IKZF1 lesions in adult acute lymphoblastic leukaemia - the chicken or the egg?

Rachel Mitchell

University College London

PhD Supervisor: Professor Adele Fielding

A thesis submitted for the degree of

Doctor of Philosophy

University College London

February 2021

Declaration

I, Rachel Jayne Mitchell, confirm that the work presented in this thesis is my own. Where information has been derived from other sources, I confirm that this has been indicated in the thesis.

Abstract

The *IKZF1* gene encodes the transcription factor IKAROS, a master regulator of lymphocyte differentiation. *IKZF1* is commonly deleted in acute lymphoblastic leukaemia (ALL), particularly in *BCR-ABL1+* ALL. Lesions in *IKZF1* carry the hallmarks of RAG mediated deletion, the expression of which is controlled by IKAROS. The title of this thesis, "*IKZF1* lesions… the chicken or the egg?", refers to the unknown sequence of events which leads up to the deletion of *IKZF1* since RAG expression dependent on IKAROS and therefore could not be deleted without RAG activity.

The most common intragenic deletion involves the removal of the DNA binding domain in exons four to seven (Δ4-7), and produces a dominant negative (DN) which inhibits wild-type IKAROS function via dimerisation. Other focal deletions involving exons two or eight cause loss of function (LOF).

Firstly, to ascertain if *IKZF1* deletions (Δ*IKZF1*) had an impact on outcome, I screened 498 patients with B-ALL by end-point PCR for the four most common deletions: Δ4-7, Δ2-7 Δ4-8 and Δ2-8. *IKZF1* lesions had no impact on outcome, despite minimal residual disease (MRD) positivity being more likely after induction therapy. A comparison of PCR and MLPA revealed a large number of discrepancies, highlighting that neither technique alone is sufficient for Δ*IKZF1* detection.

Next, I compared Ig/TCR and *BCR-ABL1* based MRD to see if one technique was better at predicting survival. Several specimens had significantly different MRD levels, though neither of technique was proven better at predicting outcome. I also show that the type and number of Ig/TCR rearrangements differ significantly based on *IKZF1* status, and that *IKZF1* breakpoint sequences differ significantly based on *BCR-ABL1* status, suggesting altered RAG activity.

Finally, I established several cell line models in order to observe the effects of DN and LOF *IKZF1* lesions on drug sensitivity. I showed that NALM-6 cells with LOF or DN *IKZF1* lesions have increased resistance to dexamethasone, and that the

presence of mesenchymal stromal cells in co-culture enhanced survival of ALL cells regardless of *IKZF1* and *BCR-ABL1* status.

The data in this thesis has shown that while there is no impact of Δ*IKZF1* on outcome in patients with ALL, it is likely that its impact is dependent on other cooperating lesions when these results are considered within the wider context of other trial data. Despite no impact seen in the clinical data, the cell line experiments have confirmed that Δ*IKZF1* contributes to a more aggressive phenotype although the cause of this remains unclear.

Impact Statement

There are around 800 new cases of acute lymphoblastic leukaemia (ALL) diagnosed each year in the UK (CRUK website). Only 50% of adults diagnosed with ALL can expect to live longer than five years after diagnosis. This stands in stark contrast to the relative success of treatment in paediatric patients, which has achieved over 90% cure rates. This demonstrates an area of unmet clinical need in adult patients. The work outlined in this thesis describes how lesions in the gene *IKZF1* impacts outcome in patients with ALL. Genetic lesions of *IKZF1*, encoding the protein IKAROS, an essential transcription factor in haematopoiesis, are an important event in the development or progression of acute lymphoblastic leukaemia (ALL).

This project was designed to dovetail with the phase three UKALL14 clinical trial and its scientific correlative studies. The specimens collected from the UKALL14 trial are heavily clinically annotated, making it possible to assess *IKZF1* lesions in different contexts. The work on trial specimens will contribute to a large body of work already performed on other trial populations, allowing clinicians to make a more informed decision based on the *IKZF1* status of a patient. This is of particular importance since a negative result was found, unlike the majority of studies previously carried out. The comparison of end-point PCR and MLPA revealed a significant number of discordant results, which could have potential implications in diagnostic laboratories.

There is some debate over how best to assess patients' treatment response via molecular minimal residual disease (MRD) monitoring. Although no significant difference was found when comparing Ig/TCR MRD and *BCR-ABL1* MRD in this project, it has highlighted that it is not uncommon for these results to differ and therefore more work needs to be done to ascertain why that is, and if this has an impact in the clinic. Further to this, the MRD assay designed around the *IKZF1* breakpoints allows for an increased repertoire by which patients can be followed, allowing for more comprehensive analysis during a patient's treatment.

Cell line models were developed in order to study the effects of the two different deletion types found in *IKZF1* in different genetic contexts. The cause of the treatment resistance observed in this project will be integral to ascertaining why some patients with *IKZF1* deletions experience a poor outcome. Use of these models in an academic setting will be necessary for this future research.

This work has the potential to improve risk stratification in patients with ALL, improve quality of life, and help in the development of different treatment options. As these are results from a national trial, the results of this project are likely to have an international reach.

Acknowledgement

Firstly, I would like to thank my supervisor Professor Adele Fielding, for her expert guidance throughout the last four years. I feel incredibly lucky to have worked with her and to have been given the opportunity of pursuing a Ph.D. in her laboratory. I would like to acknowledge my funding source, a Gordon Piller studentship from the Blood Cancer UK charity, without which this work would not have been possible.

I would also like to thank the members of the Fielding laboratory both past and present for their constant help, support, and friendship. It was a privilege to work with every member of the group.

Finally, I would like to thank my family and my partner, Adam, for their encouragement and for their belief in me.

This thesis is dedicated to the memory of Harry, Eric, and Sam.

Table of Contents

Table of figures

List of tables

Abbreviations

ABL1	ABL Proto-Oncogene 1, Non-Receptor Tyrosine Kinase
AFF1	AF4/FMR2 Family Member 1
aCGH	Array Comparative Genomic Hybridisation
ALB	Albumin
ALL	Acute Lymphoblastic Leukaemia
AMPK	AMP-Activated Protein Kinase
ASO	Allele Specific Oligonucleotides
ATAC-seq	Assay for Transposase-Accessible Chromatin-Sequencing
ATP	Adenosine Triphosphate
BCR	Breakpoint Cluster Region
BM	Bone Marrow
BMM	Bone Marrow Microenvironment
BRG1	Brahma Related Gene 1
BSA	Bovine Serum Albumin
BTG1	B-cell Translocation Gene, Anti-Proliferation Factor 1
CCND2	Cyclin D2
CD20	Cluster of Differentiation 20
CDKN2A/B	Cyclin Dependent Kinase Inhibitor 2A/B
cDNA	Complementary Deoxyribonucleic Acid
ChiP-Seq	Chromatin Immunoprecipitation-sequencing
CLP	Common Lymphoid progenitor
CML	Chronic Myeloid Leukaemia
CNS	Central Nervous System
CRISPR	Clustered Regularly Interspaced Short Palindromic Repeats
CRLF2	Cytokine Receptor Like Factor 2
cRSS	Cryptic Recombination Signal Sequences
CRUK	Cancer Research UK
CSF2RA	Colony Stimulating Factor 2 Receptor Subunit Alpha
DAPI	4,6-Diamidino-2-Phenylindole
DFS	Disease Free Survival
dH2O	Distilled water
DMEM	Dulbecco's Modified Eagle Medium
DN	Dominant Negative

DNA	Deoxyribonucleic Acid
dNTPs	2'-Deoxiribonucleoside 5'-Triphosphate
DSB	Double Stranded Break
DSMZ	Deutsche Sammlung von Mikroorganismen und Zellkulturen GmbH
DTT	Dithiothreitol
DUSP6	Dual Specificity Phosphatase 6
EBF1	Early B-Cell Factor 1
ECOG	Eastern Cooperative Oncology Group
EFS	Event Free Survival
EGFL7	Epidermal Growth Factor-Like Protein 7
Elf-1	E74-Like Factor 1
ERG	ETS Related Gene
ESLHO	European Scientific foundation for Laboratory Hemato Oncology
ETV6	ETS variant transcription factor 6
EV	Empty Vector
FACS	Fluorescence-Activated Cell Sorting
FBS	Foetal Bovine Serum
FISH	Fluorescence In Situ Hybridisation
FOXO1	Forkhead box O1
FOXP1	Forkhead box P1
GATA3	GATA Binding Protein 3
GFP	Green Fluorescent Protein
GLUT-1	Glucose Transporter 1
GUS	β – Glucuronidase
HDAC	Histone Deacetylase
HEB	HeLa E-box binding protein
HMGB1	High Mobility Group Box 1
HoTr	Low Hypodiploidy/Near Triploidy
HR	Hazard Ratio
HSC	Haematopoietic Stem Cell
IgH	Immunoglobulin Heavy chain
IgL	Immunoglobulin Light chain
Igκ	Immunoglobulin kappa
Igλ	Immunoglobulin lambda

IKZF1	Ikaros Family Zinc Finger 1
IL3RA	Interleukin 3 Receptor, Alpha
IRES	Internal Ribosome Entry Site
JAK2	Janus Kinase 2
KMT2A	Lysine Methyltransferase 2A
LMPP	Lympho-Myeloid Multipotent progenitor
LOF	Loss Of Function
LPO	Left Probe Oligonucleotide
LST1	Leukocyte Specific Transcript 1
m-BCR	Minor-Breakpoint Cluster Region
M-BCR	Major-Breakpoint Cluster Region
MLPA	Multiplex Ligation-dependent Probe Amplification
MRD	Minimal Residual Disease
mRFP	Monomer Red Fluorescent Protein
MSC	Mesenchymal Stromal Cell
MSCV	Murine Stem Cell Virus
MVA	Multivariable analysis
NAC	Non-Amplifiable Control
NF-κB	Nuclear Factor-kappa B
NGS	Next Generation Sequencing
NHEJ	Non-Homologous End Joining
NR3C1	Nuclear Receptor subfamily 3 group C member 1
NR3C2	Nuclear Receptor subfamily 3 group C member 2
ns	Not Significant
NTC	Non-Template Control
NuRD	Nucleosome Remodelling and Deacetylase
OS	Overall Survival
PAR1	Pseudoautosomal Region 1
PAX5	Paired box 5
PB	Peripheral Blood
PBS	Phosphate Buffered Saline
PCR	Polymerase Chain Reaction
Ph	Philadelphia chromosome
POQR	Positive Out Of The Quantitative Range

PRC2	Polycomb Repressive Complex 2
QC	Quality Control
QR	Quantitative Range
RAG1	Recombination Activating Gene 1
RAG2	Recombination Activating Gene 2
RB1	Retinoblastoma 1
RFS	Relapse Free Survival
RNA	Ribonucleic Acid
RNP	Ribonucleoprotein
RPMI	Roswell Park Memorial Institute
RPO	Right Probe Oligonucleotide
RSS	Recombination Signal Sequence
RT-qPCR	Real Time Quantitative Polymerase Chain Reaction
RUNX1	RUNX Family Transcription Factor 1
SCT	Stem Cell Transplant
SD	Standard Deviation
SH3BP5	SH3 Domain Binding Protein 5
SM-FRET	Single Molecule- Fluorescence Resonance Energy Transfer
SNP	Single Nucleotide Polymorphisms
SOCS2	Suppressor Of Cytokine Signalling 2
TAQ	Thermus Aquaticus
TBLXR1	TBL1X Receptor 1
TCF-1	Transcription Factor-1
TCF3	Transcription Factor 3
TCR	T-Cell Receptor
TCRα	T-Cell Receptor alpha
TCRβ	T-Cell Receptor beta
TCRγ	T-Cell Receptor gamma
TCRδ	T-Cell Receptor delta
TdT	Terminal deoxynucleotidyl Transferase
TKI	Tyrosine Kinase Inhibitors
TP53	Tumour Protein p53
TTR	Time To Relapse
UVA	Univariable Analysis

V(D)J	Variable (Diversity) Joining gene segments
WBC	White Blood Cell
WHO	World Health Organisation
WT	Wild Type
κde	Kappa Deleting

1 Introduction

1.1 Acute Lymphoblastic Leukaemia

1.1.1 Overview

Acute Lymphoblastic Leukaemia (ALL) is characterised by the clonal expansion of lymphoid cells and is a rare and heterogeneous disease. ALL involves a high rate of proliferation and an arrest in the differentiation of lymphocytes which can arise in both B- and T-cells. B-ALL is the more common of the two, with 75% of cases arising from the B-cell lineage. Between 2015 and 2017, around 800 cases were diagnosed per year in the UK (CRUK website). ALL is the most common cancer amongst children, with a median age of diagnosis of 13 years, and 60% of all diagnoses made under the age of 20 (Ma et al., 2014). Age at diagnosis follows a bimodal distribution with a peak in early childhood and after the age of 50 (**Figure 1.1**) (Brown et al., 2020).
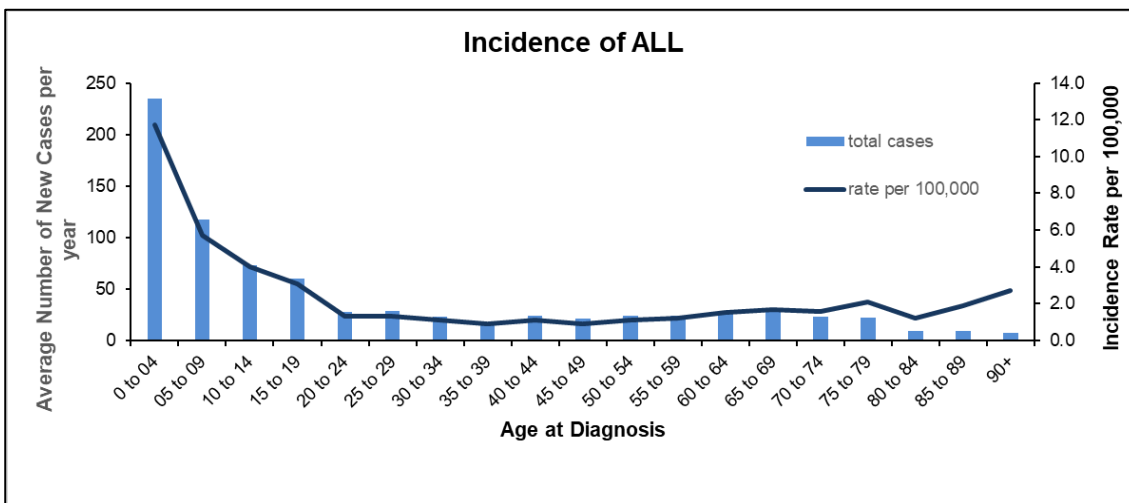
Figure 1.1: Average incidence of ALL in the UK per 100,000 and cases per age group 2015-2017. Most ALL cases diagnosed in children with a peak in incidence in early childhood, with a smaller peak in older adults. The light blue bars indicate the average number of total cases in the UK from 2015-2017. The dark blue like shows the rate per 100,000. Data modified from the CRUK website, accessed August 2020.

Outcomes have been significantly improved in paediatric ALL with cure rates exceeding 85% (Tran and Hunger, 2020, Maloney et al., 2020). This stands in stark contrast to adult patients, whose 5-year survival rate is much lower at 40-50%. A major cause in the differences in outcomes between adult and paediatric patients is that adult management of these patients; novel therapies and

diagnostic tools are necessary in order to improve outcomes in patients that historically have poor response to treatment.

1.1.2 Classification

An initial attempt was made at classifying ALL in 1976 based on cell morphology alone. The French American British classification divided ALL into 3 subgroups-L1, L2 and L3 (Bennett et al., 1976). Although this classification was useful for making initial diagnoses, it held no clinical significance. Later attempts at classifying ALL were made by the World Health Organisation (WHO) in 1997, which incorporated both morphology and cytogenetic profile. When revised in 2008, ALL was defined by two entities- T-ALL and B-ALL, with a further subdivision of the latter based on the chromosomal abnormalities present (Campo et al., 2011). The most recent update in 2016 included two new provisional entities which were added to the list of recognised genetic abnormalities, summarised in (**Table 1.1**), and hypodiploid B-ALL was further subdivided into low hypodiploid or hypodiploid with *TP53* mutations (Terwilliger and Abdul-Hay, 2017, Arber et al., 2016).

Table 1.1 2016 WHO classification of ALL

B-cell lymphoblastic leukaemia/lymphoma, not otherwise specified
B-cell lymphoblastic leukaemia/lymphoma, with recurrent genetic abnormalities
B-cell lymphoblastic leukaemia/lymphoma with hypodiploidy
B-cell lymphoblastic leukaemia/lymphoma with hyperdiploidy
B-cell lymphoblastic leukaemia/lymphoma with t(9;22)(q34;q11.2)[BCR-ABL1]
B-cell lymphoblastic leukaemia/lymphoma with t(v;11q23)[MLL rearranged]
B-cell lymphoblastic leukaemia/lymphoma with t(12;21)(p13;q22)[ETV6-RUNX1]
B-cell lymphoblastic leukaemia/lymphoma with t(1;19)(q23;p13.3)[TCF3-PBX1]
B-cell lymphoblastic leukaemia/lymphoma with t(5;14)(q31;q32)[IL3-IGH]
B-cell lymphoblastic leukaemia/lymphoma with intrachromosomal amplification of chromosome 21 (iAMP21)*
B-cell lymphoblastic leukaemia/lymphoma with translocations involving tyrosine kinases or cytokine receptors ('*BCR-ABL1*–like ALL')*
T-cell lymphoblastic leukaemia/lymphomas
Early T-cell precursor lymphoblastic leukaemia*

Modified from Arber et. al., 2016. *provisional entity

1.1.3 Prognostic and Predictive Biomarkers

Traditionally, patients have been risk stratified by factors such as age and presenting white blood cell (WBC) count. Individuals over the age of 60 at diagnosis experience a particularly poor outcome, with only a 10-20% chance of long-term survival (Gökbuget and Hoelzer, 2006). However, it is likely that older age is a surrogate for unfavourable genetic alterations associated with a poorer outcome (Rowe, 2010). Older patients are also more likely to have other co-morbidities meaning they are less likely to tolerate intensive therapies. Presenting WBC count is also likely to be a surrogate for underlying genetic alterations such as the poor risk t(4;11)(q21;q23) translocation which is associated with a high WBC count (Gu et al., 1992) and the good risk *ETV6-RUNX1* fusion is associated with a low presenting WBC count (Stanulla and Schrappe, 2009).

As well as the risk factors identified at diagnosis, the initial response to treatment is also a strong indicator of outcome. Traditionally this was assessed by morphology, a predictive biomarker, but it is now standard practice to measure minimal residual disease (MRD) by molecular techniques such as flow cytometry and real time quantitative polymerase chain reaction (RT-qPCR). This is discussed in more detail later on the chapter.

In addition to the presenting features in patients, the identification of particular genetic alterations has helped to refine this stratification. ALL can affect both children and adults and the majority of paediatric patients can expect to have a good outcome, though this is not the case for adult patients. While adult and childhood ALL present with the same overt disease phenotype, they often do not carry the same genetic lesions (Moorman et al., 2012). Childhood ALL is more likely to harbour genetic lesions associated with good outcome such as *ETV6-RUNX1*, with adult ALL more likely to harbour lesions associated with poor outcome- the Philadelphia chromosome, for example (**Figure 1.2** and reviewed in Iacobucci and Mullighan, 2017).
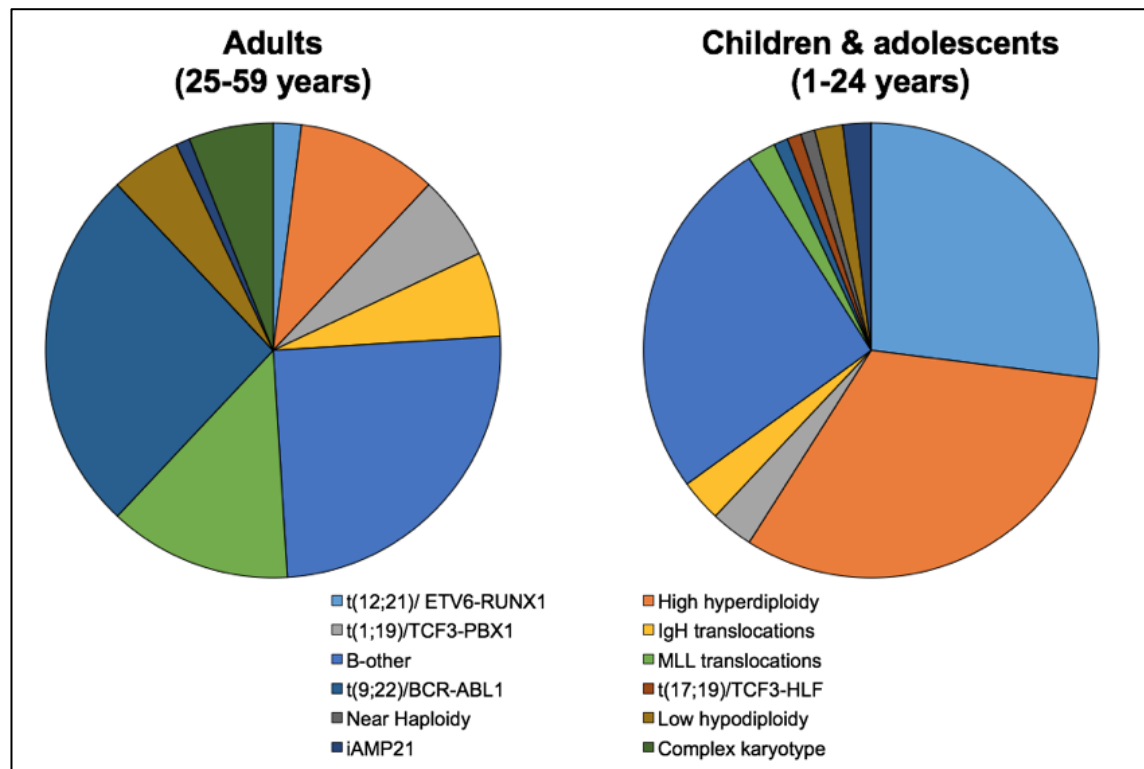
Figure 1.2: Cytogenetic subgroups in Adult and Childhood ALL. (Moorman et al., 2012)

A lot is already known about the gross genetic changes in ALL that have been studied by more traditional techniques like fluorescence in situ hybridisation (FISH). A number of sub-microscopic lesions in important genes such as *PAX5, CDKN2A/B, ETV6, EBF1,* and *IKZF1* have been identified with high resolution techniques. These lesions are of importance as these could provide an explanation as to why adult ALL patients have a significantly poorer outcome than their childhood counterparts. It may also explain why some patients that do not harbour any established genetic lesions associated with a poor risk go on to relapse.

1.1.4 Philadelphia chromosome positive ALL

The most common lesion in adult ALL is the Philadelphia chromosome, first described in 1960 (Nowell and Hungerford, 1960), and was later discovered to be the result of a reciprocal translocation between chromosomes 9 and 22 in 1973 (Rowley, 1973). This translocation brings together a breakpoint cluster region *BCR* on chromosome 22 and the oncogene *ABL1* on chromosome 9 which results in the formation of the fusion transcript *BCR-ABL1*, a tyrosine kinase (**Figure 1.3A**). The size of the fusion transcript is dependent on the breakpoints,

the most common of which is p190 (minor/m-BCR) in B-ALL, with a much smaller proportion of patients harbouring the p210 transcript (major/M-BCR) (Arana-Trejo et al., 2016). It is also worth noting that the p210 variant is much more common in chronic myeloid leukaemia (CML) and is the only genomic aberration which is sufficient to initiate leukaemogenesis, though this is not the case for *BCR-ABL1*+ ALL which requires other cooperating lesions (Reckel et al., 2017).

The breakpoints in both *BCR* and *ABL1* are highly variable but are consistently found in either introns 1 or 13/14 in *BCR*, termed minor and major breakpoint cluster regions respectively, and between exons 1b and 2 of *ABL1* (**Figure 1.3B**) (Score et al., 2010, Kang et al., 2016). The different proteins that arise from the differing fusion transcripts do not all have the same domains though all have constitutively active protein kinase activity, the domain for which is targeted by tyrosine kinase inhibitors (TKIs) such as imatinib.

Philadelphia positive (*BCR-ABL1*+) ALL accounts for around 20-30% of adult ALL patients and incidence increases with age (Moorman et al., 2007, Chiaretti et al., 2013). While patients with *BCR-ABL1*+ ALL were known for having a poorer outcome, the introduction of tyrosine kinase inhibitors in standard therapy significantly improved this (Short et al., 2017, Daver et al., 2015).
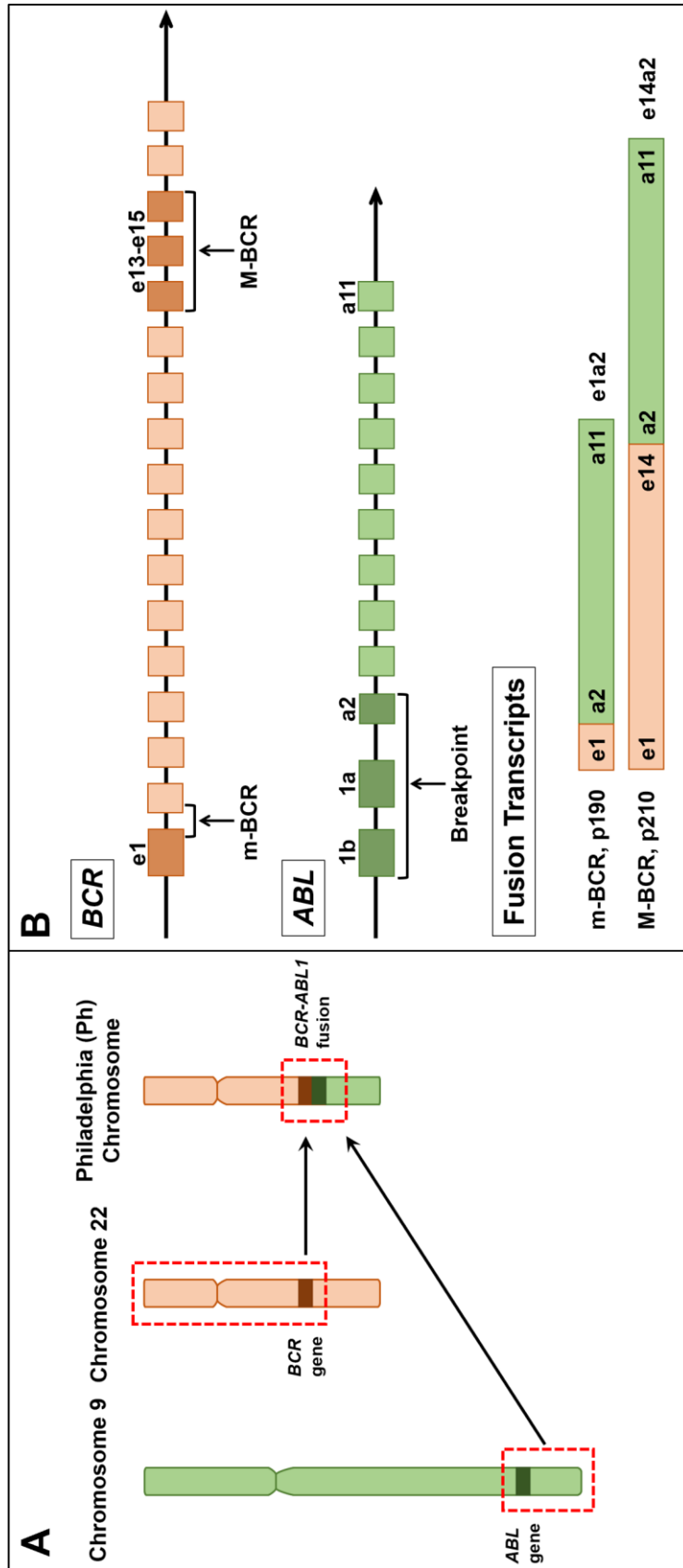
Figure 1.3: Philadelphia Chromosome. (A) The Philadelphia chromosome arises when a reciprocal translocation occurs between the long arms of Chromosomes 9 (green) and 22 (orange), generating the *BCR-ABL1* fusion transcript. **(B)** Schematic diagrams showing the minor (m-BCR) and the major (M-BCR) breakpoints in *BCR* (orange), and the breakpoint in *ABL* (green). The fusion transcripts that arise from each breakpoint are also shown.

1.1.5 "Philadelphia like" ALL

There is also a proportion of Philadelphia chromosome negative (*BCR-ABL1-*) patients that have "Philadelphia like" ALL. These are patients that have a characteristic gene expression profile associated with *BCR-ABL1+* ALL and share a similar poor outcome, but do not carry the Philadelphia chromosome (Den Boer et al., 2009). This subgroup was first discovered in paediatric ALL and has now been identified in adult patients, with incidence increasing with age and peaking in adolescence (Herold et al., 2014, Boer et al., 2015, Roberts et al., 2017). Within this group of patients, adults tend to experience poorer outcomes compared to their paediatric counterparts.

There is no clear definition for Philadelphia-like ALL, and this is partly because it was initially described by two independent groups using different methodologies. The COG-TARGET-St Jude consortium first identified high risk B-ALL *IKZF1* deleted cases with a similar gene expression pattern to *BCR-ABL1+* ALL using gene set enrichment analysis and Affymetrix microarrays, referring to this group of patients as "*BCR-ABL1* like" (Mullighan et al., 2009). This in turn identified 257 gene probe sets common to *BCR-ABL1+* and "*BCR-ABL1* like" ALL, while a Dutch study group led by Den Boer used hierarchical clustering of 110 previously defined probeset expression patterns to identify major subtypes in ALL, including the discovery of a group of patients described as having "Philadelphia-like" ALL (Den Boer et al., 2009). There is significant overlap, though there is not total concordance between the two definitions, with only 9 probesets of seven genes common between the two definitions- *ABL*, *CCND2*, *DUSP6*, *EGFL7*, *LST1*, *SH3BP5*, and *SOCS2*. Currently, there is no consistent way of identifying Philadelphia-like ALL in the clinical laboratory setting because of the unclear nature of the definition.

Like *BCR-ABL1+* ALL, these patients are more likely to harbour lesions in *IKZF1*, are found in around 15% of patients, and are almost always in the B-other subgroup, i.e. those that aren't classified by any other genetic change (Mullighan et al., 2009). Despite not having a clear definition for Philadelphia-like ALL, numerous studies have identified several underlying genetic events that make up this group of patients. Based on this, Philadelphia-like ALL can be broadly divided

into two groups. Around half are characterised by an over-expression of *CRLF2* (Roberts et al., 2012, Russell et al., 2009), and in those where this is not the case, fusions involving *JAK2*, *PDGFRB ABL1* and *ABL2* are common (Roberts et al., 2014). These are referred to as the ABL-class fusions, with *PDGFRB* being the most common fusion partner. The ABL-class fusion is one of the most important subtypes, accounting for around 10% of Ph-like ALL (Yadav et al., 2021). It occurs in 17% of paediatric patients, 9% of adolescents, 10% of young adults and 9% of older adults (Roberts et al., 2014, Roberts et al., 2017, Reshmi et al., 2017).

1.1.6 Treatment

The treatment of adult ALL has largely been based on modified childhood protocols, which typically involves three steps: Induction, consolidation/ intensification, and maintenance. The main aim of induction therapy is to eradicate leukaemic cells from the blood, bone marrow and central nervous system (CNS), allowing for normal haematopoiesis to be reinstated. Several multi-agent induction therapy regimens have been developed, and involve the use of cytotoxic chemotherapies such as vincristine and daunorubicin, and corticosteroids like dexamethasone and prednisone.

Upon the completion of induction therapy, consolidation is started in order to increase the chances of a prolonged remission being achieved. The agents used in this phase of treatment should not induce similar resistance to that of the drugs used during the induction phase of therapy. This is to reduce the chances of a patient developing a resistant clone (Narayanan and Shami, 2012).

Maintenance therapy lasts for two to three years, and consists of daily doses of 6-mercaptopurine, weekly methotrexate and vincristine, and pulses corticosteroids. There is a shorter disease free survival in patients where no maintenance therapy is given compared to those that receive it (Cuttner et al., 1991, Cassileth et al., 1992). However, maintenance beyond three years does not appear have any significant benefit in patients (Jabbour et al., 2005, Narayanan and Shami, 2012).

Relapse is common among adult patients, and so allogeneic stem cell transplant (SCT) is used to improve outcomes. Patients that are deemed high risk by either presenting features such as age and white count, or the persistence of residual disease after induction therapy are offered transplant if eligible. A number of patients are not eligible for transplant due to lack of a donor, presence of infection and other co-morbidities. It is therefore a challenge to make a comparison among the different treatments for high risk patients. Patients with *BCR-ABL1+* disease are at particular risk of relapse and cure rates are low without the use of SCT. On the international UKALLXII/ECOG2993 trial, patients with *BCR-ABL1+* ALL that underwent SCT had improved overall survival at 5 years when compared to those that did not (44% versus 36%) (Fielding et al., 2009).

CNS relapse is highly likely in adult patients where treatment is not administered prophylactically. Therapies to prevent CNS relapse include cytarabine and methotrexate, both of which have good penetration into the CNS. CNS disease can also be treated more directly by administering chemotherapy intrathecally and is given throughout treatment to prevent CNS relapse (Terwilliger and Abdul-Hay, 2017, Lenk et al., 2020).

As mentioned previously, *BCR-ABL1+* ALL is also treated with TKIs such as imatinib which specifically target the BCR-ABL1 fusion protein and has been vital in improving outcome in patients with this genetic alteration. Imatinib was first devleoped to treat CML patients, with CML being the first malignancy for which a targeted treatment was implemented (O'Brien et al., 2003). Prior to the use of TKIs, α-interferon was considered the gold standard in the treatment of CML, though toxicity was not uncommon and outcomes were poor, with a median survival time of five years (Hehlmann et al., 2003). The establishment of TKIs in the therapy of CML also made it apparent that patients also experience resistance, making it necessary for the development of second and third generation TKIs like Ponatinib (Zhou et al., 2011).

Patients with *BCR-ABL1+* ALL treated before the TKI era experienced very poor outcomes, with a five year survival rate of around 5-20% (Faderl et al., 2000, Dombret et al., 2002). The introduction of TKIs in the treatment of ALL has

significantly improved outcomes for patients with *BCR-ABL+* disease (Daver et al., 2015, Samra et al., 2020). Imatinib can induce responses as a single agent, though these are often short lived. Imatinib is most effective when given in combination with other multi-agent protocols. However, imatinib has poor CNS penetration and relapse is common. Second generation TKIs such as dasatinib have shown promise in treating CNS disease in a paediatric murine model (Porkka et al., 2008) and more recently on the CCCG-ALL-2015 clinical trial in comparison to imatinib. Patients treated with dasatinib had higher rates of event free survival (71.0% vs 48.9%), overall survival (88.4% vs 69.2%), and lower relapse rates at four years (19.8% vs 34.4%) than those treated with imatinib (Shen et al., 2020).

Despite the advent of TKI therapy, prognosis for both paediatric and adult patients with *BCR-ABL1+* ALL remains poor with high rates of relapse. Resistance to imatinib is considered one of the main causes of poorer outcomes among these patients. One major mechanism of resistance to first generation TKIs is the T315I mutation in the ABL kinase domain. Second generation TKIs like dasatinib have only partially overcome this resistance (Rousselot et al., 2016), and therefore development of third generation TKIs, e.g. ponatinib, is essential in overcoming potential resistance (Jabbour et al., 2013).

1.1.7 V(D)J Recombination and RAG

B and T cells have the ability to recognise and respond to the diverse pathogens invading the human body. This is due to the almost infinite capacity of these cells to rearrange the seven loci involved in making up the receptors that recognise these pathogens. B-cell receptors are made up of a heavy chain (IgH) and a light chain (Igκ and Igλ) whose gene loci are comprised of Variable (V) Diversity (D) and Joining (J) gene segments (Sakano et al., 1979). The sheer number of the gene segments and the random manner in which they are rearranged are the cause of the diverse nature of the heavy and light chains. In normal development, recombination is lineage specific, i.e. only complete T-cell receptor (TCR) genes are rearranged in T cells, and only complete immunoglobulin (Ig) gene rearrangement in B-cells. In developing B cells, the first recombination event is between the D and the J gene segments at the IgH locus on Chromosome 14,

followed by the V segment. This precedes the rearrangement of the light chain loci, the process of which has been summarised in **Figure 1.4** (van der Burg et al., 2002).
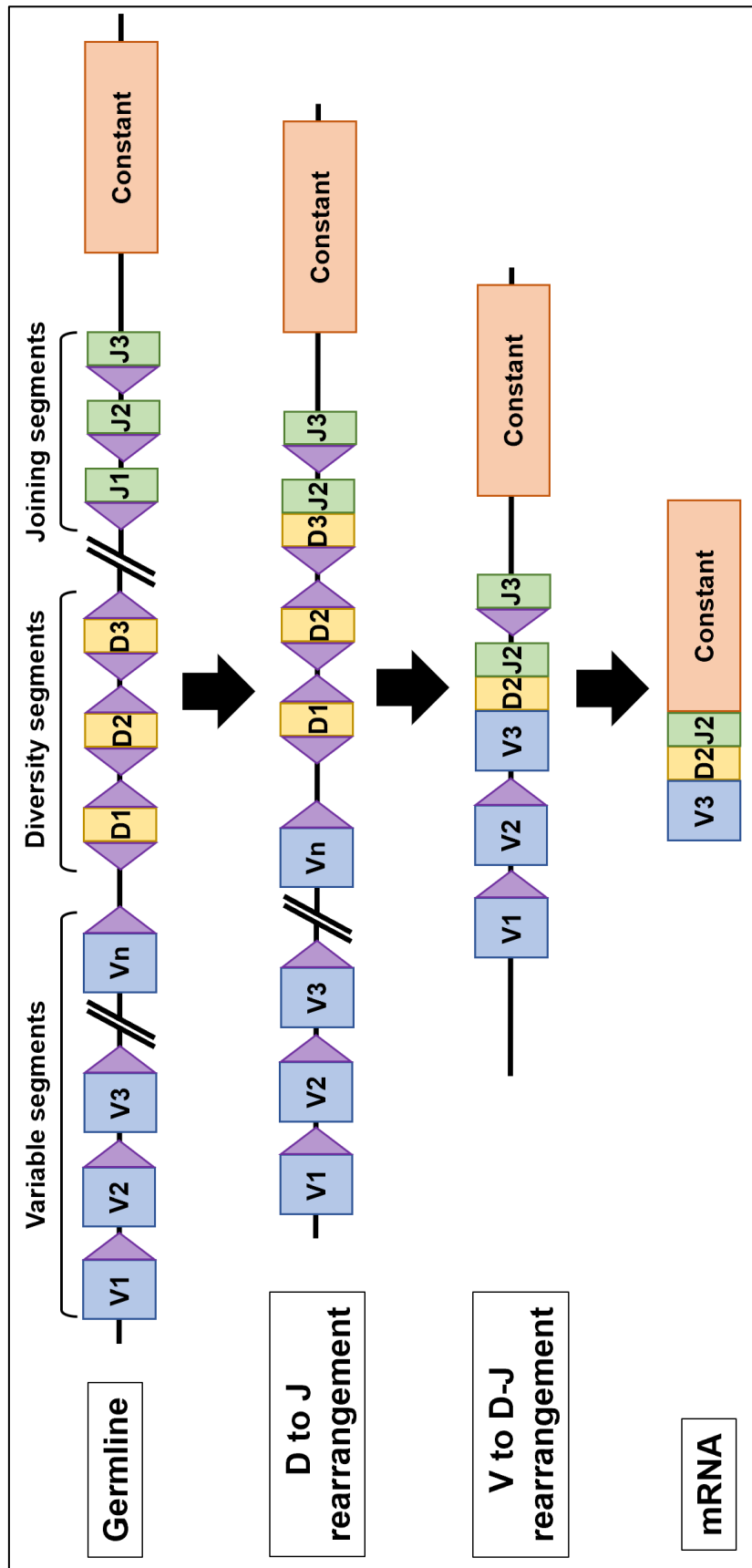
Figure 1.4: Assembly of complete antigen receptor loci. The three different types of gene segments, variable (V), diversity (D) and Joining (J) are assembled into one coding sequence by the RAG 1/2 enzyme complex. RAG recognises the recombination signal sequences (purple triangle) that flank the gene segments and makes double stranded breaks. In the case of the IgH, TCR beta and delta chains, this occurs in two steps. Initially, a D to J rearrangement occurs, then a V segment is added. The IgL, TCR gamma and alpha chains rearrange in one step since they lack D segments. For the final protein to be translated, the extra gene segments not involved in the rearrangement are spliced out of the mRNA sequence.

Haematopietic Stem Cells (HSCs) continually generate B and T cells within the bone marrow, with B-lymphocytes undergoing maturation exclusively within the bone marrow unlike T cells which develop within the thymus. During lineage commitment, T and B cells must rearrange and produce a functional TCR and BCR respectively. HSCs subsequently give rise to common Lymphoid progenitors (CLPs), which in turn develop into to B-cells (**Figure 1.5**), T-cells, dendritic cells, and innate lympoid cells (Lescale and Deriano, 2016). Commitment to a particular lineage is specified by both environmental signals and a number of transcription factors such as TCF3, EBF1, FOXO1, PAX5, and IKAROS (Miyazaki et al., 2014, Miyazaki and Miyazaki, 2021). During B cell development, the non-productive gene segments within the Ig/TCR loci are rearranged into one gene which is mediated by the recombination activating genes 1 and 2 (RAG1 and RAG2). Expression of the RAG gene locus is therefore restricted to B and T lymphocytes (Månsson et al., 2007). In both B and T lineages, expression of RAG occurs at two stages which coincides with the rearrangement of the Ig/TCR loci. In developing B cells in particular, the IgH locus is rearranged during the first stage in pro-B cells. A burst in proliferation then occurs upon the expression of a pre-BCR on the cell surface which is associated with a reduction in RAG expression in pre-B cells (**Figure 1.5**). The second wave of expression gives rise to rearrangement of the IgL chain in pre-B cells that have exited the cell cycle (Hillion et al., 2009). A number of transcription factors involved in lymphoyte differentiation have been implicated in the regaulation of the *RAG* locus including TCF3, IKAROS, PAX5, FOXP1, FOXO1 and NF-κB via binding to its promoters and other regulatory elements such as cis-regulatory elements (Kuo and Schlissel, 2009).

The *Erag* enhancer has been shown to regulate Rag in B-cells, the deletion of which results in a a reduction of Rag expression and a partial block between pro-B and pre-B cells in mice (Hsu et al., 2003). More recently, lineage specific cis-regulatory elements that control Rag1/2 expression have been identified by using ChIP-seq and ATAC-seq to assess TCF3 binding. Two B-cell specific regions were found: *R1B*, 5kb upstream of the *RAG1* promoter, and *R2B* which partially overlaps with *Erag* (Miyazaki et al., 2020). TCF3 was not the only transcription

factor to bind to these regulatory elements- Pax5 and Ikaros were among the proteins identified at these sites (Miyazaki et al., 2020).
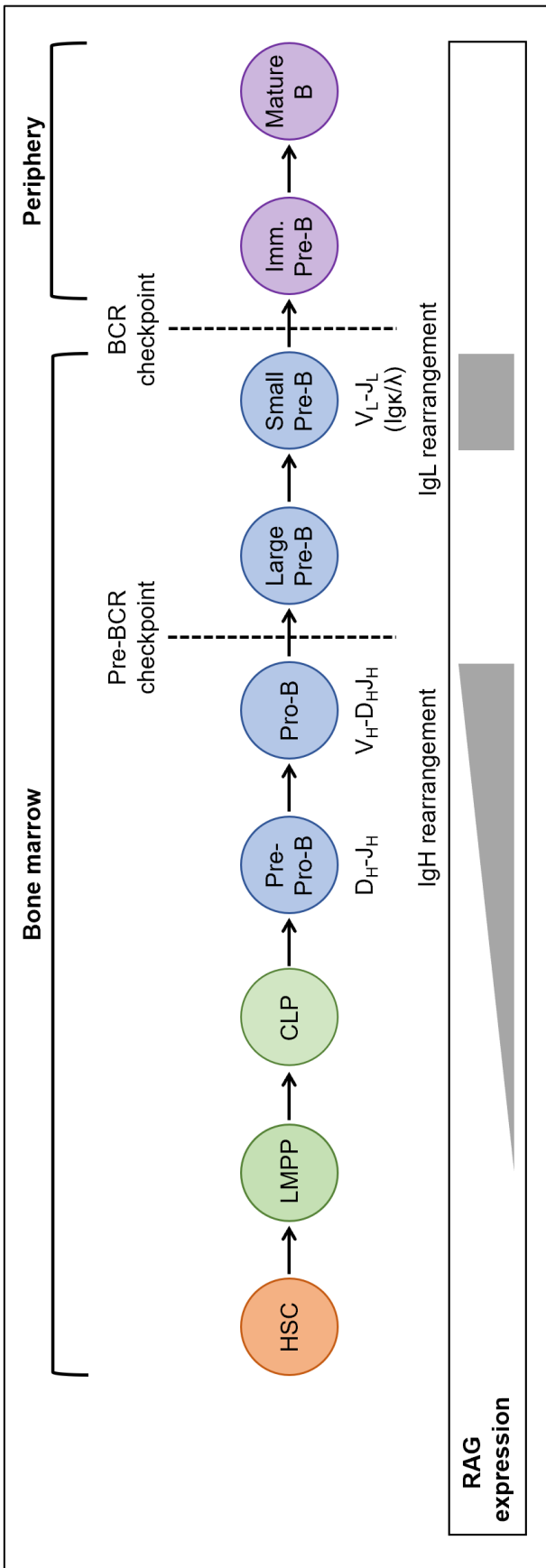
Figure 1.5: B-cell development and RAG expression. RAG expression occurs at specific stages of B-cell development in order to rearrange a productive BCR. The heavy chain (IgH) is rearranged at the pre-pro to pro-B stage, while the light chain (IgL) is rearranged at the small pre-B stage in development. BCR= B cell receptor, HSC= haematopoietic stem cell, LMPP= lympho-myeloid multipotent progenitor, CLP= common lymphoid progenitor, Imm.= immature. Modified from Lescale and Dariano, 2016.

The structure of the two RAG proteins has now been resolved. Initial functional studies identified "core" RAG residues in which portions of the proteins had been removed and still retained specific binding and cleavage activity *in vitro*. More recently, a high-resolution structure of the RAG1, RAG2 and the tetrameric complex has been identified using X-ray crystallography (Kim et al., 2015). RAG1 is elongated and consists of several structural modules including the active site and DNA binding domain. RAG2 is a doughnut shaped six-bladed propeller, termed a "Kelch repeat structure" (**Figure 1.6A**). The RAG1/2 complex is Y-shaped with the two RAG1 monomers forming the main stalk, and RAG2 sitting on top of each arm (**Figure 1.6B**). The two active sites are located in the middle of each arm, and it likely that RAG2 assists with the formation of the catalytic site and DNA cleavage due to its proximity.
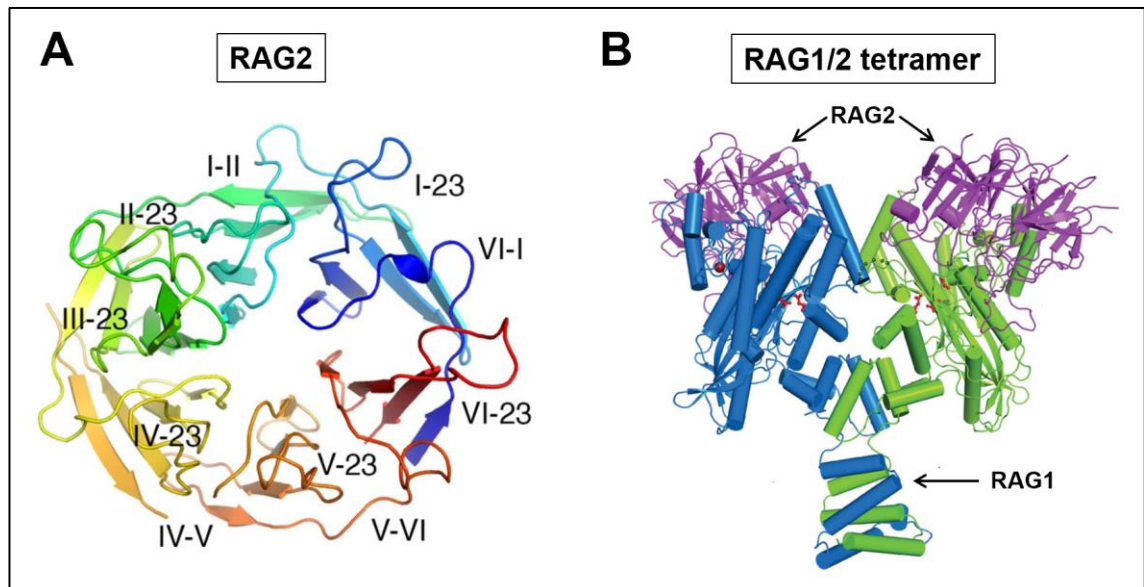
Figure 1.6: The crystal structure of RAG1/2. (A) RAG1 is a 6 bladed propeller structure. Each blade is numbered with a roman numeral. **(B)** The structure of the RAG1/2 heterotetramer is Y shaped. RAG1 (blue and green) makes up the main stalk with RAG 2 (purple) sitting on top of each arm. Modified from Kim et. al., 2015.

RAG1 and RAG2 cooperate in all their known activities. The recombinase complex recognises the recombination signal sequences (RSS) that flank the gene segments. These are comprised of a conserved heptamer (CACAGTG), either a 12 or 23 bp spacer, and a conserved nonamer (ACAAAAACC) (Sakano et al., 1979). Strictly one of each of these is required for V(D)J recombination, termed the "12/23 rule" (Lewis, 1994). The different segments are flanked by the two different RSSs which only allows recombination to occur between V, D and J segments, and not within the same gene segment type.

Initially, the RAG1/2 complex binds to one each of these motifs, forming the paired complex (steps 1 and 2, **Figure 1.7**). Next, RAG1/2 forms a nick in the DNA which leaves the exposed hydroxyl group to attack the other stand, forming a double stranded break (DSB) (step 3, **Figure 1.7**). The resulting hairpin structure that is formed is brought about by a covalent seal at the end of the segment. Finally, RAG1/2 cooperate with the machinery associated with the non-homologous end joining (NHEJ) pathway to repair the DSBs. The RSS ends are usually joined to form the signal joint, while the coding joint undergoes the addition of non-germline nucleotides via by terminal deoxynucleotidyl transferase (TdT) before being repaired (step 4, **Figure 1.7**). Both the DSB and the repair mechanisms involved are what make each rearrangement unique.

RAG1 and 2 are proposed to originate from transposable elements and are themselves capable of transposition, as was demonstrated *in vitro* (Agrawal et al., 1998). Due to the potential damaging nature of V(D)J recombination, this process is tightly regulated by limiting access to DNA. During development of ALL, the regulation of the RAG enzyme machinery breaks down, and these genes become constitutively active. This means that not only do lineage specific genes become rearranged in the wrong cell type, but RAG is able to recognise cryptic RSS (cRSS) throughout the genome. It has been hypothesised that RAG is responsible for a number of translocations and deletions common to ALL. Due to the clonal nature of ALL cells, the same V(D)J rearrangement is present in many cells making it possible to detect by PCR.
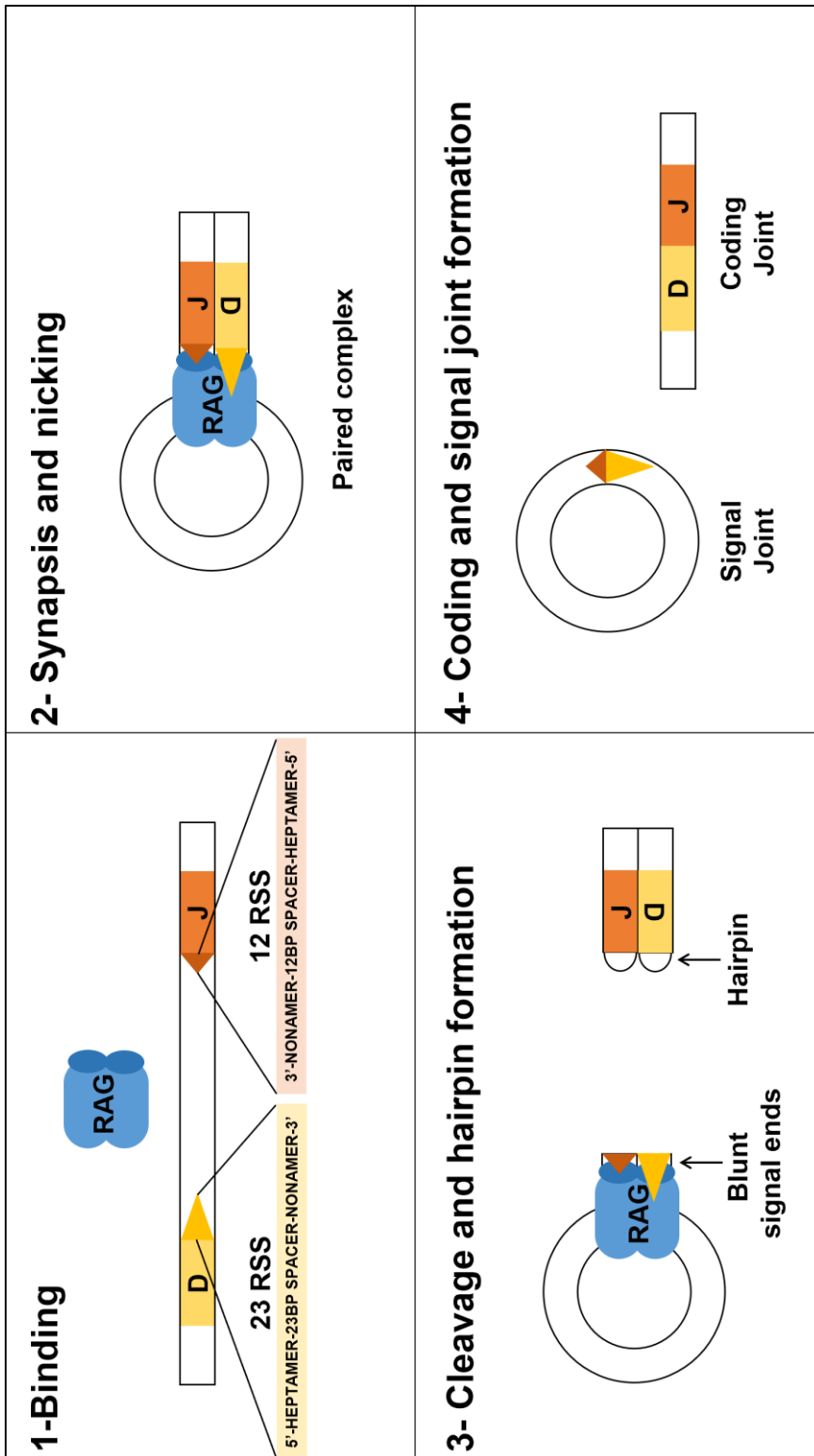
Figure 1.7: Stages of RAG mediated V(D)J recombination. Step 1: RAG recognises and bind to either the 12 (orange triangle) or 23 (yellow triangle) RSS forming the 12 or 23 RSS respectively. **Step 2:** Capture of the second RSS forms the paired complex (termed synapsis) RAG then nicks 1 strand of the DNA. **Step 3:** The free OH group then attacks the other strand producing DSBs, forming the hairpin coding end and the blunt signal ends. **Step 4:** The DSBs in the coding ends are then repaired via the NHEJ pathway after undergoing the addition of non-germline nucleotides via TdT activity. This forms the coding joint. The signal ends often join without processing to form the signal joint.

37

1.1.8 Minimal Residual Disease Monitoring

MRD detection is defined as any technique used to identify residual leukaemic cells beyond the limit of cytomorphological analysis. MRD monitoring has made it possible to assess treatment response and risk of relapse in patients, and has since become a key tool in risk stratification (Pui et al., 2015, Kruse et al., 2020). This has allowed for high risk patients to be assigned to more intense treatment strategies and to avoid toxicity in low or intermediate risk patients (Vora et al., 2013, Pieters et al., 2016). Less sensitive methodologies such as FISH used for MRD detection are incapable of differentiating between truly MRD negative low risk patients and MRD positive patients that are at risk of relapse without intervention (**Figure 1.8**). These methods of detection are not sufficiently sensitive enough and are not able to detect sub-microscopic MRD. More sensitive techniques have been developed, e.g. quantification of Ig/TCR gene loci and immunophenotyping by multi-parameter flow cytometry (Denys et al., 2013, Garand et al., 2013).
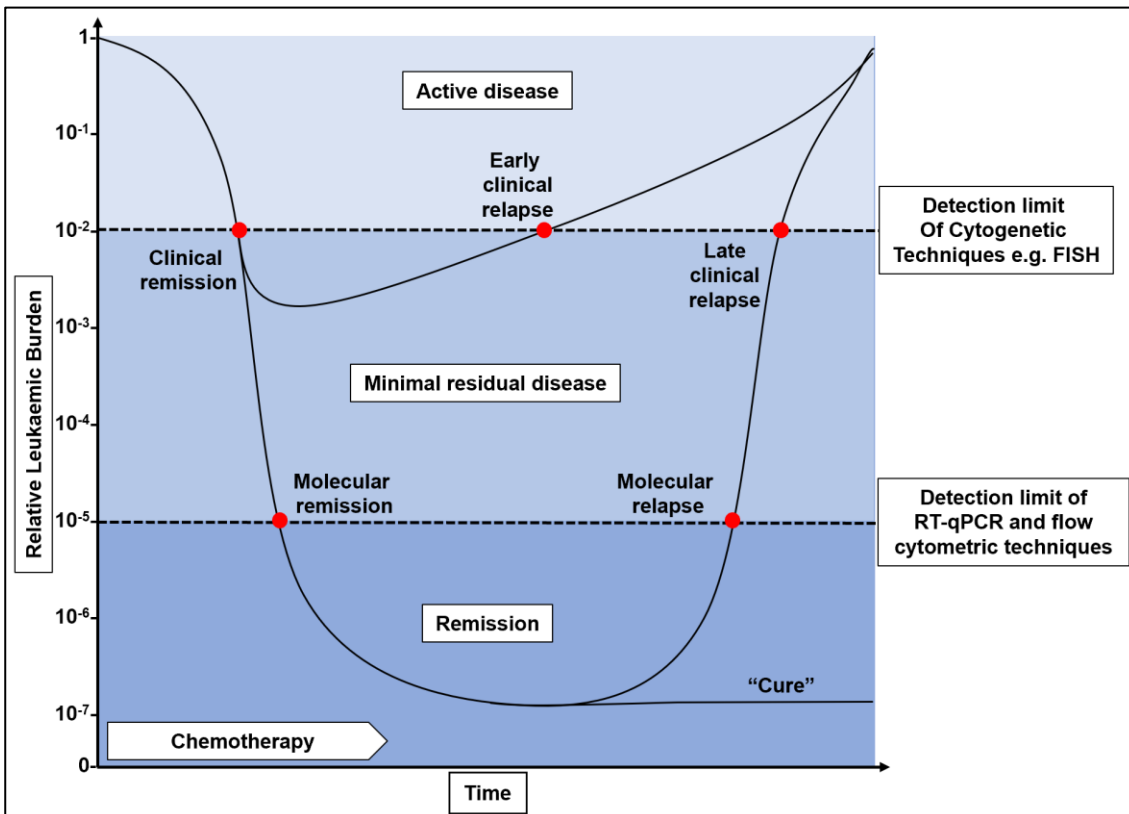
Figure 1.8: Measuring MRD over time. The hypothetical disease kinetics are shown by the solid black lines, and are monitored by the different diagnostic tools. Lower detection limits of molecular techniques (dashed black lines) have allowed for more refined MRD detection and earlier detection of relapse (red dots).

The monitoring of minimal residual disease (MRD) of ALL patients and their response to therapy has long been performed through the quantification of clonal immunoglobulin or T cell receptor loci (Ig/TCR) rearrangements. This tool has shown to be vital and is consequently incorporated into the risk stratification of both paediatric and adult patients and is regarded as the gold standard in monitoring (Brüggemann et al., 2010). MRD is typically analysed through the PCR detection of leukaemia specific clonal rearrangements of the Ig/TCR loci. To ensure this technique is comparable, large scale studies were carried out to standardise the processes involved, and quality control is performed to maintain this through groups such as ESLHO (van der Velden et al., 2007).

The basic principle of this is the comparison of follow-up specimens by quantitative real-time PCR to a patient derived standard curve made from DNA obtained from diagnostic bone marrow or peripheral blood. The patient is screened at diagnosis for a range of clonal Ig/TCR rearrangements, the rearrangements are sequenced, a patient specific oligonucleotide is designed over the junctional region, and the assay is optimised through a "limited test", i.e. only a limited number of points from the standard curve is used to determine quantitative range (QR) and appropriate T_m (van der Velden et al., 2007).

This assay is highly sensitive, with an ideal lower limit of detection of $1*10^{-4}$ (0.01%) though this is not always possible. There are a number of limitations to MRD detection by this method. It is labour intensive and to carry it out requires a significant amount of training, not every patient can be monitored, rearrangements can undergo clonal evolution due to the presence of constitutively active RAG and can lead to false negative results (Szczepanski et al., 1999). While some patients achieve MRD negativity, they go on to relapse, and so there is also some debate over whether RT-qPCR is sufficiently sensitive.

There has been a drive to move towards next generation sequencing (NGS) to resolve some of these limitations of monitoring by RT-qPCR (Faham et al., 2012, Della Starza et al., 2019). While NGS would be more sensitive, there is some question over the standardisation of these techniques and the clinical relevance of detecting such low levels of MRD. More recently, NGS has been proven to be

a better predictor of relapse in paediatric patients. In an initial study by Kotrova and colleagues, 210 specimens from 76 patients were analysed by RT-qPCR and NGS. There was a high correlation between both methods (R^2=0.72), though analysis by NGS would have caused 25 (33%) patients to be assigned to different risk group. Furthermore, NGS MRD positivity was more predictive of relapse than RT-qPCR MRD (5-year relapse free survival [RFS] NGS: -ve/+ve- 90± 5% vs 53 ± 9%, p=0.0003; PCR: -ve/+ve- 84 ± 6% vs 63 ± 8%, p=0.04) (Kotrova et al., 2015). A subsequent study from this group also found a similar result in the post SCT setting, and the low level positivity found by RT-qPCR in post-transplant patients are not likely to be genuine and are in fact negative, as found by NGS (Kotrova et al., 2017).

MRD monitoring can also be performed by quantifying the level of the *BCR-ABL1* fusion transcript in *BCR-ABL1*+ ALL, which has now been standardised after several rounds of QC (Pfeifer et al., 2019). There is some debate over whether *BCR-ABL1* MRD correlates with Ig/TCR MRD, and if there is a clinical significance to this. A group of paediatric patients has been identified in whom the *BCR-ABL1* MRD was significantly higher than that of the Ig/TCR. Subsequent analysis revealed that there was multi-lineage involvement of the Philadelphia chromosome, and that a multipotent progenitor was affected. This suggests that these patients had a "CML-like" biology and may impact their outcome (Hovorkova et al., 2017)

1.1.9 Bone marrow microenvironment

The bone marrow microenvironment (BMM) or "niche" is a collection of cells and structures that support the production of all blood cell types within the bone marrow. There are several different cell types which regulate the biology of HSCs within the BMM including arteriolar and sinusoidal endothelial cells (Kunisaki et al., 2013, Acar et al., 2015), mesenchymal stromal cells (MSCs) (Asada et al., 2017), sympathetic neuronal cells (Méndez-Ferrer et al., 2008, Kunisaki et al., 2013), osteoblasts (Calvi et al., 2003), perivascular stromal cells (Sugiyama et al., 2006), nonmyelinating Schwann cells (Yamazaki et al., 2011), adipocytes (Naveiras et al., 2009), megakaryocytes (Zhao et al., 2014) and regulatory T cells (Fujisaki et al., 2011).

MSCs are multipotent stem cells capable of differeniating into several cell types that give rise to osteocytes, chondrocytes, myoblasts, fibroblasts and adipocytes under distinct conditions *in vitro* (Dominici et al., 2006), and also responsible for the formation the extracellular matrix within the bone marrow, providing the BMM and structural support (Novoseletskaya et al., 2020). MSCs are therefore critical for the formation of the bone marrow niche in which haematopoiesis occurs.

Malignant cells are capable of hijacking the BMM, and destroying the HSC-supporting microenvironment providing survival advantages and support to leukaemic cells. This shift within the BMM changes from one where normal haematopoiesis is supported to one which allows for the rapid expansion of leukaemic cells and potentially leads to chemoresistance. More recently, it was demonstrated that B-ALL cells have the ability to remodel the BMM to create a niche in which MSCs are transformed and create an chemoprotective environment (Duan et al., 2014). Recent work within my host laboratory has described the way in which a protective niche is induced by ROS inducing chemotheraputic agents and are responsible for the generation of cancer associated fibroblasts that protect leukaemic cells by accepting damaged mitochondria via tunelling nanotubes (Burt et al., 2019).

1.2 *IKZF1* and IKAROS

1.2.1 *IKZF1* gene and protein function

The *IKZF1* gene is located on the short arm of chromosome 7 and is comprised of eight exons (**Figure 1.9**) (Georgopoulos et al., 1994, Molnár et al., 1996). While the gene contains eight exons, exon 1 is not transcribed, with the transcription start site, and ATG start codon, located in exon 2. *IKZF1* encodes for the zinc finger protein IKAROS, a member of a family of transcription factors responsible for the maturation and differentiation of haematopoietic stem cells (IKZF1-5) (Yoshida and Georgopoulos, 2014, John and Ward, 2011). IKAROS is able to directly bind DNA via the four N-terminal zinc fingers encoded by exons 4-6. The middle pair of these zinc fingers makes contact with DNA via the specific (A/G)GGAA core motif (Hu et al., 2016). The other zinc fingers within the DNA binding domain contribute to its acitvity, though they do not make direct contact with DNA (Schjerven et al., 2013, Arenzana et al., 2015). IKAROS is also able to

form homo- and heterodimers with family members via the C-terminal zinc fingers encoded by exon 8 (McCarty et al., 2003).
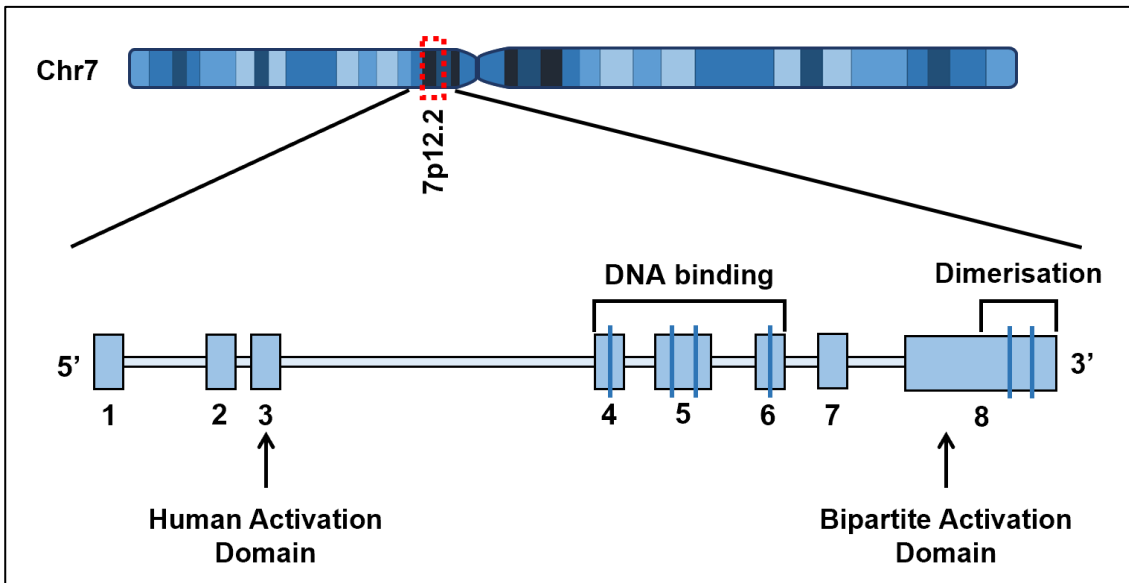
Figure 1.9: Chromosomal location and gene structure of *IKZF1*. The *IKZF1* gene is located on Chromosome 7. Blue boxes represent exons in the gene and the dark blue vertical lines represent the location of the zinc fingers.

IKAROS is essential for normal lymphopoiesis at different stages of differentiation by repressing gene expression through the alteration of chromatin structure in developing immune cells. This is achieved through the recruitment of various complexes that are able to modify chromatin at target loci (Kim et al., 1999, Oravecz et al., 2015, Yoshida and Georgopoulos, 2014). One such complex that IKAROS interacts with is the nucleosome remodelling deacetylase (NuRD) complex via the ATPase Mi2b (Schwickert et al., 2014, Schjerven et al., 2013, Yoshida et al., 2019). Both NuRD and IKAROS enrichment patterns at these target lymphoid lineage genes vary significantly during lymphocyte development, meaning that IKAROS regulates a broad range of genes (Zhang et al., 2011). It has recently been shown that IKAROS leaves highly distinct histone methylation signatures depending on its interaction with the HDAC proteins, which are components of the NuRD complex (Song et al., 2016).

In addition to the NuRD complex, IKAROS also interacts with the Polycomb Repressive Complex PRC2 during B-cell development and also double negative thymocytes (Oravecz et al., 2015, Hu et al., 2017). PRC2 is responsoble for the

presence of the H3K27me3 repressive marker, and so the loss of IKAROS leads to the loss of this (Oravecz et al., 2015). IKAROS activity is not exclusive to transcriptional repression of its target genes. IKAROS also interacts with BRG1, which makes up a part of the chromatin remodeling Switch/Sucrose Non-Fermentable complex (Kim et al., 1999, Bossen et al., 2015).

1.2.1.1 Control over early lymphoid development

Lymphocyte differentiation is dependent on a small number of proteins that bind to DNA and are able to influence transcription patterns in HSCs, the root of all haematopoietic and lymphoid lineages (van Galen et al., 2014, Ng et al., 2009). Examples of these transcription factors include TCF3, HEB, EBF1, PAX5, RUNX1, and the IKAROS family of transcription factors. HSCs exhibit low levels of gene expression patterns, termed "transcriptional priming" (Laslo et al., 2006). IKAROS plays a key role in the transcriptional priming of HSCs and subsequently lympho-myeloid multipotent progenitors (LMPPs) (Ng et al., 2009).

IKAROS is known to be expressed throughout haematopoeisis from the HSC through to terminally differentiated T and B effector cells. Early work to elucidate its function through the generation of mutant murine models led to the discovery that loss of IKAROS leads to significant defects in lymphoid development *in vivo* (Georgopoulos et al., 1994). In the same study, mice that exclusively express the DN isoforms of IKAROS have a complete lack of T, B and natural killer cells. A later study in which a heterozygous murine model was generated, found that T-cell development was normal up to one month of age, and subsequently lost double and single positive thymocyte populations. Following the loss of these populations, the heterozygous mice developed leukaemia and lymphoma which led to the conclusion that Ikaros is a tumour suppressor (Winandy et al., 1995). Disruption of the C-terminal zinc fingers were also studied in murine models. Loss of these zinc fingers in the dimerisation domain led to the absence of murine foetal T- and B-cell precursors (Wang et al., 1996). These early functional studies concluded that DNA binding and dimerisation are both essential for the normal function of Ikaros.

Despite the early work in Ikaros function pointing to its role in lymphocyte development, its specific activity during each developmental stage was not clear. Subsequent studies found that mice homozygous for an Ikaros null mutation displayed a significant reduction in the ability of HSCs to repopulate (Nichogiannopoulou et al., 1999), and that Ikaros is necessary for the activation of the lymphoid gene expression profile and the repression of stem cell genetic signatures in LMPPs.

1.2.1.2 Control of early B-cell development

Since the early murine models discussed in section 1.2.1.1 had a total lack of B-cells, a model in which the expression of Ikaros at low levels was generated in order to study its role in early B-cell development (Kirstetter et al., 2002). In this particular model, foetal B-cells were absent although were able to develop from an albeit markedly smaller population of precursors which appeared postnatally. These B-cells had significant defects in the pro- to pre-B cell stage. Other studies have since found that normal pre-B cell development and pre-BCR signalling is prevented upon a loss of Ikaros (Schwickert et al., 2014, Heizmann et al., 2013).

Ikaros is also implicated in the development of early thymocytes (Winandy et al., 1999), innate lymphoid cells (Mazzurana et al., 2019), and in the function of mature T-cells (Thomas et al., 2010) and mature B-cells (Heizmann et al., 2016), which will not be discussed in detail as they are less relevant to this thesis.

1.2.1.3 Role in adhesion and migration

IKAROS is involved in the migration and adhesion of cells, the loss of which alters both of these normal functions (Lopez et al., 2002). A loss of Ikaros function in murine models has been implicated in cells acquiring stem cell like features, self-renewal and over-expression of adhesion molecules (Churchman et al., 2016, Churchman et al., 2015). The expression of a dominant negative form of IKAROS also leads to the expansion of primitive B-cells in a murine model, but without initiating leukaemia (Beer et al., 2014).

1.2.1.4 Metabolic control of IKAROS

Malignant cells have a higher dependence on glucose metabolism, known as aerobic glycolysis (Warburg et al., 1924). More recently, the involvement of IKAROS in the prevention of malignant transformation via metabolic pathways has been investigated. It was found that IKAROS and PAX5 restrict glucose uptake via transporters below the required level for malignant transformation. This restriction activated the AMPK pathway, an energy stress sensor, which results in autophagy. DN isoforms of both proteins were shown to lift the block on glucose metabolism and relieve energy restriction, and also resulted in resistance to corticosteroids (Chan et al., 2017). This may explain the apparent treatment resistance in *IKZF1* deleted patients, though only DN IKAROS was tested and not a loss of the entire IKAROS protein.

1.2.2 Regulation of the *IKZF1* locus

Since alterations in the *IKZF1* locus are common in ALL, discussed in detail later on in this chapter, understanding its normal expression patterns and what controls this is critical. Murine studies on control of the *Ikzf1* locus have revealed the presence of two stage-specific promoters and six enhancers. One of the promoters has a major role in lymphoid-myeloid cells (**Figure 1.10**, promoter B). Only two of the six enhancers are active in T cells (**Figure 1.10**, C/D and H), and one is involved in the up-regulation of Ikaros during the transition of LMPPs from HSCs (**Figure 1.10**, C/D) (Yoshida and Georgopoulos, 2014).

The elements identified in murine models allow for control over the *Ikzf1* locus during normal lymphopoiesis (Yoshida et al., 2013, Perotti et al., 2015). A number of key transcription factors that control development of the lymphoid system display occupancy at the enhancers of *IKZF1*. Enrichment for TCF3 and HEB, enhancers of E-box proteins, RUNX1 and TCF-1 at these enhancers suggest that these are likely to contribute to the induction of IKAROS expression in HSCs (Yoshida et al., 2013).
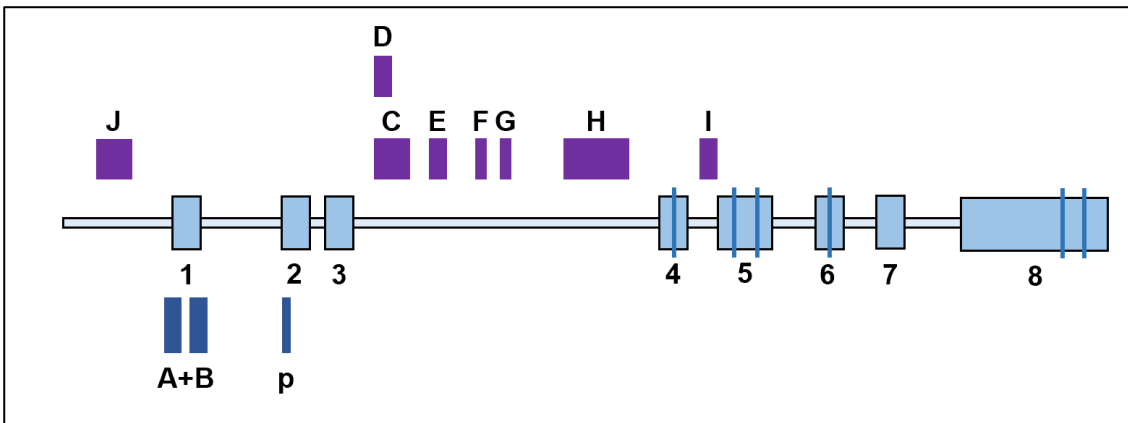
Figure 1.10: A summary of the regulatory elements controlling the murine _Ikzf1_ locus. The promoters A and B, represented by the dark blue boxes located in exon 1 are shown, along with a promoter element (p). Regions tested for enhancer activity (C-I) are represented by the purple boxes. Promoter B and the promoter element up-regulate Ikaros in HSCs and B-cells, and enhancers E, F, and H-J maintain expression in restricted chromatin environments. Enhancer C/D is required for the up regulation of Ikaros during the transition from HSCs to LMPPs. Modified from Yoshida and Georgopoulos, 2014.

1.2.3 _IKZF1_ gene mutations

IKZF1 is commonly deleted in ALL, with _IKZF1_ deletions (Δ_IKZF1_) more commonly occurring in _BCR-ABL1_+ ALL (Mullighan et al., 2008, van der Veer et al., 2014a). There are several different deletions that can affect _IKZF1_ in the progression and development of ALL, some involving the entire gene, caused through the loss of 7p or monosomy 7 (Stanulla et al., 2020, Lopes et al., 2019). Others only affect part of the gene and remove a subset of the exons. There are a number of different isoforms of IKAROS (**Figure 1.11**), the majority of which are produced through alternative splicing. This is with the exception of IK6 which is produced through the deletion of exons 4-7, the most common intragenic deletion found in _IKZF1_ (Cazzaniga et al., 2011, Iacobucci et al., 2009). The IK6 isoform is described as Dominant Negative (DN) as the four zinc fingers in the DNA binding domain become deleted, leaving the dimerisation domain intact. This means that the IK6 protein can render wild type (WT) IKAROS non-functional by dimerising with it while also being non-functional itself (Sun et al., 1996).
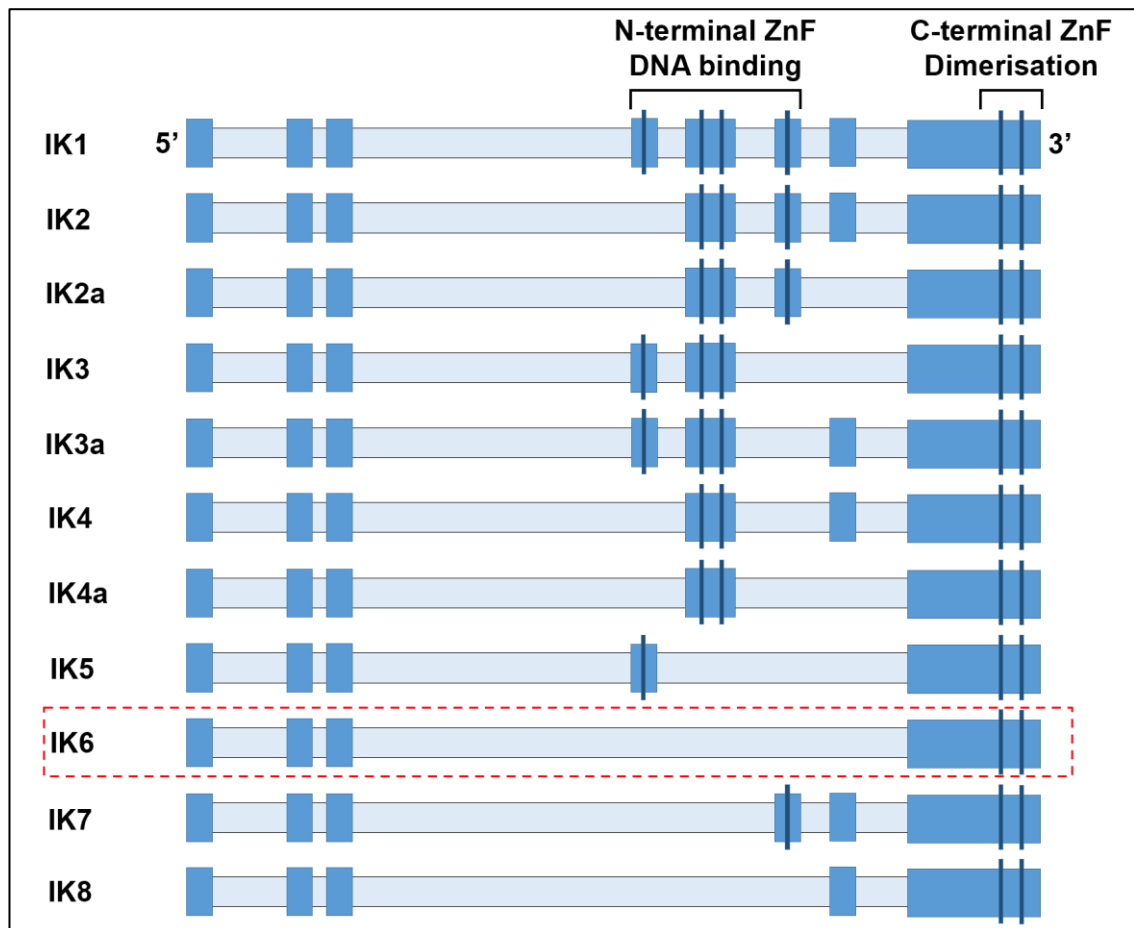
Figure 1.11: Isoforms of the IKAROS protein. There are several isoforms produced from *IKZF1* through alternate splicing with the exception of IK6 (highlighted in the red box), a dominant negative protein generated through the deletion of exons 4-7. The mid-blue boxes represent the exons, and the dark blue boxes represent the zinc fingers.

There are also other, less common deletions found in *IKZF1* that exert a different effect on the IKAROS protein. Other common deletions involve exons 2-7, 4-8 and 2-8, all of which have a loss of function effect (LOF) (Boer et al., 2016, Kastner et al., 2013). Any deletion involving either exon 2 or exon 8 would have this effect. Deletions involving exon 2 means the ATG start codon is deleted and so the gene cannot be transcribed. Deletions involving exon 8 removes the zinc fingers in the dimerisation domain, and so any protein produced cannot dimerise, and subsequently reducing activity (Kastner et al., 2013).

The intragenic deletions in *IKZF1* are thought to be caused by the aberrant activity of the RAG enzyme machinery. This is particularly evident from the breakpoints in *IKZF1* occurring closely to sequences sharing a high homology with the heptamer that RAG recognises. The breakpoints are not consistent, and

there is often the presence of a short sequence of non-germline nucleotides inserted at the breakpoint which is a hallmark of TdT activity. IKAROS is known to bind to the TdT gene, downregulate TdT in developing thymocytes (Gurel et al., 2008), and to activate the transcription of the *RAG* genes (Reynaud et al., 2008). It is unclear as to what is cause and effect in the deletion of *IKZF1*.

It is not only somatic deletions that affect the *IKZF1* locus. Single nucleotide polymorphisms (SNPs) in a number of genes such as *CDKN2A/B, GATA3* as well as *IKZF1* have been identified through genome wide association studies and found to cause a modest increase in risk to ALL susceptibility (Perez-Andreu et al., 2015, Trevino et al., 2009). Damaging SNPs in *TP53* and *ETV6* have been identified in presumed *de novo* ALL, and more recently, SNPs in *IKZF1* have been investigated (Moriyama et al., 2015). In this study, 28 SNPs in *IKZF1* were identified in paediatric patients, and found in familial ALL also. Of the 28 identified, 22 were found to be damaging and the remaining six benign. Of note, these variants were found throughout the *IKZF1* gene and not restricted to the zinc fingers (Churchman et al., 2018). All this suggests that germline variants in a number of genes including *IKZF1* have a greater role in ALL than previously thought.

1.2.4 Technical approaches for Δ*IKZF1* screening

There are several strategies that can identify intragenic *IKZF1* lesions, with differing strengths and weaknesses. Polymerase chain reaction (PCR) is a highly sensitive and specific assay. Reverse and forward primers are designed around the genomic target which anneals to the DNA, and a polymerase enzyme elongates the strand using the dNTPs available in the reaction. In the case of *IKZF1*, the primers are designed to anneal around the target breakpoint in *IKZF1* and will only produce a PCR product when brought close enough i.e., if a part of the sequence has been deleted between the primer annealing sites (**Figure 1.12**). The polymerse enzyme can only work at short range and can only produce a maximum product length of around 1Kb. PCR is fast, low cost, and easy to interpret via gel electrophoresis. While PCR highly sensitive and specific, this also means that this technique can yeild false negative results if the primer sites are disrupted, which means it is not ideal for detecting *IKZF1* deletions as the

breakpoints are not consistent, and the number of exons affected can vary. PCR is also limited to detecting the lesions where an assay has been designed. It therefore cannot detect any lesion within *IKZF1*.
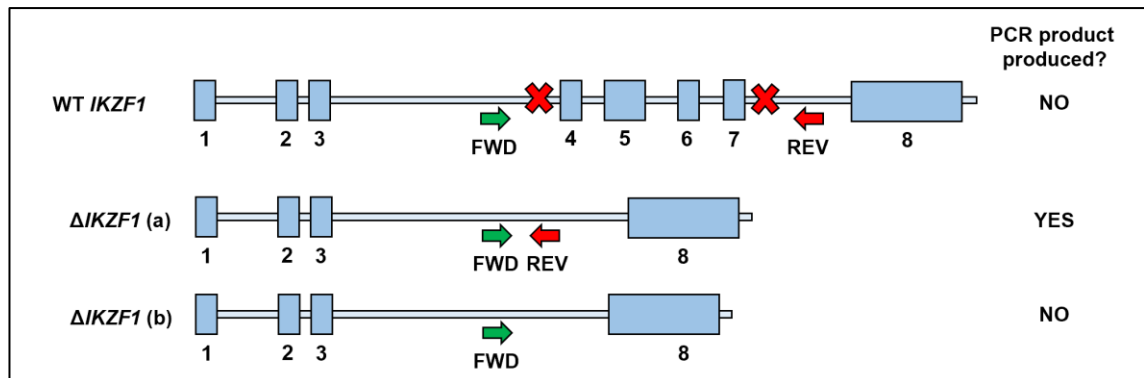
Figure 1.12: PCR based Δ*IKZF1* screening strategy. TAQ polymerase is not able to synthesise a PCR product long enough to span the distance between the forward and reverse primers in WT *IKZF1*. In (a), when exons 4-7 are deleted, the PCR primers are brought closer together and TAQ polymerase is able to elongate the strand, and will therefore only produce a positive signal on a gel if deleted. Example (b) shows one of the limitations of the PCR assay since the reverse primer site has been deleted. The breakpoints in *IKZF1* are not consistent and can yield false negative results if the primer sites are deleted. The red crosses in WT *IKZF1* represent two of the common breakpoints within the gene. FWD=forward, REV=reverse.

Multiplex Ligation-dependent Probe Amplification (MLPA) is a PCR based assay that can screen for many lesions in one reaction, making it fast and cost effective. MLPA uses probes that have two parts- the left probe oligonucleotide (LPO) and the right probe oligonucleotide (RPO). These probes contain forward and reverse PCR binding sites, a stuffer sequence, and hybridisation sequences, as seen in **Figure 1.13A**. The DNA sample is denatured to break the double strand into single stranded DNA (**Figure 1.13B**, step 1) The probes are designed to anneal to the probe target directly next to each other (**Figure 1.13B**, step 2), allowing for the sequences to be ligated by a ligase enzyme (**Figure 1.13B**, step 3). The ligated probes are then amplified by PCR (**Figure 1.13B**, step 4) and detected by capillary electrophoresis (**Figure 1.13B**, step 4). Since the probes contain a stuffer sequence, they can be identified by their defined unique length. The data are then analysed using software such as Coffalyser, comparing the leukaemic DNA sample to a healthy reference (**Figure 1.13B**, step 5). One such MLPA kit, the p335 kit, can screen the for loss of each exon of *IKZF1* independently, as well

as other genes including *RB1*, *CDKN2A/B*, *BTG1*, *ETV6*, *PAX5*, *JAK2*, *EBF1*, and the PAR1 region. Although MLPA can have a broad range of targets in one reaction, it is not as sensitive as PCR, meaning it may miss deletions in minor leukaemic clones. Furthermore, a high level of skill is required for the interpretation of MLPA. MLPA also relies on the "test" DNA sample being diploid, which is not the case for many leukaemias and hence can make interpretation of the data a challenge. Similar to PCR, MLPA is limited in that it can only detect lesion for which a probe has been designed. For example, the p335 kit has a probe designed to target each of the eight exons on *IKZF1* and so cannot detected any lesions affecting its promoter which would also reduce the amount of cellular IKAROS.

NGS based techniques would allow for all types of *IKZF1* deletion to be detected, including lesions in the promoter and intronic regions that may affect splice sites, and also damaging SNPs. While this would allow for the full spectrum of lesions in *IKZF1* to be detected, NGS is expensive which may not make it viable in the clinic, and also requires a high level of bioinformatic skill to interpret the data.
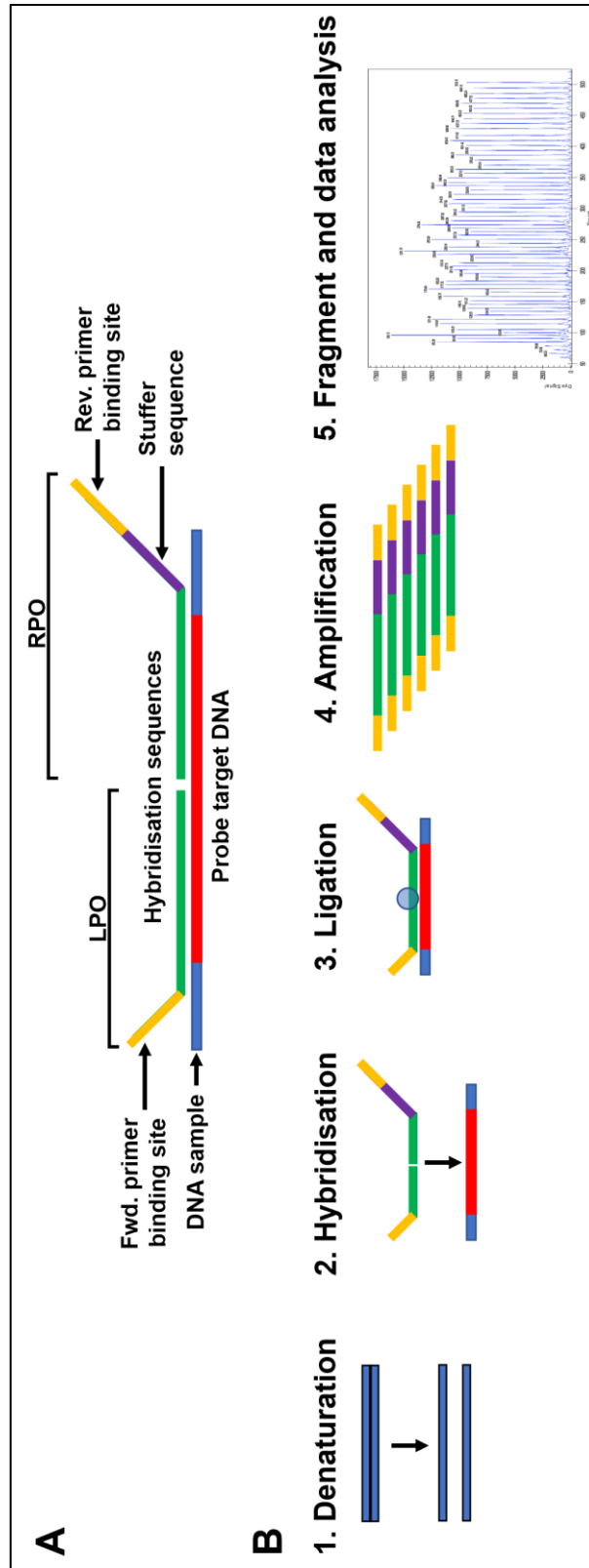
Figure 1.13: MLPA probe structure and workflow. Multiplex Ligation dependent Probe Amplification (MLPA) is a PCR based technique that allows for the screening of multiple genomic regions in one assay. (A) There are two parts to each MLPA probe. The Left and Right Probe Oligonucleotide (LPO and RPO respectively) anneal directly next to each other, allowing for ligation by a ligase enzyme. The primer sequences allow for amplification of the ligated probe. The stuffer sequence gives each probe a unique length meaning it can be distinguished from other probes during data analysis. (B) The workflow for MLPA is as follows: 1. DNA is denatured at high temperatures to break the double strands into single strands. 2. The LPO and RPO anneal to their target sequence. 3. The LPO and RPO are ligated by a ligase enzyme (represented by the blue circle. 4. The ligated probes are amplified by PCR. 5. Capillary electrophoresis is performed to determine the amount of each probe present in the sample. Test samples are normalised to a reference, and results are displayed as "peak ratios" based on the amount of each probe present in the sample. A ratio of one suggests that there has been no alteration in the test sample. A ratio below 0.5 means there has been a heterozygous deletion, and a ratio above 1.5 means there has been an amplification.

1.2.5 Δ*IKZF1* based MRD assays

MRD assays specific for Δ*IKZF1* have been developed for the monitoring of ALL patients, and found to have a strong correlation with Ig/TCR MRD (Caye et al., 2013, Venn et al., 2012). In the study led by Caye, the lower limits of sensitivity and quantitative range (QR) were similar to that of Ig/TCR MRD assays with 11 assays achieving a QR of $1*10^{-4}$ and seven achieving $5*10^{-4}$. It is worth noting that both of these studies were performed in small numbers of paediatric patients and not in adult patients. *IKZF1* deletions should only be present in leukaemic cells, and so should prove to be a highly specific marker in the detection of MRD. Moreover, as it was possible to identify sub-clonal *IKZF1* lesions, *IKZF1* MRD assays may provide a way of identifying and monitoring subclones at diagnosis that go on to become the drivers of relapse, since *IKZF1* lesions are associated with poor prognosis.   *IKZF1* deletions showed promise at increasing the repertoire of markers we can use to follow patients, which is of particular importance in adult patients where finding a sensitive marker is a challenge.

1.2.6 Prognostic impact of *IKZF1* alterations

There have been reports of differing results for the prognostic impact of *IKZF1* deletions in ALL patients. *IKZF1* has been reported as being a strong prognostic marker in paediatric patients with high risk disease (Mullighan et al., 2009). There have also been a number of studies that have identified Δ*IKZF1* as a marker for poor outcome but only in certain contexts (**Table 1.2**). For example, one study found that it is LOF and not DN deletions that are associated with poorer outcome in *BCR-ABL1-* patients on the GMALL trial (Kobitzsch et al., 2017).

There has been some suggestion that the cooperating lesions define outcome along with any *IKZF1* lesion. In particular, an *IKZF1*plus subgroup was identified in a paediatric cohort for having very poor outcome. This subgroup was defined as any *IKZF1* deletion co-occurring with deletions in either *CDKN2A*, *CDKN2B*, *PAR1*, *PAX5*, and in the absence of an *ERG* deletion (Stanulla et al., 2018). *ERG* deletions are exclusively associated with the newly described IGH-DUX4 lesion, which is associated with good risk (Zhang et al., 2016, Yasuda et al., 2016). Patients with these lesions are also likely to harbour *IKZF1* deletions (Zhang et al., 2016).

Interestingly, Dupuis and colleagues identified a relationship between IgH rearrangements and Δ*IKZF1*, and outcome (Kastner et al., 2013, Dupuis et al., 2013). Patients negative for both had the best outcome, while patients positive for Δ*IKZF1* and negative for an IgH rearrangement fared the worst. It was noted that this required repeating on other cohorts to confirm the association. This work points to a link between the activity of RAG in rearranging the IgH locus, and also the aberrant involvement in the deletion of *IKZF1.*

If Δ*IKZF1* does indeed have such a large impact on outcome, its detection in the clinical setting needs to be considered carefully. While PCR is highly sensitive, it may yield false negative results if the primer sites are deleted through the presence of an atypical breakpoint. Multiplex Ligation-dependent Probe Amplification (MLPA) would overcome this issue but is not as sensitive, and due to its technical approach struggles with the comparison of healthy individuals and patient samples harbouring large differences in ploidy. Higher throughput methods such as array Comparative Genomic Hybridisation (aCGH) and SNP arrays would overcome the issues in both PCR and MLPA, but the cost of these may not make them viable.

Table 1.2: A summary of studies focusing IKZF1 loss

Study	Method of detection	Adult/ paediatric	Number of patients	% IKZF1 altered	Outcome
Mullighan et al., 2009	SNP array	paediatric	221 "High risk" (258 validation cohort)	28%	Alterations in IKZF1 associated with very poor outcome
Dupuis et al., 2013	PCR, MLPA, aCGH	Adult and Paediatric	139	36%	More severe outcome in IKZF1 deleted paediatric patients and *BCR-ABL1-* patients.
Beldjord et al., 2014	Multiplex PCR/ MLPA	Adult	216 *BCR-ABL1-*	25%	Higher rate of relapse in patients with a focal deletion than those without
Kobitzsch et al., 2017	PCR	Adult	482 *BCR-ABL1-*	27%	LOF and not DN deletions associated with poor prognosis
Pfeifer et al., 2018	SNP array	Adult	97 *BCR-ABL1+*	76%	*IKZF1* alone was not indicative of poor outcome but was dependent on the co-occurrence of other genetic alterations
Stanulla et al., 2018	MLPA	Paediatric	991 (417 validation cohort)	15%	*IKZF1*plus (*ΔIKZF1* plus deletions in any of CDKN2A, CDKN2B, PAR1, PAX5, and absence of ERG deletion) defines a new very poor prognostic profile

1.3 Hypotheses and aims

1.3.1 Central Hypothesis

The central hypothesis of this thesis is that *IKZF1* lesions contribute to poor outcome in patients with B-ALL. The first part of this thesis addresses the central hypothesis by analysing the effects of *IKZF1* on outcome in a large clinical trial population. The subsequent parts of this thesis address how *IKZF1* lesions contribute to treatment resistance.

1.3.2 Aims

1.3.2.1 Chapter 3: *IKZF1* lesions do not contribute to poor outcome in patients with B-ALL, regardless of other cooperating lesions

Aims

- To compare PCR and MLPA for screening of *IKZF1* status
- To describe the *IKZF1* deletion status of a large patient group taking part in a national clinical trial UKALL14
- To determine the prognostic relevance of *IKZF1* and *IKZF1*^{plus} status in patients with B-ALL treated on UKALL14
- To determine the suitability and stability of Δ*IKZF1* as a marker for monitoring MRD over the timecourse of treatment

1.3.2.2 Chapter 4: Ig/TCR MRD is not more predictive of outcome than *BCR-ABL1* MRD in patients with *BCR-ABL1*+ ALL

Aims

- To compare Ig/TCR MRD and *BCR-ABL1* MRD and identify if one technique is better than the other at predicting survival
- To compare the frequency and type of Ig/TCR markers with relation to *BCR-ABL1* and *IKZF1* status
- To compare *IKZF1* breakpoint sequences in *BCR-ABL1*+ versus *BCR-ABL1*- specimens, specifically the location of the breakpoints and the non-germline insertions

1.3.2.3 Chapter 5: Lesions in *IKZF1* contribute to treatment resistance which is
abolished by *BCR-ABL1* expression

Aims

- To generate both DN and LOF *IKZF1* cell line models

- To study the effects of *IKZF1* lesions on treatment resistance

- To study the effects of mesenchymal stromal cells on treatment resistance

2 Materials & Methods

2.1 Patients

All patients were enrolled on UKALL14 (ISRCTN 66541317), a multicentre phase 3 clinical trial that recruited B-ALL and T-ALL patients aged between 20-65. Patients were recruited from December 2010 until the trial closed in July 2018. All patients gave written and informed consent to research. Where possible, cytogenetic subgroup was determined by FISH at the Northern Institute for Cancer Research, Newcastle University. In *BCR-ABL1*+ patients, the breakpoint was confirmed by PCR.

2.2 Cell lines

The ALL cell lines NALM-6, SUP-B15, SD-1 and the mesenchymal stromal cell (MSC) line HS27a (DSMZ) were cultured in RPMI 1640 (Thermo Scientific) supplemented with 10% heat inactivated foetal bovine serum (FBS) and 1% penicillin/streptomycin and L-glutamine. The packaging cell line Phoenix™-AMPHO was cultured in Dulbecco's Modified Eagle Medium (Thermo Scientific) supplemented with 10% heat inactivated FBS and 1% penicillin/streptomycin and L-glutamine. All cell lines were passaged every 3 days except for HS27a which were passaged every 7 days.

2.3 Sample processing and DNA extraction

All patient samples were processed by the National Adult ALL MRD Laboratory upon arrival. Bone marrow (BM) and peripheral blood (PB) samples were processed to isolate the white blood cell population. Samples were either diluted (BM) with RPMI 1640 or directly layered (PB) onto an equal volume of Lymphosep separation (MP Biochemicals Europe) and spun at 1,600 RPM for 30 minutes at room temperature. Where possible, DNA extraction was performed on at least $1*10^7$ cells using the DNeasy mini kit (Qiagen) according to manufacturers' instructions. DNA was diluted to a concentration between 50 and 150ng/μl using AE buffer (Qiagen). Initial concentration and purity was checked by measuring absorbance at 260nm and 280nm using a Nanodrop™ spectrophotometer (Thermo Scientific). Final DNA concentration and quality was

assessed by TaqMan™ (Thermo Scientific) real time quantitative PCR (RT-qPCR) amplification of the albumin housekeeping gene, and compared to a standard curve derived from human genomic DNA (Bioline).

2.4   Ig/TCR screening and sequence analysis

The detection of Ig/TCR rearrangement by end point PCR was performed according to EuroMRD guidelines. See **Table 7.1** in the appendix for the Ig/TCR panel of 36 primer combinations used for the 66 most common rearrangements found in B-ALL. Ig/TCR screening of patients with *BCR-ABL1+* ALL was performed by MSc student Jillian Brown as part of her research project. Ig/TCR screening is not routinely performed for patients with *BCR-ABL1+* ALL as they are followed by measuring *BCR-ABL1* transcript levels. Ig/TCR screening of patients with *BCR-ABL1-* ALL was performed as routine MRD analysis by members of MRD laboratory. To each reaction the following was added: 11.775µl dH$_2$O, 2.1µl 10x reaction buffer (Qiagen), 0.5µl 0.5mM dNTPs (Promega), 0.125µl HotStart Taq polymerase (Qiagen), 0.5µl template DNA. Cycling conditions can be found in **Table 2.1**.

Table 2.1: Cycling conditions for Ig/TCR screening

Step	Cycling condition
1	95°C for 10 minutes
2	95°C for 50 seconds
3	60°C for 50 seconds
4	72°C for 40 seconds
5	Repeat steps 2-4 for 31 more times
6	72°C for 5 minutes
7	4°C forever

PCR products were run on a 10% polyacrylamide gel with Hyperladder IV (Bioline) at 150mV for one hour. PCR products from multiplex wells were purified with using Exostar Pro (GE Healthcare) and all wells positive for an Ig/TCR rearrangement were sent for sanger sequencing to Eurofins Genomics. DNAstar Lasergene software was used to analyse sequences. The BLAST search engine was used to determine which gene segments were present in the

rearrangements. Patient specific allele specific oligonucleotides (ASO) were designed over the unique N-regions.

2.5   Patients specific standard curve preparation and ASO testing

Standard curves were serially diluted from DNA extracted from diagnostic PB and BM specimens. The initial amount of the input DNA was adjusted depending on the concentration as determined by *ALB* control gene RT-qPCR amplification. DNA was diluted with non-amplifiable control (NAC) derived from pooled healthy controls. A range from 10^{-1} to 10^{-5} was prepared. The sensitivity and specificity of ASOs were assessed by "limited testing" in which RT-qPCR was performed for 10^{-2} and 10^{-4} standard curve points in duplicate and NAC in triplicate.

2.6   Ig/TCR RT-qPCR quantification

All RT-qPCR was performed on an ABI-7500 fast machine (Thermofisher). Dilution points 10^{-1} to 10^{-3} were run in duplicates, $5*10^{-4}$ to 10^{-5} and follow up DNA specimens were run in triplicate to ensure reproducibility. Six replicates of NAC were also included to determine the sensitivity of each assay. To each reaction the following was added: 12.5µl TaqMan fast mastermix (Thermofisher), 2.5µl 0.4% bovine serum albumin (BSA), 2.25µl of each of the 10µM forward and reverse primer, 0.5µl 5µM probe (Sigma-Aldrich). Cycling conditions in **Table 2.2**.

Table 2.2: Cycling conditions for Ig/TCR and *BCR-ABL1* quantification

Step	Cycling condition
1. Hold 1	95°C for 20 seconds
2. Cycling	95°C for 3 seconds
3. Cycling	58-64°C for 30 seconds*
4. Cycling	Repeat steps 2 and 3 50 times

*A range of annealing temperatures were used depending on the optimal conditions specific to each ASO. A temperature of 60°C was used for p190 quantification

2.7 RNA extraction cDNA synthesis

RNA was extracted from BM and PB samples, and cell lines using the QIAamp RNA Blood Mini Kit (Qiagen) according to manufacturers' instructions. 1µg of RNA was made up to the volume of 20µl with dH_2O (or 20µl dH_2O for the non template control [NTC]), 1µl RNasin added and incubated at 65°C for 5 minutes in a water bath. The tubes were removed from the water bath and cooled on ice for 5 minutes before the following was added to each reaction: 10µl 5x cDNA buffer, 2.5µl 10mM dNTPs (Promega), 1µl random primers, 0.5µl DTT, 2µl reverse transcriptase, 1µl RNasin, 12µl dH_2O. Each tube was incubated at 37°C for one hour and then 10 minutes at 65°C and cooled on ice.

2.8 *BCR-ABL1* screening

Screening for the most common *BCR-ABL1* fusion transcripts was performed as part of routine MRD analysis to identify patients with *BCR-ABL1*+ ALL, and also the breakpoint, i.e. p190/minor or p210/major. To each reaction the following was added: 12.8µl dH_2O, 3µl 10x reaction buffer, 2.5µl forward primer (Merck), 2.5µl reverse primer (Merck), 0.2µl TAQ polymerase (Qiagen), 2mM dNTPs (Promega), 4µl DNA/dH_2O for the NTC. Primers are as follows (Foroni et al., 2009):

BCR-C: 5'-ACCGCATGTTCCGGGACAAAAG-3'

B2B: 5'-ACAGCATTCCGCTGACCATCAATAAG-3'

C5e-: 5'-TCCTTTGCAACCGGGTCTGAA-3'

CA3-: 5'-TGTTGACTGGCGTGATGTAGTTGCTTGG-3'

Cycling conditions can be found in **Table 2.3**. Expected band sizes and primer combinations are as follows:

- Control band- 805bp (B2B - C5e-)
- e1a2, p190/minor- 481bp (BCR-C - CA3-)
- e14a2, p210/major- 385bp (B2B - CA3-)

PCR products were run on a 2% agarose gel for one hour at 150mV.

Table 2.3: Cycling conditions for *BCR-ABL1* breakpoint detection by PCR

Step	Cycling condition
1	96°C for 5 minutes
2	96°C for 1 minute
3	64°C for 50 seconds
4	72°C for 1 minute
5	Repeat steps 2-4 for 34 more times
6	72°C for 10 minutes
7	4°C forever

2.9   *BCR-ABL1* quantification

Quantification of *BCR-ABL1* p190 and p210 fusion transcripts was performed as part of routine MRD detection on the UKALL14 trial. This was also performed to confirm p190 transcript expression in the NALM-6 IK6 and mRFP control cell lines. Both *GUS* and *ABL* were used as the housekeeping genes for *BCR-ABL* MRD. Housekeeping genes were used in order to normalise the fusion transcript level with the amount of input cells. Absolute quantification was performed by using a plasmid standard curve (Qiagen) expressing either *BCR-ABL1* or house-keeping genes. Primer and probe sequences for the quantification of the p190 transcript are as follows:

p190

Forward- 5'-CTGGCCCAACGATGGCGA-3'

Reverse- 5'-CACTCAGACCCTGAGGCTCAA-3'

Probe- 5'-[FAM]CCCTTCAGCGGCCAGTAGCATCTGA[TAMRA]-3'

GUS

Forward- 5'-GAAAATATGTGGTTGGAGAGCTCATT-3'

Reverse- 5'-CCGAGTGAAGATCCCCTTTTTA-3'

Probe- 5'-[FAM]CCAGCACTCTCGTCGGTGACTGTTCA[TAMRA]-3'

Quantification of the plasmid standard curves were performed in duplicate and follow-up cDNA was performed in triplicate. Prior to quantification the plasmids thawed on ice for two hours. For quantification using *GUS* as the house-keeping gene, each reaction included the following: 5.5µl dH$_2$O, 12.5µl TaqMan fast

mastermix (Thermofisher), 0.75µl of each of the 10µM forward and reverse primer (Merck), 0.5µl 5µM probe (Merck), 5µl cDNA template/dH$_2$O for the NTC. The Cycling conditions are the same as Ig/TCR quantification in **Table 2.2**. For quantification using *ABL* as the housekeeping gene, the Ipsogen BCR-ABL1 Mbcr Kit (CE) (Qiagen) was used according to manufacturers' instructions.

2.10   Lower limit of detection for Δ*IKZF1* PCR screen

DNA from the *IKZF1*Δ4-7 positive cell line SUPB-15, to serve as a positive control, was extracted using DNeasy mini kit (Qiagen) according to manufacturers' instructions. A standard curve was derived from the DNA by serial 1 in 10 dilutions in AE buffer, ranging from 10^{-1} to 10^{-8}. A PCR using primers (Venn et al., 2012) specific to Δ4-7 were used:

forward- 5'-TCTTAGAAGTCTGGAGTCTGTGAAGGT-3'

reverse- 5'-AGGAATAAAATGCAAATCACCTTGA-3'.

For each reaction, the following was added- 2µl 10x reaction buffer (Qiagen), 0.5µl 10mM dNTPs (Promega), 0.125µl HotStarTaq (Qiagen), 2.5µl 10mM forward and reverse primer, made up to a final volume of 20µl with 11.375µl dH$_2$O. The cycling conditions used are found in **Table 2.4**. PCR products were run on a 2% agarose gel for an hour at 150mV with hyperladder IV (Bioline) to confirm band size.

Table 2.4: Cycling conditions for Δ*IKZF1* PCR screening

Step	Cycling condition
1	95°C for 10 minutes
2	95°C for 50 seconds
3	58°C for 50 seconds
4	72°C for 50 seconds
5	Repeat steps 2-4 for 44 more times
6	72°C for 10 minutes
7	4°C forever

2.11 Δ*IKZF1* Screening

Of the 655 B-ALL patients recruited, 498 diagnostic DNA specimens were screened by end-point PCR for 4 common intergenic deletions (primers in **Table 2.5**) in *IKZF1* in a multiplex manner (**Table 2.6**). The instrument for all PCR reactions was a DYAD thermocycler. For each reaction, the following was added: 2µl 10x reaction buffer (Qiagen), 0.5µl 10mM dNTPs (Promega), 0.125µl HotStarTaq (Qiagen), 2.5µl each of the 10µM primers (**Table 2.5**), 1µl template/1µl dH$_2$O for the NTC, made up to a final volume of 20µl with 1.375µl dH$_2$O. Patient baseline characteristics were analysed to in order to identify any differences between the screened population and patient population as a whole. The primers were designed as close to the breakpoint cluster region as possible (Caye et al., 2013). Distance from the putative heptamer sequence in each of the 4 breakpoint regions can be seen in **Figure 2.1**.

Table 2.5: Primers used in Δ*IKZF1* PCR screen

	Location	Sequence
Forward Primers	Δ2a	5'-CAACAAGTGACCCATCCTTTG-3'
	Δ2b	5'-CACACACTTCAAGATTATGCATTT-3'
	Δ4	5'-TGTGAAGGTCACACCCTCTG-3'
	Albumin	5'-TGAAACATACGTTCCCAAAGAGTTT-3'
Reverse Primers	Δ7	5'-AAAGAACCCTCAGGCATTCA-3'
	Δ8	5'-GGGGACTGGAAGTCACAGAA-3'
	Albumin	5'-CTCTCCTTCTCAGAAAGTGTGCATAT-3'

Table 2.6: Multiplex screening Δ*IKZF1* PCR strategy

Well 1		Well 2	
Forward	Reverse	Forward	Reverse
Δ2a	Δ7	Δ2a	Δ8
Δ2b	-	Δ2b	-
Δ4	-	Δ4	-
Alb	Alb	Alb	Alb

Proximal intron 1
5'-GATGTAAAAG**CAACAAGTGACCCATCCTTTG**AAGCTTACAAGAAGAGAAACATTAATCTATTTCACGTCT
TGAAAACAGATCAGTTTTATTTTGCTCAAAAAGGGCACATGTACATTTTTGATCTAGGTCTTAGAAACGTAGAGTT
TCAGAGGATCAGCATTATA**CACACTG**TCACACACACA

Proximal intron 3
5'-ATTAAAATAT**TCTTAGAAGTCTGGAGTCTGTGAAGGT**CACACCCTCTGGTCTTCTCCCAGCCCATAGGG
TATAAATAATCTGAATTGACGGCATCCAGGGATCTCAGAAATTATTAGTACATCC**CACAGTG**AATTACCACCTTACT
A-3'

Distal Intron 7
5'-TGTTGAATGT**TGCTGTG**GAAACATCAAGTCTAGTGTAACTGTTTCTTCT**TCAAGGTGATTTGCATTTTATTC
CT**GAATG-3'

Distal 3' UTR
5'-AGCAGG**CACACTG**GTCCCTTTCAAGGTGTGGGCTGACATGCTGGCTCTCTTCCCTGTATGCCGAGACATG
CTTGGGATCTCCTAGCTCCACACTCTGTCTCTCATGAGTCTGAGCCCTTTGGGT**TTCTGTGACTTCCAGTCCCC**
TCCTGCCAGT-3'

TTCTGTGACT   -Primer sequence
CACACTG   -Heptamer sequence

Figure 2.1: Common breakpoint cluster regions in *IKZF1*. The four breakpoints involved in the deletions detected by Δ*IKZF1* PCR screen. The heptamer sequence is highlighted in blue, the primer sites are highlighted in red.

The albumin housekeeping gene was amplified as an internal control. DNA from the cell line SUP-B15 was used as a positive control. All PCR products were analysed on a 10% polyacrylamide gel to ensure a high band resolution. Cycling conditions for the PCR are found in **Table 2.4**. All PCR products were purified using Illustra ExoProStar (GE Healthcare) to remove unincorporated primers and dNTPs. Briefly, 0.5µl of ExoProstar was added to 5µl PCR product and incubated at 37°C for 15 minutes, and then 80°C for 15 minutes to stop the reaction. PCR products were diluted 1/100 in dH$_2$O prior to sequencing. Sanger sequencing was performed by Eurofins Genomics and analysed using Seqman Lasergene software (DNASTAR).

2.12 MLPA validation and *IKZF1*^plus profile

Where extra material was available, patients were also screened for *IKZF1* deletions using MLPA as a way of validating the PCR results. This was possible in 420 of the 498 (84%) patients that were screened by PCR. The P335-ALL-IKZF1 kit (MRC Holland) was used according to manufacturers' instructions. This kit was chosen based on its full coverage of *IKZF1,* with a specific probe to each

exon. The details of other genes also screened for in this kit are found in **Table 2.7**.

Table 2.7: Genes covered in the P335-ALL-IKZF1 kit

Gene	Location	Definition
EBF1	Chr5q33.3	Transcriptional activator involved in B-cell differentiation
JAK2	Chr9p24.1	Tyrosine kinase
CDKN2A/B	Chr9p21.3	Can induce cell cycle arrest in G1 and G2. Tumour suppressor
PAX5	Chr9p13.2	Transcription factor expressed during early B-cell differentiation
ETV6	Chr12p13.2	Transcription factor required for haematopoiesis
BTG1	Chr12q21.33	Regulates cell growth and proliferation
RB1	Chr13q14.2	Tumour suppressor. Maintains chromatin structure
PAR1 region	ChXp22.33	Pseudoautosomal region on the X chromosome. The P2RY8-CRLF2 fusion gene results in the over-expression of CRLF2, which activates JAK-STAT pathways.

Screening with this kit also allows for the detection of patients defined by the *IKZF1*[plus] which is described as any *IKZF1* lesion as well as a deletion in any of the following: *CDKN2A, CDKN2B, PAX5,* PAR1 region, in the absence of an *ERG* deletion (Stanulla et al., 2018). *ERG* deletions were only screened in 21 patients using the P327-iAMP21-ERG kit, and so the *IKZF1*[plus] profile described as "probable" in patients where this was not possible. All *IKZF1*[plus] analysis was performed with the MLPA data only. All MLPA assays were prepared in the collaborating laboratory of Anthony Moorman at the Northern Institute for Cancer Research, Newcastle University and analysed by DBS Genomics, Durham university.

2.13   MRD assessment

A similar approach was used to determine MRD by *IKZF1* breakpoint quantification in order to perform a comparison of MRD levels in patients between *IKZF1* and Ig/TCR MRD quantification (van der Velden et al., 2007). A universal forward primer and TaqMan probe was designed in intron 3 proximal to the breakpoint in *IKZF1* and a patient specific primer was designed over the

breakpoint (**Figure 2.2**). Patient 14-1-332 was used for the design of the primer and probe set due to the presence of the largest deletion of intron 3 in this cohort. The primer and probe set were designed in this way to ensure both sites were intact in all patients. The forward primer and probe sequences are as follows:

Forward primer- 5'-GTCACACCCTCTGGTCTTCTCC-3'

Probe- FAM-CAGGCCCATAGGGTATAAATAATCTGAATTGACGGC-TAMRA
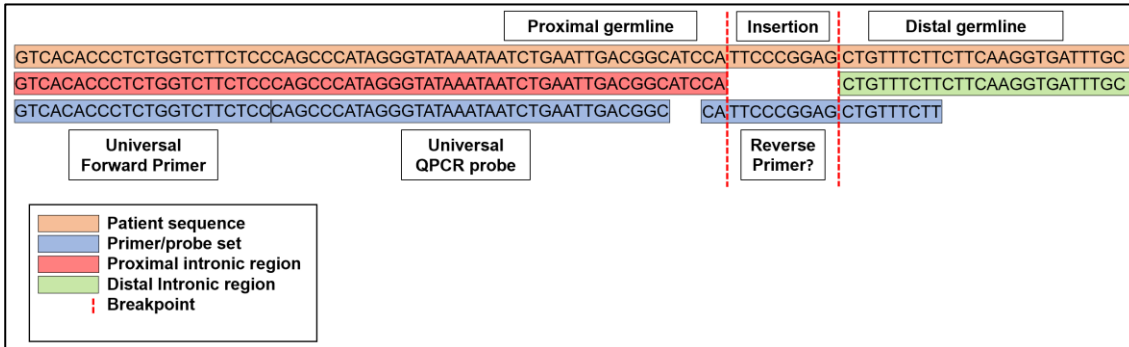
Figure 2.2: Δ*IKZF1* 4-7 RT-qPCR assay design. A universal primer and probe were designed proximal to the breakpoint, and a reverse primer unique to the patient was designed over the breakpoint.

Initial "limited testing" was performed to identify the correct annealing temperature for the patient specific primers, and also the QR. *IKZF1* MRD was performed in for 43 follow up samples in 12 patients. Details of the Ig/TCR markers used for MRD quantitation can be found in **Table 2.8**. The patients used for this were chosen due to the nature of the sequences, i.e. the unique primers designed were optimal for RT-qPCR. All follow up samples were run in triplicate where there was an adequate volume of DNA and in duplicate for samples where there was limited material. For each reaction, the following was added- 12µl TaqMan Fast Mastermix (Thermofisher), 2.5µl 0.4% bovine serum albumin, 2.25µl 10µM forward primer, 2.25µl 10µM reverse primer (Merck), 0.5µl 5µM TaqMan probe (Merck), 5µl DNA/dH$_2$O for the NTC.

Table 2.8: IKZF1 and Ig/TCR MRD RT-qPCR assay details

Patient ID	*IKZF1* QR	*IKZF1* Unique primer sequence (5'-3')*	Ig/TCR QR	Ig/TCR marker used
14-1-135	1e-04	AGACTTGATGTTTCGAGGTGTA	1e-04	IgH complete TCRδ
14-1-206	5e-04	CAGTTACACTAGACTTGGCGTACT	5e-04	IgH complete TCRβ
14-1-222	1e-04	GACTTGATGTCCTTGGGGGT	1e-04	IgH complete TCRγ
14-1-278	1e-04	TTGATGTTTCAAGGCAATTTCT	1e-04	IgH complete TCRγ
14-1-294	1e-04	CACTAGACTTGATGTTTCGGTGTA	1e-04	Igκ
14-1-306	1e-04	ACACTAGACTTGATGTTGGGAAT	1e-04	IgH complete
14-1-431	1e-04	ACAGTTACACTAGACTTGAGGTACT	1e-04	IgH complete TCRγ
14-1-456	1e-04	CTAGACTTGATGTTCGGATGTA	1e-04	TCRγ
14-1-473	1e-05	CTAGACTTGATGTTTCGATGTACT	1e-04	IgH complete TCRγ
14-1-595	5e-04	CACTAGACTTGATGTTTAAGGTACTAAT	1e-04	TCRβ TCRγ
14-1-606	5e-04	GACTTGATGTTTCGGGTGTACT	1e-04	IgH complete TCRδ-Jα
14-1-618	1e-03	AGACTTGATGTCCCTGATGTACT	1e-04	TCRγ TCRγ

*inserted nucleotides underlined

The results of the *IKZF1* and Ig/TCR MRD were log transformed to enable comparison. Where more than one Ig/TCR rearrangement was tested, the assay with the highest positivity was used for the comparison with *IKZF1* MRD quantification as this is what is used for reporting follow-up results. All MRD results were interpreted using EuroMRD guidelines, and using the reporting system for the UKALL14 trial (**Table 2.9**).

Table 2.9: Definitions of MRD results reported on UKALL14

MRD result	Definition
Negative	No MRD detectable with a quantitative range of 10^{-4}
Positive	MRD detectable and quantifiable
Positive out of the quantitative range (POQR)	MRD detectable but value falls out of quantitative range
Indeterminate	MRD not detected by quantitative range did not reach 10^{-4}

2.14   Generation of Dominant Negative NALM-6 Δ*IKZF1* model

The Murine Stem Cell Virus (MSCV)-IK6- Internal Ribosome Entry Site (IRES)-monomer Red Fluorescent Protein (mRFP), MSCV-IK6-IRES-mRFP retroviral vector (MSCV IK6) Plasmid was a kind gift to our lab from Charles Mullighan of St Jude's Childrens Research Hospital, TN, USA. The plasmid was cloned using NEB 10-beta *E. coli* (High efficiency) (New England Biolabs) according to manufacturers' instructions. The transformed bacteria were spread onto 2x TY agar containing 100µg/mL of ampicillin and incubated overnight. Single colonies were picked and cultured in 2xTY broth containing 50µg/mL ampicillin for four hours at 37°C, to allow selection of the correct plasmid, and shaken vigorously. Plasmids were isolated from the bacteria using a QIAprep® Spin Miniprep Kit (Qiagen) according to manufacturers' instructions. A plasmid that did not contain the IK6 cDNA sequence was generated (MSCV empty vector [EV]) in the lab previously to serve as a control and cloned as for the MSCV IK6 plasmid.

SD-1 and NALM-6 cell lines were retrovirally transduced with either the MSCV IK6 or the MSCV EV retroviral vector with the packaging cell line Phoenix™-AMPHO. The NALM-6 cell line had previously been transduced. SD-1 cells were transduced in a similar manner as follows:

Day1

Phoenix™-AMPHO cells were cultured in DMEM 10% FBS, 1% L-Glutamine, 1% penicillin and streptomycin until the cells became 60-80% confluent. Phoenix™-AMPHO cells were then harvested by trypsinisation, washed, and counted. $2*10^6$ cells in 10ml DMEM were incubated in 10cm culture dishes overnight.

Day 2

A transfection mix was prepared, 1 per 10cm plate:

    Solution A:

        10 µL fuGENE® (Promega)

        150 µL Opti-MEM® (Thermo Scientific)

Solution B:

    1.5 µg pCL-ampho rerovirus packaging vector (Imgenex)

    2.6 µg of either MSCV IK6 or MSCV EV

Solution A was added to solution B, mixed by gentle pipetting and incubated at room temperature for 15-20 minutes. Media from the Phoenix™-AMPHO plates was gently removed, the transfection solution added in a dropwise manner to the cell layer and fresh media re-applied carefully. The cells were incubated at 37°C overnight.

Day 3

Supernatant was removed and fresh media added to the plates.

Day 4

6 well culture dishes were treated with 2ml/well of 30ng/mL RetroNectin® (TaKaRa Biosciences) and incubated at room temperature for 2-3 hours. The RetroNectin® was removed and wells were blocked with 2mL filter sterilised 2% BSA and incubated for a further 30 minutes at room temperature. The BSA was removed and wells were washed with 3mL phosphate buffered saline (PBS) twice. $2.5*10^6$ SD-1 cells in 2.5mL were added to each well and incubated at 37°C for 30 minutes. The viral supernatant from the Phoenix™-AMPHO cells was removed from the plate, spun to remove any cell debris and added to the SD-1 cells.

Day 5

Viral supernatant was removed from each well and replaced with 5mL/well of RPMI 1640 10% FBS, 1% L-glutamine, 1% penicillin/streptomycin. The cells were incubated at 37°C for 3 days before mRFP expression was confirmed by flow cytometry. The cells were sorted for mRFP expression, and the population enriched until a positivity of >95% was achieved. As the SD-1 cell line was not an appropriate *BCR-ABL1*+ model, the NALM-6 cell lines successfully transduced with either IK6 or mRFP control were subsequently transduced with either MSCV 2.2 Mig p190 (Mig 185) GFP plasmid, a gift from Warren Pear lab (Addgene

plasmid #27483), or the MSCV 2.2 backbone control, a gift from Russell Vance (Addgene plasmid #60206). In total four NALM-6 modified cell lines were generated- IK6 p190, IK6 GFP, RFP p190, and RFP GFP and p190 expression by RT-PCR and subsequent RT-qPCR using Ipsogen BCR-ABL plasmid standards (Qiagen).

2.15   Generation of Δ*IKZF1* Loss of Function NALM-6 model

The guide RNA (IK20) used for the knockout of *IKZF1* exon 8 has previously shown to successfully knockout *IKZF1* ex8 (Fedele et al., 2018), the sequence and position of IK20 is shown in **Figure 2.3**. The IK20 guide RNA and Alt-R® ATTO 550™ tracrRNAs were re-suspended in nuclease free buffer (Integrated DNA Technologies, USA) and made up to a concentration of 10nmol and 20nmol respectively from a 200µM stock. The guideRNA:tracrRNA duplex was made by combining 10µL each of guideRNA and tracRNA and incubated at 95°C for 5 minutes, then cooled to room temperature. The ribonucleoprotein (RNP) complex was made as follows-

crRNA:tracrRNA duplex: 3.9µl

Recombinant CRISPR Cas9: 5.1µl

PBS: 6µl
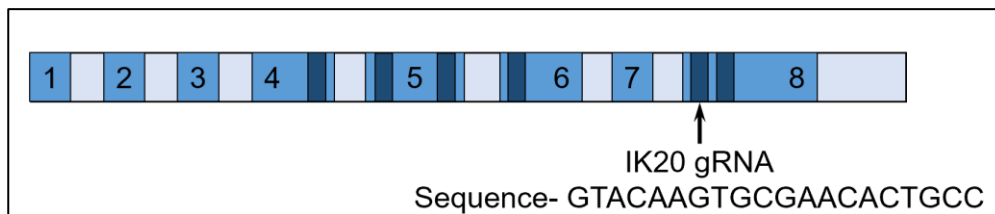
Figure 2.3: Position and sequence of the IK20 guide RNA. *IKZF1* gene showing exons (numbered) and zinc fingers in dark blue. The arrow indicates the region of *IKZF1* that the gRNA IK20 targets.

The RNP complex was incubated at room temperature for 20 minutes. While the RNP complex was incubating, $2*10^6$ NALM-6 cells were spun at 400g for 10 minutes. The supernatant was removed, and cells were washed in 5mL PBS a further 2 times to remove any RNase present in the medium. The pellet was resuspended in 60µL Ingenio® nucleofection solution (Mirus). The RNP complex was added to the cells with 3µl of 2nmol enhancer oligo (Integrated DNA technologies). The cell suspension was then electroporated in a cuvette (Mirus)

using the setting C-05 (Chicaybam et al., 2017). The cell suspension was transferred from the cuvette to 2mL pre-warmed penicillin/streptomycin free RPMI media and incubated overnight in a 12 well plate at 37°C.

To achieve accurate screening for the successful knockout of *IKZF1* ex8, the cells were single cell sorted into 10 96 well plates. Prior to sorting the electroporated cells were removed from the 12 well plate and spun at 400g for 5 minutes to remove media, and washed with 5mL PBS. The cells were stained with the TO-PRO-3™ (Thermo Scientific) viability dye and incubated for 15 minutes at room temperature. Since the tracrRNA was tagged with the ATTO550 fluorophore, it was possible to select cells based on their positivity for this. Non-electroporated cells stained with the TO-PRO-3™ viability dye served as a control. Cells were sorted into a mixture of fresh and conditioned media at a ratio of 1:1 and incubated until cells had visibly grown out. Initial attempts failed as the NALM-6 cell line required neighbouring cells present in the media for growth, and so conditioned media was required.

The wells that had successfully grown out from single cells were transferred to fresh 96 well plates, and the first 36 screened by PCR (same programme as seen in **Table 2.4**) for successful disruption of exon 8. Direct DNA extraction was performed from 50µL of each cell culture with QuickExtract™ DNA extraction solution (Lucigen) according to manufacturers' instructions. The PCR primers were first validated on normal healthy controls obtained from buffy coat. The primers sequences are:

IK20 forward- 5'-GGAGAACCTGCTGCTCT-3'

IK20 reverse- 5'-GCACATGTTGCACTCAAAAG-3'

All PCR products were run on a 10% polyacrylamide gel. Two clones, A4 and A8 were grown out and used for subsequent experimentation.

2.16   Drug Sensitivity by MTS assay

2.16.1 Monoculture

Cell viability was determined by MTS tetrazolium assay (Promega, UK). An initial serial dilution of NALM-6 cells was performed to identify the optimal number. NALM-6 cells were washed in PBS, counted and diluted with 10% FBS RPMI 1640 to make a range of concentrations from $5*10^4$ to $5*10^5$ per ml. 100µl of each concentration was added to a 96 well plate in triplicate and incubated with 20µl MTS solution for 3-4 hours at 37°C and read on a FLUOstar Omega microplate reader at an absorbance of 490nm.

Sensitivity was performed for four drugs routinely used in the treatment of ALL, and on UKALL14 (**Table 2.10**). At 0 hours, for each drug at each concentration, $1*10^5$ cells in 100µL RPMI 1640+ drug was added to a well of a 96 well plate in triplicate. Data was recorded at 24 hours, 48 hours and 72 hours of exposure and a non-drug control was also included. At each time point, 20µL of MTS solution was added to each well and incubated at 37°C for 3-4 hours. Data was recorded using FLUOstar Omega microplate reader at an absorbance of 490nm. The drug concentrations used are in **Table 2.11**.

Table 2.10: Drugs used for sensitivity assays

Drug	Mechanism or action
Daunorubicin	Forms complexes with DNA, inhibits topoisomerase II
Vincristine	Inhibits microtubule formation in the mitotic spindle. Leads to mitotic arrest and cell death
Cytarabine	Causes DNA damage by incorporation. Primarily kills cells in S phase
Dexamethasone	Steroid- glucocorticoid agonist

Table 2.11: The range of concentrations used for each drug

	Daunorubicin (nM)	Vincristine (nM)	Cytarabine (nM)	Dexamethasone (nM)
1	1000	1000	2000	2000
2	100	100	500	500
3	10	10	100	100
4	1	1	10	10

2.16.2 Co-culture

Prior to performing co-culture MTS assays, HS27a cells were assessed for sensitivity to dexamethasone at the concentrations used for the monoculture experiments (**Table 2.11**). For co-culture assays, HS27a cells were plated 24h prior to adding the ALL cells and performed as described above for three conditions- HS27a alone, HS27a and ALL cell co-culture, and ALL cells alone. This was performed for NALM-6 IK6 and EV cells only, and only dexamethasone was assessed. The ALL cells alone were to act as a control for the efficacy of dexamethasone in culture. Assessing the HS27a cells alone allowed for the mean absorbance value to be subtracted from the absorbance of the co-culture equivalent in order to identify the activity that was due to the ALL cells alone.

2.17   Drug Sensitivity assessment by Flow Cytometry

As the MTS assays were not a suitable method for co-culture drug sensitivity assays, flow cytometry was used as an alternative. $1*10^5$ HS27a cells were allowed to adhere in 6 well plates overnight in 2mL RPMI 1640 media. $4*10^5$ ALL cells in 2mL media were added 24h later along with dexamethasone at a concentration of 500nm, see **Table 2.12** for a summary of the conditions tested. At each time point, the ALL cells were removed from the plates and washed with 4mL PBS before being transferred to a FACS tube. For the co-culture wells, ALL cells were removed from the plates, 1mL trypsin was added and plates were incubated for two minutes at 37°C. HS27a cells were then added to the corresponding ALL cells prior to the wash with PBS. This was to ensure that any ALL cells that remained attached to the MSC layer were not missed. Once the PBS was removed, the cell pellets were resuspended in 490μL PBS with and

10μL DAPI at a concentration of 0.5μg/mL. RFP expression was used to identify the ALL cells and were analysed on a Fortessa™ X20 (BD Biosciences). Cells incubated at 60°C for 15 minutes were used as a positive control for the DAPI viability stain.

Table 2.12: The conditions tested in flow cytometry drug sensitivity assays

Cell line	Culture Type	+/-Dex
IK6 p190	Co-culture	+
		-
	Monoculture	+
		-
IK6 GFP	Co-culture	+
		-
	Monoculture	+
		-
RFP p190	Co-culture	+
		-
	Monoculture	+
		-
RFP GFP	Co-culture	+
		-
	Monoculture	+
		-

2.18 *IKZF1* Breakpoint and Ig/TCR rearrangement analysis

As a way of assessing the differences in RAG activity between *BCR-ABL1*+ versus *BCR-ABL1*- B-ALL patients, the number of nucleotides deleted relative to the putative heptamer in the proximal and distal breakpoints were counted in *IKZF1* deleted patients. All breakpoints were analysed with the exception of 5 due to poor sequence quality.

The number and type of Ig/TCR rearrangements in *BCR-ABL1+* patients were compared to *BCR-ABL1-* patients. This was to identify any differences in the proportion of different rearrangements present in these patients, as it may indicate a different stage of developmental arrest. A positive Ig/TCR rearrangement was defined as one that could be sequenced, as a number of faint bands appear on the acrylamide gels but are not strong enough to be sequenced, so it is not clear if these are genuine rearrangements or non-specific amplification. Patients were screened with a primer panel developed by the UK MRD Laboratory Network and EuroMRD (Pongers-Willemse et al., 1999). A total of 160 patients were included in this analysis, 55 *BCR-ABL1+* and 105 *BCR-ABL1-* patients.

2.19   Statistical Analyses

For drug sensitivity assays, data was analysed using the software package GraphPad Prism. An unpaired t test was used for the differences in the number of Ig/TCR rearrangements as the data followed a normal distribution when plotted on a histogram for both *BCR-ABL1+* versus *BCR-ABL1-* and also when separated based on *IKZF1* deletion status. To test if the number of Ig/TCR rearrangements differed depending on *IKZF1* deletion status, Fisher's exact test was used. The Wilcoxon-Mann-Whitney test was used to assess the differences in *IKZF1* deleted patients based on *BCR-ABL1* status.

For both MLPA and *IKZF1* screening, Event Free Survival (EFS) and Overall Survival (OS) were used as for outcome in a univariable analysis. EFS and OS times were calculated from the date of randomisation until the date of the first event (relapse and death for EFS or death for OS) with patients not experiencing event censored at the date last seen. Comparisons between groups were made using Chi-squared or Fisher's exact tests (discrete variables), Wilcoxon Mann-Whitney tests (continuous variables) or Cox regression and the log-rank test (time to event variables). The assumption of proportional hazards was tested using the Schoenfeld residuals. Analyses were performed using STATA version 15.1 (STATACorp, Texas) All outcome analysis and baseline characteristics were analysed by Amy Kirkwood at UCL Cancer Trial Centre.

3 *IKZF1* lesions do not contribute to poor outcome in patients with B-ALL, regardless of other cooperating lesions

3.1 Introduction

3.1.1 Differential impact of Δ*IKZF1* on trial populations

The treatment of paediatric patients with ALL has been incredibly successful, with cure rates exceeding 80%, and in certain subtypes cure rates of 98% have been achieved (Gaynon et al., 2010). This is not the case for adult ALL, which has a markedly higher rate of relapse and death despite a significant number of patients achieving a complete remission after induction therapy (Pulte et al., 2014, Sive et al., 2012). A large proportion of these patients will have been classified as standard risk by traditional cytogenetics and baseline characteristics such as age and presenting white cell count. Therefore, there is a need to refine risk stratification through the identification of other poor risk markers that are not currently assessed in routine diagnostic laboratories.

There have been numerous reports on the impact of Δ*IKZF1* on outcome in both adult and paediatric trial populations. A study on high risk paediatric patients found that Δ*IKZF1* was a strong predictor of poor outcome and was further validated on a reference cohort (Mullighan et al., 2009). Patients with ALL positive for Δ*IKZF1* were more likely to exhibit a gene expression profile similar to that of *BCR-ABL1+* ALL, with activated kinase pathways now known to be "Philadelphia like" ALL. More recently, Δ*IKZF1* was only found to refine risk stratification in patients with high risk disease and not standard risk disease, which is arguably where a refinement of risk stratification is needed most (Palmi et al., 2013).

The functional effect of different focal deletions also has a differential effect on outcome. In one study on *BCR-ABL1-* ALL, loss of function *IKZF1* lesions found in 56 (12%) patients had a negative impact on outcome (overall survival at 5 years 28% vs 59%) (Kobitzsch et al., 2017). Dominant negative deletions, found in 50 patients, did not have a prognostic impact in this trial cohort. This is an unexpected result, as DN deletions would be anticipated to be more deleterious

than LOF deletions in terms of effect on phenotype. The DN IK6 isoform, produced by a deletion of exons 4-7, should be more deleterious than an LOF deletion as it cannot bind DNA itself and also renders WT IKAROS non-functional as it is still capable of dimerising. Interestingly, a small number of patients harboured both types of deletion (22 patients, 5%) whose outcome was comparable to the LOF only deleted patients. It is worth noting that only patients with an LOF deletion in a major leukaemic clone had a poorer outcome and that patients where $\Delta IKZF1$ resided in a small fraction of leukaemic cells did not.

A recent study from the German ALL group showed that $\Delta IKZF1$ did not significantly impact outcome in patients with *BCR-ABL1*+ ALL undergoing allogeneic bone marrow transplant, without the occurrence of other lesions; *CDKN2A* lesions were instead found as the strongest predictor of poor outcome in a univariate analysis for overall survival (p=0.023), disease-free survival (p=0.012), and remission duration (p=0.036) and this trend was retained in multivariate analysis (Pfeifer et al., 2018). By contrast, the French cooperative ALL group found such a strong impact of $\Delta IKZF1$ on the GRAALL 2003 and 2005 trials on outcome, that they adopted *IKZF1* status for individual treatment stratification (Beldjord et al., 2014) on their subsequent trial. The outcome of this strategy is not yet known. Based on these studies, it is becoming increasingly clear that there is no consensus on the prognostic impact of $\Delta IKZF1$.

3.1.2   *IKZF1*^{plus} Profile

There is accumulating evidence that the impact of $\Delta IKZF1$ is dependent on other co-operating lesions present (Clappier et al., 2014, Scheijen et al., 2017). Stanulla and colleagues developed a profile that identified patients with very poor outcome, termed *IKZF1*^{plus}. The PCR-based technique MLPA was used to screen specimens from 991 paediatric patients for lesions in *IKZF1* along with *PAX5, ETV6, RB1, BTG1, EBF1, CDKN2A, CDKN2B*, and the PAR1 region (*CRLF2, CSF2RA* and *IL3RA*). Not all the deletions screened for contributed to poorer outcome when they co-occurred with $\Delta IKZF1$; deletions of *ETV6, RB1, BTG1,* and *EBF1* did not have a significant influence on outcome.

Interestingly, *ERG* deletions seem to attenuate the negative impact on *IKZF1* deleted paediatric patients. A French study showed that despite Δ*IKZF1* 4-7 frequently co-occurring with *ERG* deletions, patients typically had a very good outcome (Clappier et al., 2014). It is worth noting that ERG deletions exclusively co-occur with the IGH-DUX4 rearrangement and are often associated with *IKZF1* deletions (Yasuda et al., 2016, Zhang et al., 2016)

ERG deletions were also taken into consideration when developing the *IKZF1*^{plus} profile. Unlike the French study, Stanulla and colleagues found *ERG* deletions were rare in high risk patients with Δ*IKZF1* and a lesion in the other genes found to contribute to a poorer outcome, though these patients did not experience a relapse. *ERG* deleted patients were subsequently excluded from the *IKZF1*^{plus} profile. Thus, the *IKZF1*^{plus} profile is defined as patients with an *IKZF1* deletion and at least one additional deletion in *PAX5*, *CDKN2A*, *CDKN2B*, or a PAR1 rearrangement, but in the absence of an *ERG* deletion.

More recently, *IKZF1*^{plus} has been identified by RNA sequencing and aCGH (Schieck et al., 2020). aCGH also revealed other high-risk lesions that would have otherwise been missed and patients would have remained in the B-other category and presumed standard risk. It is worth noting that outcome analysis was not performed in this study, presumably due to the size of the cohort (Schieck et al., 2020).

A recent report from the Dutch Children's Oncology Group found that *IKZF1*^{plus} predicted poor outcome in paediatric patients in the DCOG-ALL10 cohort and was associated with drug resistance (Steeghs et al., 2019). It was suggested that this was caused by an over-representation of *BCR-ABL1* like subtypes within this profile, and therefore the prognostic value of *IKZF1*^{plus} was linked to subtype related drug resistance. These studies have shown that *IKZF1*^{plus} is easily screened for, and may play a major role in risk stratifying patients in the future.

3.1.3 *IKZF1* as an MRD marker in ALL

The real time PCR quantification of clonal immunoglobulin and T-cell receptor gene loci (Ig/TCR) has long been the gold standard for the detection of MRD in ALL. Ig/TCR markers are not pathogenic themselves but are a unique genetic "fingerprint" of malignant clonal cells. Although this is the gold standard for MRD quantification, there are some limitations to using Ig/TCR as an MRD marker. Ig/TCR markers are susceptible to ongoing clonal evolution, such that patient specific oligonucleotides designed are no longer able to anneal and give false negative results. Additionally, finding suitable markers in adult patients is a challenge, especially in older adults as seen in patients monitored by the national MRD laboratory for adult ALL in the UK. The median age for patients without a marker was 48 (95% CI ±2.03) whereas the median age for those with a useable marker was 42 (95% CI ±0.98, p=0.003) (Alapi et al., 2018). *IKZF1* lesions may provide an opportunity to monitor ALL patients by a marker associated with leukaemic transformation, unlike Ig/TCR.

There are two approaches to designing an MRD assay of Δ*IKZF1* based primer location. The primer and probe set could be 'patient specific' by generating one of the primers with the ability to anneal to the unique breakpoint present in *IKZF1*. This would be similar in principle to Ig/TCR MRD and would allow for all breakpoints to be used as an MRD assay, i.e. even patient sequences with atypical breakpoints could have a specific assay designed. However, it is not clear that Δ*IKZF1* is vulnerable to clonal evolution in the same way as Ig/TCR markers. Another approach to assay design would be to produce a primer and probe set that is specific to the germline *IKZF1* sequence immediately proximal and distal to the breakpoint. This would be less time consuming as Sanger sequencing for the breakpoint would not be necessary but may exclude some patients as they harbour non-typical breakpoints.

Δ*IKZF1* has previously been assessed for its suitability as a marker with promising results (Caye et al., 2013, Venn et al., 2012) but only for Δ*IKZF1* 4-7 lesions which are the most common focal deletion. The correlation between Ig/TCR MRD and Δ*IKZF1* MRD was strong in both studies (Caye et al.,

R^2=0.9232, Venn et al., R^2=0.985), suggesting that the Ig/TCR markers likely reside in the same clone as $\Delta IKZF1$.

Quantification of the *BCR-ABL1* fusion transcript is another method of monitoring MRD, recently standardised for the p190 transcript by EuroMRD (Pfeifer et al., 2019). Quantification by this method should also be taken into account, it was recently found that *BCR-ABL1* MRD did not correlate with Ig/TCR MRD in a subset of paediatric patients. In 20% of patients, the *BCR-ABL1* MRD was significantly higher than the Ig/TCR MRD levels by more than a log (Hovorkova et al., 2017). The cells from these patients were flow sorted, which revealed that the *BCR-ABL* fusion protein was present in non-B-ALL cells such as granulocytes and myeloid cell. Hovorkova and colleagues concluded that these patients' disease had a "CML like" biology and not the original diagnosis of B-ALL. It remains unclear how $\Delta IKZF1$ correlates with *BCR-ABL1* MRD quantification.

3.1.4   UKALL14 Trial

UKALL14 is a phase 3 clinical trial that recruited 655 B-ALL patients aged between 25 and 60 from December 2010 to July 2018. The trial protocol was based on a previous UKALLXII trial with some modifications and asked a number of questions. The only question of relevance to this thesis is:

- Does the addition of the anti CD20 monoclonal antibody Rituximab to standard induction chemotherapy improve EFS?

UKALL14 stratified patients according to baseline and treatment-related risk factors which are of relevance to this chapter because they are elements on which pre-determined subgroup analyses were planned. The high-risk factors for UKALL14 are summarised in **Table 3.1**.

Table 3.1: Summary of high-risk classifiers on UKALL14

Risk stratification factor for B-ALL	High risk
White blood cell count	A presenting count of $\geq 30 \times 10^9$/L
Age	Patients aged over 40 at diagnosis
Cytogenetic subgroups	• Philadelphia chromosome (t9;22)(q34;q11) • MLL-AF4 (now *KMT2A-AFF1*) (t4;11)(q21;q23) • Low hypodiploidy/near triploidy (HoTr) • Complex karyotype- five or more chromosomal abnormalities in the absence of an established translocation
MRD	Any residual MRD at the end of the second induction treatment block

3.1.5 Approach in this chapter

The approach I took was to develop and validate a PCR-based assay for screening of patients for the four most common *IKZF1* lesions found in ALL and to compare it with MLPA in order to determine the prognostic relevance of these lesions in this treatment setting and the optimal screening process. The MLPA will also make it possible to identify *IKZF1*^plus patients and analyse their outcome. Finally, I developed an RT-qPCR MRD assay based on the breakpoints in *IKZF1* deleted patients from the sequencing data obtained from the PCR screening. I was able to assess its suitability as an MRD assay by quantifying follow-up specimens taken throughout the timecourse of treatment to allow for correlation between *IKZF1* MRD and Ig/TCR MRD.

3.2 Hypothesis

Δ*IKZF1* contributes to poor survival outcomes in adult ALL patients

3.2.1 Aims

- To compare PCR and MLPA for screening of *IKZF1* status
- To describe the *IKZF1* deletion status of a large patient group taking part in a national clinical trial UKALL14
- To determine the prognostic relevance of *IKZF1* and *IKZF1*^plus status in patients with B-ALL treated on UKALL14
- To determine the suitability and stability of Δ*IKZF1* as a marker for monitoring MRD over the timecourse of treatment

3.3   Methods

3.3.1 Outcome analysis

3.3.1.1   UKALL14 protocol amendment

The UKALL14 treatment protocol changed in April 2012 due to a high level of toxicity caused by pegylated asparaginase (Patel et al., 2017). Ninety-one patients enrolled between December 2010 and April 2012. This has been taken into account in multivariable analyses. Patients treated on UKALL14 prior to a protocol change which was mandated by an excess of deaths in the *BCR-ABL1+* arm were excluded from the analysis because the high rate death in *BCR-ABL1+* population would lead to bias as *IKZF1* is more common in *BCR-ABL1+* ALL.

3.3.1.2   ECOG scores

Eastern Cooperative Oncology Group (ECOG) performance status was developed to encourage standardisation when conducting clinical trials and allowing for more consistency (Oken et al., 1982). ECOG scores, ranging from 1-5, were included in baseline characteristics and in univariable and multivariable analyses. ECOG scores of 2 and 3 have been grouped in the analyses. **Table 3.2** summarises ECOG performance status.

Table 3.2: ECOG classifier definitions

Grade	Performance status
0	Fully active, able to carry out all pre-disease performance without restriction
1	Restricted in physically strenuous activity but Ambulatory and able to carry out work of a light sedentary nature
2	Ambulatory and capable of all self-care but Unable to carry out work activities. Up and about for >50% waking hours
3	Capable of only limited self-care, confined to bed for >50% of waking hours
4	Completely disabled. Cannot carry out self-care. Totally confined to bed/chair
5	Dead

3.3.1.3   Refined paediatric genetic risk group

Risk status on UKALL14 classified patients as either "standard risk" or "high risk". More recently, there has been analyses in paediatric trial populations that stratifies patients based on their cytogenetics into good risk, intermediate risk, and poor risk groups. This additional analysis has also been applied.

The refined cytogenetic risk group was developed (Moorman et al., 2014) and validated (Hamadeh et al., 2019) in paediatric patients. **Table 3.3** summarises the genetic lesions in each group. *BCR-ABL1* was analysed as a separate group.

Table 3.3: Refined cytogenetic risk groups

Group	Definition
Good Risk (CYTO-GR)	• High hyperdiploidy • *ETV6-RUNX1* • *ZNF384* fusions
Intermediate Risk (CYTO-IR)	• B-other
Poor Risk (CYTO-PR)	• *KMT2A* fusions • Low hypodiploidy/ near haploidy • Complex karyotype • *JAK-STAT* abnormalities (*IGH-CRLF2*, *P2RY8-CRLF2*, and *JAK2* fusions) • iAMP2 • *BCR-ABL1*

3.4   Results

3.4.1   *IKZF1* Screening

Δ*IKZF1* screening by PCR was performed in a multiplex manner to make screening fast, but was done in two different reactions to allow for Sanger sequencing to be carried out more easily (**Figure 3.1A**). Patient specimens with *IKZF1* lesions of known sizes were used to validate this approach (**Figure 3.1B**). The lower limit of detection of the PCR assay was determined as 10^{-4} by serial 10-fold dilutions of the *IKZF1* Δ4-7 positive cell line SUP-B15 (**Figure 3.2**). Cell line material harbouring the other deletions (Δ2-8, Δ4-8, Δ2-7) which were

screened was not available and hence could not be assessed for the lower limit of detection.
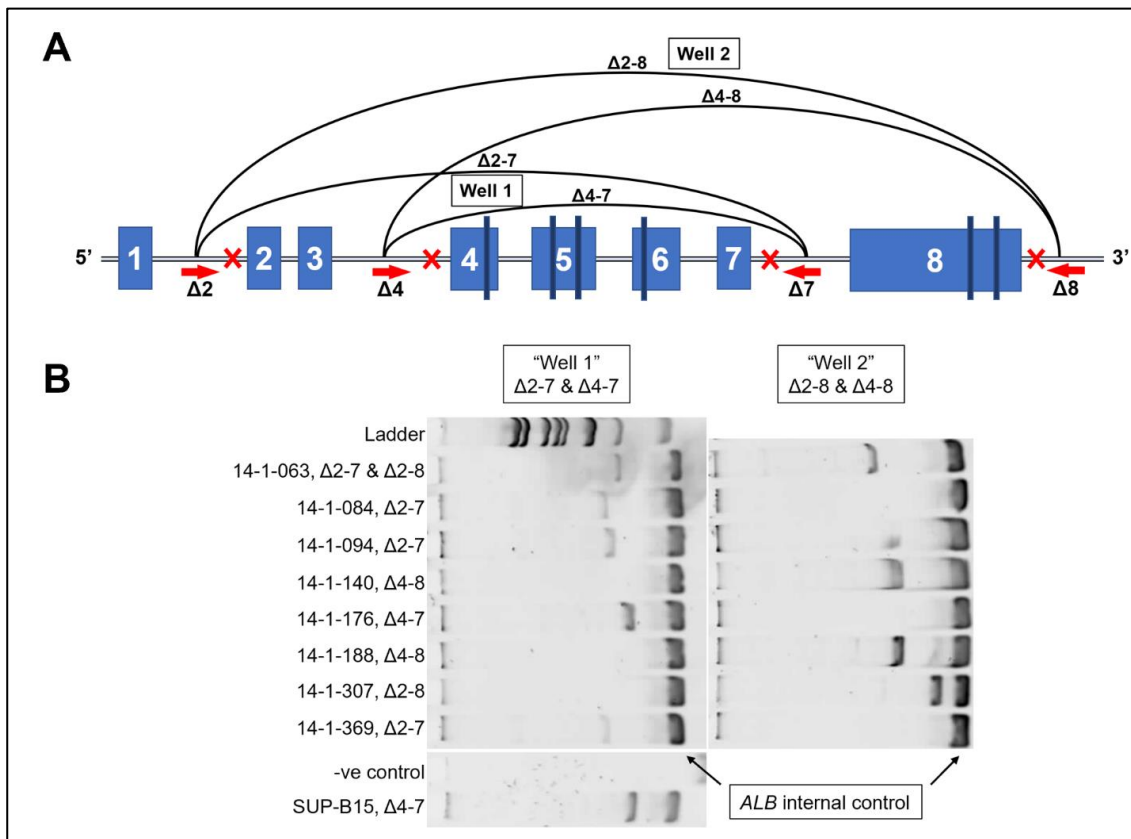
Figure 3.1: PCR assay design and validation. (A) Schematic representation of the *IKZF1* gene showing the primer sites and direction (red arrows) and common breakpoints (red crosses). The blue boxes represent exons and the dark blue boxes represent the zinc fingers. Two different reactions were used to screen patients for Δ*IKZF1:* well 1= Δ2-7 and Δ4-7, well 2= Δ2-8 and Δ4-8. **(B)** 8 patients with Δ*IKZF1* of known sizes were used to validate this screening strategy. The housekeeping gene *ALB* served as an internal control.
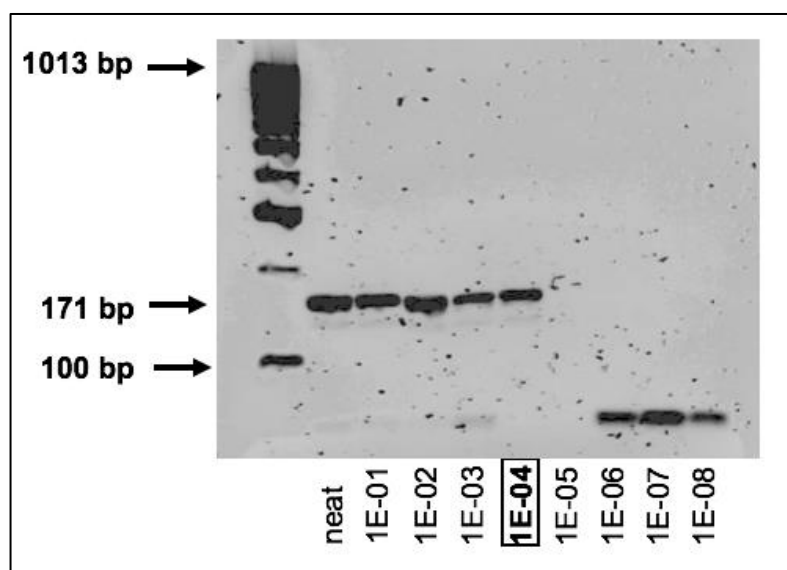
Figure 3.2: Sensitivity of the *IKZF1* assay. An agarose gel showing 10-fold dilutions from neat SUP-B15 DNA. The lower limit of detection of *IKZF1* is screen $1*10^{-4}$

3.4.1.1 Summary of PCR results

Out of a possible 655 B-ALL patients enrolled, 498 were able to be screened by multiplex end point PCR. The reasons why patients could not be screened are summarised in **Figure 3.3**. The most common reason why patients were not able to be screened was due to the diagnostic specimen becoming depleted, the likely cause of this was the material being used for MRD analysis.
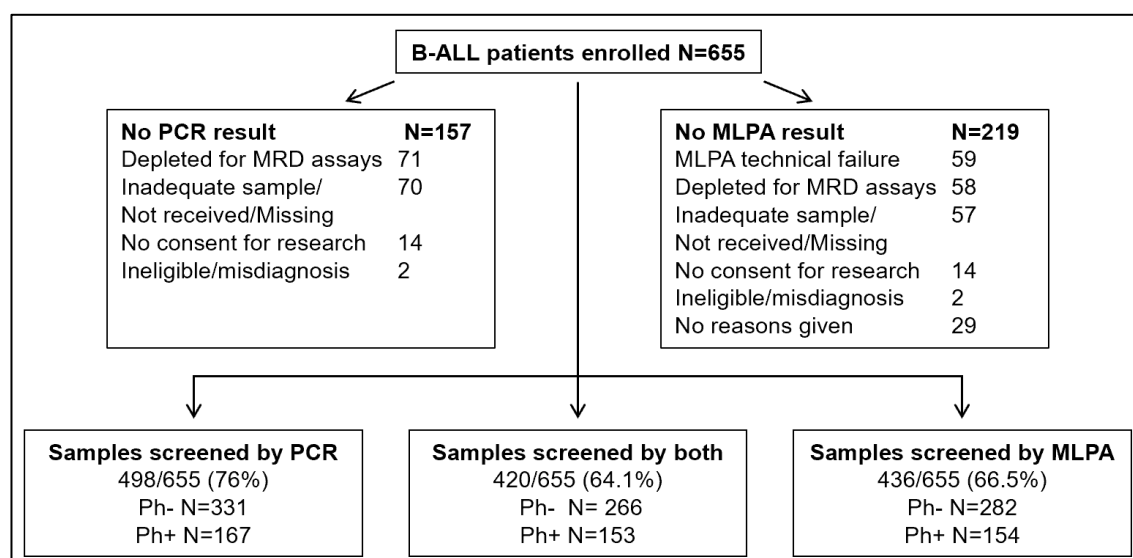
Figure 3.3: Reasons why patients could not be screened. Of those patients not screened, the most common reason was due to diagnostic specimen depletion. The likely cause of the depletion is due to a large amount of DNA required for MRD analysis.

Overall, 123 deletions were detected in 114/498 (22.9%) patients by PCR (**Figure 3.4A**). Of those that were positive, 9/114 were positive for two deletions. As expected, Δ4-7 (n=66, 53.6%) was the most common deletion detected, followed by Δ2-7 (n=29, 23.7%) and Δ4-8 (n=22, 17.9%), with Δ2-8 (n=6, 4.8%) being the rarest deletion. As expected, Δ*IKZF1* was more common in *BCR-ABL1+* ALL than in *BCR-ABL1-* ALL (PCR: 60.5% *BCR-ABL1+* vs. 39.5% *BCR-ABL1-*, MLPA: 57.6% vs. 42.4% *BCR-ABL1-*).
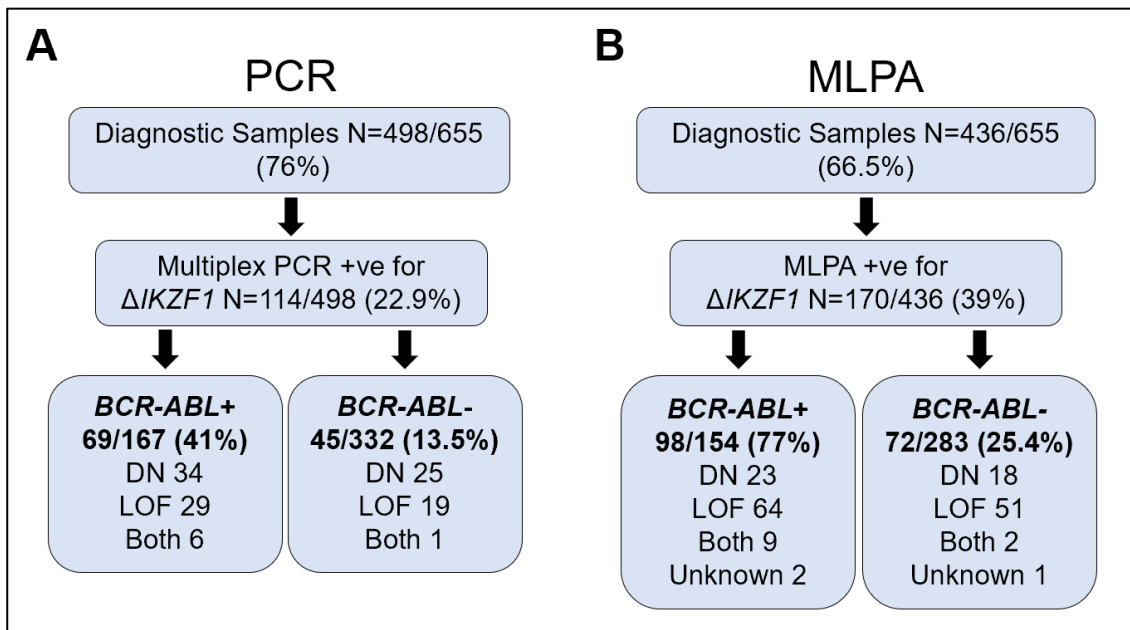
Figure 3.4: MLPA and PCR assay summaries. The flow diagrams show the number of B-ALL patients screened for Δ*IKZF1* by either (A) PCR or (B) MLPA.

3.4.1.2   Summary of MLPA data

Of the 436 specimens screened by MLPA (**Figure 3.4B**), 420 were also screened by PCR. Consistent with the technical approach, MLPA found a wider range of deletions in 170 patients- Δ1-2 (n=9, 4.9%), Δ1-3 (n=4, 2.2%), Δ1-7 (n=4, 2.2%), Δ1-8 (n=37, 20.3%), Δ2-3 (n=6, 3.3%), Δ2-7 (n=34, 18.7%), Δ2-8 (n=14, 7.7%), Δ4-7 (n=51, 28%), Δ4-8 (n=19, 10.4%), Δ6-8 (n=1, 0.6%). The probe ratios were such that the size of the deletion in *IKZF1* could not be confidently called in 3 (1.6%) cases.

3.4.1.3   Comparison of PCR and MLPA

Between the MLPA and PCR data, 95 discrepancies were identified (**Table 3.4**). Fifty-six (58.9%) of these were as expected due to the technical differences between the two approaches, i.e. deletions that the PCR could not detect. Fifteen deletions were detected by PCR and not MLPA, likely explained by the fact that PCR has a greater sensitivity. Twenty-one deletions were identified by MLPA and not by PCR, which cannot be explained by the differences between the two techniques. In these patients, it is likely that the binding sites for the PCR primers have been deleted as the breakpoints were atypical, and the MLPA probe binding sites have remained intact. Sixteen patients were positive for Δ*IKZF1* but the results were incongruous, i.e. a different deletion was identified by both techniques. Four of these are expected, as a second deletion was picked up by MLPA that PCR could not detect (**Table 3.5**).

Table 3.4: A summary of the incongruous results between patients screening by MLPA and PCR

PCR	MLPA	No. of patients	Total
Neg	**Neg**	240	359
	Pos **(discordant-expected)** Δ1-2 n=7 Δ1-3 n=3 Δ2-3 n=4 Δ1-7 n=3 Δ1-8 (WG) n=34 Δ1-2+Δ6-8 n=1 Gain n=1	53 (54 alterations total)	
	Pos **(discordant-unexpected)** Δ2-8, n=7 Δ4-8, n=4 Δ2-7 n=4 Δ4-7 n=2 unknown del, n=1 Δ2-7(+Δ2-3), n=2 Δ4-8(+Δ1-2), n=1	21	
	Fail	45	
Pos	**Pos** Δ2-8 n=3 Δ2-7+2-8, n=1 Δ4-8, n=11 Δ2-7+4-7, n=3 Δ2-7 n=15 Δ4-7+4-8, n=3 Δ4-7, n=39	75	112
	Pos, Incongruous (see **Table 3.5** for details)	Expected n=4 Not expected, n=11 Unknown del (MLPA), n=2	
Pos 4-7, n=8 2-7, n=2 4-8, n=4	**Neg**	14	
Pos 4-7, n=4 4-8, n=2	**Fail**	6	

Table 3.5: Details of patients positive by both MLPA and PCR with incongruous results

Trial Number	PCR result	MLPA result	Expected?
14-1-006	2-8	2-8, 4-7	No
14-1-084	2-7	1-8, 2-7	Yes
14-1-176	4-7	2-7	No
14-1-261	2-7	2-7, 2-3	Yes
14-1-269	4-7	1-8, 4-7	Yes
14-1-285	2-7, 4-8	2-7	No
14-1-289	2-7	2-7, 4-7	No
14-1-332	4-7	2-7	No
14-1-378	4-8	2-8	No
14-1-405	2-7	2-3, 4-7	No
14-1-422	4-7, 2-8	DEL UNKNOWN	?
14-1-445	4-7	2-7	No
14-1-551	2-7	1-7	No
14-1-595	4-7	2-7	No
14-1-607	4-7	DEL UNKNOWN	?
14-1-628	2-7	1-8, 2-7	Yes
14-1-643	4-7	2-8, 4-7	No

Of the remaining incongruous results, six deletions found by PCR were smaller than the deletion found by MLPA. MLPA may be detecting two different deletions, but as they are both present in the same clone, they are assigned the same probe ratios. For example, in patient 14-1-176, MLPA may have identified a Δ2-3 and Δ4-7 while the PCR could only identify Δ4-7. These cases could be resolved by using a higher resolution technique, such as NGS. There were several patients identified by both techniques found to harbour two deletions (9 by PCR and 18 by MLPA). These could either be bi-allelic and reside in the same cell, or biclonal, having arisen separately in two distinct clones, though it is not possible to assess this by the PCR based assays used here.

3.4.2 Patient baseline characteristics

All baseline characteristics of the PCR cohort, MLPA cohort and PCR+MLPA cohort are summarised in **Table 3.6**. Baseline characteristics are analysed to ascertain if the screened populations are representative of the whole trial population. The p-values represent a comparison between each screened cohort and the whole B-ALL population enrolled onto UKALL14. The baseline white count (p<0.001 for all cohorts) and *BCR-ABL1* status (p<0.001 for all cohorts) was significantly different for all three cohorts compared to the whole B-ALL population on UKALL14. Patients with *BCR-ABL1+* ALL are more likely to have DNA spare since it is not required for their MRD analysis, unlike the patients followed by an Ig/TCR rearrangement. This is the likely cause for *BCR-ABL1+* ALL to be enriched in the screened cohorts. Similarly, white count is likely to be skewed as there would have been excess DNA extracted if there were more cells present in the diagnostic specimen. Age was significantly different between the MLPA (p=0.0009) and PCR+MLPA (p=0.0022), and all B-ALL patients. It is less clear why there would be a significant difference, though this may have been caused by *BCR-ABL1+* ALL being more common in older patients. The UKALL14 cytogenetic risk factor was significantly different between the PCR only cohort (p=0.029) also. Baseline characteristics for patients only treated after the 2012 protocol amendment can be found in Appendix **Table 7.2**.

Table 3.6: Baseline patient characteristics for patients screened for Δ*IKZF1* on UKALL14

	PCR cohort N=498	p-val.*	MLPA cohort N=436	p-val.*	PCR + MLPA N=420	p-val.*	UKALL14 B-ALL patients N=655
Age (years)	46.0 (23-65)	0.11	45.0 (23-65)	0.0009	45.0 (23-65)	0.0022	46 (22-65)
Age group, N (%)		0.26		0.003		0.013	
40 or under at randomisation	183 (36.7)		172 (39.4)		164 (39.0)		233 (35.6)
Over 40 at randomisation	315 (63.3)		264 (60.6)		256 (61.0)		422 (64.4)
Sex, N (%)		0.95		0.91		0.68	
Male	270 (54.2)		239 (54.8)		231 (55.0)		358 (54.7)
Female	227 (45.6)		196 (45.0)		187 (44.8)		296 (45.2)
Intersex- genetically male, identifies as female	1 (0.2)		1 (0.2)		1 (0.2)		1 (0.2)
Baseline WBC	9.7 (0.11-889.6)	<0.001	10.7 (0.11-889.6)	<0.001	11.4 (0.11-889.6)	<0.001	8.0 (0.11-889.6)
Baseline WBC group, N (%)		0.028		0.008		0.003	
<30	356 (71.5)		306 (70.2)		293 (69.8)		485 (74.0)
30-100	85 (17.1)		78 (17.7)		74 (17.6)		101 (15.4)
>=100	57 (11.4)		53 (12.2)		53 (12.6)		69 (10.5)
Philadelphia Chromosome, N (%)		<0.001		<0.001		<0.001	
Present	331 (66.5)		282 (64.7)		266 (63.3)		457 (69.8)
Absent	167 (33.5)		154 (35.3)		154 (36.7)		198 (30.2)
Any UKALL14 cytogenetic risk factor, N (%)		0.029		0.083		0.83	
Absent	158 (37.4)		156 (42.3)		143 (40.2)		214 (39.9)
Present	264 (61.8)		213 (57.7)		213 (59.8)		323 (60.1)
Missing	76		67		64		118
Risk Group at Randomisation, N (%)		0.23		0.11		0.47	
Standard risk	58 (11.6)		59 (13.5)		54 (12.9)		77 (11.6)
High risk	420 (84.3)		356 (81.7)		347 (82.6)		546 (3.4)
Assumed Standard- missing information	20 (4.0)		21 (4.8)		19 (4.5)		32 (4.9)

*p-values are a comparison between the screened cohort i.e. PCR, MLPA and PCR+MLPA and the whole UKALL14 B-ALL population.

3.4.3 Δ*IKZF1* impact on outcome

The impact of Δ*IKZF1* on outcome and MRD was analysed for patients recruited after an amendment in the treatment protocol in April 2012. Induction chemotherapy was altered as treatment related mortality was higher than expected, particularly in older patients with *BCR-ABL1*+ ALL. The likely cause of this was an interaction between imatinib and pegylated asparaginase (Patel et al., 2017). Based on this, the final number of patients analysed for each group was: PCR only n=437, MLPA only n=384, both techniques n=370.

Patients positive for any *IKZF1* lesion were more likely to be MRD positive after phase 2 induction therapy (PCR p=0.0009, MLPA p=0.038), which was found for both screening techniques (**Table 3.7**). This significance appears to have been driven by the patients with *BCR-ABL1-* ALL (PCR, p=0.0057, MLPA, p=0.084), as the number of MRD+ patients with *BCR-ABL1*+ ALL was not significantly different at phase 2 induction therapy (PCR, p=0.25, MLPA, p=0.79) (**Table 3.7**). Despite the apparent difference based on *BCR-ABL1* status, the interaction did not reach significance (PCR p=0.096, MLPA p=0.17).

Chapter 3 Results

Table 3.7: The relationship between Δ*IKZF1* and MRD status after phase 2 induction therapy

	PCR ΔIKZF1	PCR IKZF1 WT†	p-value	MLPA ΔIKZF1	MLPA IKZF1 WT	p-value
End of induction MRD value N(%)						
Negative	21 (27.6)	80 (33.5)		21 (29.6)	64 (36.2)	
POQR#	13 (17.1)	48 (20.1)		13 (18.5)	33 (18.6)	
Indeterminate	5 (6.6)	44 (18.4)		5 (11.1)	29 (16.4)	
Positive	37 (48.7)	67 (28.0)		37 (40.7)	51 (28.8)	
Missing	22	100		22	58	
All patients						
Negative*	39 (51.3)	172 (72.0)	0.0009	39 (59.3)	126 (71.2)	0.038
Positive	37 (48.7)	67 (28.0)		37 (40.7)	51 (28.8)	
***BCR-ABL1* negative**						
Negative*	18 (52.9)	131 (76.2)	0.0057	18 (62.7)	99 (75.6)	0.084
Positive	16 (47.1)	41 (23.8)		16 (37.3)	32 (24.4)	
***BCR-ABL1* positive**						
Negative*	21 (50.0)	41 (61.2)	0.25	21 (56.1)	27 (58.7)	0.79
Positive	21 (50.0)	26 (38.8)		21 (43.9)	19 (41.3)	

#POQR = positive outside quantitative range

†WT = wild type

* for this analysis, negative was grouped together with indeterminate and POQR as this was how patients without a positive result were stratified to treatment

EFS and OS were analysed separately for both MLPA and PCR due to the large number of discrepancies between the two methods. For PCR detected lesions, there was no significant impact of Δ*IKZF1* on EFS in a univariable (UVA, HR=0.91, 95% CI= 0.66-1.24, p=0.54) or multivariable analysis (MVA, HR=0.87, 95% CI= 0.62-1.22, p=0.43) (**Table 3.8**). The same was true for the MLPA cohort, the data can be found in **Table 3.9**. Δ*IKZF1* did not have an impact on OS for either screening technique, the analyses can be found in **Table 7.2, 7.3, and 7.4** in the Appendix. Despite the relationship between Δ*IKZF1* and MRD positivity at phase 2 of induction therapy, a high-risk feature on UKALL14, this did not translate into a significant difference in either OS or EFS.

DN and LOF lesions were analysed separately to assess their impact on outcome, and no association was found between either deletion type and poor outcome in either UVA or MVA (Appendix **Tables 7.3-7.6**). All MVA were also re-run to include the randomised treatment arms for standard of care alone or standard of care with rituximab and, again, no interaction was seen with Δ*IKZF1*.

Table 3.8: Univariable and multivariable analysis of EFS on PCR screened cohort

Risk factor	Events/N	Complete cases univariable		Multivariable (post April 2012)	
		HR (95% CI)	p-value	HR (95% CI)	p-value
Age (increase of 10 years, centred at 23) [1]	220/387	1.36 (1.21, 1.53)	<0.001	1.35 (1.20 – 1.53)	<0.001
Sex					
Male	112/207	1.00	0.23	1.00	0.44
Female	108/180	1.18 (0.90, 1.53)		1.11 (0.85 – 1.45)	
ECOG					
ECOG 0	112/207	1.00	0.077[2]	1.00	0.030
ECOG 1	80/139	1.04 (0.79, 1.38)		1.07 (0.81 – 1.42)	
ECOG 2-3	12/13	2.75 (1.52, 4.98)		2.37 (1.29 – 4.35)	
Log WBC	220/387	1.10 (1.02, 1.20)	0.019	1.09 (1.00 – 1.19)	0.048
Genetic risk [1]					
Good risk	5/18	0.45 (0.18, 1.13)		0.58 (0.23 – 1.47)	
Standard risk	51/96	1.00	0.0026	1.00	0.012
High risk	86/130	1.59 (1.13, 2.26)		1.46 (1.01 – 2.09)	
BCR-ABL1+	78/143	1.12 (0.78, 1.59)		0.95 (0.65 – 1.39)	
***IKZF1* deletion by PCR**					
No deletion	168/293	1.00	0.54	1.00	0.43
Deletion	52/94	0.91 (0.66, 1.24)		0.87 (0.62 – 1.22)	

[1] Fails the assumption of proportional hazards (MVA did not fail). [2] Test for trend

Table 3.9: Univariable and multivariable analysis of EFS on MLPA screened cohort

Risk factor	Events/N	Complete cases univariable		Multivariable (post April 2012)	
		HR (95% CI)	p-value	HR (95% CI)	p-value
Age (increase of 10 years)[1]	194/342	1.32 (1.16, 1.49)	<0.001	1.30 (1.14 – 1.49)	<0.001
Sex					
Male	103/186	1.00	0.61	1.00	0.88
Female	91/156	1.08 (0.81, 1.43)		1.02 (0.77 – 1.36)	
ECOG					
ECOG 0	103/186	1.00	0.49*	1.00	0.096
ECOG 1	66/123	0.88 (0.65, 1.19)		0.91 (0.67 – 1.25)	
ECOG 2-3	11/12	2.45 (1.32, 4.56)		2.01 (1.07 – 3.77)	
Log WBC[1]	194/342	1.13 (1.03, 1.23)	0.009	1.11 (1.01 – 1.22)	0.025
Genetic Risk[1]					
Good risk	5/17	0.41 (0.16, 1.02)		0.45 (0.18 – 1.14)	
Standard risk	55/97	1.00	0.015	1.00	0.049
High risk	63/95	1.40 (0.98, 2.02)		1.18 (0.79 – 1.74)	
Ph+	71/133	0.99 (0.69, 1.40)		0.79 (0.53 – 1.16)	
IKZF1					
No deletion	143/263	1.00	0.047	1.00	0.36
IKZF1 deletion	30/64	0.79 (0.53, 1.18)		0.90 (0.58 – 1.40)	
*IKFF1*plus	51/79	1.36 (0.98, 1.89)		1.23 (0.87 – 1.74)	

[1]Fails the assumption of proportional hazards

3.4.4 Impact of *IKZF1*^{plus} profile on outcome

While Δ*IKZF1* had no impact on EFS or OS in the trial population regardless of *BCR-ABL1* status, further analysis was performed to examine the impact of the *IKZF1*^{plus} profile on outcome. This was made largely possible as the existing dataset since probes in the MLPA p335 kit cover all but *ERG* (Stanulla et al., 2018). It was not possible to determine *ERG* status in most patients and in this case were termed "probable" when otherwise positive for *IKZF1*^{plus}.

IKZF1^{plus} profiling could only be performed for patients where MLPA data was available. A total of 93/436 (21.3%) patients were positive for the *IKZF1*^{plus} profile in the whole cohort including patients treated before the April 2012 amendment. The proportion of patients positive for *IKZF1*^{plus} is high in comparison to the previous reports, with only 6% of high-risk paediatric patients treated on the AIEOP-BFM ALL 2000 trial previously defined as such (Stanulla et al., 2018). This is likely to be because patients with both *BCR-ABL1* negative and positive patients were included, whereas only *BCR-ABL1-* patients were analysed by Stanulla and colleagues. However, even when grouping patients based on *BCR-ABL1* status, the proportion of patients positive for *IKZF1*^{plus} is still relatively high in comparison (*BCR-ABL1*+=11.2%, *BCR-ABL1*-=10.1%).

Since it was not possible to determine *ERG* status in all patients, these were termed as "probable" for *IKZF1*^{plus} as the frequency of *ERG* deletions were low with only five patients positive for *IKZF1*^{plus} previously (Stanulla et al., 2018). With the "no deletion" group used as the reference, UVA revealed that the *IKZF1*^{plus} profile did have a significant impact on EFS (p=0.047), but this was not retained in the MVA (p=0.36) suggesting the difference in outcome was driven by something else. The data can be found in **Table 3.9**.

3.4.5 MRD assessment by Δ*IKZF1*

Δ*IKZF1* was assessed for its suitability as an MRD maker in 12 patients with 43 available follow up specimens at a variety of time-points. In order to determine its suitability as a marker, it was compared with Ig/TCR MRD. To allow for atypical breakpoints to be quantified, and also ensure a high level of specificity and to

reduce the chances of contamination from other patients, primers were designed specific to each patient sequence. The forward primer and probe were universal, and reverse primer designed over the unique *IKZF1* breakpoint in each patient. The majority of the follow up specimens tested by both methods were concordant with 14/43 positive by both methods, 18/43 were negative by both methods, and 4/43 positive out of the quantitative range (POQR) by both methods (**Figure 3.5**). Four samples were POQR by one method and negative by the other; this would not make a difference in the treatment approach in the adult setting as POQR is regarded as negative in terms of risk stratification. However, 4 of 43 patients with a POQR result by *IKZF1* MRD had a quantifiably positive result by Ig/TCR MRD (highlighted by the red box in **Figure 3.5A**). This difference would have a differential effect on how the patient was treated if one MRD method was taken above another.

However, among the samples that were MRD positive for both Ig/TCR and Δ*IKZF1*, the correlation of the quantitation was fairly poor (R^2=0.695, **Figure 3.5B**) when compared with previous studies (Caye et al., R^2=0.9232, Venn et al., R^2=0.98). Several results were different by more than half a log, suggesting either that the Ig/TCR marker tested was either present in a different clone to Δ*IKZF1*, or the deletion in *IKZF1* occurred at a different stage of leukaemogenesis than the Ig/TCR rearrangement. Results were inconsistently different, i.e. when there was a marked difference between one method and another, no method was giving consistently lower or higher positivity than the other (**Figure 3.5B**).

For Ig/TCR MRD detection, the QR should ideally reach 10^{-4} and at least 2 loci should be used to cover more than one clone to reduce the chances of false negative results. For 11/12 patients, a QR of 10^{-4} was achieved for the Ig/TCR MRD quantification (**Table 2.8**). This was also the case for 8/11 patients for the *IKZF1* MRD assay. For four patients, the QR was different for each MRD assay, with three patients having a poorer QR for the *IKZF1* assay, and for one patient a better QR was achieved with the *IKZF1* assay than Ig/TCR. These data suggest that Δ*IKZF1* could make a stable and sensitive MRD marker in adult ALL patients if used alongside Ig/TCR rearrangements.
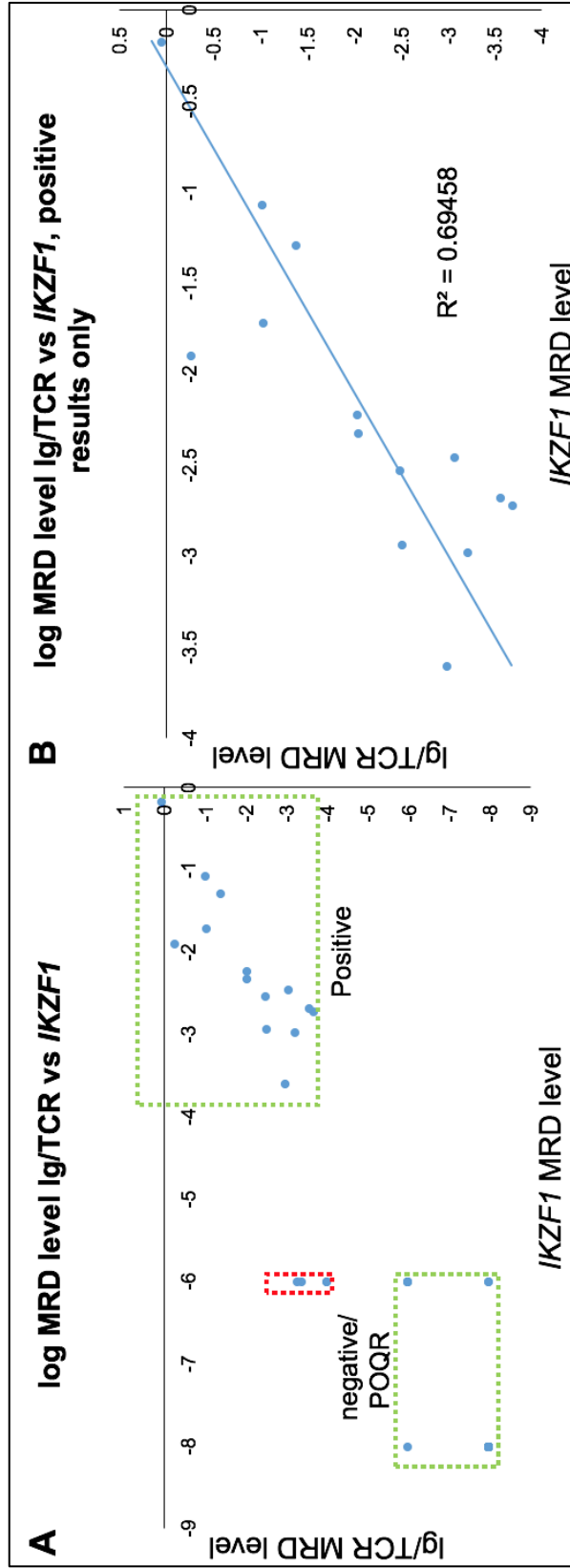
Figure 3.5: *IKZF1* **MRD correlation with Ig/TCR MRD. (A)** All samples quantified by both *IKZF1* and Ig/TCR MRD plotted on a log scale. The green boxes show samples that are positive by both methods, or negative/POQR by both methods. Samples highlighted in the red box were positive by one method and negative by another. Negative samples were given the value of 10^{-8} and POQR samples were given the value of 10^{-6}. **(B)** Correlation of samples quantifiably positive by both methods only.

3.5   Discussion

The results from screening a large clinical trial population for Δ*IKZF1*, has revealed that *IKZF1* lesions do not have an impact on outcome regardless of deletion type, size, and also on screening method. The large number of patients included means it is unlikely there was insufficient statistical power, i.e. the results are likely to be genuine and reliable. It is interesting that *IKZF1* lesions had absolutely no impact on outcome, no matter how the data were analysed. The outcome analysis was also performed based on deletion type, i.e. DN vs LOF deletions.

The expression of the DN isoform IK6 arises when the deletion of exons 4-7 occurs, removing the DNA binding domain from IKAROS. DN isoforms are not only unable to carry out their normal function but can still dimerise with WT IKAROS and render full length isoforms non-functional as well. Δ*IKZF1*4-7 is potentially more deleterious than LOF deletions though this was not evident in this trial cohort. This stands in contrast to the work of Kobitzsch and colleagues in which 482 patients with *BCR-ABL1-* ALL were screened for *IKZF1* lesions by PCR. Only LOF lesions present in a large fraction of leukaemic cells had an adverse impact on outcome (OS at 5 years 28% vs. 59%, p<0.0001). Neither DN lesions or deletions present at low levels had a prognostic impact (Kobitzsch et al., 2017).

Despite MRD positivity being more likely at the end of induction therapy in *IKZF1* deleted patients, this relationship did not persist for EFS and did not lead to an adverse outcome in these patients. This is not expected as MRD positivity is considered a high-risk feature on UKALL14. Even though there was no impact on outcome, the significant difference in MRD appears to have been driven by patients with *BCR-ABL1-* disease and not the patients with *BCR-ABL1+* ALL, which is unexpected and is in contrast to what has been seen previously. In one study on 191 paediatric patients, Δ*IKZF1* was found to have a strong impact on disease free survival (DFS) in *BCR-ABL1+* ALL. Patients positive for Δ*IKZF1* were significantly more likely to have a shorter DFS than those positive for any type *IKZF1* lesion both before (30.0± 6.8% vs 57.5± 9.4%, p=0.01) and after

(55.5± 9.5% vs 75.0± 13.9%, p=0.03) the introduction of TKI therapy (van der Veer et al., 2014b).

The differences in impact of Δ*IKZF1* could be due to the presence of other cooperating lesions, though not seen here it is likely that the impact of Δ*IKZF1* is context dependent. In one report on 97 adult patients with *BCR-ABL1*+ ALL that received an allogeneic transplant, Δ*IKZF1* alone was not sufficient to predict poor outcome. Aside from *IKZF1*, six of the most commonly occurring lesions in ALL were also investigated by SNP array and validated by MLPA: *IKZF1*, *PAX5*, *CDKN2A/2B*, *BTG1*, *EBF1*, *ETV6*, and *RB1*. The study concluded that Δ*IKZF1* required the presence of one of the other six common co-occurring lesions, and only lesions in *CDKN2A/2B* had any impact on outcome when occurring alone (Pfeifer et al., 2018).

The *IKZF1*[plus] profile also takes into account other deletions and incorporates cooperating lesions in defining a very poor risk group in paediatric ALL (Stanulla et al., 2018). Although UVA identified *IKZF1*[plus] as having a significant impact on EFS in this trial cohort, this was not evident in the multivariable analyses, suggesting the significance was not driven by the *IKZF1*[plus] profile alone. Ultimately, *IKZF1* lesions do not have an impact on outcome either alone, or in the presence of cooperating lesions even though there was a high number of patients positive for *IKZF1*[plus] on UKALL14.

The studies previously performed on several trial populations have differed in a number of ways, such as the genetic subtype, median age, and treatment. Despite these differences, they have found an adverse effect of *IKZF1* lesions on outcome in these trail populations. The main difference between previous studies and UKALL14 is that this trial recruited, on average, the oldest patients screened for Δ*IKZF1* to date with a median age of 46 years, which is potentially why no impact of Δ*IKZF1* was seen.

Both MLPA and PCR have proven to be easy and rapid assays in the screening of ALL specimens for Δ*IKZF1*, though there are limitations to both techniques

which is evident from the large number of discrepancies. MLPA, while it is able to detect a deletion of any exon, cannot detect deletions present in leukaemic sublcones due to low sensitivity. It is also evident that it cannot discern between two deletions of consecutive exons present in the same clone and a single deletion in only one allele. MLPA also requires a higher level of skill to interpret in comparison to PCR. PCR can detect deletions residing in a small proportion of the leukaemic population but is restricted to where the primers are designed around the breakpoints, which was evident from 21 lesions MLPA detected that the PCR was designed to screen for. PCR may therefore miss lesions where the primer sites have been deleted and yield false negative results.

The discrepancies in the screening results between MLPA and PCR have highlighted that the two techniques used are not adequate for $\Delta IKZF1$ detection alone, due to differences in sensitivity and specificity. $IKZF1$ lesions have been previously missed by PCR assays when breakpoints occur at atypical loci. In one study, a patient expressing IK6 mRNA was negative for a 4-7 deletion by PCR, but upon further investigation by aCGH a deletion was found (Dupuis et al., 2013). Deletions upstream of exon 1 in $IKZF1$ affecting its promoter were also detected in the same study and were predicted to lead to a loss of transcription. Subsequent immunofluorescence assays confirmed a lower level of cellular WT IKAROS (Dupuis et al., 2013). Without the other techniques used to identify $IKZF1$ lesions, these would have been missed by both MLPA and PCR. While it is unlikely that identifying more patients on UKALL14 with $IKZF1$ alterations will affect the results in this chapter, other ways of identifying $IKZF1$ lesions may lead to a more accurate method of detection and could be of importance in future. Expression of the IKAROS isoforms would be a more accurate way of identifying patients harbouring a lesion that affected levels of IKAROS, and assessing how IKAROS negatively affects outcome in ALL patients. This could be achieved either through reverse transcriptase RT-qPCR, or directly assessing protein levels via western blot.

When assessing $\Delta IKZF1$4-7 as an MRD marker, it proved to be both a stable and sensitive method for MRD monitoring. Using $\Delta IKZF1$ in combination with Ig/TCR

markers would provide more comprehensive monitoring and may give a way of following patients in whom no Ig/TCR marker could be identified. Though the correlation between the MRD positive follow-up specimens was low compared with previous studies (Venn et al., 2012, Caye et al., 2013), almost all results did agree. The number of follow up samples analysed by Δ*IKZF1* MRD was fairly small at 42, and so the low correlation with Ig/TCR MRD could be explained by this. Δ*IKZF1* would, however, suffer from the same limitations affecting Ig/TCR MRD in that it requires a high level of skill to perform and is labour intensive. Only the Δ4-7 lesion was assessed for its suitability as an MRD marker. LOF lesions could also be used and there is no reason why an assay could not be developed for those lesions. However, it is not clear if LOF lesions would be as stable as DN lesions over the timecourse of treatment since they produce a different phenotype, and hence prone to different selection pressures.

In conclusion, the results presented here have shown that *IKZF1* lesions are easy to screen for by PCR and MLPA, but great caution should be taken when choosing the method of detection. It is of the highest importance that the true *IKZF1* status of a patient is known if it is to be used to risk stratify patients and make decisions about treatment in the clinic in future. Furthermore, the data presented in this chapter have demonstrated that Δ*IKZF1* should not necessarily be accepted as a biomarker for poor outcome, and that the relationship between poor outcome with Δ*IKZF1* may be age related.

4 Ig/TCR MRD is not more predictive of outcome than *BCR-ABL1* MRD in patients with *BCR-ABL1*+ ALL

4.1 Introduction

4.1.1 IKAROS interacts with RAG and Immunoglobulin and T cell receptor gene loci

Regulation of V(D)J recombination, mediated by the RAG enzyme complex, is controlled in two main processes:

- Regulation of the convergent expression of the RAG1/2 locus
- Accessibility of immunoglobulin and T cell receptor (Ig/TCR) loci

It was established that IKAROS simultaneously performs both of these processes at the pro-B cell stage of lymphocyte development, in which healthy B-cells must rearrange IgH and IgL to form the pre-BCR complex (Reynaud et al., 2008). Chromatin immunoprecipitation assays confirmed that IKAROS directly binds to several regulatory elements of RAG, and knockout experiments revealed that *IKZF1* null cells were defective in the expression of RAG and the complete rearrangement of the immunoglobulin heavy chain. Cells were able to rearrange D to J gene segments but were not able to add the V segment to complete the rearrangement. Furthermore, these cells did not express TdT, the enzyme responsible for N-region diversity. This resulted in the rearranged D-JH region lacking the addition of any non-germline nucleotides. In contrast, not only was RAG expression induced by transducing the *IKZF1* null cells with the full length IK-1 isoform, but these cells were also able to undergo further differentiation (Reynaud et al., 2008). To further support this finding, gene expression analysis in a study on 62 *IKZF1* deleted patients revealed that 422 genes were de-regulated in the absence of functional IKAROS, and, more specifically, included a down-regulation of RAG 1/2 (Iacobucci et al., 2012).

IKAROS not only controls access to the IgH locus and its subsequent recombination, but is also implicated in controlling activity at other Ig/TCR loci. A mouse thymoma cell line, JE131, was used in one study to assess Ikaros activity at the TCRα locus. JE131 was positive for a DN isoform of Ikaros, with only one functional TCRβ gene and no fully rearranged TCRα. Once full length Ikaros was

introduced, there was a dramatic increase in TCRαβ positive cells (Collins et al., 2013). Another study generated an *Ikzf1* knockout murine model in which there was a complete block in B-cell differentiation *in vivo*, but did not lead to the development of leukaemia. However, exit from the cell cycle and cell surface expression of Igκ and Igλ was induced upon re-introduction of full length Ikaros. Furthermore, Igκ transcripts could be seen as early as 4 hours post Ikaros introduction in an *in vitro* model (Heizmann et al., 2013). This further supports the idea that IKAROS is a master regulator of RAG, V(D)J recombination in both B- and T-cells and, more widely, the differentiation of several cell lineages.

4.1.2 RAG mediated lesions in ALL

Several lesions in haematological malignancies carry the hallmarks of RAG mediated deletion, such as non-germline sequences and heptamer RSSs present at genomic breakpoints. RAG becomes constitutively active during leukaemogenesis and it not only continues to rearrange Ig/TCR loci throughout clonal evolution, but can also cause both deletions and chromosomal translocations through illegitimate off-target activity. Cryptic RSSs are scattered throughout the genome and constitutively active RAG is able to recognise these and generate double stranded DNA breaks.

A prime example of this off-target activity is the *ETV6-RUNX1* fusion gene. The RAG enzyme machinery is responsible for the balanced translocation between chromosomes 12 and 21 which generates the *ETV6-RUNX1* fusion gene, found in around 25% of paediatric ALL. Through the study of monozygotic twins with ALL and retrospective analysis of blood spot tests, it was established that the translocation causing the *ETV6-RUNX1* fusion arises in utero and is not sufficient for malignant transformation alone (Ford et al., 1998). Further postnatal genetic lesions which often also carry the hallmarks of RAG mediated deletion are required for leukaemogenesis (Papaemmanuil et al., 2014). This demonstrates that RAG activity requires tight regulation in order to prevent damaging events from occurring, and therefore the activity of IKAROS is essential for the safe rearrangement of Ig/TCR loci during lymphocyte differentiation.

Intragenic *IKZF1* lesions carry the hallmarks of RAG mediated deletion, which causes a circular argument. IKAROS induces RAG expression and RAG deletes *IKZF1* which leads to no functional IKAROS expression. At this point RAG expression should cease, so does RAG itself becomes constitutively active during this process? RAG expression cannot go ahead without IKAROS otherwise. Being able to understand what fundamentally underpins this process would give insight into the RAG mediated lesions required for the malignant transformation that causes ALL.

4.1.3 Measuring RAG activity

A key question regarding the interaction between IKAROS and RAG has yet to be addressed. It is not certain at what point in leukaemogenesis that *IKZF1* becomes deleted by RAG, and if IKAROS activity has an influence over its own deletion. This could be made possible by observing the activity of the RAG enzyme machinery. Extra-chromosomal recombination assays allow RAG activity to be measured. This assay was developed to determine if off-target RAG activity was responsible for several aberrations common to ALL. This involves the transduction of leukaemic cells with plasmids containing potential two target sequences separated by a termination signal. Once the signal has been removed by recombination via RAG, the sequence is fully transcribed and can be detected (Score et al., 2010).

However, ideally the assay should allow for the real-time observation of RAG activity. There are several ways to do this, such as with single molecule-fluorescence resonance energy transfer (SM-FRET), or tethered bead assays. SM-FRET is a biophysical tool that can monitor the interactions between molecules. A pair of fluorophores are used where the emission spectrum of one fluorophore overlaps with the absorption spectrum of the other, termed the donor and acceptor. By measuring the energy emitted from the donor and acceptor, the amount of energy transferred can be determined. A schematic can be found in **Figure 4.1A**. A change in the distance between the fluorophores is indicated by energy transfer, or FRET and acts as a "spectroscopic ruler". SM-FRET has been used to determine the relationship between RAG and the 12 and 23 RSSs.

Specific sequences tagged with fluorophores were attached to a glass coverslip and visualised with total internal reflection fluorescence microscopy. Several aspects of RAG:DNA interactions were resolved, including conformation of DNA when interacting with the RAG enzyme complex, that HMGB1 acts as a cofactor, and also that both the 12 and 23 RSS are required for sequence specificity by measuring the dwell time on a particular DNA sequence (Zagelbaum et al., 2016).
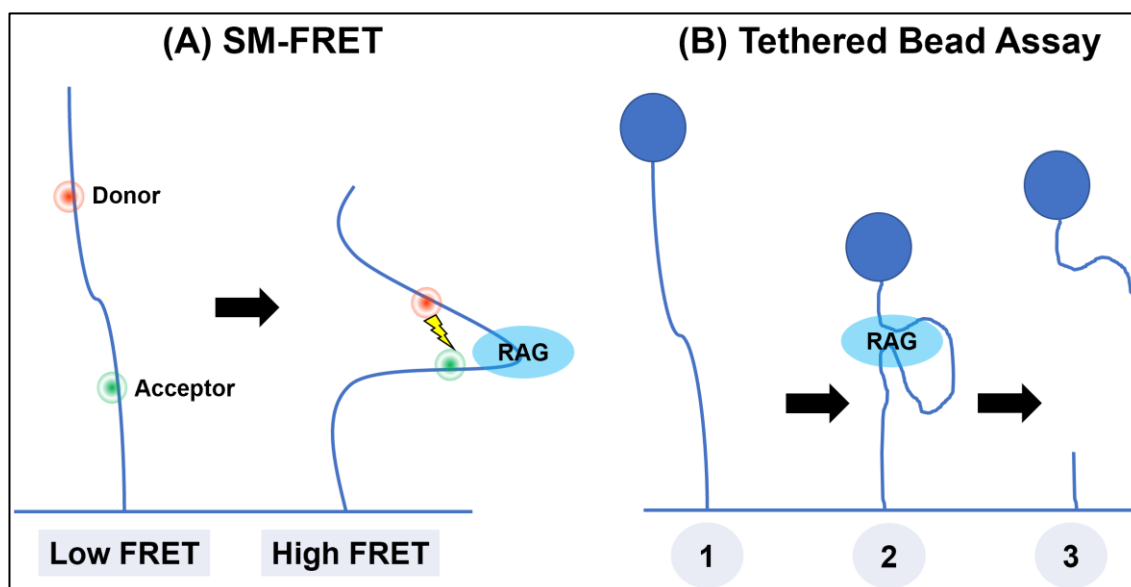
Figure 4.1: Two methods for the direct measurement of RAG activity. (A) SM-FRET. Energy is only transferred between the two fluorophores, termed the donor and acceptor, when they are in close proximity to each other **(B)** Tethered bead assays. Similar to SM-FRET, DNA is attached to a glass slide and a polystyrene bead at the free end. It is possible to measure the position of the bead and infer RAG activity from that- (1) no interaction (2) shortening of the strand via synapsis and nicking (3) detachment from the slide after DSB in the DNA.

Similar to SM-FRET, tethered bead assays are a single molecule technique in which a strand of DNA is attached to a glass coverslip, but instead of fluorophores, a polystyrene bead is attached to the free end. A schematic of this is seen in **Figure 4.1B**. Using brightfield microscopy, the root mean displacement of the bead can be determined over time when RAG interacts with the tethered DNA. This has allowed for the RAG-RSS interaction to be observed, and has revealed that single nucleotide changes of the RSS can significantly change the likelihood of RAG mediated cleavage (Hirokawa et al., 2020). Both SM-FRET and tethered bead assays have allowed the direct observation of the RAG:RSS interaction.

However, it is not possible to perform these techniques in vitro and as such not suitable for assessing the influence of IKAROS on RAG in a leukaemic cell. For this reason, measuring RAG activity in real-time is not suitable for this project.

4.1.4 Ig/TCR versus *BCR-ABL1* MRD

The two most common targets used in PCR-based assays for MRD detection are Ig/TCR rearrangements and the *BCR-ABL1* fusion gene. Ig/TCR MRD has long since been the gold standard of measuring MRD throughout the treatment of patients with ALL. While RT-qPCR monitoring via Ig/TCR rearrangements are highly sensitive, there are limitations to measuring MRD in this manner. Ig/TCR rearrangements are vulnerable to ongoing RAG activity via clonal evolution throughout the time course of treatment and lead to false negative results since the assays are sequence specific. Minor clones not detected at diagnosis have the potential emerge while the clone being followed is lost at relapse, again also leading to false negatives.

MRD can also be monitored through the quantification of the *BCR-ABL1* transcript which assesses the expression levels of *BCR-ABL1*, rather than the levels of a genomic rearrangement- a "fingerprint" rather than something that directly contributes to leukaemogenesis in ALL. The advantage of quantifying MRD by *BCR-ABL1* fusion transcript levels is that no patient specific assay is necessary as the breakpoints are consistent. The design of Ig/TCR assays is labour intensive, costly, and requires intensive technical training.

Ig/TCR MRD positivity is now widely accepted as a predictor of poor outcome and is integral to decision making in the clinic, but despite this there is still a significant number of MRD negative patients that still experience relapse. There is a possibility that patients with *BCR-ABL1+* ALL have differing MRD results depending on which target is quantified. There have been a number of studies comparing the two techniques, as it is not clear which is the better predictor of outcome. The most recent of these studies assessed Ig/TCR and BCR-ABL MRD in 64 paediatric patients with ALL. A small subset of patients were MRD positive (Hovorkova et al., 2017)

4.1.5 Approach in this chapter

I compared Ig/TCR MRD and *BCR-ABL1* MRD in patients with *BCR-ABL1*+ ALL their ability to predict poor outcome. Since patients with *BCR-ABL1*+ ALL were screened for Ig/TCR markers, it was also possible to compare the differences in the number and type of Ig/TCR rearrangements based on both *BCR-ABL1* and *IKZF1* status. IKAROS has an influence over V(D)J recombination and RAG itself, so the hallmarks of RAG activity were examined in order to indirectly identify any differences between *IKZF1* non-deleted and deleted specimens. The type and frequency of Ig/TCR rearrangements were analysed depending on *IKZF1* and *BCR-ABL1* status. The breakpoints in *IKZF1* deleted patients were also analysed for the breakpoint positions and the nucleotide insertions mediated by TdT activity, as RAG also mediates intragenic deletions in *IKZF1*.

4.2 Hypothesis

Ig/TCR MRD is more predictive of outcome than *BCR-ABL1* MRD in patients with *BCR-ABL1*+ ALL

4.2.1 Aims

- To compare Ig/TCR MRD and *BCR-ABL1* MRD and identify if one technique is better than the other at predicting survival
- To compare the frequency and type of Ig/TCR markers with relation to *BCR-ABL1* and *IKZF1* status
- To compare *IKZF1* breakpoint sequences in *BCR-ABL1*+ versus *BCR-ABL1*- specimens, specifically the location of the breakpoints and the non-germline insertions

4.3 Methods

4.3.1 Statistical Analysis

All baseline characteristics and outcome analyses were performed by UKALL14 trial statistician Amy Kirkwood. The Unpaired students T test was used to compare the number or Ig/TCR rearrangements in patients based on *BCR-ABL1* and *IKZF1* status. The Fisher's Exact test was used to compare the presence of types of Ig/TCR rearrangements in *IKZF1* deleted and non- deleted patients. The Mann-Whitney test was used for *IKZF1* breakpoint analysis.

4.4 Results

4.4.1 A comparison of Ig/TCR and BCR-ABL MRD quantification as a predictor of outcome

4.4.1.1 Assay Characteristics

Fifty-five patients were screened for Ig/TCR rearrangements making it possible to compare Ig/TCR and *BCR-ABL1* MRD quantification. However, only 39 of those had available follow up material and a working Ig/TCR MRD assay (**Figure 4.2A**). Patients with a working Ig/TCR MRD assay and available follow-up material had a total of 72 follow up specimens analysed. The patient samples were collected between 19/05/2011 and 18/09/2017 and at several different points throughout the course of treatment, summarised in **Figure 4.2B**. Forty-two of 72 were taken at after either phase 1 or 2 induction therapy, the remaining 30 were taken beyond phase 2.

A total of 128 sequences were analysed from 39 patients (**Figure 4.2A**). The most common rearrangements used for patient specific MRD assays were TCRγ, followed by complete IgH rearrangements (**Table 4.1**). Just over half of the 39 diagnostic specimens had at least one assay that achieved the expected quantitative range of $1*10^{-4}$ (20/39, 51.3%). Of those assays that did not achieve a QR of $1*10^{-4}$, 11 had a QR of $5*10^{-4}$ (28.2%), seven had a QR of $1*10^{-3}$ (17.9%) and one had a QR of $1*10^{-2}$ (2.6%). The number of specimens not achieving a QR of $1*10^{-4}$ appears to be relatively high in comparison to paediatric patients.

Table 4.1:The Ig/TCR rearrangements used for MRD assays

Rearrangement	Number of Assays
IgH Complete	17
TCRγ	12
IgH Incomplete	2
Igκ-κde	6
TCRδ	5
TCRδ$_V$–α$_J$	2
TCRβ Incomplete	2
TCRβ complete	1

Figure 4.2: Patients included in the study and the number of samples collected per timepoint. (A) The total number of patients with *BCR-ABL1+* ALL screened of Ig/TCR rearrangements was 55, but only 28 patients had available material for Ig/TCR quantification and a working assay **(B)** From the 39 patients with a working Ig/TCR marker, 72 samples were collected. The majority of the samples collected were taken after phase 1 and 2 induction therapy.

4.4.1.2   Comparison and congruity between *BCR-ABL1* and Ig/TCR MRD

MRD was successfully quantified in all 72 follow-up specimens according to the guidelines published by the EuroMRD consortium on acceptable limits of sensitivity and specificity. MRD assessment by Ig/TCR RT-qPCR assay found 47/72 were negative, and 6/72 were POQR. The remaining 19 samples were quantifiably positive, ranging from 0.0032% to 173.4%. Thirteen of the MRD positive samples were collected at phase 1 and three were post phase 2.

For the majority (54/72, 75%) of the patient samples assessed, MRD results were congruous between the Ig/TCR and *BCR-ABL1* assays. However, nine of 72 patient samples were negative by one assay and positive by another, of these eight samples nine were positive by *BCR-ABL1* MRD and negative by Ig/TCR. One patient specimen, trial number 14-1-245, was MRD positive by Ig/TCR but negative by *BCR-ABL1*. The patient information for these discordant follow-up samples is shown in **Table 4.2**. A further four specimens were POQR by one method and quantifiably positive by another. Three of the four were quantifiably positive by *BCR-ABL1* MRD and POQR by Ig/TCR, and the reverse was true for only one patient sample (**Table 4.2**). A small proportion of samples were positive by both assays but were not congruous as they differed by more than one log (**Table 4.3**).

Table 4.2: Details for specimens with incongruous results

Trial No.	*BCR-ABL1* MRD	Ig/TCR MRD	Sample Timepoint	Breakpoint	Ig/TCR Assay Sensitivity
14-1-027	0.02%	0.00%	Phase 1	p210	1×10^{-4}
14-1-109	0.30%	0.00%	Phase 1	p210	1×10^{-3}
14-1-126	POQR	5.7%	Phase 1	p190	1×10^{-4}
14-1-127	0.02%	0.00%	Phase 2	p210	1×10^{-3}
14-1-132	0.002%	POQR	After phase 2	p190	1×10^{-4}
14-1-218	6.14%	0.00%	Phase 2	p190	1×10^{-3}
14-1-245	0.00%	0.015%	After phase 2	p210	1×10^{-4}
14-1-357	0.01%	0.00%	Phase 2	p190	1×10^{-3}
14-1-364	59.8%	0.00%	Phase 2	p210	1×10^{-3}
14-1-372	0.004%	POQR	Phase 1	p190	1×10^{-3}
14-1-580	1.87%	POQR	Phase 2	p210	5×10^{-4}
14-1-637	0.008%	0.00%	Phase 1	p190	5×10^{-4}
14-1-655	0.31%	0.00%	Phase 1	p210	5×10^{-4}

Table 4.3: Details of specimens MRD positive by both Ig/TCR and *BCR-ABL1* that differed by more than 1 log

Trial No.	BCR-ABL MRD	Ig/TCR MRD	Sample Timepoint	Breakpoint	Ig/TCR Assay Sensitivity
14-1-146	0.44%	0.0032%	Phase 1	p190	1×10^{-4}
14-1-252	0.016%	0.20%	Phase 2	p190	1×10^{-4}
14-1-364	62.73%	0.30%	Phase 1	p210	1×10^{-3}
14-1-365	0.0032%	0.043%	Phase 1	p190	1×10^{-4}
14-1-530	0.0029%	0.10%	Phase 1	p210	1×10^{-3}

The *BCR-ABL1* quantification diverged from the Ig/TCR quantification in numerous cases. Only 27/72 (37.5%) samples were negative by *BCR-ABL1* quantification, as compared with 47/72 (23.5%) by Ig/TCR quantification. A higher proportion of specimens were determined as POQR by Ig/TCR than *BCR-ABL1* MRD (47 vs 17, **Figure 4.2**). Therefore, more follow up specimens were quantifiably positive by *BCR-ABL1* MRD than Ig/TCR MRD, ranging from 5.56% to 1335.138%.

4.4.1.3   Predictive value of Ig/TCR MRD versus *BCR-ABL1* MRD

Analysis on outcome was performed in order to determine which is the best predictor, especially since a number of patients with differing Ig/TCR and *BCR-ABL1* MRD results were identified. Baseline characteristics of the patients with *BCR-ABL1+* ALL were compared to the *BCR-ABL1+* population as a whole to ensure they were representative of *BCR-ABL1+* enrolled onto UKALL14 (**Table 4.4**). Presenting white count was significantly higher (p=0.014), which typically suggests that excess material is more likely to be banked for patients with higher presenting WBC count.

EFS and time to relapse (TTR, a secondary endpoint on UKALL14) were examined for the 21 phase 2 samples collected. MRD evaluated by either Ig/TCR or *BCR-ABL1* did not differ in their ability to predict poor outcome despite the differences in the number of MRD positive and negative samples found by each technique (7/21 MRD positive by *BCR-ABL1,* 11/21 MRD positive by Ig/TCR), as summarised in the statistical analysis in **Table 4.5**.

Table 4.4: Baseline characteristics for the 39 patients with *BCR-ABL1*+ ALL screened for Ig/TCR markers

	MRD samples	B-cell, Ph+, no MRD samples	B-cell, Ph+ No MRD Samples ,achieved remission phase 1 or 2	p-value
	N (%) N=39	N (%) N=159	N (%) N=139	
Age at randomisation (range)	43.0 (25.0-62.0)	48.0 (22.0-65.0)	47.0 (22.0-65.0)	0.41*
40 or under	15 (38.5)	49 (30.8)	47 (33.8)	0.59
Over 40 at randomisation	24 (61.5)	110 (69.2)	92 (66.2)	
WBC at randomisation, median (range)	32.9 (1.1-269.3)	12.7 (0.6-378.6)	12.7 (0.6-378.6)	0.014*
<30	18 (46.2)	107 (67.3)	93 (66.9)	0.048
30-100	13 (33.3)	35 (22.0)	32 (23.0)	
>=100	8 (20.5)	17 (10.7)	14 (10.1)	
Sex				
Male	22 (56.4)	89 (56.0)	78 (56.1)	0.97
Female	17 (43.6)	70 (44.0)	61 (43.9)	
***IKZF1* deletion**				
Absent	16 (42.1)	72 (55.8)	66 (58.9)	0.072
Present	22 (57.9)	57 (44.2)	46 (41.1)	
Missing	1	30	27	

The p-value compares patients with MRD samples to those without but who are B-cell, *BCR-ABL1*+ and achieved remission in phase 1 or 2. Chi-squared unless otherwise stated. *Wilcoxon- Mann-Whitey.

Table 4.5: Summary of the end of phase 2 statistical analysis

MRD	Events/N	HR (95% CI)	p-value
Event free survival			
BCR-ABL			
Log (MRD value)*	10/21	1.06 (0.80 – 1.41)	0.68
MRD negative	6/13	1.00	0.62
MRD Positive	4/8	1.40 (0.39 – 4.92)	
IgTCR			
Log (MRD value)*	10/21	1.13 (0.79 – 1.62)	0.50
MRD negative	6/10	1.00	0.45
MRD Positive	4/11	0.61 (0.17 – 2.17)	
Time to relapse			
BCR-ABL			
Log (MRD value)*	8/21	1.14 (0.85 – 1.53)	0.39
MRD negative	4/13	1.00	0.32
MRD Positive	4/8	2.04 (0.51 – 8.24)	
IgTCR			
Log (MRD value)*	8/21	1.23 (0.85 – 1.80)	
MRD negative	5/10	1.00	0.41
MRD Positive	3/11	0.55 (0.13 – 2.31)	

*for an increase in 1 log. Patients with 0 values were set as 0.00001 before the log was taken.

**Deaths from other causes are not included as events.

As seen in the Kaplan-Meier curves in **Figure 4.3** when correlating EFS and TTR with MRD status, it appears that patients with an MRD positive result determined by Ig/TCR have a longer EFS and are less likely to relapse which is the opposite to what is expected clinically but interpretation here is limited by the small sample size. The Kaplan-Meier curves for *BCR-ABL1* MRD show very little separation between MRD positive and MRD negative patients for EFS (p=0.68, HR: 1.06, 95% CI: 0.8-1.41), suggesting there is no impact of *BCR-ABL1* MRD on EFS (**Figure 4.3A**, left graph). For TTR (**Figure 4.3B**), there is a small separation between the two curves. Patients with MRD positive disease by *BCR-ABL1* may be more likely to experience a relapse, although our data do not show a statistically significant difference (p=0.5, HR: 1.14, 95% CI: 0.85-1.53).
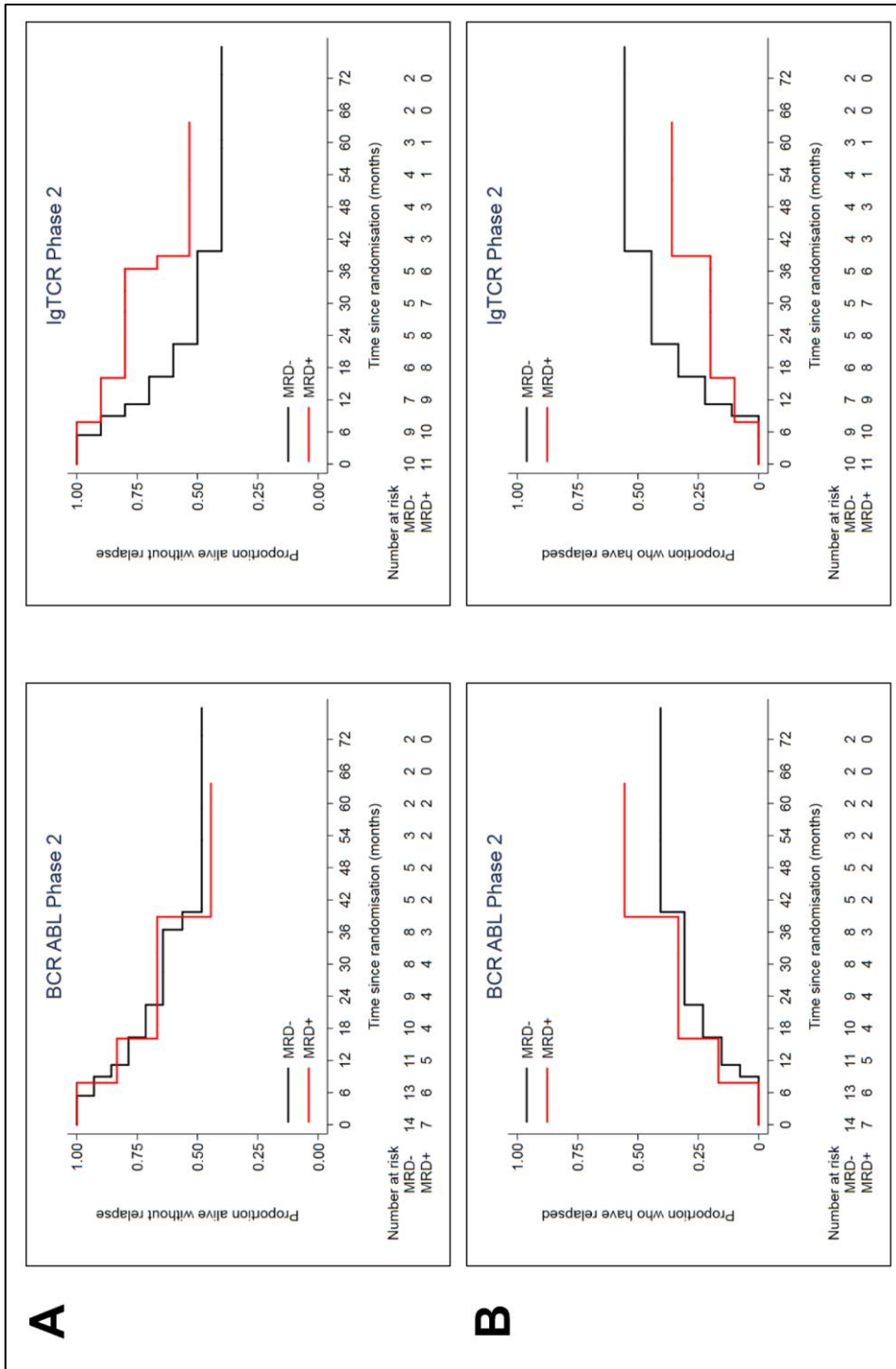
Figure 4.3: Kaplan-Meier survival curves. Displaying the correlation between MRD status at the end of phase 2 for (A) Event-Free Survival and (B) Time To Relapse.

4.4.2 The number of Ig/TCR rearrangements per patient is dependent on *IKZF1* status and not *BCR-ABL1* status

Since Ig/TCR screening was performed for the comparison of Ig/TCR and *BCR-ABL1* MRD, it was possible to analyse the number and type of Ig/TCR rearrangements found based on Philadelphia and *IKZF1* status. IKAROS is known to the activate the RAG genes, and so differences in the activity of IKAROS, either due to the presence of a DN protein or a LOF deletion, may affect the activity of the RAG enzyme machinery in rearranging Ig or TCR loci. *BCR-ABL1+* patients are more likely to harbour *IKZF1* lesions which are mediated by the RAG enzyme machinery, whose normal function is the rearrangement of the Ig and TCR loci. It was hypothesized that the presence of the Philadelphia chromosome increased the off-target activity of RAG and also its rearrangement of the Ig/TCR loci. For these reasons, the number of Ig/TCR markers was analysed in 105 *BCR-ABL1-* and 55 *BCR-ABL1+* patients, and groups separated based on both *BCR-ABL1* and *IKZF1* status. The range of the number of markers found per patient did not vary by much between the groups (**Table 4.6**). The average number of markers per patient is slightly higher for both *IKZF1* deleted groups when compared with the *IKZF1* wild type groups.

Table 4.6: Summary of the Ig/TCR rearrangements analysed

	BCR-ABL+ Δ*IKZF1+*	*BCR-ABL-* Δ*IKZF1+*	*BCR-ABL+* Δ*IKZF1-*	*BCR-ABL-* Δ*IKZF1-*
Total patients analysed	31	47	24	58
Range	0-7	0-8	0-5	0-8
No. with no marker (%)	4 (12.9)	1 (2.13)	2 (8.33)	8 (13.8)
Average per patient	3.6	3.1	2.5	2.7
Total rearrangements found	112	147	59	154

When analysing the groups separated based on Philadelphia status alone, there was no significant difference in the number of rearrangements per patient between *BCR-ABL1+* and *BCR-ABL1-* groups. However, there was a highly significant difference in the number of rearrangements between *IKZF1* deleted and non-deleted specimens (**Figure 4.4**). The suggestion that *BCR-ABL1+* ALL harbours a larger number of Ig/TCR rearrangements may be driven by the fact

that there are more *IKZF1* deleted cases present in the *BCR-ABL1+* population, and not by the presence of the Philadelphia chromosome itself.
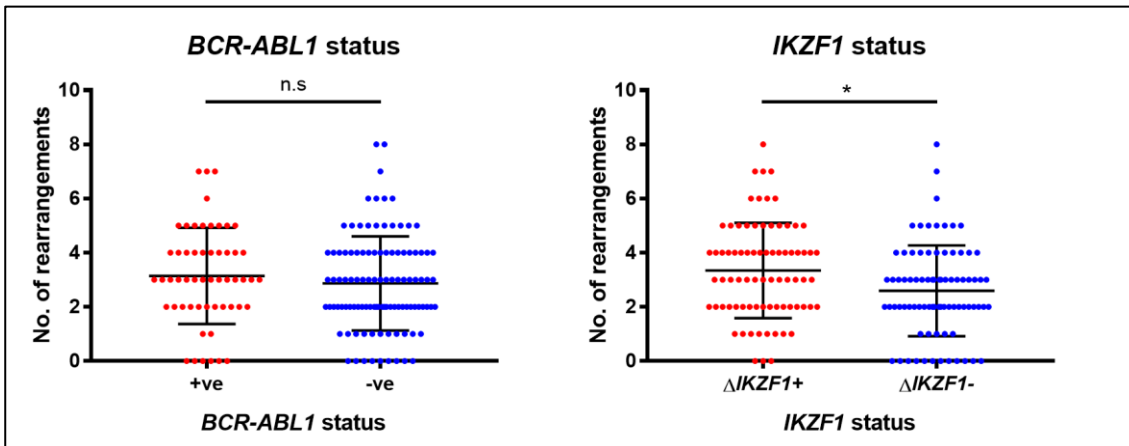
Figure 4.4: Ig/TCR rearrangements analysis. The number of Ig/TCR rearrangements were analysed. Patients were grouped based on *BCR-ABL1* status and *IKZF1* status. Error bars represent mean and SD. *p=0.0065.

The number of specimens in whom no marker was found was the highest for *BCR-ABL1- IKZF1* non-deleted specimens (**Table 4.6**). The type of Ig/TCR rearrangements found in each group was also analysed based on *IKZF1* status, due to the significance in the rearrangement data (**Figure 4.5**). A total of 472 rearrangements were detected in 160 patients. During normal the normal V(D)J rearrangement of the IgH locus, the first gene segments to be arranged is the D to the J, with the V segment being added at a later stage. An assumption can be made that a leukaemic clone with an incomplete IgH rearrangement arrested earlier in development than a clone with a complete rearrangement (Alt et al., 1984). When looking at IgH rearrangements only, there is a greater proportion of incomplete rearrangements seen in *IKZF1* WT patients when compared to the *IKZF1* deleted patients (32.1% versus 10.1%, p<0.0001, **Figure 4.5**). It is possible that *IKZF1* is deleted in more mature clones after the IgH locus has already undergone rearrangement. The prevalence of two other Ig/TCR rearrangements were significantly higher in *IKZF1* deleted than WT specimens- TCRγ (p=0.015) and Igκ (p=0.001).
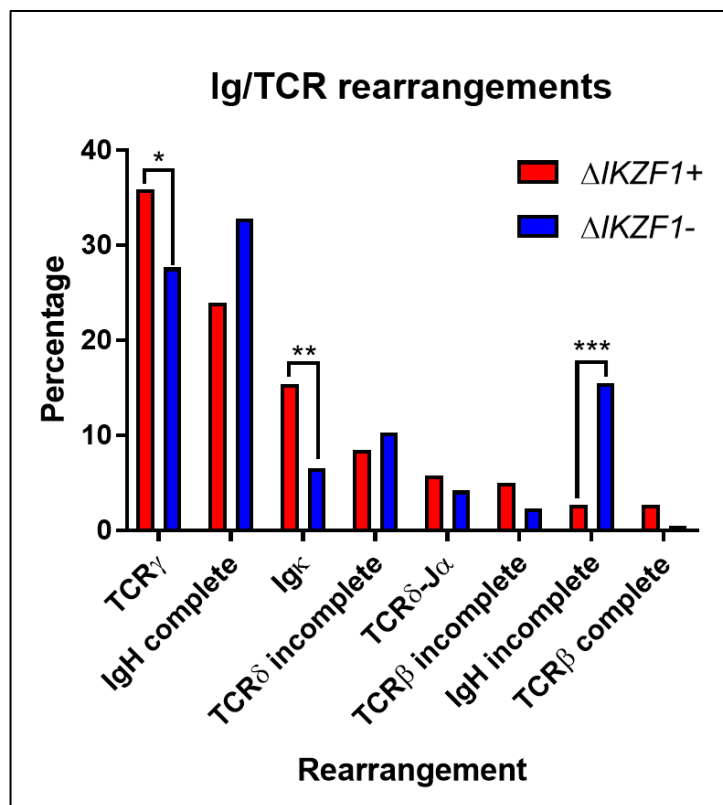
Figure 4.5: Type of Ig/TCR rearrangements and their proportion based on *IKZF1* status. A significant difference between *IKZF1* deleted and WT for TCRγ (p=0.015), Igκ (p=0.001) and Incomplete IgH rearrangements (p=<0.0001).

4.4.3 *IKZF1* breakpoint analysis- A significant difference between *BCR-ABL1+* and *BCR-ABL1-* patients

IKAROS interacts with the RAG enzyme machinery, which is responsible for normal V(D)J recombination of the immunoglobulin and TCR loci in developing B and T cells. In turn, the deletions in *IKZF1* are mediated by the RAG enzyme complex (Mullighan et al., 2008) As seen in clinical data, the effects of *IKZF1* deletions in ALL may be context dependent, i.e. in the presence or absence of the Philadelphia chromosome. More recently, an algorithm for risk stratification in children with ALL has been determined, termed *IKZF1*plus. This not only includes *IKZF1* deletions, but also deletions in *CDKN2A*, *CDKN2B*, *PAR1*, *PAX5*, and in the absence of an *ERG* deletion. As a way of examining the differences in RAG activity in *BCR-ABL1+* versus *BCR-ABL1-* the breakpoints for all but five sequences were analysed for their insertions and deletions. An example can be seen in **Figure 4.6**.

Figure 4.6: *IKZF1* **breakpoint analysis, an example.** The example shows how the number of nucleotides inserted and deleted around the breakpoint in *IKZF1*. The arrows indicate the end of the heptamer (underlined) where the counting started. In the example, the breakpoint is 8 nucleotides away from the end of the heptamer in the distal breakpoint.

All breakpoints were subject to Sanger sequencing and confirmed a unique sequence. This was expected due to the nature of the RAG enzyme as it does not break the DNA in a consistent way at the putative heptamer as seen in **Figure 4.7**. It is evident that the DSBs caused by RAG are more likely to occur either immediately 5' in the proximal breakpoint, or immediately after the heptamer in the 3' distal breakpoints (**Figure 4.7**).

Figure 4.7: Breakpoint position and frequency in *IKZF1.* Sanger sequencing of patient *IKZF1* sequences allowed for the analysis of the position and frequency of each breakpoint found in the regions immediately proximal and distal to the heptamers. Arrows indicate unique breakpoint; number indicates the frequency at which the breakpoint was observed. The putative heptamer is underlined.

122

The TdT activity at the breakpoint means that a random number and sequence of nucleotides are inserted. It is not possible to study the RAG activity in patient specimens, as the Ig/TCR loci have already been previously rearranged during the development of their ALL.

Although the RAG enzyme complex recognises the RSSs flanking Ig/TCR gene segments, RAG does not break DNA in exactly the same place every time, i.e. a variable number of nucleotides are deleted near to the RSS or in this instance, the cRSS in *IKZF1* (**Figure 4.7**). Patients with *BCR-ABL1+* ALL are more likely to be positive for an *IKZF1* lesion, so it is also possible that there are differences in the breakpoints in *BCR-ABL1+* versus *BCR-ABL1-* ALL due to altered RAG activity and subsequent repair of the DSBs. Since the observation of the direct activity of RAG was not possible, the number of nucleotides deleted relative to the putative heptamer in *IKZF1* deleted specimens were counted as a surrogate marker for the differences in RAG activity between *BCR-ABL1+* and *BCR-ABL1-* patients (**Figure 4.8**).

Figure 4.8: *IKZF1* **breakpoint analysis, a difference based on** *BCR-ABL1* **status.** For all four deletions screened for by PCR, the number of nucleotides deleted, prior to the heptamer in the proximal breakpoint, beyond the heptamer in the distal breakpoint was counted, and inserted at the breakpoint were counted, and compared in *BCR-ABL1*+ versus *BCR-ABL1*- patients. Error bars represent mean and SD.

During the normal repair of DNA via non-homologous end joining after RAG generates DSBs, a small number of nucleotides are inserted at the breakpoint by TdT. Again, the *BCR-ABL1* status of the patient may have an effect on TdT activity since RAG "shepherds" DSBs into the NHEJ pathway (Lee et al., 2004). The number of nucleotides and inserted through TdT activity around the breakpoint was also assessed. Off-target RAG activity is potentially higher in the presence of *BCR-ABL1* as Δ*IKZF1* are more common in *BCR-ABL1*+ ALL and mediated by RAG. It was expected that there was an increase in TdT activity at the breakpoint site in *IKZF1* also, i.e. a larger number of non-germline nucleotides present. This was also expected in the position of the break relative to the heptamer mediated by RAG. The range of nucleotides deleted did not vary greatly depending on the position of the breakpoint, and nor did the number of nucleotides inserted based on the four different deletions screened.

Patients with *BCR-ABL1*+ ALL had significantly more nucleotides deleted from the distal breakpoint relative to the heptamer sequence, and also significantly more nucleotides inserted at the breakpoint. While significance was not reached for the proximal breakpoint, a similar trend was observed as with the insertion and distal breakpoints.

4.5   Discussion

It was previously revealed that differences in *BCR-ABL1* and Ig/TCR MRD could have a biological basis, and that patients with higher *BCR-ABL1* MRD levels than Ig/TCR have a different disease biology as the Philadelphia chromosome has multilineage involvement (Hovorkova et al., 2017). Aside from any biological basis, the differences in MRD levels could also be attributed to the different targets, i.e. genomic Ig/TCR versus measuring the expression of *BCR-ABL1* indirectly via cDNA. Ig/TCR MRD monitors one copy of one rearrangement per cell at the genomic level, whereas *BCR-ABL1* MRD based assays monitor the expression of fusion transcripts which relies on measuring a housekeeping gene for normalisation, though expression of these genes is not uniform. Both *GUS* and *ABL* have been used as the control gene in the monitoring of patients with

BCR-ABL1+ ALL and CML, though the choice between these remains controversial. The true level of *BCR-ABL1* expression could be either under- or overestimated depending on the number of control gene copies that are quantified and this normalisation makes a direct comparison between Ig/TCR and *BCR-ABL1* MRD levels difficult. There have been several studies investigating the use of the genomic *BCR-ABL1* fusion as an MRD target in CML, and could overcome the differences in *BCR-ABL1* expression and the genomic Ig/TCR targets.

In our small sample size, we did not demonstrate that Ig/TCR or *BCR-ABL1* was a better predictor of outcome over the other, although the study was underpowered to detect modest differences. Completing Ig/TCR screening on the patients with *BCR-ABL1+* ALL on UKALL14 will add more data and provide a more statistically robust output. Furthermore, the p210 patients with differing MRD results should be investigated further, especially those MRD positive by *BCR-ABL1* and negative by Ig/TCR as seen in paediatric patients with a CML-like disease (Hovorkova et al., 2017). The p210 variant is more prevalent in CML, so it is more likely that these patients would display a "CML- like" biology. If available, flow cytometric analysis of their diagnostic specimens may reveal the true cause of this discrepancy, as this would reveal if the Philadelphia chromosome has multilineage involvement. It is worth noting that Hovorkova and colleagues worked on paediatric samples, whereas this current analysis was performed on samples from adult patients wherein the disease biology is likely quite different.

IKAROS interacts with the machinery responsible for V(D)J recombination in developing B-cells. IKAROS represses TdT expression, the enzyme that increases the junctional diversity of Ig/TCR loci (Gurel et al., 2008) by binding a regulatory element upstream and displacing Elf-1, a transcriptional activator (Trinh et al., 2001). IKAROS transcriptionally activates the convergently expressed RAG1/2 gene locus (Reynaud et al., 2008). The data from both the *IKZF1* breakpoint and the Ig/TCR rearrangements suggests there are differences in both RAG and TdT activity in patients based on *IKZF1* deletion and *BCR-ABL1*

status. *IKZF1* deleted specimens were more likely to have Igκ, TCRγ or TCRβ rearrangements than *IKZF1* WT specimens, and the reverse was true for incomplete IgH rearrangements. The results for the incomplete IgH rearrangements were unexpected biologically, since IKAROS has control over IgH locus access and also induces RAG expression (Reynaud et al., 2008). The presence of the Philadelphia chromosome could potentially alter the gene expression profile that leads to a difference in RAG activity, which subsequently initiates *IKZF1* gene deletions and greater TdT activity at the *IKZF1* breakpoint. This would suggest that IKAROS expression is lower in *BCR-ABL1*+ ALL, since the number of nucleotides inserted at the *IKZF1* breakpoint was significantly higher in patients with *BCR-ABL1*+ ALL than in *BCR-ABL1*-.

The cellular levels of WT IKAROS are not only affected by intragenic deletions but are also removed with the deletion of the whole p arm of chromosome 7, which has been observed in B-ALL (Dabaja et al., 1999). Other mutations including SNPs and lesions affecting the promoter affect the abundance of IKAROS in pre-leukaemic cells (Dupuis et al., 2013, Churchman et al., 2018). These lesions could also have an effect on RAG activity since IKAROS induces the expression of RAG1/2.

Other RAG mediated co-occurring lesions could also be assessed, as the promiscuous nature of RAG in leukaemia could affect other loci in the same way as the *IKZF1* locus. RAG also causes lesions in *CRLF2*, *TBL1XR1*, *CDKN2*, *NR3C1*, *NR3C2*, and *BTG1* in *ETV6-RUNX1* rearranged paediatric B-ALL (Papaemmanuil et al., 2014). It is also not known that once *IKZF1* has been deleted if this has any effect on ongoing RAG activity at the Ig/TCR loci and clonal evolution which has an effect on MRD markers followed. Ultimately, *in vivo* experiments may provide answers.

It may be of clinical relevance that patients positive for Δ*IKZF1* the absence of an IgH rearrangement had a poorer outcome than those with an IgH rearrangement (Kastner et al., 2013, Dupuis et al., 2013). Furthermore, blast crisis transformation in CML is associated with distinct patterns of deletions in IgH and TCR loci, and

the loss of the short arm of chromosome 7 where *IKZF1* resides, suggesting the link between RAG activity and IKAROS has implications in other haematological malignancies (Nacheva et al., 2010). This was performed as a way of assessing RAG activity, as the direct observation of RAG mediated DNA cleavage cannot be performed *in vitro*, and so any DN or LOF cell line model cannot be used. Previous attempts at measuring RAG activity have employed biochemical assays in solution and not performed *in vitro*, making it not possible to study the effects of IKAROS on RAG enzyme activity (Zagelbaum et al., 2016, Hirokawa et al., 2020). Ultimately, the best way to examine the damaging nature of the interaction between RAG and IKAROS will be via a real-time assay *in vitro*. While it is not possible to assess the activity of the RAG enzyme machinery in real-time, these data suggest that there is a difference in RAG and TdT activity dependent on the presence of the Philadelphia chromosome.

There has been some evidence that RAG may play a role in initiating the generation of the t(9;22) translocation that gives rise to the *BCR-ABL1* fusion gene, but specifically only in ALL (Score et al., 2010). It was previously hypothesised that the different breakpoints that generate the p190 and p210 variants are present in differing frequencies in CML and ALL due to the developmental stage at which they occur, i.e. p190 occurs later than p210 since the lymphoid lineage has already been committed to and hence more common in ALL. This led the authors to hypothesise that there are different mechanisms that cause each of the *BCR-ABL1* variants. Candidate cRSSs were identified around the breakpoints in *BCR-ABL1* sequences from patients with *BCR-ABL1+* ALL, and while this could simply be by chance as they are likely to occur around every 5000 base pairs, further experimentation revealed RAG could have been responsible. Representative *BCR-ABL1* sequences from CML and ALL patients were used in extra-chromosomal recombination assays to assess if there was a functional link between the cRSSs identified and their proximity to the breakpoint. There was no strong evidence for recurrent RAG recognition sites, though the proximal breakpoint in one ALL sequence was recapitulated in multiple experiments, which was only seen in p190 sequences and not the CML p210 sequences (Score et al., 2010). The *IKZF1* status of these patients was not

analysed in this study, and so any potential interaction with IKAROS could not be identified.

A case report on two pairs of monozygotic twins has identified the sequence of leukaemia initiating events in *BCR-ABL1*+ ALL (Cazzaniga et al., 2011). One pair of twins were discordant for ALL, with one twin developing *BCR-ABL1*+ ALL and the other remaining leukaemia free with low levels of *BCR-ABL1* present in their blood (around $1*10^{-4}$). Other leukaemia initiating events were required for malignant transformation and while the twin without ALL had other genetic changes present *IKZF1* remained intact, and the twin with ALL was positive for a deletion in *IKZF1.* In a second pair of twins, both developed *BCR-ABL1*+ ALL but with differing secondary aberrations, one of which was an *IKZF1* deletion and was the likely cause of treatment failure (Cazzaniga et al., 2011). *IKZF1* was not the only differing CNA, though previous murine models have shown that *IKZF1* lesions accelerate leukaemogenesis in *BCR-ABL1*+ ALL (Virely et al., 2010), and that the normal function of IKAROS pushes pre-leukaemic cells towards cell cycle exit in the presence of *BCR-ABL1* (Trageser et al., 2009). Monozygotic twins discordant for ALL are rare and so evidence is largely anecdotal, though analysis of these pairs of twins' ALL suggest that *IKZF1* is a secondary event to *BCR-ABL1* and arose postnatally.

This points to RAG over-activity being the initiating event, and that the occurrence of *IKZF1* lesions and the minor *BCR-ABL1* variant are potentially a product of this. Since the normal function of IKAROS is necessary for the expression of RAG in developing lymphocytes, the constitutive activation of RAG must be necessary prior to any *IKZF1* deletion or translocation events between chromosomes 9 and 22.

The data presented in this chapter suggests that IKAROS, RAG and TdT activity are altered in the presence of the Philadelphia chromosome, and that differences in MRD as detected by two different targets, Ig/TCR and *BCR-ABL1*, may be able to identify patients with distinct disease biology. However, it remains unclear as

to which MRD target is the better predictor of outcome in adult patients with *BCR-ABL1*+ ALL.

5 Lesions in *IKZF1* contribute to treatment resistance which is abolished by *BCR-ABL1* expression

5.1 Introduction

5.1.1 *IKZF1* lesions - importance of context

There have been numerous reports on the impact of *IKZF1* lesions on outcome from clinical trial studies, both in adult and paediatric patients but without consensus on the overall impact of *IKZF1* deletions (Δ*IKZF1*). Δ*IKZF1* was reported as being a strong prognostic marker in paediatric patients with high risk disease, and that these patients were more likely to have a gene expression pattern similar to that of the high risk *BCR-ABL1+* ALL (Mullighan et al., 2009). A specific profile, termed *IKZF1*plus has been developed in order to identify very high-risk paediatric ALL (Stanulla et al., 2018). Deletion type may also be important for outcome: Kobitzsch et al showed that LOF lesions and not DN deletions are a marker for poor outcome in *BCR-ABL1-* patients (Kobitzsch et al., 2017).

The overall results from these analyses suggests that the negative impact on outcome associated with Δ*IKZF1* is likely context dependent and may require the presence of other genetic lesions. Based on these studies, this chapter aims to model the contexts in which Δ*IKZF1* arises and to determine their impact on chemoresistance.

5.1.2 Corticosteroid resistance in ALL

Glucocorticoid steroids were among the first antileukemic agents to be used in the treatment of ALL and still play critical role in the clinic. Two of the most common corticosteroids used are prednisolone and dexamethasone, both synthetic derivatives of cortisol. They work by binding to the glucocorticoid receptor, which in turn effects change within the cell by altering gene expression, results in a reduction of cytokine production (Arya et al., 1984), and eventually cell cycle arrest and apoptosis (Wyllie, 1980, Harmon et al., 1979). The effect of corticosteroids is tissue dependent, but it is not yet clear why they have a specific pro-apoptotic effect in haematopoietic cells. Corticosteroid resistance has been

reported as an adverse prognostic factor in ALL, and that a shift in gene expression to increase glucose metabolism is a hallmark of this (Tissing et al., 2006, Hulleman et al., 2009).

Studies performed on trial populations have noted that post-induction residual MRD is more likely in paediatric patients with *IKZF1* deletions (Mullighan et al., 2009, Dorge et al., 2013). Treatment resistance brought about by *IKZF1* deletions is thought to be caused by the role of IKAROS in cellular metabolism. IKAROS is able to stop malignant transformation by blocking the increased uptake of glucose required for aerobic glycolysis. When IKAROS is non-functional, the block on the uptake of glucose is removed, and so a higher dose of corticosteroid is required to overcome the increase in glycolysis (Chan et al., 2017).

5.1.3 The Role of the Microenvironment in ALL treatment resistance

The bone marrow microenvironment supports the healthy development of haematopoietic cells. ALL cells are able to hijack this and form a niche capable of supporting leukaemic cells, thereby providing protection from therapeutic agents, i.e. contribute to resistant residual disease (Duan et al., 2014). To better refine models of treatment resistance in ALL, several studies have used mesenchymal stromal cells (MSCs) as a way of mimicking the bone marrow microenvironment. One such study found that certain drugs are more likely to induce niche formation based on ROS production, and that mitochondria were transferred from MSCs to leukaemic cells via tunnelling nanotubes (TNTs) (Burt et al., 2019).

IKAROS plays a role in the adhesion and migration of developing lymphocytes, and the loss of IKAROS function in ALL has been shown to contribute to disease resistance and an increase in dependency on stromal cells (Churchman et al., 2015, Joshi et al., 2014). ALL cells in contact with MSCs may alter their metabolic activity differentially depending on *IKZF1* status and whether other energy demanding cooperating lesions such as *BCR-ABL1* are present.

Based on the findings from chapter 3, *BCR-ABL1+* and *BCR-ABL1-* models were chosen due to the differential effect of the Philadelphia chromosome on outcome in ALL patients enrolled onto UKALL14. *BCR-ABL1+* ALL is also the largest subtype of ALL, and *IKZF1* is much more commonly deleted in this subgroup.

5.1.4 Approach taken in this chapter

I plan to establish models in order to observe the effects of *IKZF1* lesions by using *BCR-ABL1+* and *BCR-ABL1-* cell lines that do not harbour any *IKZF1* lesions. I will use retroviral transduction to over-express the isoform IK6 to model a DN lesion. I will use the CRISPR-cas9 system to knock out exon 8, the dimerisation domain, of *IKZF1* to model LOF lesions in *IKZF1* deleted ALL. **Figure 5.1** summarises the strategies used to generate the cell lines.
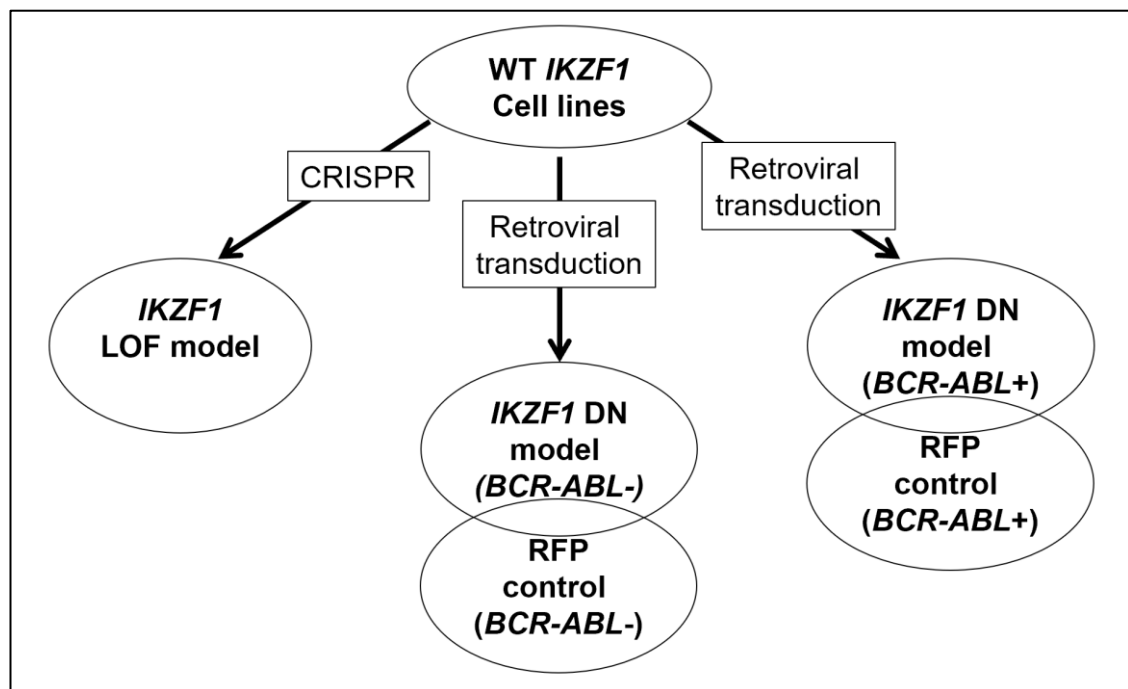
Figure 5.1: Figure 15: Strategies for modelling *IKZF1* lesions in vitro. In order to model the effects of *IKZF1* lesions in ALL cell lines, the models proposed are as follows: A DN model generated by retroviral transduction introducing IK6 into a *BCR-ABL1* positive and negative cell line. The cell lines used must have both alleles of *IKZF1* intact. An LOF model will be generated through knockout of exon 8 using CRISPR-Cas9 technology.

5.2 Hypothesis

Lesions in *IKZF1* contribute differently to treatment resistance in *BCR-ABL1+* and *BCR-ABL1-* cell line models.

5.2.1 Aims

- To generate both DN and LOF *IKZF1* cell line models
- To study the effects of *IKZF1* lesions on treatment resistance
- To study the effects of mesenchymal stromal cells on treatment resistance in the context of *IKZF1* lesions

5.3 Methods

5.3.1 PCR confirmation of p190 plasmid

To confirm the correct plasmid containing the p190 fusion protein was selected prior to retroviral transduction, PCR amplification of the p190 *BCR-ABL1* fusion gene was performed. To each reaction the following was added: 12.8μl ddH$_2$O, 3μl 10x reaction buffer, 2.5μl forward primer (Merck), 2.5μl reverse primer (Merck), 0.2μl TAQ polymerase (Qiagen), 2mM dNTPs (Promega), 4μl DNA/dH$_2$O for the NTC. Primer sequences are as follows:

Forward- 5'-ACCGCATGTTCCGGGACAAAA G-3'

Reverse- 5'-TGTTGACTGGCGTGATGTAGTTGCTTGG-3'

Cycling conditions can be found in **Table 5.1**. PCR products were run on a 2% agarose gel for one hour at 150mV.

Table 5.1: Cycling conditions for PCR amplification of *BCR-ABL1* transcript

Step	Cycling condition
1	96°C for 5 minutes
2	96°C for 1 minute
3	64°C for 50 seconds
4	72°C for 1 minute
5	Repeat steps 2-4 for 34 more times
6	72°C for 10 minutes
7	4°C forever

5.4   Results

5.4.1   Generation of NALM-6 and SD-1 IK6

In order to further investigate the apparent context dependent prognostic relevance of *IKZF1* lesions, two B-ALL cell lines, NALM-6 (*BCR-ABL1*-) and SD-1 (*BCR-ABL1*+) were retrovirally transduced with a plasmid overexpressing the DN IK6 isoform of the IKAROS protein (**Figure 5.2A**). Prior to the retroviral transduction of NALM-6 and SD-1 cell lines, selection of the correct plasmid was confirmed by PCR (**Figure 5.2B**). After the cell lines were retrovirally transduced, they were flow-sorted on mRFP expression, and the population enriched until mRFP expression by >95% of the population was achieved (**Figure 5.3**).
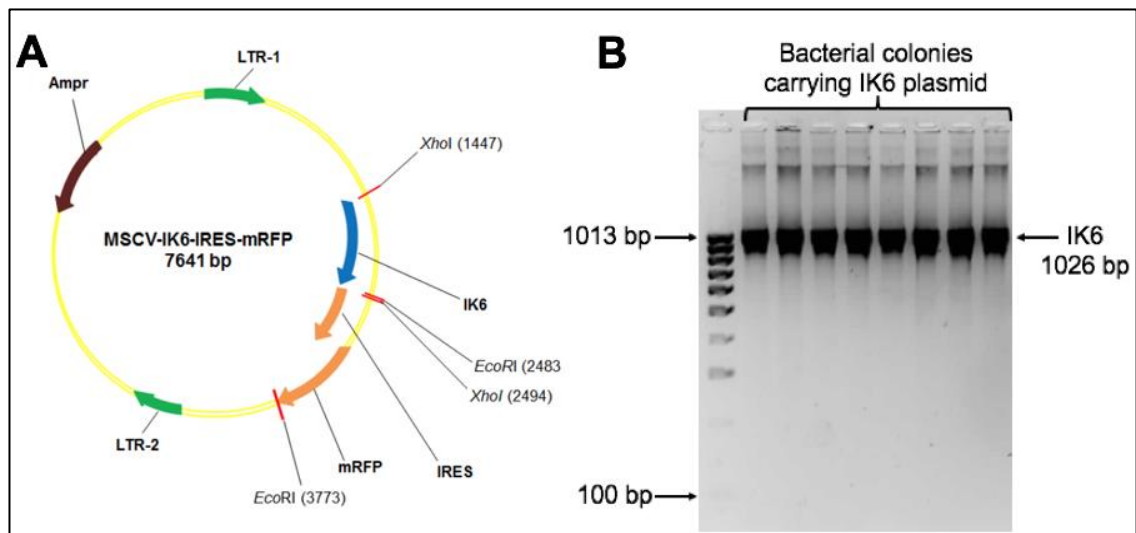
Figure 5.2: MSCV IK6 IRES mRFP plasmid. (A) Schematic diagram of MSCV IK6, the plasmid used for the retroviral transduction of the *BCR-ABL* negative NALM-6 cell line and the *BCR-ABL* positive SD-1 cell line. The plasmid either contained the DN IK6 (MSCV IK6) gene or was removed (MSCV EV) to serve as a negative control. **(B)** Agarose gel showing strong PCR product signal, indicating correct bacterial colonies were selected. After cloning, the IK6 gene was amplified to ensure the correct plasmid had been selected for.
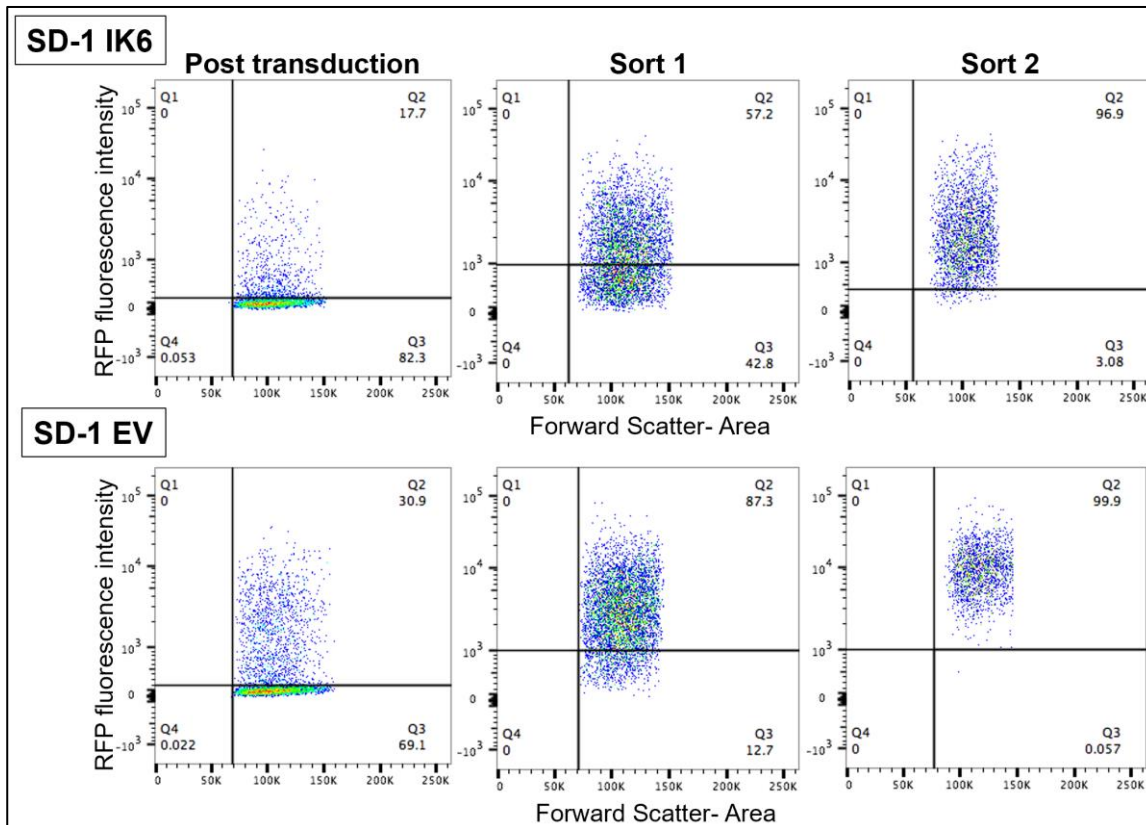
Figure 5.3: Flow plots after flow sorting on mRFP expression. SD-1 cells were sorted twice post induction to achieve RFP positivity of at least 95%. SD-1 WT cells served as a negative control. Side scatter height and area were plotted in order to remove cell doublets from the analysis. Top panel- SD-1 IK6 cells Bottom panel- SD-1 EV cells after initial transduction, and subsequent enrichment of mRFP positivity following two further flow sorts.

5.4.2 Generation of LOF *IKZF1* model by CRISPR

The CRISPR-Cas9 system was used to knock out exon 8 in the NALM-6 cell line. Exon 8 was chosen as the target as this is where the zinc fingers that mediate dimerisation reside. IKAROS activity becomes reduced and wild type proteins non-functional when IKAROS is not able to dimerise. Indeed, myeloma cells die when the IKAROS dimerisation domain is knocked out due to their dependence on IKAROS to function normally (Fedele et al., 2018). After exposure to the CRISPR-guide RNA complex, cells were single cell sorted based on their positivity for ATTO550, the fluorophore conjugated to the CRISPR nucleoprotein. A PCR screen was used to confirm the disruption of exon 8. The primers were first validated using five separate aliquots of DNA pooled from twelve healthy controls as used in Ig/TCR RT-qPCR assays (non-amplifiable control, NAC) (**Figure 5.4**).
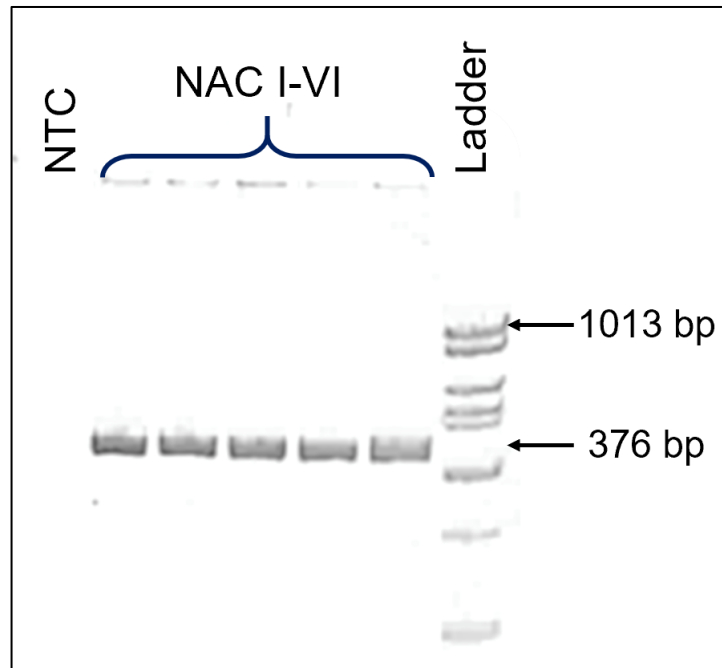
Figure 5.4: Validation of primers for CRISPR screening. An image of an acrylamide gel confirming the primers amplified exon 8 of *IKZF1* correctly. Pooled genomic DNA (Non-amplifiable control, NAC) from healthy controls was used to validate the primers for the PCR CRISPR screen.

After sorting, 381/960 (39.7%) wells containing single cells successfully grew into colonies. The first 36 were screened for disruption of exon 8. 10/36 (25%) displayed disruption at the exon 8 locus, as multiple PCR products of different sizes were observed (**Figure 5.5**). Clones from wells A4 and A8 were chosen for subsequent experimentation, since the PCR signals on the acrylamide gel were strongest for these wells. In order to confirm the differences between germline and the disrupted clones, PCR products were picked from the acrylamide gel and re-amplified in order to Sanger sequence the products. The Sanger sequencing data was not interpretable due to more than one sequence present in the reaction, and so successful disruption of exon eight of *IKZF1* could not be confirmed.
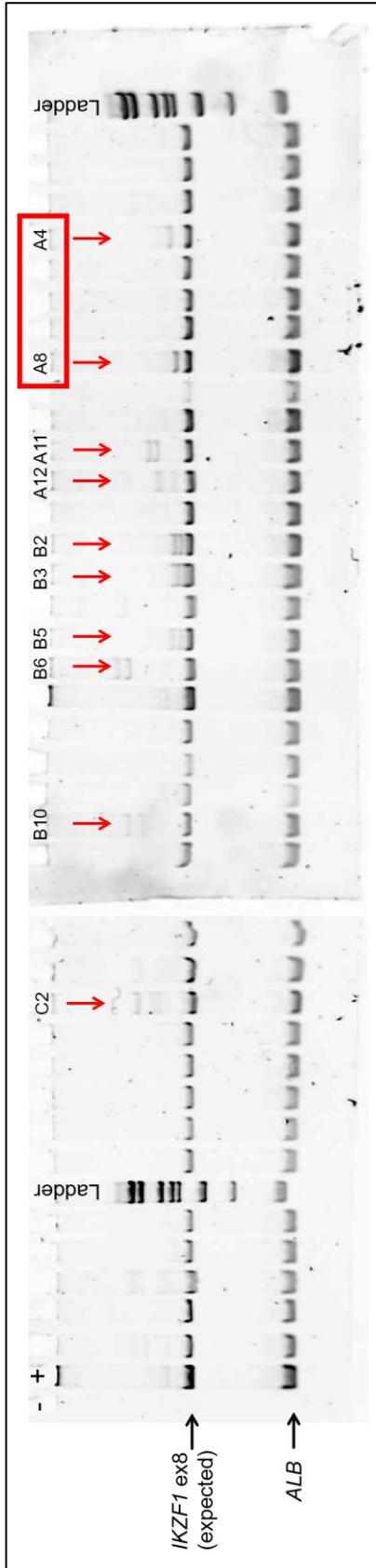
Figure 5.5: PCR screen for CRISPR disruption. After NALM-6 cells were exposed to the CRISPR-gRNA complex, DNA was extracted from the first 36 cultures that had successfully grown out and IKZF1 ex8 was amplified to identify clones that display disruption at that locus. The *ALB* gene served as an internal control for DNA quality. Red arrows indicate clones that have undergone disruption at the ex8 locus, i.e., a band of an unexpected size. The red box indicates the clones used in subsequent experiments.

5.4.3 Drug sensitivity of NALM-6 IK6 and SD1 IK6 compared to wild type cells

Previous studies found that *IKZF1* deletions contribute to treatment resistance in murine models (Marke et al., 2015) and trial populations (Imamura et al., 2016). Drug sensitivity assays were performed. The four drugs were chosen as they are commonly used in the treatment of adult ALL. The optimal cell number for the assay was established so as to be within the linear range of the assay resulting in a choice of cell number of $1*10^5$ in 100µL media for this experiment (**Figure 5.6**).
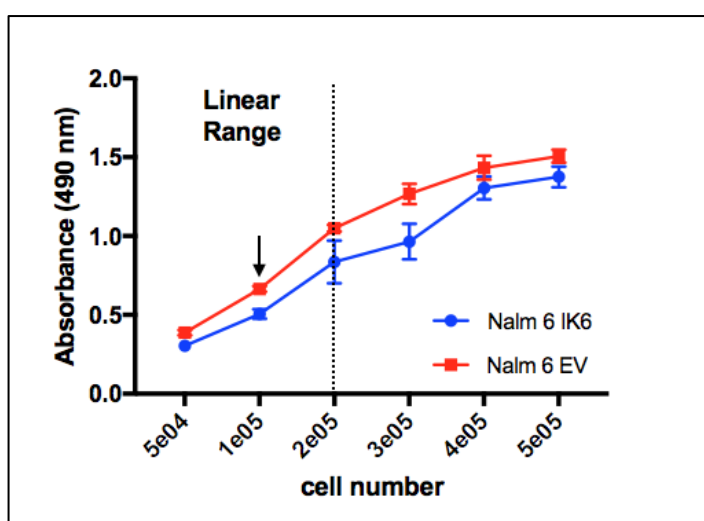
Figure 5.6: Optimal cell number for MTS assays. Cell viability was assessed by MTS assay and absorbance was measured between three and four hours of exposure to MTS solution Based on the linear range of the assay, $1*10^5$ cell per well was in subsequent drug sensitivity assays (indicated by arrow). Error bars represent SD of the mean.

There was no difference between NALM-6 IK6 and NALM-6 EV cell lines in sensitivity to cytarabine, daunorubicin or vincristine at any concentration and three timepoints (**Figure 5.7A**, **B** and **C**). By contrast, when the cells were treated with dexamethasone, the IK6 cell line had a higher cell viability at 72 hours. There was a statistically significant difference in cell viability at 500nM of dexamethasone between the IK6 and EV cells, suggesting that the presence of the DN IK6 protein contributes to glucocorticoid resistance in this *BCR-ABL1* negative model (**Figure 5.7D**). In the same experiment performed on SD-1 cells

no such difference was observed after exposure to dexamethasone (**Figure 5.8**). The SD-1 cell line was resistant to both cytarabine and dexamethasone (**Figure 5.8A** and **D**), even at higher concentrations (**Figure 5.9A and B**). Hence, SD-1 was rejected as a model for investigating chemoresistance induced by IK6.
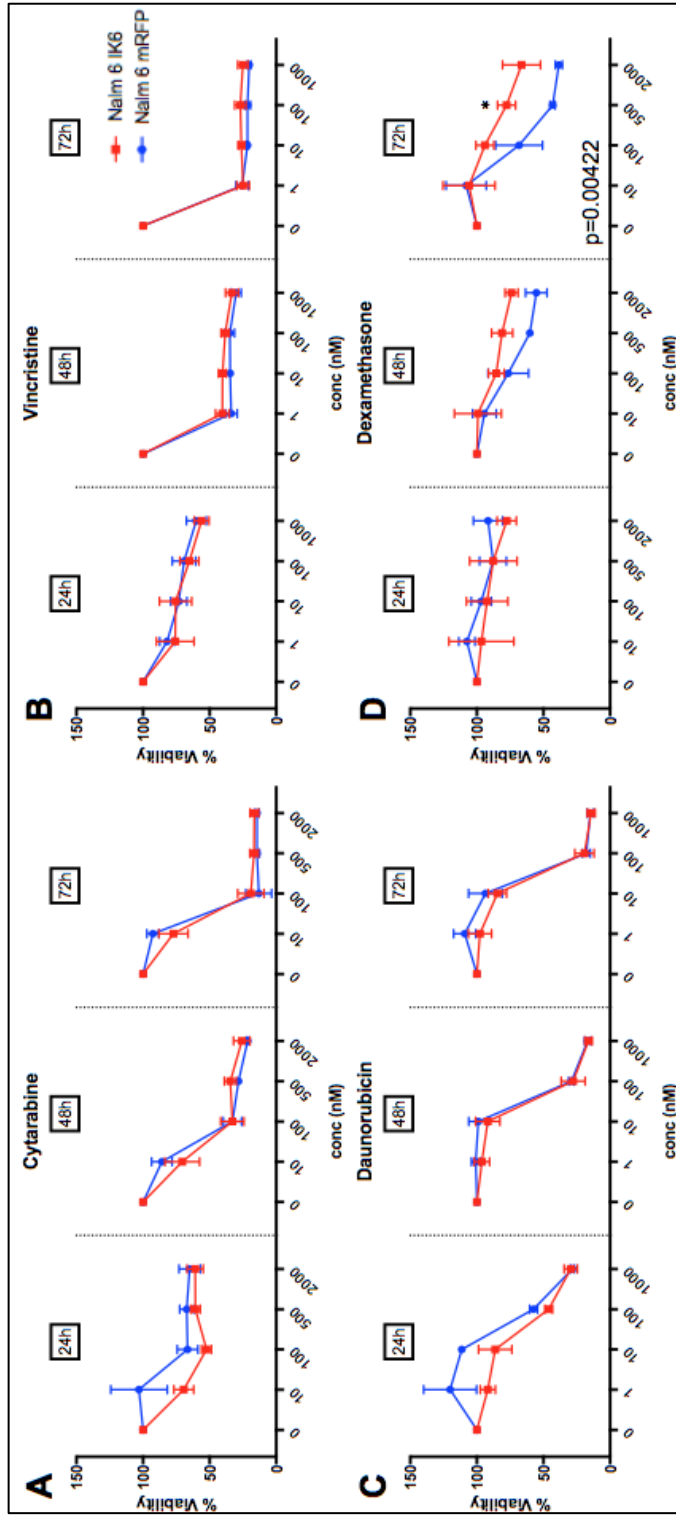
Figure 5.7: Drug Sensitivity in NALM6 IK6 expressing cell vs mRFP control. Cell viability was assessed by MTS assay and absorbance was measured between three and four hours of exposure to MTS solution. Experiments were done in triplicate at 3 different timepoints- 24, 48 and 72 hours. The no drug control in each for each drug was defined as 100% viability for each experiment. Error bars represent SD of the mean. Performed for four different drugs (A) Cytarabine, (B) Vincristine, (C) Daunorubicin, (D) Dexamethasone. N=3
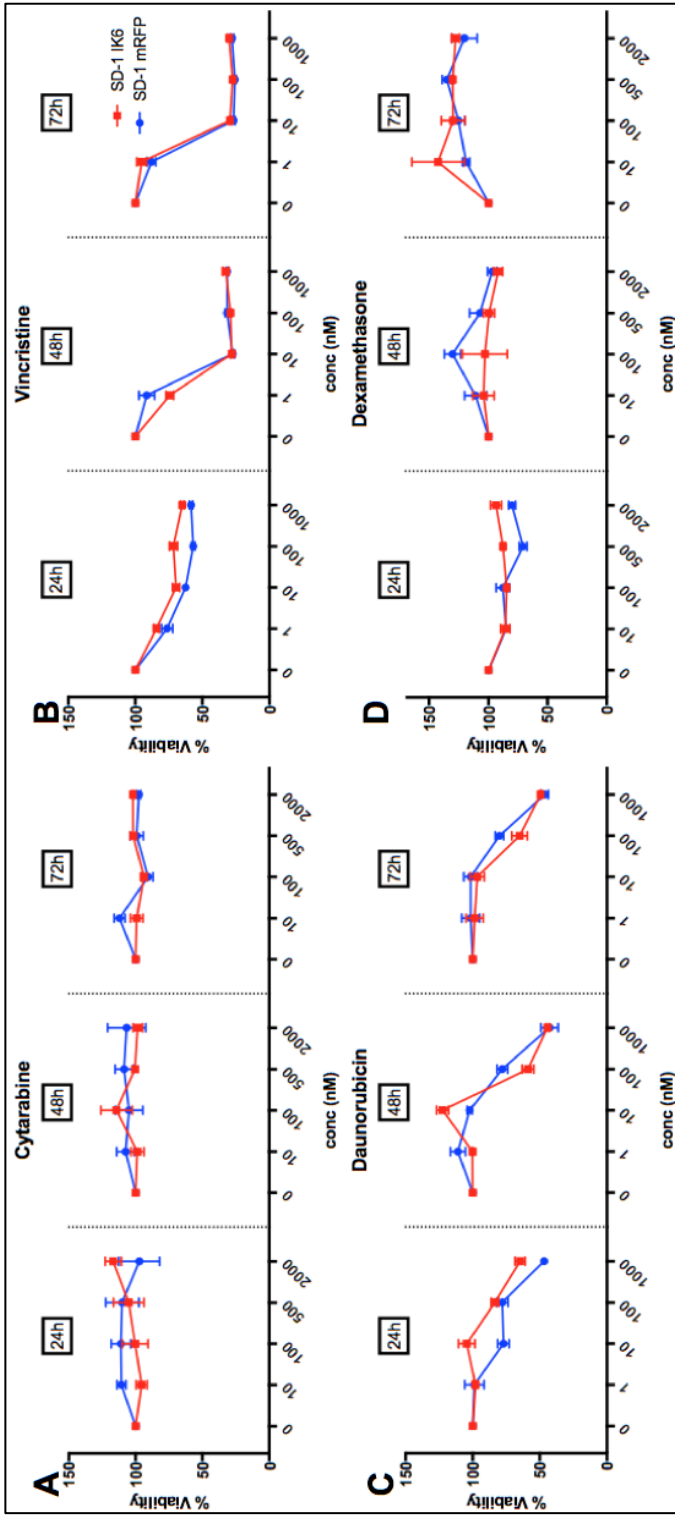
Figure 5.8: Drug Sensitivity in SD-1 IK6 expressing cell vs mRFP control. The SD-1 IK6 RFP expressing cell line and RFP only control were assessed by MTS assay to determine cell viability. Experiments were done in triplicate at three different timepoints- 24, 48 and 72 hours. The no drug control in each for each drug was defined as 100% viability for each experiment. Error bars represent SD of the mean. Performed for four different drugs (A) Cytarabine, (B) Vincristine, (C) Daunorubicin, (D) Dexamethasone. N=3

142
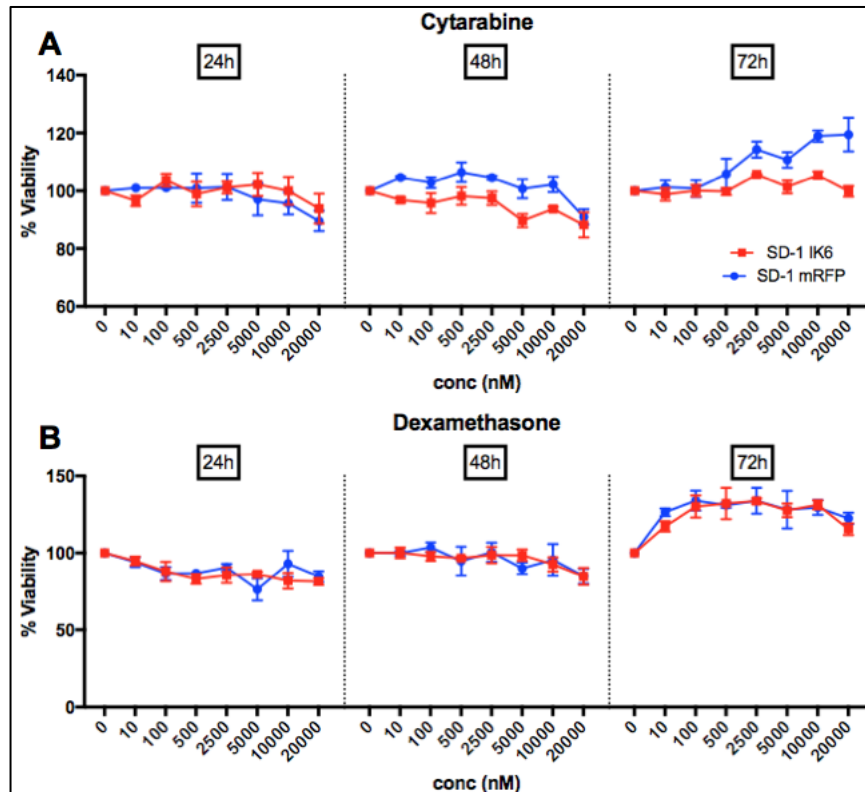
Figure 5.9: Drug Sensitivity in SD-1 IK6 expressing cell vs mRFP control, confirming resistance for cytarabine and dexamethasone. To assess the extent of their resistance, SD-1 cells were exposed to higher concentrations of cytarabine and dexamethasone via MTS assay. Experiments were done in triplicate at three different timepoints- 24, 48 and 72 hours. The no drug control in each for each drug was defined as 100% viability for each experiment. Error bars represent SD of the mean. **(A)** Cytarabine, **(B)** Dexamethasone. N=1

5.4.4 Generation of NALM-6 IK6 *BCR-ABL1+* model

As the SD-1 cell line was rejected as a suitable model due to baseline dexamethasone resistance, a *BCR-ABL1+* model was still required to examine the effects of *IKZF1* lesions in this context based on the results from the clinical outcome data. It was not possible to find an *IKZF1* wild type *BCR-ABL1+* cell lines, hence I decided to introduce a plasmid expressing a p190 fusion transcript- or the backbone alone as a control- to NALM-6 cells previously transduced with IK6. The p190 transcript was chosen as this is the most commonly occurring transcript in *BCR-ABL1+* B-ALL. The marker in the p190 plasmid is GFP, so the existing RFP did not interfere when selecting for the successfully transduced cells. **Figure 5.10** shows that the correct plasmid was selected prior to transduction.
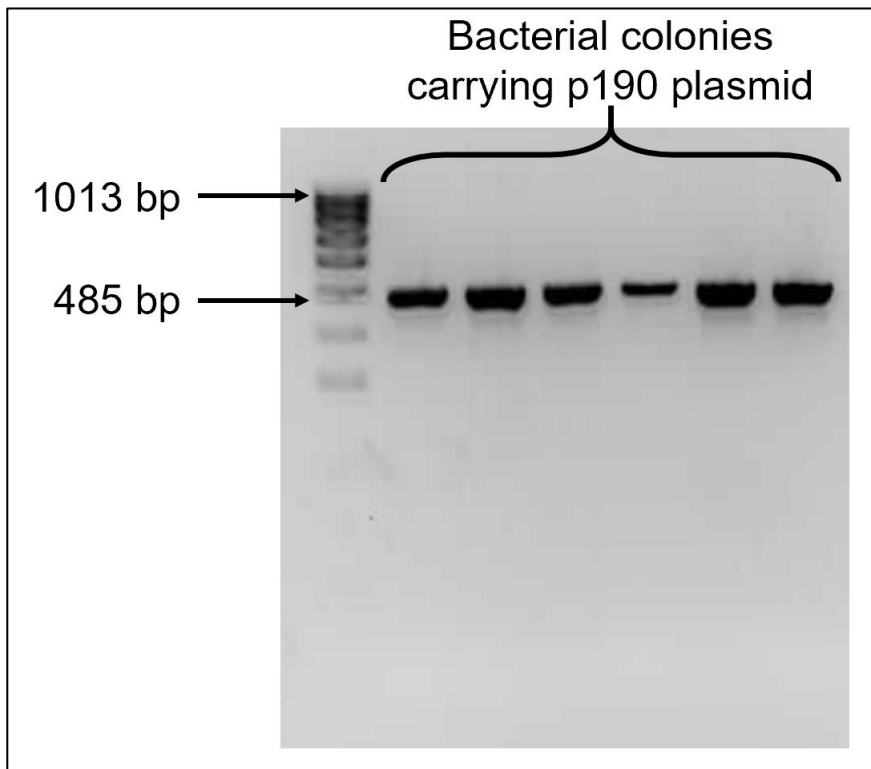
Figure 5.10: Agarose gel showing the correct plasmid was selected for. After cloning, the p190 fusion transcript was amplified to ensure the correct plasmid had been selected for in six clones. PCR products were run on a 2% agarose gel.

After transduction with the correct plasmid, the cells were flow sorted until RFP and GFP positivity reached >95%. This performed in a similar manner to the NALM-6 IK6 and RFP controls. Both GFP and RFP markers were used to identify the successfully transduced cells were selected and enriched >95% of the population (**Figure 5.11**). To ensure the p190 transcript was present, RT-qPCR was performed for all four cell lines. *GUS*, a control gene, was quantified in order to test the quality of the cDNA (

Table 5.2). The four cell lines are referred to as NALM-6 IK6 GFP, IK6 p190, RFP p190, and RFP GFP hereafter.
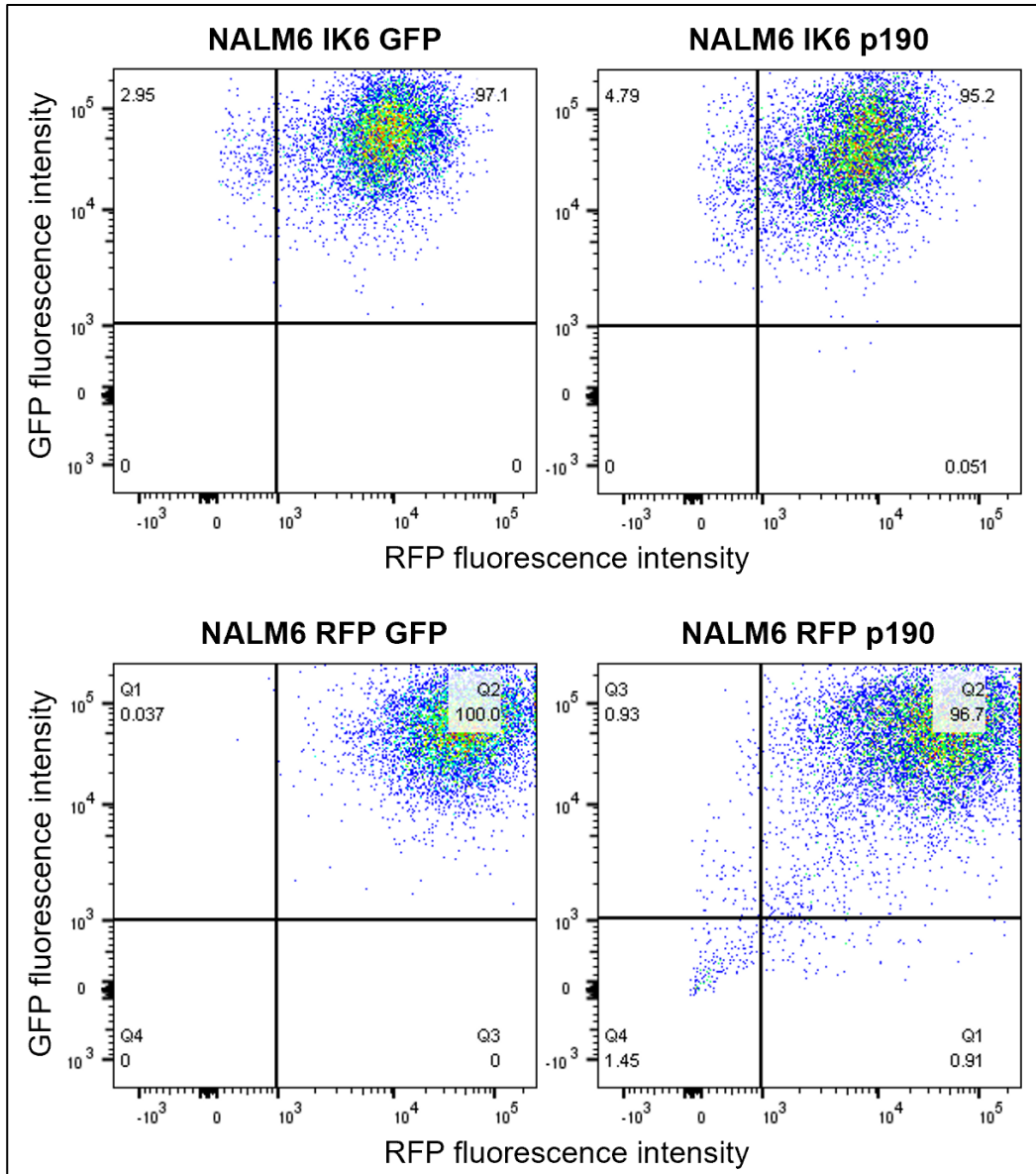
Figure 5.11: Flow plots after flow sorting on RFP and GFP positivity.
Flow plots to check for >95% positivity for each of the four RFP and GFP
positive cell lines generated after enrichment by flow sorting. Prior to plotting
the GFP and RFP fluorescence intensity, side scatter area and height were
plotted to remove cell doublets from the analysis. NALM-6 WT cells served
as a negative control to ensure the gates were set appropriately.

146

Table 5.2: Results from p190 and *GUS* transcript level quantification

Sample	GUS		p190		BCR-ABL:GUS ratio
	Average Ct	No. of molecules	Average Ct	No. of molecules	
RFP p190	21.40	371668.88	19.10	2965392.75	797.859%
IK6 p190	22.00	226298.31	18.60	3034964.5	1341.134%
RFP GFP	22.20	198059.11	0.00	0.00	0.00%
IK6 GFP	22.00	322811.00	0.00	0.00	0.00%

5.4.5 The presence of *BCR-ABL1* diminishes IK6 induced corticosteroid resistance in the NALM-6 DN cell line model

Since corticosteroid resistance is linked to an increase in glucose metabolism, and that *BCR-ABL1* exerts a high energy demand, dexamethasone resistance was assessed in the p190 cell line models. As expected, the same significant difference in sensitivity seen in the NALM-6 IK6 and RFP control (72h, 100nM p=0.042, 500nM p=0.042) was also seen in the NALM-6 IK6 GFP and RFP GFP cell lines (**Figure 5.12A**), though this same pattern was not evident in the p190 cell lines (**Figure 5.2B**). The presence of p190 alone increased dexamethasone resistance in NALM-6 cells (72h, 500nM p=0.039, **Figure 5.12C**) but the increased resistance of either IK6 or p190 alone is not evident when both are present in the same model, best demonstrated in **Figure 5.12D** at 72 hours.
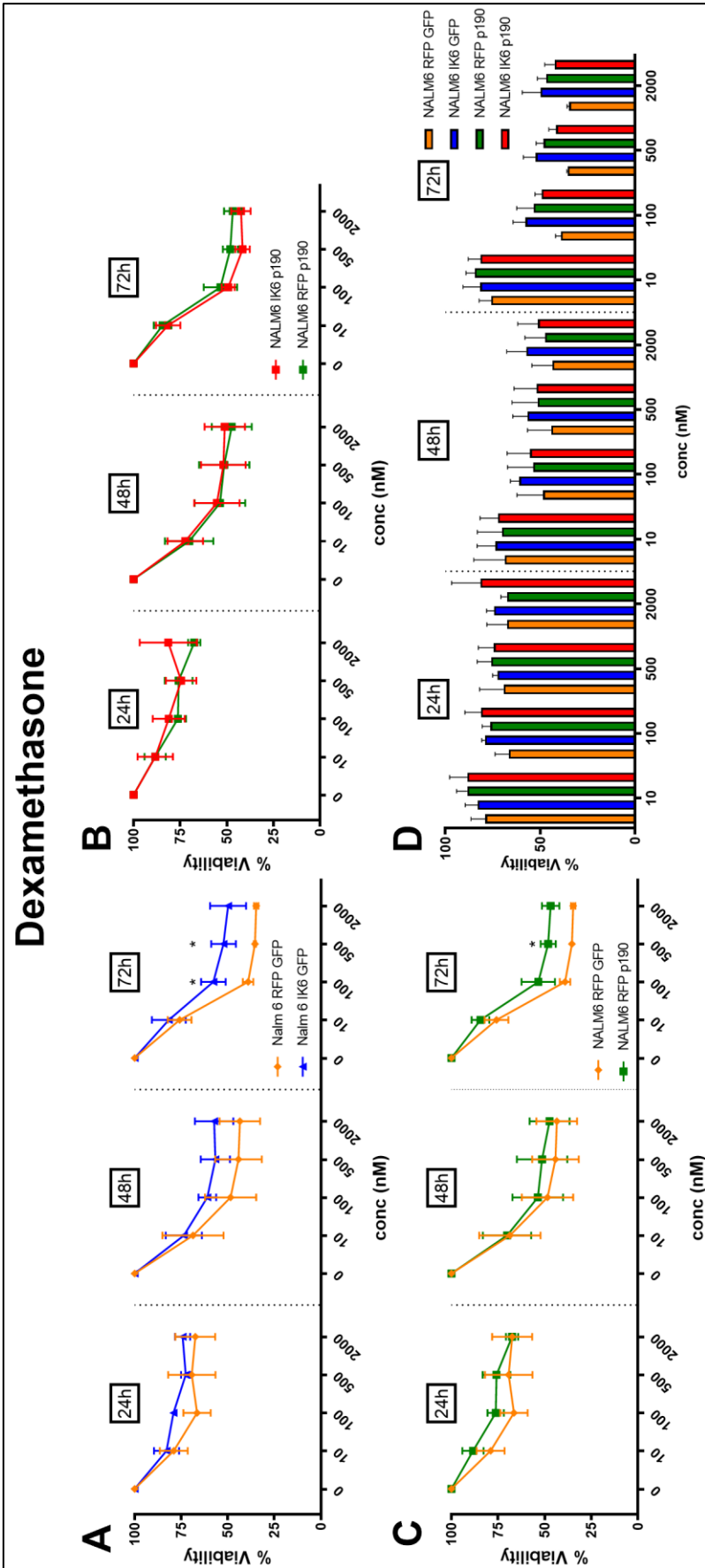
Figure 5.12: Dexamethasone sensitivity assays for NALM-6 IK6, p190 and RFP and GFP controls. To examine the effect of IK6 and *BCR-ABL1* on sensitivity the dexamethasone, each of the four cell lines was exposed to the dexamethasone at three different timepoints in triplicate- 24, 48 and 72 hours. Cell viability was assessed by MTS assay. The no drug control was defined as 100% viability for each experiment. Error bars represent SD of the mean. The asterisks represent a significant difference in viability of $p<0.05$ (A) NALM6 RFP and IK6 GFP controls only (B) NALM6 RFP and IK6 p190 cell lines only (C) NALM6 RFP GFP and p190 cell lines only (D) a comparison of all cell lines on a bar graph to make interpretation easier. N=3

5.4.6 Role of stromal cells

5.4.6.1   MTS is not a suitable method of assessment

The role of IKAROS in the adhesion and migration of cells within the bone marrow niche plays an important role in treatment resistance (Schwickert et al., 2014). The role of the bone marrow microenvironment in treatment resistance is of interest to my host laboratory and is an ongoing project. Loss of Ikaros in a murine model arrests cells in an adherent phase dependent on stroma for survival (Joshi et al., 2014). Mesenchymal stromal cells have shown to be critical for the survival of ALL cells in the bone marrow niche (Ebinger et al., 2016, Duan et al., 2014), and that MSCs themselves secrete adhesion molecules (Wagner et al., 2007). Therefore, loss of IKAROS or the expression of a DN isoform could potentially have a different effect on treatment resistance in the presence of stromal cells.

I used the model developed in my host laboratory, in which the human MSC cell line HS27a is used as a stromal layer. First, the performance of drug sensitivity assays were evaluated using the IK6 DN models. HS27a cells alone were exposed to dexamethasone to ensure this cell line was not sensitive at the concentrations used. **Figure 5.13** shows that HS27a viability did not drop below 90% for any concentration at any of the three timepoints. Next, three conditions were tested by MTS assay- ALL cells alone, HS27a cells alone and MSC and ALL cells in co-culture. The intention was to subtract the mean absorbance value from the HS27a cells from that of the co-culture values in order to ascertain how much of the viability in each well was attributable to the ALL cells. This method of assessing viability did not give reliable and consistent results (**Figure 5.14A** and **B**). It was also not possible to ascertain if any apparent differences in cell survival are due to the increased cell survival of the ALL cells, or an increase in metabolic activity. For this reason, flow cytometric based cell viability was used to assess viability in the co-culture models.
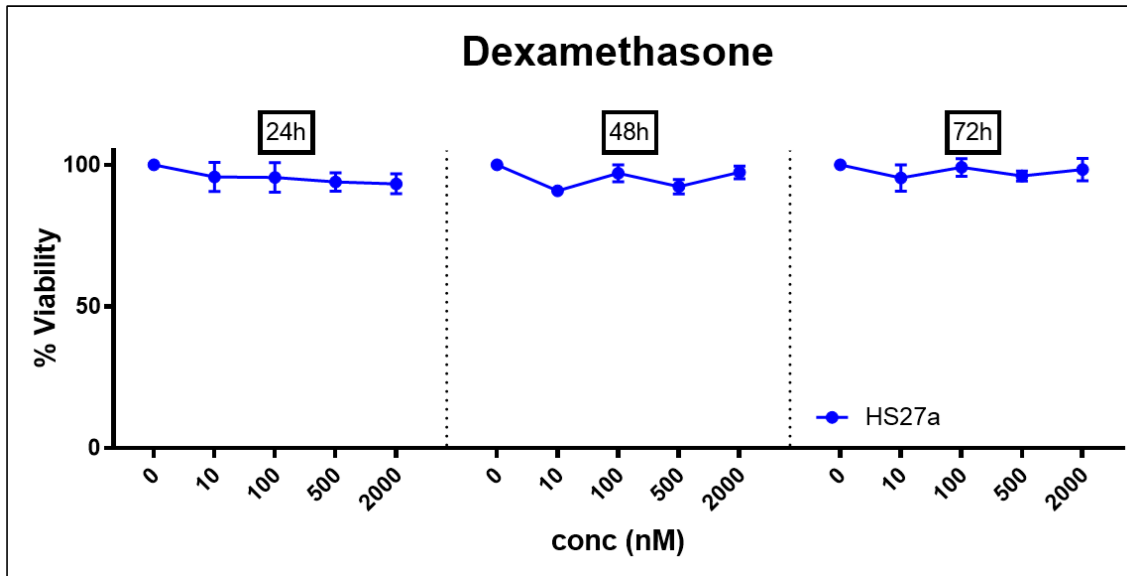
Figure 5.13: HS27a dexamethasone sensitivity assay. The HS27a cell line was exposed to four different concentrations of dexamethasone and assessed by MTS assay to confirm that the cell line was not sensitive, and viability was not reduced. The no drug control was defined as 100% viability for each experiment. Error bars represent SD of the mean. Performed at three different timepoints used in subsequent coculture expeirments- 24, 48, and 72 hours. N=1
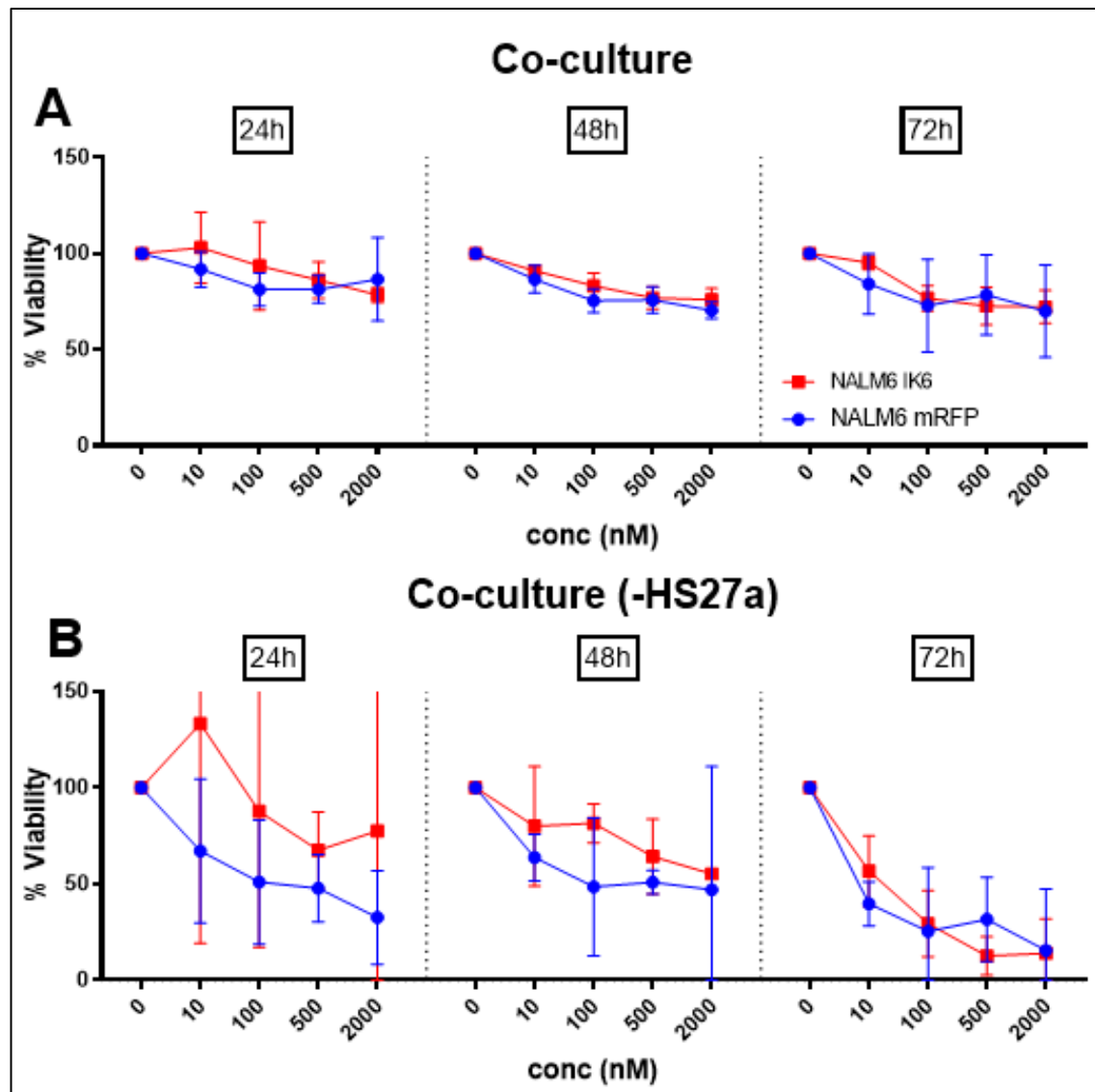
Figure 5.14: MTS coculture assays. MTS was assessed for its suitability for use in coculture assays. The no drug control was defined as 100% viability for each experiment. Error bars represent SD of the mean. Performed at three different timepoints- 24, 48 and 72 hours. (A) Viability based on total absorbance (B) Viability based on mean absorbance values of HS27a subtracted from absorbance values of co-culture wells. N=3

5.4.6.2 Flow cytometric analysis of drug sensitivity gives consistent results for co-culture assays

The ability to gate on individual cell populations when using flow cytometry to assess cell viability makes it more suitable than MTS assays for co-culture experiments. RFP and GFP were used as the marker for the four cell lines- IK6 p190, IK6 GFP, RFP p190 and the RFP GFP control. Representative flow plots can be seen in **Figure 5.15**. The stromal layer appears to provide a protective effect to ALL cells when exposed to dexamethasone regardless of *IKZF1* or *BCR-*

ABL1 status since all cell lines have enhanced survival when cultured with HS27a cells compared to the respective monoculture controls at 72 hours in particular (**Figure 5.16A**). The flow results reflect those of the monoculture MTS assays in that the IK6 and p190 only cell lines display lower cell death when exposed to dexamethasone compared to the RFP GFP controls (**Figure 5.12A** and **C**, **Figure 5.16A** and **C**). Again, reflective of the MTS assays, the *BCR-ABL1* fusion protein in the IK6 p190 cell line appears to abolish the ability of the DN IK6 protein to resist dexamethasone mediated cell death in monoculture and coculture (**Figure 5.12B and Figure 5.16B** and **C**). Despite previous findings by Lopez and colleagues showing that loss of IKAROS leads to the arrest of cells in an adherent state (Lopez et al., 2002), the presence of the stromal layer with IK6 does not appear to enhance resistance to dexamethasone when compared to the monoculture experiments (**Figure 5.16B** and **C**).
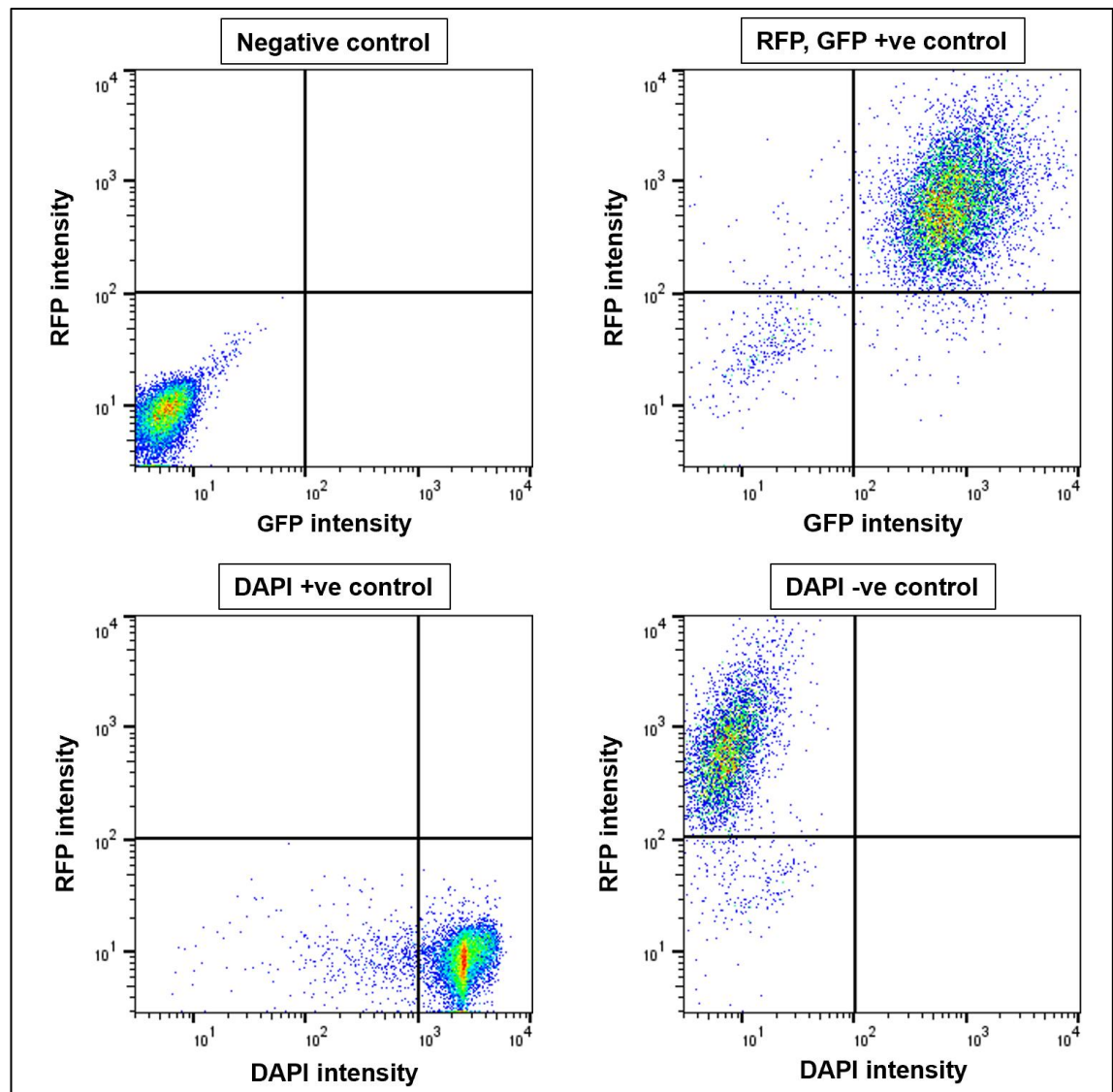
Figure 5.15: Representative flow plots for coculture experiments. To select the desired cell population, initially single cells were selected by plotting side scatter area and height, removing any cell doublets. To select the correct gating strategy, NALM-6 WT cells were used as a negative unstained control (top left panel). To ensure only the ALL cells were being analysed, only RFP and GFP positive cells were selected for (top right panel). NALM-6 WT cells were incubated for at least 15 minutes at 60°C in a water bath to kill them, and stained with the DAPI to serve as a positive control for DAPI positive cells (bottom left panel). RFP and GFP positive cells were analysed without the DAPI stain to confirm the gates had been set correctly (bottom right panel). N=3.
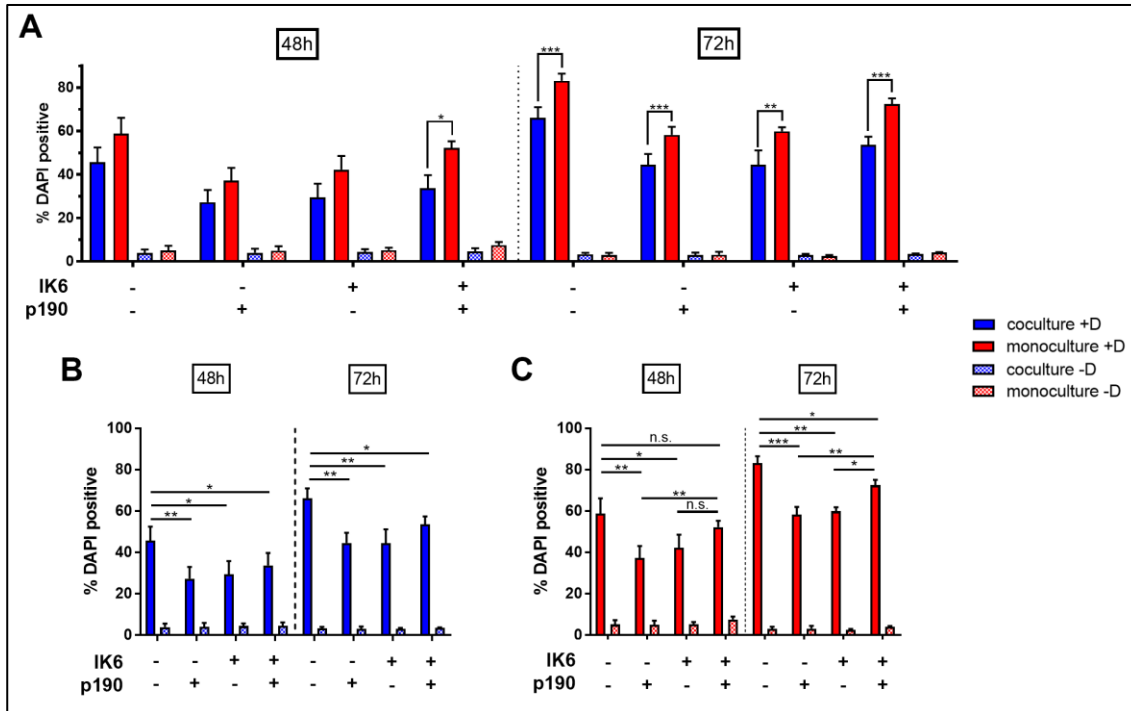
Figure 5.16: Coculture flow cytometry assays. To examine the effects of stromal cells on ALL cell viability and resistance to dexamethasone, NALM-6 IK6 cells were cultured with and without the MSC cell line HS27a. ALL cells were cultured +/- dexamethasone and +/- HS27a cells and assessed for DAPI positivity at two timepoints- 48h and 72h. The percentage of positive cells is based on the bulk population positive for RFP and GFP. Experiments were done in triplicate at each time point. Error bars represent SD of the mean **(A)** data for all conditions **(B)** coculture only **(C)** monoculture only. *p<0.5, **p<0.05, ***p<0.005. "D"=dexamethasone. N=3.

5.4.7 Loss of IKAROS function leads to increased resistance when exposed to dexamethasone in the NALM-6 cell line

As with DN drug sensitivity assays, daunorubicin, cytarabine, dexamethasone and vincristine were used. As was seen in the DN IK6 expressing NALM-6 cell line, no difference in sensitivity was observed between either of the A4 an A8 LOF cell lines and the WT control when exposed to daunorubicin (**Figure 5.17C**). Unlike the IK6 cell line, in the A8 LOF cell line in particular, an increased viability was seen at 48h and 72h when exposed to cytarabine (**Figure 5.17A**, 48h: 500nM p=0.043, 2000nM p=0.019, 72h: 500nM p=0.009, 2000nM p=0.007) and vincristine (**Figure 5.17B**, 48h: 1000nM p=0.029, 72h: 1000nM p=0.022). A significant difference in viability at both 48h (100nM p=0.018, 500nM p=0.017, 2000nM p=0.021) and 72h (10n p=0.021 (A8 LOF), 100nM p= 0.006 (A8 LOF), p= 0.013 (A4 LOF), 500nM p=0.005 (A8 LOF), 2000nM p=0.0007 (A8 LOF)) was

also observed when the A4 LOF and A8 LOF cell lines were exposed to dexamethasone, consistent with the results from the DN drug sensitivity assays. There was a differential sensitivity between the A4 and A8 LOF clones, most pronounced for when exposed to dexamethasone, despite successful knockout of exon eight in both clones (**Figure 5.17D**).
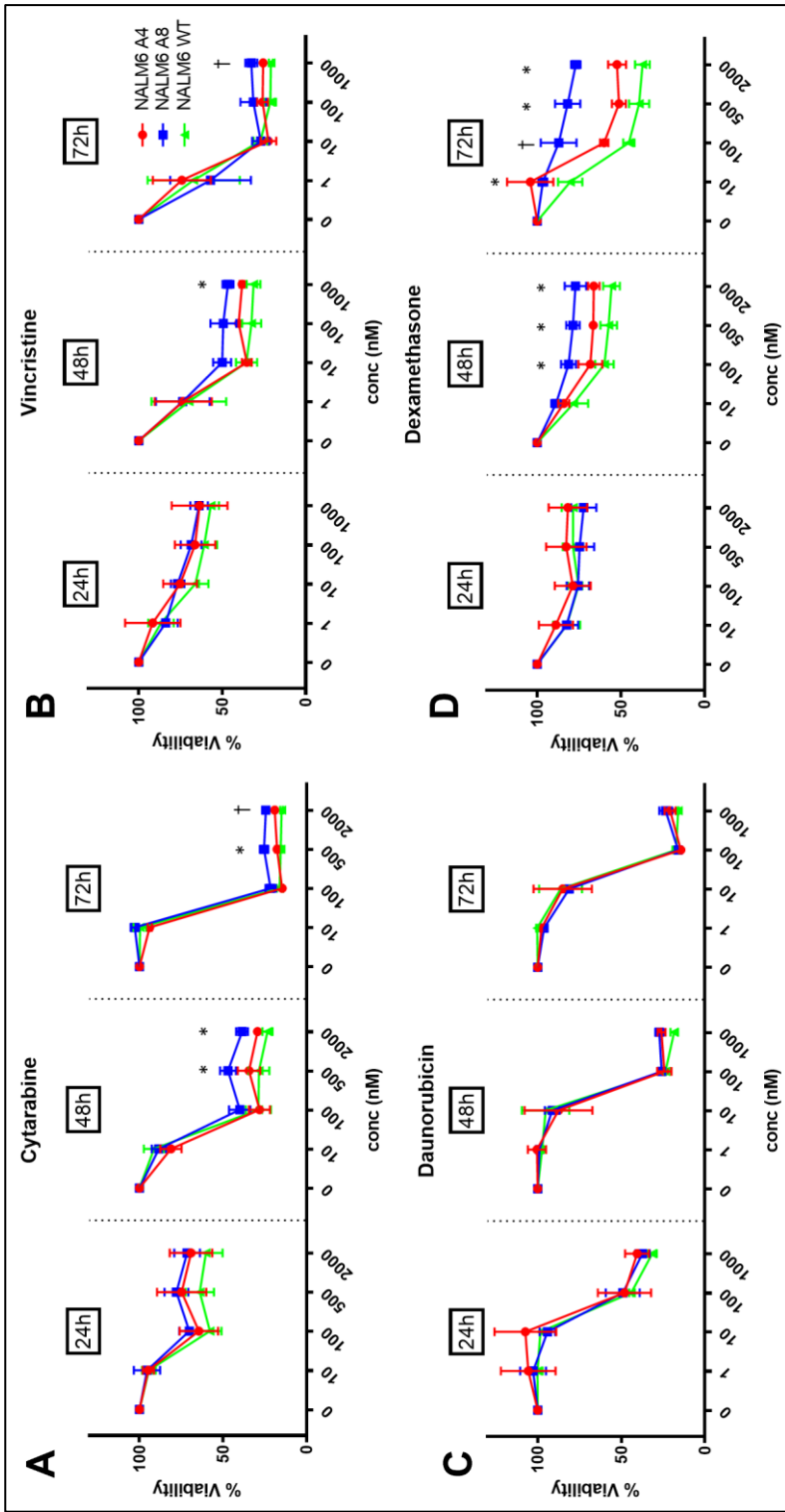
Figure 5.17: Drug Sensitivity in NALM-6 A4 LOF and A8 LOF clones vs WT control. To test the effects of LOF lesions on drug sensitivity, two cell lines NALM-6 A4 and A8 were exposed to four drugs commonly used in the treatment of ALL. Experiments were done in triplicate at three different timepoints- 24, 48 and 72 hours. The no drug control in each for each drug was defined as 100% viability for each experiment. Error bars represent SD of the mean. * represents $p<0.05$ for A8 v WT only, † represents $p<0.05$ for A4 LOF v WT and A8 LOF v WT. Performed for four different drugs **(A)** Cytarabine, **(B)** Vincristine, **(C)** Daunorubicin, **(D)** Dexamethasone. N=3.

5.5   Discussion

In this chapter, I have explored the potential ways in which *IKZF1* lesions lead to a more aggressive phenotype in several ALL cell line models. As seen in the drug sensitivity assays, the presence of IK6 confers resistance to the corticosteroid dexamethasone only, and not to cytarabine, daunorubicin or vincristine. This further confirms previous studies' findings in both the clinic and the laboratory setting that have also found that a loss of IKAROS causes resistance to corticosteroids. Corticosteroids play a critical role the in treatment of ALL, and if the *IKZF1* status of a patient is known it may be possible to overcome this resistance with altered treatment regimens.

As *IKZF1* lesions and the *BCR-ABL1* fusion often co-occur, it was necessary to test this also. The *BCR-ABL1* positive SD-1 cell line was initially transduced with the DN IK6 isoform but was rejected as a model due to its resistance to dexamethasone even at very high concentrations, and a dose dependent response was not seen. For this reason, the existing DN NALM-6 model was successfully transduced with the *BCR-ABL1* p190 fusion protein.

The results from the drug sensitivity assays on *BCR-ABL1* positive cell lines were unexpected. The presence of *BCR-ABL1* alone did increase resistance to dexamethasone in comparison to the NALM-6 RFP GFP control. While *IKZF1* deletions and the Philadelphia chromosome often co-occur, the presence of both of these lesions do not appear to give a survival advantage in this model, or indeed in the trial population enrolled on UKALL14 studied in chapter 3. This is does not confirm the findings of previous studies.

The Philadelphia chromosome exerts a high metabolic demand since it promotes cellular proliferation and is able to increase glucose metabolism to facilitate this (Kim et al., 2005). It is thought that lesions in *IKZF1* are necessary for malignant transformation by lifting the block on glucose uptake and metabolism. The cause of the decreased resistance could also be that while there is high expression of *BCR-ABL1* (**Table 5.2**) the expression of *BCR-ABL1* alone is not able to exert the necessary changes in the metabolic profile of the cell necessary for corticosteroid

resistance since other cooperating lesions (aside from *IKZF1*) are required, thereby not giving any survival advantage in this model. The NALM-6 cell line used in this model is *BCR-ABL1* negative, and the addition of this oncogene into an already established ALL cell may simply not be sufficient for the apparent resistance normally observed in *BCR-ABL1* positive ALL in the clinic. Other cooperating lesions during leukaemogenesis of *BCR-ABL1* positive ALL may need to be acquired in order for *BCR-ABL1* to exploit the cellular metabolic programme. One possible explanation is that both endogenous WT alleles of *IKZF1* are still intact and are able to overcome the presence of IK6, and to block the increased uptake of glucose demanded by *BCR-ABL1*.

If the presence of *BCR-ABL1* was not able to sufficiently increase glucose uptake and metabolism required in the NALM-6 cell line, then corticosteroids may be able to better exploit the increased metabolic pressure exerted by the presence of *BCR-ABL1.* This dependence on glucose is demonstrated by *BCR-ABL1+* CML cells displaying a high affinity to the glucose transporter GLUT-1, and a subsequent reduction in cell surface GLUT-1 when treated with imatinib (Barnes et al., 2005). More recently, *BCR-ABL1+* B-ALL cells were found to be dependent on the GLUT-1 transporter for survival and growth *in vivo* (Liu et al., 2014). This dependency on glucose uptake caused by the presence of *BCR-ABL1* could in turn increase sensitivity to corticosteroids. Based on the data presented in this chapter, the deletion of *IKZF1* is simply a hallmark of *BCR-ABL1+* ALL since it does not enhance the pro-leukaemic effects of *BCR-ABL1*, is purely coincidental, and does not exert a selective pressure or evolutionary advantage to the leukaemic cell.

The reduction in cell viability in the *BCR-ABL1* positive models could also be due to a flaw in the cell line model since it may not have all conditions necessary to display a more aggressive phenotype upon exposure to dexamethasone. *IKZF1* along with the transcription factor *PAX5* can be described as "metabolic gatekeepers" and lesions in these genes are required for malignant transformation due to an increased demand for glucose utilisation (Chan et al., 2017). It has been previously shown that lesions in *PAX5* are required to remove

the restriction on glucose uptake and metabolism (as seen in the "Warburg effect") that is necessary for leukaemogenesis (Chan et al., 2017), though there is no such lesion present in *PAX5* in NALM-6 cells.

Since there are a number of different lesions that affect *IKZF1* function, it was necessary to model these also. The deletion of exons 4-7 still allows for the expression of the DN IK6 isoform as the transcription start site and dimerisation domain remain intact. Other lesions either deleting the entire gene, or involving the transcription start site in exon 2 or dimerisation domain in exon 8 cause a loss of function of IKAROS. This is thought to lead to a less aggressive phenotype than a DN lesion as it leaves the other allele intact and fully functional, unlike in the presence of IK6. To model LOF lesions, loss of IKAROS was successfully achieved by using the CRISPR-Cas9 system to knock out exon 8 where the dimerisation domain resides. The loss of this domain led to a significantly higher viability compared to the WT NALM-6 cell line when exposed to vincristine and cytarabine, as well as dexamethasone. No such difference was seen for daunorubicin, as with the IK6 model. The apparent resistance to cytarabine could potentially be due to the specific vulnerability of leukaemic cells during the S-phase of the cell cycle, the point at which cytarabine can damage and prevent DNA synthesis (Li et al., 2012). This is the point at which there is also a reduction in IKAROS DNA binding activity. With the loss of IKAROS in the model, it could potentially allow for cells to enter a prolonged S-phase of the cell cycle and so a higher concentration of cytarabine is required for the same level of efficacy. Cell cycle analysis of these models when challenged with antileukaemic agents could confirm this. The potential cause of the vincristine resistance in this LOF model is less clear, though it has been previously reported that *IKZF1* null cells are modestly resistant to vincristine *in vitro* (Rogers et al., 2018).

Despite successful knockout of exon eight in *IKZF1* in both A4 and A8 LOF cell lines as seen in the PCR products for these clones (**Figure 5.5**), a differential sensitivity to dexamethasone was observed between them (**Figure 5.17D**). This could be due to the random nature of TdT and NHEJ when repairing locus after

CRISPR disruption. However, without the sanger sequencing data, it is not possible to confirm this.

The resistance to these agents *in vitro* is not consistent with the clinical data presented in chapter 3. No difference in outcome was observed between *IKZF1* deleted vs non-deleted patients. There are significant differences in the way this resistance was modelled *in vitro* as compared to the clinical setting. Monotherapy is not typical for the treatment of ALL in the clinic, as seen in the cell line models, and so further testing of multiple agents simultaneously would better refine this.

The higher level of resistance to vincristine and cytarabine in the A4 and A8 LOF cell lines as compared to the DN cell line was not expected. The DN isoforms of IKAROS are thought to also render WT IKAROS non-functional and so has a greater effect than an LOF deletion in *IKZF1*. This could be caused by the way both of these cell lines were generated. Expression of IK6 via retroviral transduction leaves both genomic copies of *IKZF1* intact. There are two strategies using the current models to rule out if this is what is causing the apparent higher sensitivity. The first involves knocking out one of the WT alleles using the CRISPR-Cas9 system as used to generate the A4 and A8 LOF cell lines. Alternatively, the CRISPR-Cas9 system could be used to remove exons 4-7 in WT NALM-6 cells in order to induce expression of IK6.

Use of a stromal layer has allowed for a more accurate model of the bone marrow microenvironment when testing drug sensitivity. Stromal cells have been shown to be critical in the response of ALL cells to therapeutic agents. While this was not well tested via MTS assay, flow cytometric analysis gave consistent and reliable results. Loss of IKAROS is known to cause cell cycle arrest at a stage where cells exhibit a high level of adhesion (Joshi et al., 2014). While the stromal layer appears to give a protective effect to all cell lines regardless of lesions present, it does not appear that the presence of IK6 enhances the protective effects of the stromal layer compared to the IK6 negative cell lines despite any potential interaction brought about by increased adhesion. My laboratory has already demonstrated that MSCs can provide support to ALL cells in the BM niche

via TNTs (Burt et al., 2019). With these cells in closer proximity to the supportive MSC layer, the ability to form TNTs should be more efficient as there would be more physical contact between the two cell types within the BM niche, though this has not been seen here. There are further questions to be answered on exactly how MSCs could be providing support and contributing to resistance.

This experiment focussed on dexamethasone, mainly due to the results from the initial drug sensitivity analysis performed on the DN IK6 model. While there was no difference in resistance to vincristine, cytarabine or daunorubicin, the presence of MSCs may cause a differential effect as they may provide additional support to IK6 expressing cells because of the altered adhesion and increased physical proximity to the supporting stromal layer.

Together these data confirm that loss of IKAROS, either by LOF or DN activity, lead to increased resistance to dexamethasone in the DN IK6 model, and dexamethasone as well as vincristine and cytarabine in the A4 and A8 LOF models generated. The resistance observed in the DN IK6 model appears to be context dependent, since the presence of *BCR-ABL1* abolishes such resistance to dexamethasone.

5.5.1 Planned experiments

5.5.1.1 Metabolic reprogramming of leukaemic cells by Δ*IKZF1*

It has been known for a long time that malignant cells rely on aerobic glycolysis for ATP production, first described by Otto Warburg (Warburg et al., 1924). This is the process by which cancerous cells rely on glycolysis for their ATP production and not mitochondrial respiration. This process helps to protect cells against oxidative stress caused by mitochondrial respiration via the electron transport chain. The intermediate steps of glycolysis supplies metabolites for fatty acid synthesis, pentose phosphate pathway and amino acid synthesis, all of which are required for an increased rate of proliferation and is caused by oncogenic signalling and external environmental pressures.

Certain genetic lesions result in very high energy demands within the cell; the fusion gene *BCR-ABL1* is an example of this. The tyrosine kinase *BCR-ABL1* promotes an increased uptake of glucose via the hexose transporter GLUT-1, and it has been shown that *BCR-ABL1*+ B-ALL is partially reliant on this transporter for cell survival (Liu et al., 2014). The use of TKIs have been shown to reduce glucose utilisation, and use of the mitochondrial inhibitor oligomycin enhances the sensitivity of leukaemic cells to TKI treatment (Alvarez-Calderon et al., 2015).

IKAROS, along with another transcription factor PAX5, are known to block malignant transformation, by not allowing an increase in uptake and utilisation of glucose required for elevated rates of proliferation seen in cancerous cells (Chan et al., 2017). *IKZF1* lesions and the subsequent inactivation of IKAROS often co-occur with *BCR-ABL1* in adult ALL. This could be necessary for an altered metabolic programme in order to meet the increased energetic demand from *BCR-ABL1*.

Further experimentation was planned in order to gain a better understanding of the metabolic reprogramming leukaemic cells undergo when *IKZF1* becomes deleted. Analysis of the levels of aerobic and anaerobic respiration were to be analysed by measuring oxygen consumption and extracellular acidification rates via Seahorse analysis (Agilent technologies) in these cell lines when exposed to corticosteroids. Further analysis of the gene expression profiles by RNA sequencing of the cell line models developed for this project was also planned in the hope of giving an explanation as to why corticosteroid resistance was observed and the unexpected results in the *BCR-ABL1*+ cell lines. In light of the Covid-19 pandemic, these experiments were unfortunately abandoned.

6 General Conclusions

This thesis presents an investigation into the context dependent impact of Δ*IKZF1* in the clinic and experimentally. This is in response to the mounting evidence that Δ*IKZF1* has an adverse effect on patient outcome. The data presented in this thesis has contributed to the substantial body of clinical data on Δ*IKZF1* in patients with B-ALL. Since no impact on outcome was found, it is of importance that this is taken into consideration for the management of patients with ALL in the future. The subsequent parts of this thesis attempt to address the differential impact of the Philadelphia chromosome on RAG activity on the deleted *IKZF1* locus and also on the Ig/TCR rearrangements. Finally, the impact of Δ*IKZF1* on drug sensitivity was examined to ascertain why *IKZF1* lesions might have an impact on outcome.

6.1 The chicken or the egg?

The title of this thesis "*IKZF1* lesions in adult acute lymphoblastic leukaemia - the chicken or the egg?" refers to the mechanisms that cause the common intragenic lesions in *IKZF1*. *IKZF1* lesions carry the hallmarks of RAG mediated deletion, as the breakpoints commonly occur at putative cRSSs and a number of non-germline nucleotides are present. Since *IKZF1* is involved in the expression of the RAG enzyme machinery, it remains unclear exactly which of these proteins is cause and effect. The initial plan for this project was to use an assay to study the direct activity of RAG. Based on current technology such as SM-FRET and tethered bead assays, it is not possible to do this within a leukaemic cell.

In terms of addressing the question in the title of this thesis, the data presented here do go some way giving an answer. As a direct measurement of RAG activity was not possible, and as a way of studying the hallmarks of RAG activity, the Ig/TCR rearrangements were assessed in *IKZF1* deleted versus non deleted ALL specimens. *IKZF1* deleted specimens were more likely to have at least one Ig/TCR rearrangement present especially in the presence of *BCR-ABL1* (**Table 4.6**), and had a significantly higher average number of rearrangements when

compared with *IKZF1* non-deleted (**Figure 4.4**). Since RAG mediates both Ig/TCR rearrangements and the intragenic deletions of *IKZF1*, it would appear the aberrant RAG activity is higher in *IKZF1* deleted cells. While it is not possible to determine why this might be, it suggests one of two possible reasons:

1. The baseline RAG activity is higher in certain subtypes of ALL prior to the loss of IKAROS, after which RAG expression would be abolished due to the lack of IKAROS protein

2. RAG expression has been de-regulated, IKAROS has lost control over its expression and the off-target activity of RAG has deleted *IKZF1*, allowing RAG to rearrange the Ig/TCR loci.

Had the Covid-19 pandemic not halted experiments, it may have been possible to ascertain at which points these events occur during clonal evolution via next generation sequencing techniques. Unfortunately, it is not possible to know at what point RAG becomes constitutively expressed, the Ig/TCR loci are rearranged, or when *IKZF1* becomes deleted during malignant transformation and so the initial question cannot be fully answered.

6.2 *IKZF1* lesions do not contribute to poor outcome in B-ALL patients on UKALL14

In order to examine the impact of Δ*IKZF1* on outcome in patients with B-ALL, patients recruited onto the UKALL14 trial were screened by PCR and validated by MLPA for the four most common lesions found in *IKZF1*. The results from the clinical data presented in Chapter 3 contradict the working hypothesis that Δ*IKZF1* does have an impact on patient outcome. Δ*IKZF1* had no impact on outcome regardless of how the data was analysed. It is unlikely this finding is not genuine- patient follow up time and the number of patients analysed on the study are adequate for sufficient statistical power. There are some potential reasons no impact was found. Firstly, this is the oldest population studied for Δ*IKZF1*. It may simply be the case that Δ*IKZF1* only has a strong association with poor outcome in paediatric patients, first seen in a study by Mullighan and colleagues (Mullighan et al., 2008). Secondly, a significant proportion of patients on UKALL14 were considered having high risk features and hence went onto have an SCT as per

the trail protocol. It is possible that transplant may have masked the effects of Δ*IKZF1* on outcome in these high-risk patients. This data is potentially of particular importance to older patients with ALL, especially as the prevalence of *BCR-ABL1+* ALL positively correlates with age. To investigate this further, assessing trials recruiting older patients may be of importance, such as the phase II UKALL60+ trial. Alternatively, if future trials are examined for Δ*IKZF1*, patients should be assessed separately based on their age. In order to refine the analyses on the impact of Δ*IKZF1* in older patients with ALL, a meta-analysis involving a broad range of age and risk status could help to identify any age-related impact on outcome.

IKZF1 lesions are likely context dependent, hence why *IKZF1*plus was investigated in chapter 3. This was made possible as a large proportion of patients were screened by an MLPA kit that covered most of the genes involved in the *IKZF1*plus profile. As with *IKZF1* alone, *IKZF1*plus did not have an impact on outcome. However, in the initial study performed by Stanulla and colleagues, only high-risk paediatric patients were included (Stanulla et al., 2018). Patients of any risk status were included for the analysis presented in chapter 3, and, again, patients recruited to UKALL14 were adult rather than paediatric. This could be the reason why no association with poor outcome was found. Despite this, the development of the profile itself points towards the impact of Δ*IKZF1* on outcome being context dependent and requires other cooperating lesions, specifically in high-risk paediatric patients. To strengthen the analyses on older adults, this needs to be expanded to include other trial populations, and the risk status of these patients should be considered.

Where possible, patients were screened by both PCR and MLPA. It was evident that neither MLPA nor PCR are not sufficient to detect Δ*IKZF1* alone due to their limitations. While both methods are rapid, neither captured the entire landscape of Δ*IKZF1* since both methods missed patients that were positive for *IKZF1* lesions. This is best demonstrated by the large number of discrepancies between the PCR and MLPA data. While PCR is highly sensitive and can deliver a rapid result, it is limited by its specificity and vulnerable to false negative results if primer

sites become deleted. In contrast, MLPA can detect a deletion of any size but sensitivity is not adequate to detect deletions in minor clones or where sample purity is low.

Higher resolution techniques such as NGS as used in the 100,000 genomes project are necessary for tailoring treatment to each individual and will be vital for personalised medicine in the future. This could be utilised to detect any lesion affecting *IKZF1* including SNPs that have been identified as damaging to IKAROS function and lesions affecting the promoter and hence expression of *IKZF1*. NGS would also be able to detect minor and subclones at diagnosis, though it is not clear if sublcones harbouring Δ*IKZF1* contribute to poor outcome in the same way as in major clones. Some studies have found that only major clones contribute to poor outcome in patients.

IKZF1 lesions can also be used as a sensitive marker in detected MRD levels, and is a direct measure of disease levels unlike Ig/TCR. A comparison of *IKZF1* MRD and *BCR-ABL1* may be more informative. *IKZF1* based MRD was only performed for a small number of patients and 4-7 lesions. There is scope to expand this analysis and, if material were available, a comparison between Δ*IKZF1* and *BCR-ABL1* based MRD would be possible, similar to the analysis in chapter 4.

6.3 A comparison of Ig/TCR and *BCR-ABL1* based MRD monitoring

The results in chapter 4 attempted to compare Ig/TCR and *BCR-ABL1* based MRD. It was not possible ascertain if either Ig/TCR or *BCR-ABL1* based MRD monitoring is a more accurate method of predicting outcome in patients with *BCR-ABL1*+ disease. This is likely, in part, because of the small number of patients included in this study. There is scope to expand on this by completing Ig/TCR screening on patients with *BCR-ABL1*+ ALL with sufficient material on UKALL14. Something yet to be explored is why were there differences in MRD levels between Ig/TCR and *BCR-ABL1*. If available cells stored from the diagnostic

specimens were available, it would be possible to use flow cytometric analysis. If the Philadelphia chromosome were present in non- B-lymphoid haematopoietic subpopulations, it could indicate atypical disease biology as found by Hovorkova and colleagues in paediatric patients (Hovorkova et al., 2017).

In normal developing lymphocytes, IKAROS controls both access to the Ig/TCR loci and RAG activity (Reynaud et al., 2008). The intragenic lesions in *IKZF1* carry the hallmarks of RAG mediated deletion, and the impact of Δ*IKZF1* may be context dependent. The second part of Chapter 4 addressed the potential context dependent differences between *IKZF1* lesions in *BCR-ABL1+* versus *BCR-ABL1-* ALL. Aberrant RAG activity is potentially more common in *BCR-ABL1+* ALL as Δ*IKZF1* is more prevalent in this genetic subtype. Intragenic *IKZF1* breakpoints and insertions mediated by TdT activity appear to be affected by presence of Philadelphia chromosome. The breakpoints in *IKZF1* were significantly further away from the heptamer proximal to the breakpoint in patients with *BCR-ABL1+* ALL than *BCR-ABL1-* (p=0.043), and there was a trend towards this for the distal breakpoint (p=0.067). There were also significantly more non-germline nucleotides inserted at the breakpoint in *BCR-ABL1+* ALL (p=0.027).

With *IKZF1* deletions more common in *BCR-ABL1+* ALL, this points to interactions between *BCR-ABL1* and the off-target activity of RAG and subsequent repair of the DSB via the NHEJ pathway. It is not known if the pattern in these breakpoints as presented in chapter 4 are the same in other RAG deleted genes in ALL such as the glucocorticoid receptor gene *NR3C1*. In the absence of this, the number and type of Ig/TCR rearrangements were analysed. Further analysis via single cell sequencing reveal which Ig/TCR rearrangements were present in the cells with *IKZF1* or Philadelphia chromosome

An assay for directly measuring real-time RAG activity *in vitro* would be ideal for assessing its interaction with IKAROS. In the absence of this, the structure of *IKZF1* lesions, and the number and type of Ig/TCR rearrangements were analysed as surrogates for measuring RAG activity. Revealing the true interaction between RAG and IKAROS is key to further understanding pathogenesis in ALL,

especially in the context of the Philadelphia chromosome based on the findings in chapter 4. If directly measuring the RAG activity is not possible, or its off-target effects in pre-leukaemic cells, examining the clonal architecture of ALL specimens may provide answers at which point in its pathogenesis RAG becomes constitutively active, and when deletions mediated by RAG occur in genes like *IKZF1*.

6.4   Treatment resistance in *IKZF1* deleted cell line models

The results presented in chapter 5 demonstrate that *IKZF1* lesions do contribute to treatment resistance, despite no impact in outcome seen in the clinical data in chapter 3. In order to test the effects of *IKZF1* lesions in ALL, the NALM-6 cell line was transduced with DN IK6 isoform of IKAROS. To examine the effects LOF lesions in ALL and to generate an appropriate model, exon 8 of *IKZF1* was successfully disrupted by the CRISPR-Cas9 system in NALM-6 cells.

The DN and LOF models were assessed for their sensitivity to four drugs commonly used in the treatment of ALL: cytarabine, daunorubicin, dexamethasone and vincristine. There was no difference in sensitivity between the IK6 cell line and the negative controls aside from dexamethasone, where there was a significant difference found at 72 hours of treatment. The LOF model displayed resistance to dexamethasone, as well as cytarabine and vincristine. The increase in resistance to antileukaemic agents in the LOF model compared with DN was unexpected. DN isoforms are thought to me more deleterious than LOF lesions, since the IK6 protein also renders WT IKAROS when dimerised, whereas LOF lesions only affect the deleted allele. This observed difference could be due to how the cell lines were generated. Since IK6 expression was brought about by retroviral transduction, the two genomic alleles of *IKZF1* remained intact, and so the WT activity of IKAROS may not be totally abolished by the presence of IK6. To make a fairer comparison with the LOF model, a DN model could be generated using the CRISPR-Cas9 system to knock out exons 4-7 of *IKZF1*. The resistance to the corticosteroid dexamethasone seen in both DN and LOF cell line models may go some way to explain why patients positive for Δ*IKZF1* were more likely to be MRD positive at the end of induction therapy

where high doses of dexamethasone are administered as seen in the data from chapter three.

To develop the NALM-6 DN model, and to observe the impact of the Philadelphia chromosome on treatment resistance, the NALM-6 IK6 cell line was transduced further with the p190 variant of the *BCR-ABL1* fusion protein. Again, despite no differential impact seen in the context of the Philadelphia chromosome in chapter 3, the presence of the p190 fusion protein in the DN model had an unexpected detrimental effect on the resistance to dexamethasone conferred by the presence of the DN IK6 protein.

The resistance to dexamethasone observed in both the DN and LOF models has a metabolic basis. Corticosteroid resistance has been reported as an adverse prognostic factor in ALL, and an altered gene expression profile increasing glucose uptake in response to corticosteroid treatment is a hallmark of this (Hulleman et al., 2009). In healthy lymphocytes, IKAROS blocks malignant transformation by blocking the increase uptake of glucose required for malignant transformation (Chan et al., 2017). Revealing the metabolic reprogramming of *IKZF1* deleted cells will be key to understanding the mechanisms causing resistance. Prior to the COIVD-19 pandemic, metabolic analysis via Seahorse assays was planned in order to measure the oxygen consumption rate (OCR) and the extracellular acidification rate (ECAR), which are indirect measurements of aerobic and anaerobic respiration, respectively. The measurement of this is of particular importance particularly in response to dexamethasone treatment.

Another experiment planned prior to the outbreak of the COVID-19 pandemic was RNA sequencing of the cell line models after exposure to dexamethasone. This was planned in order to determine why any potential metabolic differences were observed from the seahorse assays. For example, a recent publication has described the way in which IKAROS down-regulates the expression of BCL-XL, anti-apoptotic mitochondrial transmembrane protein which leads to resistance to doxorubicin, dexamethasone and vincristine (Song et al., 2020). This is just one

of the myriad of proteins involved in mitochondrial processes whose expression is altered without functional IKAROS present.

The cytarabine resistance observed in the LOF cell lines could be investigated further. Cytarabine exploits cells during the S-phase of the cell cycle, the same point at which there is a reduction in the level of IKAROS (Li et al., 2012). Flow cytometric cell cycle analysis could provide answers as to why the LOF cell line displayed increased resistance to cytarabine, particularly if IKAROS deficient cells appeared to be entering a prolonged S-phase and hence required a higher concentration of cytarabine to overcome this.

Since IKAROS is involved in the adhesion and migration of developing lymphocytes (Schwickert et al., 2014), and loss of IKAROS arrests cells in an adherent state (Joshi et al., 2014), it was important to understand the role of supportive stromal layer in treatment resistance. The results from the flow cytometry experiment showed that the stromal layer provided support to the NALM-6 cell line, irrespective of the genetic aberrations present, and that despite loss of IKAROS leading to a more adherent state in a previous study, this was not observed here when compared to the controls.

There are some aspects to these experiments that may explain the differences between the clinical data and the *in vitro* cell line models. *In vitro* experiments are not the perfect model, they do not replicate the environment in which blast cells reside within a patients' bone marrow. All of these experiments only tested anti-leukaemic agents in monotherapy which does not mimic the way in which patients are treated.

Aside from the differences between what was observed clinically and the cell line model data, there are some other aspects to these experiments that could be developed further. LOF lesions were not explored within the context of the Philadelphia chromosome, which is necessary to complete the lesions that observed in patients with ALL. The other anti-leukaemic agents used in the monoculture experiments should be performed in coculture. While no difference

in sensitivity was seen in the DN cell line models, that does not mean to say the presence of the supportive stromal layer could enhance the ability of cells expressing IK6 to survive being challenged by cytarabine, daunorubicin, or vincristine.

6.5 Future plans

In order to address the contrasting results from the clinical data presented in Chapter 3, a wider meta-analysis would ideally be performed to reveal the true cause of this. Analyses should include patients with a broad range in age, risk status, and in the pre- and post- transplant setting. While the overall conclusion from other studies state that there is an association between poor outcome and *IKZF1* lesions, there is no clear message since the analyses have been in varying settings and trial populations. The current literature on the impact of *IKZF1* lesions in patients with ALL need to give a clear and concise message regarding its true impact.

The suitability of Δ*IKZF1* as an MRD marker was also presented in chapter 3. To confirm that it is indeed a suitable MRD marker, the small study in chapter 3 should be expanded. Although there was a fairly strong correlation of Δ*IKZF1* MRD with Ig/TCR MRD, it was not as convincing as previous studies (R^2=0.695, **Figure 3.5B**, Caye et al., R^2=0.9232, Venn et al., R^2=0.98). As well as expanding the number of DN lesions investigated, an assay for LOF lesions should also be developed and assessed, as only the Δ4-7 lesion in a relatively small sample size was considered in this project.

Where possible, an investigation into the discrepancies between Ig/TCR and *BCR-ABL1* MRD seen in the results from chapter 4 should be performed. Flow cytometric analysis and sorting of cells from the primary diagnostic specimens (where available) may give insights into which cells are *BCR-ABL1* positive, if the Ig/TCR rearrangements are present in the same clones, and if indeed there is the presence of a "CML like" biology in the patients where a discrepant result was seen. The differences in the number and type of Ig/TCR rearrangements between

IKZF1 deleted and non-deleted specimens may have a biological basis that requires further examination.

If and when it is possible to directly measure the activity of RAG in a leukaemic cell, it is critical that this is done to better understand the sequence of events which leads up to the intragenic deletion of *IKZF1*, and what exactly causes the differences in RAG activity. Only then will it be possible to attempt to address what this project set out to do. In the absence of such an assay, the clonal architecture of *IKZF1* deleted specimens could be studied through NGS techniques to ascertain the true sequence of events.

The cell line models generated in Chapter 5 require refinement. The DN IK6 expressing cell lines were generated through retroviral transduction, and so the two genomic alleles of *IKZF1* remain intact. A more "true to life" model could be generated through the knockout of exons 4-7 *IKZF1* using CRISPR-Cas9, as was the case with the LOF cell line. Furthermore, *BCR-ABL1* was only studied in the DN cell lines and should also be studied with LOF lesions also. This would not be difficult to achieve as the LOF cell lines could be transduced with the plasmids used for the DN cell lines. Despite seeing no enhanced effect of MSCs in coculture with *IKZF1* deleted cell lines in comparison to their WT controls, this could be explored further. IKAROS has been implicated in the adhesion and migration of cells within the BMM, and so lesions in *IKZF1* could affect how closely ALL cells interact with MSCs. As seen in previous work from my host laboratory, damaged mitochondria are transferred from ALL cells to MSCs via tunnelling nanotubes when exposed to ROS inducing chemotherapeutic agents. This may be of importance as *IKZF1* deletions affect the metabolic status of leukaemic cells, and there may be a difference in how leukaemic cells interact with supporting MSCs based on their *IKZF1* status.

Finally, as mentioned at the end of chapter 5, had the Covid-19 pandemic not halted all experimentation, the final part of this project would have investigated the metabolic activity associated with *IKZF1* deletions, and to ascertain if this is the true cause of corticosteroid resistance in *IKZF1* deleted cell lines. Analysis of

aerobic and anaerobic activity of the cell lines under different conditions generated in chapter 5 could be achieved by using a Seahorse instrument (Agilent Technologies). The conditions tested should include exposure to dexamethasone, and also limiting glucose supply to ascertain if *IKZF1* deleted cell lines are more dependent on glycolysis. RNA sequencing was also planned as a way of identifying the metabolic pathways that are up- and down-regulated depending on *IKZF1* status and the presence of dexamethasone.

7 Appendix

Table 7.1 Screening panel and primer pairs for the detection of clonal Ig/TCR rearrangements in patients with B-ALL on UKALL14

Mix	Well	Primers
1	A1	VH1-JHC
2	B1	VH2-JHC
3	C1	VH3-JHC
4	D1	VH4-JHC
5	E1	VH5-JHC
6	F1	VK1-KDE
7	G1	VK2-KDE
8	H1	VK3-KDE
9	A2	VK4-KDE
10	B2	VK INT-KDE
11	C2	VG1-JG1.1
12	D2	VG1-JG1.3
13	E2	VG2-JG1.1
14	F2	VG2-JG1.3
15	G2	VG4-JG1.1
16	H2	VG4-JG1.3
17	A3	VD2-DD3
18	B3	DD2-DD3
19	C3	VD2-JA29
20	D3	DH1-JHC
21	E3	DH2-JHC
22	F3	DH3-JHC
23	G3	DH4-JHC
24	H3	DH5-JHC
25	A4	DH6-JHC
26	B4	DH7-JHC
27	C4	(VB20,VB12b/13c/14, VB19, VB10, VB2, VB3/12a/15)-JB2.2
28	D4	(VB20,VB12b/13c/14, VB19, VB10, VB2, VB3/12a/15)-JB2.3
29	E4	(VB20,VB12b/13c/14, VB19, VB10, VB2, VB3/12a/15)-JB2.5
30	F4	(VB20,VB12b/13c/14, VB19, VB10, VB2, VB3/12a/15)-JB2.7
31	G4	(DB1+DB2)-JB2.2
32	H4	(DB1+DB2)-JB2.3
33	A5	(DB1+DB2)-JB2.5
34	B5	(DB1+DB2)-JB2.7
35	C5	VD2-(JA9,JA30,JA48)
36	D5	VD2-(JA54,JA58,JA61)
37	E5	VG3-JG1.1
38	F5	VG3-JG1.3

Table 7.2: Baseline characteristics of patients only treated after the 2012 protocol amendment

	PCR Cohort N=437	p-value	MLPA Cohort N=384	p-value	PCR and MLPA Cohort N=370	p-value	All UKALL 14 patients N=577
Rituximab, N (%)		-		-		-	
No	210 (48.1)		186 (48.4)		176 (47.6)		288 (49.9)
Yes	227 (51.9)		198 (51.6)		194 (52.4)		289 (50.1)
Age (years)	45.0(23 - 65)	0.20	44.0(23 - 65)	0.0006	44.0(23 - 65)	0.0014	46.0(22 - 65)
Age group, N (%)		0.27		0.001		0.004	
40 or under at randomisation	166 (38.0)		159 (41.4)		152 (41.1)		212 (36.7)
Over 40 at randomisation	271 (62.0)		225 (58.6)		218 (58.9)		365 (63.3)
Sex, N (%)		0.47		0.79		0.90	
Male	237 (54.2)		210 (54.7)		203 (54.9)		318 (55.1)
Female	199 (45.5)		173 (45.1)		166 (44.9)		258 (44.7)
Intersex - genetically male, identifies as female	1 (0.2)		1 (0.3)		1 (0.3)		1 (0.2)
ECOG, N (%)		0.68*		0.33*		0.47*	
0	264 (61.0)		264 (61.0)		226 (61.6)		226 (61.6)
1	154 (35.6)		154 (35.6)		128 (34.9)		128 (34.9)
2	12 (2.8)		12 (2.8)		12 (3.3)		12 (3.3)
3	3 (0.7)		3 (0.7)		1 (0.3)		1 (0.3)
Missing	4		4		3		3
Baseline WBC	9.7(.11 - 889.6)	0.0001	10.7(.11 - 889.6)	<0.0001	11.4(.11 - 889.6)	<0.0001	8.0(.11 - 889.6)
Baseline WBC group, N (%)		0.035		0.020		0.004	
<30	312 (71.4)		270 (70.3)		257 (69.5)		427 (74.0)
30-100	79 (18.1)		71 (18.5)		70 (18.9)		93 (16.1)
>=100	46 (10.5)		43 (11.2)		43 (11.6)		57 (9.9)
Philadelphia chromosome, N (%)		0.004		<0.001		<0.001	
Absent	293 (67.0)		250 (65.1)		236 (63.8)		405 (70.2)
Present	144 (33.0)		134 (34.9)		134 (36.2)		172 (29.8)
Any UKALL 14 cytogenetic risk factor, N (%)		0.071		0.056		0.65	
Absent	145 (38.8)		144 (43.8)		132 (41.6)		196 (40.9)
Present	229 (61.2)		185 (56.2)		185 (58.4)		283 (59.1)
Missing	63		55		53		98
Genetic Risk group**		0.025*		0.001*		0.001*	
Genetic good risk	18 (4.6)		17 (4.9)		16 (4.8)		23 (4.6)
Standard risk	99 (25.3)		100 (28.9)		89 (26.7)		142 (28.4)
High risk	131 (33.4)		95 (27.5)		94 (28.2)		163 (32.6)
Ph+	144 (36.7)		134 (38.7)		134 (40.2)		172 (34.4)
Missing	45		38		37		77
UKALL 14 risk group at randomisation, N (%)		0.28		0.068		0.41	
Standard risk	57 (13.0)		59 (15.4)		54 (14.6)		76 (13.2)
High risk	364 (83.3)		308 (80.2)		301 (81.4)		475 (82.3)
Assumed Standard - missing info	16 (3.7)		17 (4.4)		15 (4.1)		26 (4.5)

*Fisher's exact test

Table 7.3: Overall survival multivariable analysis for PCR, complete cases only

Risk Factor	Events/N	Complete cases univariable		Multivariable	
		HR (95% CI)	p-value	HR (95% CI)	p-value
Age (increase of 10 years)	188/387	1.41 (1.24, 1.61)	<0.001	1.42 (1.24 – 1.63)	<0.001
Sex					
Male	94/207	1.00	0.22	1.00	0.42
Female	94/180	1.19(0.90, 1.59)		1.13 (0.84 – 1.50)	
ECOG					
ECOG 0	94/207	1.00	0.048[2]	1.00	0.011
ECOG 1	68/139	1.03 (0.76, 1.40)		1.07 (0.79 - 1.46)	
ECOG 2-3	12/13	3.29 (1.81, 5.99)		2.91 (1.58 – 5.38)	
Log WBC	188/387	1.09 (1.00, 1.20)	0.050	1.09 (0.99 – 1.19)	0.072
Genetic Risk					
Good risk	5/18	0.52 (0.21, 1.32)		0.71 (0.28 – 1.79)	
Standard risk	45/96	1.00	0.0032	1.00	0.0057
High risk	77/130	1.52 (1.05, 2.20)		1.37 (0.93 – 2.02)	
Ph+	61/143	0.91 (0.62, 1.33)		0.73 (0.48 – 1.11)	
PCR					
No deletion	144/293	1.00	0.47	1.00	0.60
Deletion	44/94	0.88 (0.63, 1.24)		0.91 (0.63 – 1.31)	

[1]Test for trend

176

Table 7.4: Overall survival multivariable analysis for MLPA, complete cases only

Risk factor	Events/N	Complete cases univariable		Multivariable	
		HR (95% CI)	p-value	HR (95% CI)	p-value
Age (increase of 10 years)	163/342	1.36 (1.18, 1.56)	<0.001	1.37 (1.19 – 1.59)	<0.001
Sex					
Male	85/186	1.00	0.53	1.00	0.78
Female	78/156	1.10 (0.81, 1.50)		1.04 (0.77 – 1.43)	
ECOG					
ECOG 0	85/186	1.00	0.43[1]	1.00	0.018
ECOG 1	54/123	0.83 (0.60, 1.16)		0.87 (0.62 – 1.22)	
ECOG 2-3	11/12	2.96 (1.58, 5.53)		2.53 (1.34 – 4.79)	
Log WBC	163/342	1.14 (1.04, 1.26)	0.007	1.15 (1.04 – 1.27)	0.009
Genetic Risk					
Good risk	5/17	0.45 (0.18, 1.13)		0.47 (0.18 – 1.23)	
Standard risk	49/97	1.00	0.012	1.00	0.010
High risk	55/95	1.33 (0.90, 1.96)		1.03 (0.67 – 1.58)	
Ph+	54/133	0.79 (0.54, 1.17)		0.58 (0.38 – 0.89)	
IKZF1					
No deletion	121/263	1.00	0.075	1.00	0.51
IKZF1 deletion	23/64	0.68 (0.43, 1.07)		0.86 (0.53 – 1.40)	
*IKZF1*plus	42/79	1.23 (0.85, 1.76)		1.16 (0.79 – 1.71)	

[1]Test for trend

**Table 7.5: Event Free Survival univariable analysis –
all patients with PCR or MLPA data**

Baseline risk	Events/N	HR (95% CI)	p-value
Age (increase of 10 years)*	255/451	1.35 (1.21, 1.51)	<0.001
Sex			
Male	130/244	1.00	0.21
Female	124/206	1.17 (0.92, 1.50)	
ECOG			
ECOG 0	130/244	1.00	0.039
ECOG 1	95/161	1.13 (0.87, 1.46)	
ECOG 2-3	13/15	2.25 (1.27, 3.97)	
Log WBC	255/451	1.08 (1.00, 1.17)	0.053
Genetic Risk			
Good risk	6/19	0.47 (0.20, 1.08)	
Standard risk	61/110	1.00	0.0037
High risk	88/132	1.50 (1.08, 2.08)	
BCR-ABL+	79/144	1.05 (0.75, 1.46)	
PCR			
No deletion	191/339	1.00	0.64
Deletion	54/98	0.93 (0.69, 1.26)	
PCR deletion type			
No deletion	191/339	1.00	0.88
Dominant negative (4-7)	32/58	0.95 (0.65, 1.38)	
Non-dominant negative	22/40	0.90 (0.58, 1.40)	
MLPA			
No deletion	133/235	1.00	0.64
Deletion	84/149	1.07 (0.81, 1.40)	
MLPA deletion type			
No deletion	133/235	1.00	0.63
Dominant negative (4-7)	28/46	1.21 (0.81, 1.83)	
Non-dominant negative	54/100	1.00 (0.73, 1.38)	
***IKZF1*plus**			
No	164/301	1.00	0.036
Yes	53/83	1.39 (1.02, 1.90)	
***IKZF1*plus**			
No deletion	164/301	1.00	0.062
IKZF1 deleted only	31/66	0.80 (0.54, 1.18)	
*IKZF1*plus	53/83	1.33 (0.97, 1.83)	

Table 7.6: Overall Survival univariable analysis – all patients with PCR or MLPA data

Baseline risk	Events/N	HR (95% CI)	p-value
Age (increase of 10 years)	217/451	1.39 (1.23, 1.56)	<0.001
Sex			
Male	111/244	1.00	0.33
Female	105/206	1.14 (0.88, 1.49)	
ECOG			
ECOG 0	111/244	1.00	0.054
ECOG 1	80/161	1.09 (0.82, 1.44)	
ECOG 2-3	12/15	2.52 (1.39, 4.56)	
Log WBC	217/451	1.08 (0.99, 1.17)	0.093
Genetic Risk			
Good risk	6/19	0.52 (0.22, 1.20)	
Standard risk	54/110	1.00	0.003
High risk	79/132	1.46 (1.03, 2.07)	
BCR-ABL+	62/144	0.87 (0.60, 1.25)	
PCR			
No deletion	164/339	1.00	0.36
Deletion	44/98	0.86 (0.61, 1.20)	
PCR deletion type			
No deletion	164/339	1.00	0.47
Dominant negative (4-7)	28/58	0.95 (0.64, 1.43)	
Non-dominant negative	16/40	0.73 (0.44, 1.22)	
MLPA*			
No deletion	116/235	1.00	0.52
Deletion	66/149	0.91 (0.67, 1.23)	
MLPA deletion type			
No deletion	116/235	1.00	0.79
Dominant negative (4-7)	22/46	1.01 (0.64, 1.59)	
Non-dominant negative	44/100	0.89 (0.63, 1.26)	
***IKZF1*plus**			
No	139/301	1.00	0.17
Yes	43/83	1.27 (0.90, 1.79)	
***IKZF1*plus**			
No deletion	139/301	1.00	0.062
IKZF1 deletion only	23/66	0.64 (0.41, 1.00)	
*IKZF1*plus	43/83	1.16 (0.82, 1.65)	

Reference List

ACAR, M., KOCHERLAKOTA, K. S., MURPHY, M. M., PEYER, J. G., OGURO, H., INRA, C. N., JAIYEOLA, C., ZHAO, Z., LUBY-PHELPS, K. & MORRISON, S. J. 2015. Deep imaging of bone marrow shows non-dividing stem cells are mainly perisinusoidal. *Nature,* 526**,** 126-30.

AGRAWAL, A., EASTMAN, Q. M. & SCHATZ, D. G. 1998. Transposition mediated by RAG1 and RAG2 and its implications for the evolution of the immune system. *Nature,* 394**,** 744-51.

ALAPI, K., MITCHELL, R. J., NAUGHTON, T., MUIRHEAD, R. C. J., LEE, S. & FIELDING, A. K. 2018. Minimal residual disease testing on the UKALL14 trial; an overview of the UK's first use of MRD-based risk stratification in adult acute lymphoblastic leukaemia. *British Journal of Haematology,* 181**,** 5-211.

ALT, F. W., YANCOPOULOS, G. D., BLACKWELL, T. K., WOOD, C., THOMAS, E., BOSS, M., COFFMAN, R., ROSENBERG, N., TONEGAWA, S. & BALTIMORE, D. 1984. Ordered rearrangement of immunoglobulin heavy chain variable region segments. *Embo j,* 3**,** 1209-19.

ALVAREZ-CALDERON, F., GREGORY, M. A., PHAM-DANIS, C., DERYCKERE, D., STEVENS, B. M., ZABEREZHNYY, V., HILL, A. A., GEMTA, L., KUMAR, A., KUMAR, V., WEMPE, M. F., POLLYEA, D. A., JORDAN, C. T., SERKOVA, N. J., GRAHAM, D. K. & DEGREGORI, J. 2015. Tyrosine kinase inhibition in leukemia induces an altered metabolic state sensitive to mitochondrial perturbations. *Clin Cancer Res,* 21**,** 1360-72.

ARANA-TREJO, R. M., IGNACIO, G., AMADOR-SÁNCHEZ, R., CRUZ-RICO, J., HERNÁNDEZ, M.-P., SALDIVAR, I., LUGO, Y., SOLÍS-POBLANO, J.-C., PÉREZ, O., TEJEDA, M., ARTRISTIAN, A. & SOLÍS-ANAYA, L. 2016. Frequency of p190 and p210 BCR-ABL Fusions Genes in Acute Lymphoblastic Leukemia in a Long Group of Adults and Childhood. *Blood,* 128**,** 5273-5273.

ARBER, D. A., ORAZI, A., HASSERJIAN, R., THIELE, J., BOROWITZ, M. J., LE BEAU, M. M., BLOOMFIELD, C. D., CAZZOLA, M. & VARDIMAN, J. W. 2016. The 2016 revision to the World Health Organization classification of myeloid neoplasms and acute leukemia. *Blood,* 127**,** 2391-405.

ARENZANA, T. L., SCHJERVEN, H. & SMALE, S. T. 2015. Regulation of gene expression dynamics during developmental transitions by the Ikaros transcription factor. *Genes Dev,* 29**,** 1801-16.

ARYA, S. K., WONG-STAAL, F. & GALLO, R. C. 1984. Dexamethasone-mediated inhibition of human T cell growth factor and gamma-interferon messenger RNA. *J Immunol,* 133**,** 273-6.

ASADA, N., KUNISAKI, Y., PIERCE, H., WANG, Z., FERNANDEZ, N. F., BIRBRAIR, A., MA'AYAN, A. & FRENETTE, P. S. 2017. Differential cytokine contributions of perivascular haematopoietic stem cell niches. *Nat Cell Biol,* 19**,** 214-223.

BARNES, K., MCINTOSH, E., WHETTON, A. D., DALEY, G. Q., BENTLEY, J. & BALDWIN, S. A. 2005. Chronic myeloid leukaemia: an investigation into the role of Bcr-Abl-induced abnormalities in glucose transport regulation. *Oncogene,* 24**,** 3257-67.

BEER, PHILIP A., KNAPP, DAVID J. H. F., KANNAN, N., MILLER, PAUL H., BABOVIC, S., BULAEVA, E., AGHAEEPOUR, N., RABU, G., ROSTAMIRAD, S., SHIH, K., WEI, L. & EAVES, CONNIE J. 2014. A Dominant-Negative Isoform of IKAROS Expands Primitive Normal Human Hematopoietic Cells. *Stem Cell Reports,* 3**,** 841-857.

BELDJORD, K., CHEVRET, S., ASNAFI, V., HUGUET, F., BOULLAND, M.-L., LEGUAY, T., THOMAS, X., CAYUELA, J.-M., GRARDEL, N., CHALANDON, Y., BOISSEL, N., SCHAEFER, B., DELABESSE, E., CAVÉ, H., CHEVALLIER, P., BUZYN, A., FEST, T., REMAN, O., VERNANT, J.-P., LHÉRITIER, V., BÉNÉ, M. C., LAFAGE, M., MACINTYRE, E., IFRAH, N., DOMBRET, H. & ON BEHALF OF THE GROUP FOR RESEARCH ON ADULT ACUTE LYMPHOBLASTIC, L. 2014. Oncogenetics and minimal residual disease are independent outcome predictors in adult patients with acute lymphoblastic leukemia. *Blood,* 123**,** 3739-3749.

BENNETT, J. M., CATOVSKY, D., DANIEL, M. T., FLANDRIN, G., GALTON, D. A., GRALNICK, H. R. & SULTAN, C. 1976. Proposals for the classification of the acute leukaemias. French-American-British (FAB) co-operative group. *Br J Haematol,* 33**,** 451-8.

BOER, J. M., KOENDERS, J. E., VAN DER HOLT, B., EXALTO, C., SANDERS, M. A., CORNELISSEN, J. J., VALK, P. J., DEN BOER, M. L. & RIJNEVELD, A. W. 2015. Expression profiling of adult acute lymphoblastic leukemia identifies a BCR-ABL1-like subgroup characterized by high non-response and relapse rates. *Haematologica,* 100**,** e261-4.

BOER, J. M., VAN DER VEER, A., RIZOPOULOS, D., FIOCCO, M., SONNEVELD, E., DE GROOT-KRUSEMAN, H. A., KUIPER, R. P., HOOGERBRUGGE, P., HORSTMANN, M., ZALIOVA, M., PALMI, C., TRKA, J., FRONKOVA, E., EMERENCIANO, M., DO SOCORRO POMBO-DE-OLIVEIRA, M., MLYNARSKI, W., SZCZEPANSKI, T., NEBRAL, K., ATTARBASCHI, A., VENN, N., SUTTON, R., SCHWAB, C. J., ENSHAEI, A., VORA, A., STANULLA, M., SCHRAPPE, M., CAZZANIGA, G., CONTER, V., ZIMMERMANN, M., MOORMAN, A. V., PIETERS, R. & DEN BOER, M. L. 2016. Prognostic value of rare IKZF1 deletion in childhood B-cell precursor acute lymphoblastic leukemia: an international collaborative study. *Leukemia,* 30**,** 32-8.

BOSSEN, C., MURRE, C. S., CHANG, A. N., MANSSON, R., RODEWALD, H.-R. & MURRE, C. 2015. The chromatin remodeler Brg1 activates enhancer repertoires to establish B cell identity and modulate cell growth. *Nature immunology,* 16**,** 775-784.

BROWN, P., INABA, H., ANNESLEY, C., BECK, J., COLACE, S., DALLAS, M., DESANTES, K., KELLY, K., KITKO, C., LACAYO, N., LARRIER, N., MAESE, L., MAHADEO, K., NANDA, R., NARDI, V., RODRIGUEZ, V., ROSSOFF, J., SCHUETTPELZ, L., SILVERMAN, L., SUN, J., SUN, W., TEACHEY, D., WONG, V., YANIK, G., JOHNSON-CHILLA, A. & OGBA, N. 2020. Pediatric Acute Lymphoblastic Leukemia, Version 2.2020, NCCN Clinical Practice Guidelines in Oncology. *J Natl Compr Canc Netw,* 18**,** 81-112.

BRÜGGEMANN, M., SCHRAUDER, A., RAFF, T., PFEIFER, H., DWORZAK, M., OTTMANN, O. G., ASNAFI, V., BARUCHEL, A., BASSAN, R., BENOIT,

Y., BIONDI, A., CAVÉ, H., DOMBRET, H., FIELDING, A. K., FOÀ, R., GÖKBUGET, N., GOLDSTONE, A. H., GOULDEN, N., HENZE, G., HOELZER, D., JANKA-SCHAUB, G. E., MACINTYRE, E. A., PIETERS, R., RAMBALDI, A., RIBERA, J. M., SCHMIEGELOW, K., SPINELLI, O., STARY, J., VON STACKELBERG, A., KNEBA, M., SCHRAPPE, M. & VAN DONGEN, J. J. 2010. Standardized MRD quantification in European ALL trials: proceedings of the Second International Symposium on MRD assessment in Kiel, Germany, 18-20 September 2008. *Leukemia,* 24**,** 521-35.

BURT, R., DEY, A., AREF, S., AGUIAR, M., AKARCA, A., BAILEY, K., DAY, W., HOOPER, S., KIRKWOOD, A., KIRSCHNER, K., LEE, S.-W., LO CELSO, C., MANJI, J., MANSOUR, M. R., MARAFIOTI, T., MITCHELL, R. J., MUIRHEAD, R. C., CHEUK YAN NG, K., POSPORI, C., PUCCIO, I., ZUBORNE-ALAPI, K., SAHAI, E. & FIELDING, A. K. 2019. Activated stromal cells transfer mitochondria to rescue acute lymphoblastic leukemia cells from oxidative stress. *Blood,* 134**,** 1415-1429.

CALVI, L. M., ADAMS, G. B., WEIBRECHT, K. W., WEBER, J. M., OLSON, D. P., KNIGHT, M. C., MARTIN, R. P., SCHIPANI, E., DIVIETI, P., BRINGHURST, F. R., MILNER, L. A., KRONENBERG, H. M. & SCADDEN, D. T. 2003. Osteoblastic cells regulate the haematopoietic stem cell niche. *Nature,* 425**,** 841-6.

CAMPO, E., SWERDLOW, S. H., HARRIS, N. L., PILERI, S., STEIN, H. & JAFFE, E. S. 2011. The 2008 WHO classification of lymphoid neoplasms and beyond: evolving concepts and practical applications. *Blood,* 117**,** 5019-5032.

CASSILETH, P. A., ANDERSEN, J. W., BENNETT, J. M., HOAGLAND, H. C., MAZZA, J. J., O'CONNELL, M. C., PAIETTA, E. & WIERNIK, P. 1992. Adult acute lymphocytic leukemia: the Eastern Cooperative Oncology Group experience. *Leukemia,* 6 Suppl 2**,** 178-81.

CAYE, A., BELDJORD, K., MASS-MALO, K., DRUNAT, S., SOULIER, J., GANDEMER, V., BARUCHEL, A., BERTRAND, Y., CAVE, H. & CLAPPIER, E. 2013. Breakpoint-specific multiplex polymerase chain reaction allows the detection of IKZF1 intragenic deletions and minimal residual disease monitoring in B-cell precursor acute lymphoblastic leukemia. *Haematologica,* 98**,** 597-601.

CAZZANIGA, G., VAN DELFT, F. W., LO NIGRO, L., FORD, A. M., SCORE, J., IACOBUCCI, I., MIRABILE, E., TAJ, M., COLMAN, S. M., BIONDI, A. & GREAVES, M. 2011. Developmental origins and impact of BCR-ABL1 fusion and IKZF1 deletions in monozygotic twins with Ph+ acute lymphoblastic leukemia. *Blood,* 118**,** 5559-64.

CHAN, L. N., CHEN, Z., BRAAS, D., LEE, J.-W., XIAO, G., GENG, H., COSGUN, K. N., HURTZ, C., SHOJAEE, S., CAZZANIGA, V., SCHJERVEN, H., ERNST, T., HOCHHAUS, A., KORNBLAU, S. M., KONOPLEVA, M., PUFALL, M. A., CAZZANIGA, G., LIU, G. J., MILNE, T. A., KOEFFLER, H. P., ROSS, T. S., SÁNCHEZ-GARCÍA, I., BORKHARDT, A., YAMAMOTO, K. R., DICKINS, R. A., GRAEBER, T. G. & MÜSCHEN, M. 2017. Metabolic gatekeeper function of B-lymphoid transcription factors. *Nature,* 542**,** 479-483.

CHIARETTI, S., VITALE, A., CAZZANIGA, G., MARIA ORLANDO, S., SILVESTRI, D., FAZI, P., GRAZIA VALSECCHI, M., ELIA, L., MARIA TESTI, A., MANCINI, F., CONTER, V., KRONNIE, G., FERRARA, F., DI RAIMONDO, F., TEDESCHI, A., FIORITONI, G., FABBIANO, F., MELONI, G., SPECCHIA, G. & FOA, R. 2013. *Clinico-biologic features of 5202 acute lymphoblastic leukemia patients enrolled in the Italian AIEOP and GIMEMA Protocols and stratified in age-cohorts.*

CHICAYBAM, L., BARCELOS, C., PEIXOTO, B., CARNEIRO, M., LIMIA, C. G., REDONDO, P., LIRA, C., PARAGUASSÚ-BRAGA, F., VASCONCELOS, Z. F. M. D., BARROS, L. & BONAMINO, M. H. 2017. An Efficient Electroporation Protocol for the Genetic Modification of Mammalian Cells. *Frontiers in Bioengineering and Biotechnology,* 4.

CHURCHMAN, M. L., EVANS, K., RICHMOND, J., ROBBINS, A., JONES, L., SHAPIRO, I. M., PACHTER, J. A., WEAVER, D. T., HOUGHTON, P. J., SMITH, M. A., LOCK, R. B. & MULLIGHAN, C. G. 2016. Synergism of FAK and tyrosine kinase inhibition in Ph(+) B-ALL. *JCI insight,* 1**,** e86082.

CHURCHMAN, M. L., LOW, J., QU, C., PAIETTA, E. M., KASPER, L. H., CHANG, Y., PAYNE-TURNER, D., ALTHOFF, M. J., SONG, G., CHEN, S. C., MA, J., RUSCH, M., MCGOLDRICK, D., EDMONSON, M., GUPTA, P., WANG, Y. D., CAUFIELD, W., FREEMAN, B., LI, L., PANETTA, J. C., BAKER, S., YANG, Y. L., ROBERTS, K. G., MCCASTLAIN, K., IACOBUCCI, I., PETERS, J. L., CENTONZE, V. E., NOTTA, F., DOBSON, S. M., ZANDI, S., DICK, J. E., JANKE, L., PENG, J., KODALI, K., PAGALA, V., MIN, J., MAYASUNDARI, A., WILLIAMS, R. T., WILLMAN, C. L., ROWE, J., LUGER, S., DICKINS, R. A., GUY, R. K., CHEN, T. & MULLIGHAN, C. G. 2015. Efficacy of Retinoids in IKZF1-Mutated BCR-ABL1 Acute Lymphoblastic Leukemia. *Cancer Cell,* 28**,** 343-56.

CHURCHMAN, M. L., QIAN, M., TE KRONNIE, G., ZHANG, R., YANG, W., ZHANG, H., LANA, T., TEDRICK, P., BASKIN, R., VERBIST, K., PETERS, J. L., DEVIDAS, M., LARSEN, E., MOORE, I. M., GU, Z., QU, C., YOSHIHARA, H., PORTER, S. N., PRUETT-MILLER, S. M., WU, G., RAETZ, E., MARTIN, P. L., BOWMAN, W. P., WINICK, N., MARDIS, E., FULTON, R., STANULLA, M., EVANS, W. E., RELLING, M. V., PUI, C. H., HUNGER, S. P., LOH, M. L., HANDGRETINGER, R., NICHOLS, K. E., YANG, J. J. & MULLIGHAN, C. G. 2018. Germline Genetic IKZF1 Variation and Predisposition to Childhood Acute Lymphoblastic Leukemia. *Cancer Cell,* 33**,** 937-948.e8.

CLAPPIER, E., AUCLERC, M. F., RAPION, J., BAKKUS, M., CAYE, A., KHEMIRI, A., GIROUX, C., HERNANDEZ, L., KABONGO, E., SAVOLA, S., LEBLANC, T., YAKOUBEN, K., PLAT, G., COSTA, V., FERSTER, A., GIRARD, S., FENNETEAU, O., CAYUELA, J. M., SIGAUX, F., DASTUGUE, N., SUCIU, S., BENOIT, Y., BERTRAND, Y., SOULIER, J. & CAVÉ, H. 2014. An intragenic ERG deletion is a marker of an oncogenic subtype of B-cell precursor acute lymphoblastic leukemia with a favorable outcome despite frequent IKZF1 deletions. *Leukemia,* 28**,** 70-7.

COLLINS, B., CLAMBEY, E. T., SCOTT-BROWNE, J., WHITE, J., MARRACK, P., HAGMAN, J. & KAPPLER, J. W. 2013. Ikaros promotes rearrangement of TCR α genes in an Ikaros null thymoma cell line. *European journal of immunology,* 43**,** 521-532.

CUTTNER, J., MICK, R., BUDMAN, D. R., MAYER, R. J., LEE, E. J., HENDERSON, E. S., WEISS, R. B., PACIUCCI, P. A., SOBOL, R., DAVEY, F. & ET AL. 1991. Phase III trial of brief intensive treatment of adult acute lymphocytic leukemia comparing daunorubicin and mitoxantrone: a CALGB Study. *Leukemia*, 5**,** 425-31.

DABAJA, B. S., FADERL, S., THOMAS, D., CORTES, J., O'BRIEN, S., NASR, F., PIERCE, S., HAYES, K., GLASSMAN, A., KEATING, M. & KANTARJIAN, H. M. 1999. Deletions and losses in chromosomes 5 or 7 in adult acute lymphocytic leukemia: incidence, associations and implications. *Leukemia*, 13**,** 869-72.

DAVER, N., THOMAS, D., RAVANDI, F., CORTES, J., GARRIS, R., JABBOUR, E., GARCIA-MANERO, G., BORTHAKUR, G., KADIA, T., RYTTING, M., KONOPLEVA, M., KANTARJIAN, H. & O'BRIEN, S. 2015. Final report of a phase II study of imatinib mesylate with hyper-CVAD for the front-line treatment of adult patients with Philadelphia chromosome-positive acute lymphoblastic leukemia. *Haematologica*, 100**,** 653-61.

DELLA STARZA, I., DE NOVI, L. A., SANTORO, A., SALEMI, D., TAM, W., CAVALLI, M., MENALE, L., SOSCIA, R., APICELLA, V., ILARI, C., VITALE, A., TESTI, A. M., INGHIRAMI, G., CHIARETTI, S., FOÀ, R. & GUARINI, A. 2019. Digital droplet PCR and next-generation sequencing refine minimal residual disease monitoring in acute lymphoblastic leukemia. *Leukemia & Lymphoma*, 1-3.

DEN BOER, M. L., VAN SLEGTENHORST, M., DE MENEZES, R. X., CHEOK, M. H., BUIJS-GLADDINES, J. G., PETERS, S. T., VAN ZUTVEN, L. J. C. M., BEVERLOO, H. B., VAN DER SPEK, P. J., ESCHERICH, G., HORSTMANN, M. A., JANKA-SCHAUB, G. E., KAMPS, W. A., EVANS, W. E. & PIETERS, R. 2009. A subtype of childhood acute lymphoblastic leukaemia with poor treatment outcome: a genome-wide classification study. *The Lancet Oncology*, 10**,** 125-134.

DENYS, B., VAN DER SLUIJS-GELLING, A. J., HOMBURG, C., VAN DER SCHOOT, C. E., DE HAAS, V., PHILIPPÉ, J., PIETERS, R., VAN DONGEN, J. J. & VAN DER VELDEN, V. H. 2013. Improved flow cytometric detection of minimal residual disease in childhood acute lymphoblastic leukemia. *Leukemia*, 27**,** 635-41.

DOMBRET, H., GABERT, J., BOIRON, J. M., RIGAL-HUGUET, F., BLAISE, D., THOMAS, X., DELANNOY, A., BUZYN, A., BILHOU-NABERA, C., CAYUELA, J. M., FENAUX, P., BOURHIS, J. H., FEGUEUX, N., CHARRIN, C., BOUCHEIX, C., LHÉRITIER, V., ESPÉROU, H., MACINTYRE, E., VERNANT, J. P. & FIÈRE, D. 2002. Outcome of treatment in adults with Philadelphia chromosome-positive acute lymphoblastic leukemia--results of the prospective multicenter LALA-94 trial. *Blood*, 100**,** 2357-66.

DOMINICI, M., LE BLANC, K., MUELLER, I., SLAPER-CORTENBACH, I., MARINI, F. C., KRAUSE, D. S., DEANS, R. J., KEATING, A., PROCKOP, D. J. & HORWITZ, E. M. 2006. Minimal criteria for defining multipotent mesenchymal stromal cells. The International Society for Cellular Therapy position statement. *Cytotherapy*, 8**,** 315-317.

DORGE, P., MEISSNER, B., ZIMMERMANN, M., MORICKE, A., SCHRAUDER, A., BOUQUIN, J. P., SCHEWE, D., HARBOTT, J., TEIGLER-SCHLEGEL,

A., RATEI, R., LUDWIG, W. D., KOEHLER, R., BARTRAM, C. R., SCHRAPPE, M., STANULLA, M. & CARIO, G. 2013. IKZF1 deletion is an independent predictor of outcome in pediatric acute lymphoblastic leukemia treated according to the ALL-BFM 2000 protocol. *Haematologica,* 98**,** 428-32.

DUAN, C. W., SHI, J., CHEN, J., WANG, B., YU, Y. H., QIN, X., ZHOU, X. C., CAI, Y. J., LI, Z. Q., ZHANG, F., YIN, M. Z., TAO, Y., MI, J. Q., LI, L. H., ENVER, T., CHEN, G. Q. & HONG, D. L. 2014. Leukemia propagating cells rebuild an evolving niche in response to therapy. *Cancer Cell,* 25**,** 778-93.

DUPUIS, A., GAUB, M. P., LEGRAIN, M., DRENOU, B., MAUVIEUX, L., LUTZ, P., HERBRECHT, R., CHAN, S. & KASTNER, P. 2013. Biclonal and biallelic deletions occur in 20% of B-ALL cases with IKZF1 mutations. *Leukemia,* 27**,** 503-507.

EBINGER, S., OZDEMIR, E. Z., ZIEGENHAIN, C., TIEDT, S., CASTRO ALVES, C., GRUNERT, M., DWORZAK, M., LUTZ, C., TURATI, V. A., ENVER, T., HORNY, H. P., SOTLAR, K., PAREKH, S., SPIEKERMANN, K., HIDDEMANN, W., SCHEPERS, A., POLZER, B., KIRSCH, S., HOFFMANN, M., KNAPP, B., HASENAUER, J., PFEIFER, H., PANZER-GRUMAYER, R., ENARD, W., GIRES, O. & JEREMIAS, I. 2016. Characterization of Rare, Dormant, and Therapy-Resistant Cells in Acute Lymphoblastic Leukemia. *Cancer Cell,* 30**,** 849-862.

FADERL, S., KANTARJIAN, H. M., THOMAS, D. A., CORTES, J., GILES, F., PIERCE, S., ALBITAR, M. & ESTROV, Z. 2000. Outcome of Philadelphia chromosome-positive adult acute lymphoblastic leukemia. *Leuk Lymphoma,* 36**,** 263-73.

FAHAM, M., ZHENG, J., MOORHEAD, M., CARLTON, V. E., STOW, P., COUSTAN-SMITH, E., PUI, C. H. & CAMPANA, D. 2012. Deep-sequencing approach for minimal residual disease detection in acute lymphoblastic leukemia. *Blood,* 120**,** 5173-80.

FEDELE, P. L., WILLIS, S. N., LIAO, Y., LOW, M. S., RAUTELA, J., SEGAL, D. H., GONG, J. N., HUNTINGTON, N. D., SHI, W., HUANG, D. C. S., GRIGORIADIS, G., TELLIER, J. & NUTT, S. L. 2018. IMiDs prime myeloma cells for daratumumab-mediated cytotoxicity through loss of Ikaros and Aiolos. *Blood,* 132**,** 2166-2178.

FIELDING, A. K., ROWE, J. M., RICHARDS, S. M., BUCK, G., MOORMAN, A. V., DURRANT, I. J., MARKS, D. I., MCMILLAN, A. K., LITZOW, M. R., LAZARUS, H. M., FORONI, L., DEWALD, G., FRANKLIN, I. M., LUGER, S. M., PAIETTA, E., WIERNIK, P. H., TALLMAN, M. S. & GOLDSTONE, A. H. 2009. Prospective outcome data on 267 unselected adult patients with Philadelphia chromosome-positive acute lymphoblastic leukemia confirms superiority of allogeneic transplantation over chemotherapy in the pre-imatinib era: results from the International ALL Trial MRC UKALLXII/ECOG2993. *Blood,* 113**,** 4489-4496.

FORD, A. M., BENNETT, C. A., PRICE, C. M., BRUIN, M. C., VAN WERING, E. R. & GREAVES, M. 1998. Fetal origins of the TEL-AML1 fusion gene in identical twins with leukemia. *Proceedings of the National Academy of Sciences of the United States of America,* 95**,** 4584-4588.

FORONI, L., GERRARD, G., NNA, E., KHORASHAD, J. S., STEVENS, D., SWALE, B., MILOJKOVIC, D., REID, A., GOLDMAN, J. & MARIN, D. 2009. Technical aspects and clinical applications of measuring BCR-ABL1 transcripts number in chronic myeloid leukemia. *Am J Hematol,* 84**,** 517-22.

FUJISAKI, J., WU, J., CARLSON, A. L., SILBERSTEIN, L., PUTHETI, P., LAROCCA, R., GAO, W., SAITO, T. I., LO CELSO, C., TSUYUZAKI, H., SATO, T., CÔTÉ, D., SYKES, M., STROM, T. B., SCADDEN, D. T. & LIN, C. P. 2011. In vivo imaging of Treg cells providing immune privilege to the haematopoietic stem-cell niche. *Nature,* 474**,** 216-9.

GARAND, R., BELDJORD, K., CAVÉ, H., FOSSAT, C., ARNOUX, I., ASNAFI, V., BERTRAND, Y., BOULLAND, M. L., BROUZES, C., CLAPPIER, E., DELABESSE, E., FEST, T., GARNACHE-OTTOU, F., HUGUET, F., JACOB, M. C., KUHLEIN, E., MARTY-GRÈS, S., PLESA, A., ROBILLARD, N., ROUSSEL, M., TKACZUK, J., DOMBRET, H., MACINTYRE, E., IFRAH, N., BÉNÉ, M. C. & BARUCHEL, A. 2013. Flow cytometry and IG/TCR quantitative PCR for minimal residual disease quantitation in acute lymphoblastic leukemia: a French multicenter prospective study on behalf of the FRALLE, EORTC and GRAALL. *Leukemia,* 27**,** 370-6.

GAYNON, P. S., ANGIOLILLO, A. L., CARROLL, W. L., NACHMAN, J. B., TRIGG, M. E., SATHER, H. N., HUNGER, S. P. & DEVIDAS, M. 2010. Long-term results of the children's cancer group studies for childhood acute lymphoblastic leukemia 1983-2002: a Children's Oncology Group Report. *Leukemia,* 24**,** 285-97.

GEORGOPOULOS, K., BIGBY, M., WANG, J. H., MOLNAR, A., WU, P., WINANDY, S. & SHARPE, A. 1994. The Ikaros gene is required for the development of all lymphoid lineages. *Cell,* 79**,** 143-56.

GÖKBUGET, N. & HOELZER, D. 2006. Treatment of adult acute lymphoblastic leukemia. *Hematology Am Soc Hematol Educ Program***,** 133-41.

GU, Y., CIMINO, G., ALDER, H., NAKAMURA, T., PRASAD, R., CANAANI, O., MOIR, D. T., JONES, C., NOWELL, P. C., CROCE, C. M. & ET AL. 1992. The (4;11)(q21;q23) chromosome translocations in acute leukemias involve the VDJ recombinase. *Proc Natl Acad Sci U S A,* 89**,** 10464-8.

GUREL, Z., RONNI, T., HO, S., KUCHAR, J., PAYNE, K. J., TURK, C. W. & DOVAT, S. 2008. Recruitment of ikaros to pericentromeric heterochromatin is regulated by phosphorylation. *J Biol Chem,* 283**,** 8291-300.

HAMADEH, L., ENSHAEI, A., SCHWAB, C., ALONSO, C. N., ATTARBASCHI, A., BARBANY, G., DEN BOER, M. L., BOER, J. M., BRAUN, M., DALLA POZZA, L., ELITZUR, S., EMERENCIANO, M., FECHINA, L., FELICE, M. S., FRONKOVA, E., HALTRICH, I., HEYMAN, M. M., HORIBE, K., IMAMURA, T., JEISON, M., KOVÁCS, G., KUIPER, R. P., MLYNARSKI, W., NEBRAL, K., IVANOV ÖFVERHOLM, I., PASTORCZAK, A., PIETERS, R., PIKO, H., POMBO-DE-OLIVEIRA, M. S., RUBIO, P., STREHL, S., STARY, J., SUTTON, R., TRKA, J., TSAUR, G., VENN, N., VORA, A., YANO, M., HARRISON, C. J., MOORMAN, A. V. & INTERNATIONAL, B. F. M. S. G. 2019. Validation of the United Kingdom

copy-number alteration classifier in 3239 children with B-cell precursor ALL. *Blood advances,* 3**,** 148-157.

HARMON, J. M., NORMAN, M. R., FOWLKES, B. J. & THOMPSON, E. B. 1979. Dexamethasone induces irreversible G1 arrest and death of a human lymphoid cell line. *J Cell Physiol,* 98**,** 267-78.

HEHLMANN, R., BERGER, U., PFIRRMANN, M., HOCHHAUS, A., METZGEROTH, G., MAYWALD, O., HASFORD, J., REITER, A., HOSSFELD, D. K., KOLB, H. J., LÖFFLER, H., PRALLE, H., QUEISSER, W., GRIESSHAMMER, M., NERL, C., KUSE, R., TOBLER, A., EIMERMACHER, H., TICHELLI, A., AUL, C., WILHELM, M., FISCHER, J. T., PERKER, M., SCHEID, C., SCHENK, M., WEISS, J., MEIER, C. R., KREMERS, S., LABEDZKI, L., SCHMEISER, T., LOHRMANN, H. P. & HEIMPEL, H. 2003. Randomized comparison of interferon alpha and hydroxyurea with hydroxyurea monotherapy in chronic myeloid leukemia (CML-study II): prolongation of survival by the combination of interferon alpha and hydroxyurea. *Leukemia,* 17**,** 1529-37.

HEIZMANN, B., KASTNER, P. & CHAN, S. 2013. Ikaros is absolutely required for pre-B cell differentiation by attenuating IL-7 signals. *The Journal of experimental medicine,* 210**,** 2823-2832.

HEIZMANN, B., SELLARS, M., MACIAS-GARCIA, A., CHAN, S. & KASTNER, P. 2016. Ikaros limits follicular B cell activation by regulating B cell receptor signaling pathways. *Biochem Biophys Res Commun,* 470**,** 714-720.

HEROLD, T., BALDUS, C. D. & GÖKBUGET, N. 2014. Ph-like Acute Lymphoblastic Leukemia in Older Adults. *New England Journal of Medicine,* 371**,** 2235-2235.

HILLION, S., ROCHAS, C., YOUINOU, P. & JAMIN, C. 2009. Signaling pathways regulating RAG expression in B lymphocytes. *Autoimmun Rev,* 8**,** 599-604.

HIROKAWA, S., CHURE, G., BELLIVEAU, N. M., LOVELY, G. A., ANAYA, M., SCHATZ, D. G., BALTIMORE, D. & PHILLIPS, R. 2020. Sequence-dependent dynamics of synthetic and endogenous RSSs in V(D)J recombination. *Nucleic Acids Research*.

HOVORKOVA, L., ZALIOVA, M., VENN, N. C., BLECKMANN, K., TRKOVA, M., POTUCKOVA, E., VASKOVA, M., LINHARTOVA, J., MACHOVA POLAKOVA, K., FRONKOVA, E., MUSKOVIC, W., GILES, J. E., SHAW, P. J., CARIO, G., SUTTON, R., STARY, J., TRKA, J. & ZUNA, J. 2017. Monitoring of childhood ALL using BCR-ABL1 genomic breakpoints identifies a subgroup with CML-like biology. *Blood,* 129**,** 2771-2781.

HSU, L. Y., LAURING, J., LIANG, H. E., GREENBAUM, S., CADO, D., ZHUANG, Y. & SCHLISSEL, M. S. 2003. A conserved transcriptional enhancer regulates RAG gene expression in developing B cells. *Immunity,* 19**,** 105-17.

HU, Y., YOSHIDA, T. & GEORGOPOULOS, K. 2017. Transcriptional circuits in B cell transformation. *Curr Opin Hematol,* 24**,** 345-352.

HU, Y., ZHANG, Z., KASHIWAGI, M., YOSHIDA, T., JOSHI, I., JENA, N., SOMASUNDARAM, R., EMMANUEL, A. O., SIGVARDSSON, M., FITAMANT, J., EL-BARDEESY, N., GOUNARI, F., VAN ETTEN, R. A. & GEORGOPOULOS, K. 2016. Superenhancer reprogramming drives a B-cell-epithelial transition and high-risk leukemia. *Genes Dev,* 30**,** 1971-90.

HULLEMAN, E., KAZEMIER, K. M., HOLLEMAN, A., VANDERWEELE, D. J., RUDIN, C. M., BROEKHUIS, M. J. C., EVANS, W. E., PIETERS, R. & DEN BOER, M. L. 2009. Inhibition of glycolysis modulates prednisolone resistance in acute lymphoblastic leukemia cells. *Blood,* 113**,** 2014-2021.

IACOBUCCI, I., IRACI, N., MESSINA, M., LONETTI, A., CHIARETTI, S., VALLI, E., FERRARI, A., PAPAYANNIDIS, C., PAOLONI, F., VITALE, A., STORLAZZI, C. T., OTTAVIANI, E., GUADAGNUOLO, V., DURANTE, S., VIGNETTI, M., SOVERINI, S., PANE, F., FOÀ, R., BACCARANI, M., MÜSCHEN, M., PERINI, G. & MARTINELLI, G. 2012. IKAROS deletions dictate a unique gene expression signature in patients with adult B-cell acute lymphoblastic leukemia. *PloS one,* 7**,** e40934-e40934.

IACOBUCCI, I., STORLAZZI, C. T., CILLONI, D., LONETTI, A., OTTAVIANI, E., SOVERINI, S., ASTOLFI, A., CHIARETTI, S., VITALE, A., MESSA, F., IMPERA, L., BALDAZZI, C., D'ADDABBO, P., PAPAYANNIDIS, C., LONOCE, A., COLAROSSI, S., VIGNETTI, M., PICCALUGA, P. P., PAOLINI, S., RUSSO, D., PANE, F., SAGLIO, G., BACCARANI, M., FOÀ, R. & MARTINELLI, G. 2009. Identification and molecular characterization of recurrent genomic deletions on 7p12 in the IKZF1 gene in a large cohort of BCR-ABL1–positive acute lymphoblastic leukemia patients: on behalf of Gruppo Italiano Malattie Ematologiche dell'Adulto Acute Leukemia Working Party (GIMEMA AL WP). *Blood,* 114**,** 2159-2167.

IMAMURA, T., YANO, M., ASAI, D., MORIYA-SAITO, A., SUENOBU, S. I., HASEGAWA, D., DEGUCHI, T., HASHII, Y., KAWASAKI, H., HORI, H., YUMURA-YAGI, K., HARA, J., HORIBE, K. & SATO, A. 2016. IKZF1 deletion is enriched in pediatric B-cell precursor acute lymphoblastic leukemia patients showing prednisolone resistance. *Leukemia,* 30**,** 1801.

JABBOUR, E., KANTARJIAN, H., THOMAS, D. A., RAVANDI, F., CORTES, J. E., FADERL, S. H., PEMMARAJU, N., KADIA, T. M., GARRIS, R., HILLARY, P., GARCIA-MANERO, G., BORTHAKUR, G., WIERDA, W. G. & O'BRIEN, S. 2013. Phase II Study Of Combination Of Hyper-CVAD With Ponatinib In Front Line Therapy Of Patients (pts) With Philadelphia Chromosome (Ph) Positive Acute Lymphoblastic Leukemia (ALL). *Blood,* 122**,** 2663-2663.

JABBOUR, E. J., FADERL, S. & KANTARJIAN, H. M. 2005. Adult acute lymphoblastic leukemia. *Mayo Clin Proc,* 80**,** 1517-27.

JOHN, L. B. & WARD, A. C. 2011. The Ikaros gene family: transcriptional regulators of hematopoiesis and immunity. *Mol Immunol,* 48**,** 1272-8.

JOSHI, I., YOSHIDA, T., JENA, N., QI, X., ZHANG, J., VAN ETTEN, R. A. & GEORGOPOULOS, K. 2014. Loss of Ikaros DNA-binding function confers integrin-dependent survival on pre-B cells and progression to acute lymphoblastic leukemia. *Nature immunology,* 15**,** 294-304.

KANG, Z.-J., LIU, Y.-F., XU, L.-Z., LONG, Z.-J., HUANG, D., YANG, Y., LIU, B., FENG, J.-X., PAN, Y.-J., YAN, J.-S. & LIU, Q. 2016. The Philadelphia chromosome in leukemogenesis. *Chinese Journal of Cancer,* 35**,** 48.

KASTNER, P., DUPUIS, A., GAUB, M.-P., HERBRECHT, R., LUTZ, P. & CHAN, S. 2013. Function of Ikaros as a tumor suppressor in B cell acute lymphoblastic leukemia. *American journal of blood research,* 3**,** 1-13.

KIM, J., SIF, S., JONES, B., JACKSON, A., KOIPALLY, J., HELLER, E., WINANDY, S., VIEL, A., SAWYER, A., IKEDA, T., KINGSTON, R. &

GEORGOPOULOS, K. 1999. Ikaros DNA-binding proteins direct formation of chromatin remodeling complexes in lymphocytes. *Immunity,* 10**,** 345-55.

KIM, J. H., CHU, S. C., GRAMLICH, J. L., PRIDE, Y. B., BABENDREIER, E., CHAUHAN, D., SALGIA, R., PODAR, K., GRIFFIN, J. D. & SATTLER, M. 2005. Activation of the PI3K/mTOR pathway by BCR-ABL contributes to increased production of reactive oxygen species. *Blood,* 105**,** 1717-23.

KIM, M.-S., LAPKOUSKI, M., YANG, W. & GELLERT, M. 2015. Crystal structure of the V(D)J recombinase RAG1–RAG2. *Nature,* 518**,** 507-511.

KIRSTETTER, P., THOMAS, M., DIERICH, A., KASTNER, P. & CHAN, S. 2002. Ikaros is critical for B cell differentiation and function. *Eur J Immunol,* 32**,** 720-30.

KOBITZSCH, B., GÖKBUGET, N., SCHWARTZ, S., REINHARDT, R., BRÜGGEMANN, M., VIARDOT, A., WÄSCH, R., STARCK, M., THIEL, E., HOELZER, D. & BURMEISTER, T. 2017. Loss-of-function but not dominant-negative intragenic IKZF1 deletions are associated with an adverse prognosis in adult BCR-ABL-negative acute lymphoblastic leukemia. *Haematologica,* 102**,** 1739-1747.

KOTROVA, M., MUZIKOVA, K., MEJSTRIKOVA, E., NOVAKOVA, M., BAKARDJIEVA-MIHAYLOVA, V., FISER, K., STUCHLY, J., GIRAUD, M., SALSON, M., POTT, C., BRÜGGEMANN, M., FÜLLGRABE, M., STARY, J., TRKA, J. & FRONKOVA, E. 2015. The predictive strength of next-generation sequencing MRD detection for relapse compared with current methods in childhood ALL. *Blood,* 126**,** 1045-1047.

KOTROVA, M., VAN DER VELDEN, V. H. J., VAN DONGEN, J. J. M., FORMANKOVA, R., SEDLACEK, P., BRÜGGEMANN, M., ZUNA, J., STARY, J., TRKA, J. & FRONKOVA, E. 2017. Next-generation sequencing indicates false-positive MRD results and better predicts prognosis after SCT in patients with childhood ALL. *Bone Marrow Transplantation,* 52**,** 962-968.

KRUSE, A., ABDEL-AZIM, N., KIM, H. N., RUAN, Y., PHAN, V., OGANA, H., WANG, W., LEE, R., GANG, E. J., KHAZAL, S. & KIM, Y. M. 2020. Minimal Residual Disease Detection in Acute Lymphoblastic Leukemia. *Int J Mol Sci,* 21.

KUNISAKI, Y., BRUNS, I., SCHEIERMANN, C., AHMED, J., PINHO, S., ZHANG, D., MIZOGUCHI, T., WEI, Q., LUCAS, D., ITO, K., MAR, J. C., BERGMAN, A. & FRENETTE, P. S. 2013. Arteriolar niches maintain haematopoietic stem cell quiescence. *Nature,* 502**,** 637-43.

KUO, T. C. & SCHLISSEL, M. S. 2009. Mechanisms controlling expression of the RAG locus during lymphocyte development. *Current opinion in immunology,* 21**,** 173-178.

LASLO, P., SPOONER, C. J., WARMFLASH, A., LANCKI, D. W., LEE, H.-J., SCIAMMAS, R., GANTNER, B. N., DINNER, A. R. & SINGH, H. 2006. Multilineage Transcriptional Priming and Determination of Alternate Hematopoietic Cell Fates. *Cell,* 126**,** 755-766.

LEE, G. S., NEIDITCH, M. B., SALUS, S. S. & ROTH, D. B. 2004. RAG Proteins Shepherd Double-Strand Breaks to a Specific Pathway, Suppressing Error-Prone Repair, but RAG Nicking Initiates Homologous Recombination. *Cell,* 117**,** 171-184.

LENK, L., ALSADEQ, A. & SCHEWE, D. M. 2020. Involvement of the central nervous system in acute lymphoblastic leukemia: opinions on molecular mechanisms and clinical implications based on recent data. *Cancer Metastasis Rev,* 39**,** 173-187.

LESCALE, C. & DERIANO, L. 2016. V(D)J Recombination: Orchestrating Diversity without Damage. *In:* BRADSHAW, R. A. & STAHL, P. D. (eds.) *Encyclopedia of Cell Biology.* Waltham: Academic Press.

LEWIS, S. M. 1994. The mechanism of V(D)J joining: lessons from molecular, immunological, and comparative analyses. *Adv Immunol,* 56**,** 27-150.

LI, Z., SONG, C., OUYANG, H., LAI, L., PAYNE, K. J. & DOVAT, S. 2012. Cell cycle-specific function of Ikaros in human leukemia. *Pediatric Blood & Cancer,* 59**,** 69-76.

LIU, T., KISHTON, R. J., MACINTYRE, A. N., GERRIETS, V. A., XIANG, H., LIU, X., ABEL, E. D., RIZZIERI, D., LOCASALE, J. W. & RATHMELL, J. C. 2014. Glucose transporter 1-mediated glucose uptake is limiting for B-cell acute lymphoblastic leukemia anabolic metabolism and resistance to apoptosis. *Cell death & disease,* 5**,** e1470-e1470.

LOPES, B. A., MEYER, C., BARBOSA, T. C., POUBEL, C. P., MANSUR, M. B., DUPLOYEZ, N., BASHTON, M., HARRISON, C. J., ZUR STADT, U., HORSTMANN, M., POMBO-DE-OLIVEIRA, M. S., PALMI, C., CAZZANIGA, G., VENN, N. C., SUTTON, R., ALONSO, C. N., TSAUR, G., GUPTA, S. K., BAKHSHI, S., MARSCHALEK, R. & EMERENCIANO, M. 2019. IKZF1 Deletions with COBL Breakpoints Are Not Driven by RAG-Mediated Recombination Events in Acute Lymphoblastic Leukemia. *Translational Oncology,* 12**,** 726-732.

LOPEZ, R. A., SCHOETZ, S., DEANGELIS, K., O'NEILL, D. & BANK, A. 2002. Multiple hematopoietic defects and delayed globin switching in Ikaros null mice. *Proceedings of the National Academy of Sciences of the United States of America,* 99**,** 602-607.

MA, H., SUN, H. & SUN, X. 2014. Survival improvement by decade of patients aged 0-14 years with acute lymphoblastic leukemia: a SEER analysis. *Sci Rep,* 4**,** 4227.

MALONEY, K. W., DEVIDAS, M., WANG, C., MATTANO, L. A., FRIEDMANN, A. M., BUCKLEY, P., BOROWITZ, M. J., CARROLL, A. J., GASTIER-FOSTER, J. M., HEEREMA, N. A., KADAN-LOTTICK, N., LOH, M. L., MATLOUB, Y. H., MARSHALL, D. T., STORK, L. C., RAETZ, E. A., WOOD, B., HUNGER, S. P., CARROLL, W. L. & WINICK, N. J. 2020. Outcome in Children With Standard-Risk B-Cell Acute Lymphoblastic Leukemia: Results of Children's Oncology Group Trial AALL0331. *J Clin Oncol,* 38**,** 602-612.

MÅNSSON, R., HULTQUIST, A., LUC, S., YANG, L., ANDERSON, K., KHARAZI, S., AL-HASHMI, S., LIUBA, K., THORÉN, L., ADOLFSSON, J., BUZA-VIDAS, N., QIAN, H., SONEJI, S., ENVER, T., SIGVARDSSON, M. & JACOBSEN, S. E. 2007. Molecular evidence for hierarchical transcriptional lineage priming in fetal and adult stem cells and multipotent progenitors. *Immunity,* 26**,** 407-19.

MARKE, R., HAVINGA, J., CLOOS, J., DEMKES, M., POELMANS, G., YUNIATI, L., VAN INGEN SCHENAU, D., SONNEVELD, E., WAANDERS, E., PIETERS, R., KUIPER, R. P., HOOGERBRUGGE, P. M., KASPERS, G.

J. L., VAN LEEUWEN, F. N. & SCHEIJEN, B. 2015. Tumor suppressor IKZF1 mediates glucocorticoid resistance in B-cell precursor acute lymphoblastic leukemia. *Leukemia,* 30**,** 1599.

MAZZURANA, L., FORKEL, M., RAO, A., VAN ACKER, A., KOKKINOU, E., ICHIYA, T., ALMER, S., HÖÖG, C., FRIBERG, D. & MJÖSBERG, J. 2019. Suppression of Aiolos and Ikaros expression by lenalidomide reduces human ILC3-ILC1/NK cell transdifferentiation. *Eur J Immunol,* 49**,** 1344-1355.

MCCARTY, A. S., KLEIGER, G., EISENBERG, D. & SMALE, S. T. 2003. Selective Dimerization of a C2H2 Zinc Finger Subfamily. *Molecular Cell,* 11**,** 459-470.

MÉNDEZ-FERRER, S., LUCAS, D., BATTISTA, M. & FRENETTE, P. S. 2008. Haematopoietic stem cell release is regulated by circadian oscillations. *Nature,* 452**,** 442-7.

MIYAZAKI, K. & MIYAZAKI, M. 2021. The Interplay Between Chromatin Architecture and Lineage-Specific Transcription Factors and the Regulation of Rag Gene Expression. *Frontiers in immunology,* 12**,** 659761-659761.

MIYAZAKI, K., MIYAZAKI, M. & MURRE, C. 2014. The establishment of B versus T cell identity. *Trends Immunol,* 35**,** 205-10.

MIYAZAKI, K., WATANABE, H., YOSHIKAWA, G., CHEN, K., HIDAKA, R., AITANI, Y., OSAWA, K., TAKEDA, R., OCHI, Y., TANI-ICHI, S., UEHATA, T., TAKEUCHI, O., IKUTA, K., OGAWA, S., KONDOH, G., LIN, Y. C., OGATA, H. & MIYAZAKI, M. 2020. The transcription factor E2A activates multiple enhancers that drive Rag expression in developing T and B cells. *Sci Immunol,* 5.

MOLNÁR, A., WU, P., LARGESPADA, D. A., VORTKAMP, A., SCHERER, S., COPELAND, N. G., JENKINS, N. A., BRUNS, G. & GEORGOPOULOS, K. 1996. The Ikaros gene encodes a family of lymphocyte-restricted zinc finger DNA binding proteins, highly conserved in human and mouse. *J Immunol,* 156**,** 585-92.

MOORMAN, A. V., ENSHAEI, A., SCHWAB, C., WADE, R., CHILTON, L., ELLIOTT, A., RICHARDSON, S., HANCOCK, J., KINSEY, S. E., MITCHELL, C. D., GOULDEN, N., VORA, A. & HARRISON, C. J. 2014. A novel integrated cytogenetic and genomic classification refines risk stratification in pediatric acute lymphoblastic leukemia. *Blood,* 124**,** 1434-1444.

MOORMAN, A. V., HARRISON, C. J., BUCK, G. A., RICHARDS, S. M., SECKER-WALKER, L. M., MARTINEAU, M., VANCE, G. H., CHERRY, A. M., HIGGINS, R. R., FIELDING, A. K., FORONI, L., PAIETTA, E., TALLMAN, M. S., LITZOW, M. R., WIERNIK, P. H., ROWE, J. M., GOLDSTONE, A. H. & DEWALD, G. W. 2007. Karyotype is an independent prognostic factor in adult acute lymphoblastic leukemia (ALL): analysis of cytogenetic data from patients treated on the Medical Research Council (MRC) UKALLXII/Eastern Cooperative Oncology Group (ECOG) 2993 trial. *Blood,* 109**,** 3189-97.

MOORMAN, A. V., SCHWAB, C., ENSOR, H. M., RUSSELL, L. J., MORRISON, H., JONES, L., MASIC, D., PATEL, B., ROWE, J. M., TALLMAN, M., GOLDSTONE, A. H., FIELDING, A. K. & HARRISON, C. J. 2012. IGH@

Translocations, CRLF2 Deregulation, and Microdeletions in Adolescents and Adults With Acute Lymphoblastic Leukemia. *Journal of Clinical Oncology,* 30**,** 3100-3108.

MORIYAMA, T., METZGER, M. L., WU, G., NISHII, R., QIAN, M., DEVIDAS, M., YANG, W., CHENG, C., CAO, X., QUINN, E., RAIMONDI, S., GASTIER-FOSTER, J. M., RAETZ, E., LARSEN, E., MARTIN, P. L., BOWMAN, W. P., WINICK, N., KOMADA, Y., WANG, S., EDMONSON, M., XU, H., MARDIS, E., FULTON, R., PUI, C.-H., MULLIGHAN, C., EVANS, W. E., ZHANG, J., HUNGER, S. P., RELLING, M. V., NICHOLS, K. E., LOH, M. L. & YANG, J. J. 2015. Germline genetic variation in ETV6 and risk of childhood acute lymphoblastic leukaemia: a systematic genetic study. *The Lancet Oncology,* 16**,** 1659-1666.

MULLIGHAN, C. G., MILLER, C. B., RADTKE, I., PHILLIPS, L. A., DALTON, J., MA, J., WHITE, D., HUGHES, T. P., LE BEAU, M. M., PUI, C.-H., RELLING, M. V., SHURTLEFF, S. A. & DOWNING, J. R. 2008. BCR–ABL1 lymphoblastic leukaemia is characterized by the deletion of Ikaros. *Nature,* 453**,** 110.

MULLIGHAN, C. G., SU, X., ZHANG, J., RADTKE, I., PHILLIPS, L. A. A., MILLER, C. B., MA, J., LIU, W., CHENG, C., SCHULMAN, B. A., HARVEY, R. C., CHEN, I. M., CLIFFORD, R. J., CARROLL, W. L., REAMAN, G., BOWMAN, W. P., DEVIDAS, M., GERHARD, D. S., YANG, W., RELLING, M. V., SHURTLEFF, S. A., CAMPANA, D., BOROWITZ, M. J., PUI, C.-H., SMITH, M., HUNGER, S. P., WILLMAN, C. L. & DOWNING, J. R. 2009. Deletion of IKZF1 and Prognosis in Acute Lymphoblastic Leukemia. *New England Journal of Medicine,* 360**,** 470-480.

NACHEVA, E. P., BRAZMA, D., VIRGILI, A., HOWARD-REEVES, J., CHANALARIS, A., GANCHEVA, K., APOSTOLOVA, M., VALGAÑON, M., MAZZULLO, H. & GRACE, C. 2010. Deletions of Immunoglobulin heavy chain and T cell receptor gene regions are uniquely associated with lymphoid blast transformation of chronic myeloid leukemia. *BMC Genomics,* 11**,** 41.

NARAYANAN, S. & SHAMI, P. J. 2012. Treatment of acute lymphoblastic leukemia in adults. *Crit Rev Oncol Hematol,* 81**,** 94-102.

NAVEIRAS, O., NARDI, V., WENZEL, P. L., HAUSCHKA, P. V., FAHEY, F. & DALEY, G. Q. 2009. Bone-marrow adipocytes as negative regulators of the haematopoietic microenvironment. *Nature,* 460**,** 259-63.

NG, S. Y.-M., YOSHIDA, T., ZHANG, J. & GEORGOPOULOS, K. 2009. Genome-wide Lineage-Specific Transcriptional Networks Underscore Ikaros-Dependent Lymphoid Priming in Hematopoietic Stem Cells. *Immunity,* 30**,** 493-507.

NICHOGIANNOPOULOU, A., TREVISAN, M., NEBEN, S., FRIEDRICH, C. & GEORGOPOULOS, K. 1999. Defects in hemopoietic stem cell activity in Ikaros mutant mice. *J Exp Med,* 190**,** 1201-14.

NOVOSELETSKAYA, E., GRIGORIEVA, O., NIMIRITSKY, P., BASALOVA, N., EREMICHEV, R., MILOVSKAYA, I., KULEBYAKIN, K., KULEBYAKINA, M., RODIONOV, S., OMELYANENKO, N. & EFIMENKO, A. 2020. Mesenchymal Stromal Cell-Produced Components of Extracellular Matrix Potentiate Multipotent Stem Cell Response to Differentiation Stimuli. *Frontiers in Cell and Developmental Biology,* 8.

NOWELL, P. C. & HUNGERFORD, D. A. 1960. Chromosome studies on normal and leukemic human leukocytes. *J Natl Cancer Inst,* 25**,** 85-109.

O'BRIEN, S. G., GUILHOT, F., LARSON, R. A., GATHMANN, I., BACCARANI, M., CERVANTES, F., CORNELISSEN, J. J., FISCHER, T., HOCHHAUS, A., HUGHES, T., LECHNER, K., NIELSEN, J. L., ROUSSELOT, P., REIFFERS, J., SAGLIO, G., SHEPHERD, J., SIMONSSON, B., GRATWOHL, A., GOLDMAN, J. M., KANTARJIAN, H., TAYLOR, K., VERHOEF, G., BOLTON, A. E., CAPDEVILLE, R. & DRUKER, B. J. 2003. Imatinib compared with interferon and low-dose cytarabine for newly diagnosed chronic-phase chronic myeloid leukemia. *N Engl J Med,* 348**,** 994-1004.

OKEN, M. M., CREECH, R. H., TORMEY, D. C., HORTON, J., DAVIS, T. E., MCFADDEN, E. T. & CARBONE, P. P. 1982. Toxicity and response criteria of the Eastern Cooperative Oncology Group. *American Journal of Clinical Oncology,* 5.

ORAVECZ, A., APOSTOLOV, A., POLAK, K., JOST, B., LE GRAS, S., CHAN, S. & KASTNER, P. 2015. Ikaros mediates gene silencing in T cells through Polycomb repressive complex 2. *Nat Commun,* 6**,** 8823.

PALMI, C., VALSECCHI, M. G., LONGINOTTI, G., SILVESTRI, D., CARRINO, V., CONTER, V., BASSO, G., BIONDI, A., KRONNIE, G. T. & CAZZANIGA, G. 2013. What is the relevance of Ikaros gene deletions as a prognostic marker in pediatric Philadelphia-negative B-cell precursor acute lymphoblastic leukemia? *Haematologica,* 98, 1226.

PAPAEMMANUIL, E., RAPADO, I., LI, Y., POTTER, N. E., WEDGE, D. C., TUBIO, J., ALEXANDROV, L. B., VAN LOO, P., COOKE, S. L., MARSHALL, J., MARTINCORENA, I., HINTON, J., GUNDEM, G., VAN DELFT, F. W., NIK-ZAINAL, S., JONES, D. R., RAMAKRISHNA, M., TITLEY, I., STEBBINGS, L., LEROY, C., MENZIES, A., GAMBLE, J., ROBINSON, B., MUDIE, L., RAINE, K., O'MEARA, S., TEAGUE, J. W., BUTLER, A. P., CAZZANIGA, G., BIONDI, A., ZUNA, J., KEMPSKI, H., MUSCHEN, M., FORD, A. M., STRATTON, M. R., GREAVES, M. & CAMPBELL, P. J. 2014. RAG-mediated recombination is the predominant driver of oncogenic rearrangement in ETV6-RUNX1 acute lymphoblastic leukemia. *Nat Genet,* 46**,** 116-25.

PATEL, B., KIRKWOOD, A. A., DEY, A., MARKS, D. I., MCMILLAN, A. K., MENNE, T. F., MICKLEWRIGHT, L., PATRICK, P., PURNELL, S., ROWNTREE, C. J., SMITH, P. & FIELDING, A. K. 2017. Pegylated-asparaginase during induction therapy for adult acute lymphoblastic leukaemia: toxicity data from the UKALL14 trial. *Leukemia,* 31**,** 58-64.

PEREZ-ANDREU, V., ROBERTS, K. G., XU, H., SMITH, C., ZHANG, H., YANG, W., HARVEY, R. C., PAYNE-TURNER, D., DEVIDAS, M., CHENG, I. M., CARROLL, W. L., HEEREMA, N. A., CARROLL, A. J., RAETZ, E. A., GASTIER-FOSTER, J. M., MARCUCCI, G., BLOOMFIELD, C. D., MROZEK, K., KOHLSCHMIDT, J., STOCK, W., KORNBLAU, S. M., KONOPLEVA, M., PAIETTA, E., ROWE, J. M., LUGER, S. M., TALLMAN, M. S., DEAN, M., BURCHARD, E. G., TORGERSON, D. G., YUE, F., WANG, Y., PUI, C. H., JEHA, S., RELLING, M. V., EVANS, W. E., GERHARD, D. S., LOH, M. L., WILLMAN, C. L., HUNGER, S. P.,

MULLIGHAN, C. G. & YANG, J. J. 2015. A genome-wide association study of susceptibility to acute lymphoblastic leukemia in adolescents and young adults. *Blood,* 125**,** 680-6.

PEROTTI, E. A., GEORGOPOULOS, K. & YOSHIDA, T. 2015. An Ikaros Promoter Element with Dual Epigenetic and Transcriptional Activities. *PLOS ONE,* 10**,** e0131568.

PFEIFER, H., CAZZANIGA, G., VAN DER VELDEN, V. H. J., CAYUELA, J. M., SCHÄFER, B., SPINELLI, O., AKIKI, S., AVIGAD, S., BENDIT, I., BORG, K., CAVÉ, H., ELIA, L., RESHMI, S. C., GERRARD, G., HAYETTE, S., HERMANSON, M., JUH, A., JURCEK, T., CHILLÓN, M. C., HOMBURG, C., MARTINELLI, G., KAIRISTO, V., LANGE, T., LION, T., MUELLER, M. C., PANE, F., RAI, L., DAMM-WELK, C., SACHA, T., SCHNITTGER, S., TOULOUMENIDOU, T., VALERHAUGEN, H., VANDENBERGHE, P., ZUNA, J., SERVE, H., HERRMANN, E., MARKOVIC, S., DONGEN, J. & OTTMANN, O. G. 2019. Standardisation and consensus guidelines for minimal residual disease assessment in Philadelphia-positive acute lymphoblastic leukemia (Ph + ALL) by real-time quantitative reverse transcriptase PCR of e1a2 BCR-ABL1. *Leukemia,* 33**,** 1910-1922.

PFEIFER, H., RAUM, K., MARKOVIC, S., NOWAK, V., FEY, S., OBLÄNDER, J., PRESSLER, J., BÖHM, V., BRÜGGEMANN, M., WUNDERLE, L., HÜTTMANN, A., WÄSCH, R., BECK, J., STELLJES, M., VIARDOT, A., LANG, F., HOELZER, D., HOFMANN, W.-K., SERVE, H., WEISS, C., GOEKBUGET, N., OTTMANN, O. G. & NOWAK, D. 2018. Genomic CDKN2A/2B deletions in adult Ph+ ALL are adverse despite allogeneic stem cell transplantation. *Blood,* blood-2017-07-796862.

PIETERS, R., DE GROOT-KRUSEMAN, H., VAN DER VELDEN, V., FIOCCO, M., VAN DEN BERG, H., DE BONT, E., EGELER, R. M., HOOGERBRUGGE, P., KASPERS, G., VAN DER SCHOOT, E., DE HAAS, V. & VAN DONGEN, J. 2016. Successful Therapy Reduction and Intensification for Childhood Acute Lymphoblastic Leukemia Based on Minimal Residual Disease Monitoring: Study ALL10 From the Dutch Childhood Oncology Group. *J Clin Oncol,* 34**,** 2591-601.

PONGERS-WILLEMSE, M. J., SERIU, T., STOLZ, F., D'ANIELLO, E., GAMEIRO, P., PISA, P., GONZALEZ, M., BARTRAM, C. R., PANZER-GRÜMAYER, E. R., BIONDI, A., SAN MIGUEL, J. F. & VAN DONGEN, J. J. M. 1999. Primers and protocols for standardized detection of minimal residual disease in acute lymphoblastic leukemia using immunoglobulin and T cell receptor gene rearrangements and TAL1 deletions as PCR targets. Report of the BIOMED-1 CONCERTED ACTION: Investigation of minimal residual disease in acute leukemia. *Leukemia,* 13**,** 110-118.

PORKKA, K., KOSKENVESA, P., LUNDÁN, T., RIMPILÄINEN, J., MUSTJOKI, S., SMYKLA, R., WILD, R., LUO, R., ARNAN, M., BRETHON, B., ECCERSLEY, L., HJORTH-HANSEN, H., HÖGLUND, M., KLAMOVA, H., KNUTSEN, H., PARIKH, S., RAFFOUX, E., GRUBER, F., BRITO-BABAPULLE, F., DOMBRET, H., DUARTE, R. F., ELONEN, E., PAQUETTE, R., ZWAAN, C. M. & LEE, F. Y. 2008. Dasatinib crosses the blood-brain barrier and is an efficient therapy for central nervous system Philadelphia chromosome-positive leukemia. *Blood,* 112**,** 1005-12.

PUI, C. H., PEI, D., COUSTAN-SMITH, E., JEHA, S., CHENG, C., BOWMAN, W. P., SANDLUND, J. T., RIBEIRO, R. C., RUBNITZ, J. E., INABA, H., BHOJWANI, D., GRUBER, T. A., LEUNG, W. H., DOWNING, J. R., EVANS, W. E., RELLING, M. V. & CAMPANA, D. 2015. Clinical utility of sequential minimal residual disease measurements in the context of risk-based therapy in childhood acute lymphoblastic leukaemia: a prospective study. *Lancet Oncol,* 16**,** 465-74.

PULTE, D., JANSEN, L., GONDOS, A., KATALINIC, A., BARNES, B., RESSING, M., HOLLECZEK, B., EBERLE, A., BRENNER, H. & GROUP, G. C. S. W. 2014. Survival of adults with acute lymphoblastic leukemia in Germany and the United States. *PloS one,* 9**,** e85554-e85554.

RECKEL, S., HAMELIN, R., GEORGEON, S., ARMAND, F., JOLLIET, Q., CHIAPPE, D., MONIATTE, M. & HANTSCHEL, O. 2017. Differential signaling networks of Bcr–Abl p210 and p190 kinases in leukemia cells defined by functional proteomics. *Leukemia,* 31**,** 1502-1512.

RESHMI, S. C., HARVEY, R. C., ROBERTS, K. G., STONEROCK, E., SMITH, A., JENKINS, H., CHEN, I. M., VALENTINE, M., LIU, Y., LI, Y., SHAO, Y., EASTON, J., PAYNE-TURNER, D., GU, Z., TRAN, T. H., NGUYEN, J. V., DEVIDAS, M., DAI, Y., HEEREMA, N. A., CARROLL, A. J., 3RD, RAETZ, E. A., BOROWITZ, M. J., WOOD, B. L., ANGIOLILLO, A. L., BURKE, M. J., SALZER, W. L., ZWEIDLER-MCKAY, P. A., RABIN, K. R., CARROLL, W. L., ZHANG, J., LOH, M. L., MULLIGHAN, C. G., WILLMAN, C. L., GASTIER-FOSTER, J. M. & HUNGER, S. P. 2017. Targetable kinase gene fusions in high-risk B-ALL: a study from the Children's Oncology Group. *Blood,* 129**,** 3352-3361.

REYNAUD, D., DEMARCO, I. A., REDDY, K. L., SCHJERVEN, H., BERTOLINO, E., CHEN, Z., SMALE, S. T., WINANDY, S. & SINGH, H. 2008. Regulation of B cell fate commitment and immunoglobulin heavy-chain gene rearrangements by Ikaros. *Nat Immunol,* 9**,** 927-36.

ROBERTS, K. G., GU, Z., PAYNE-TURNER, D., MCCASTLAIN, K., HARVEY, R. C., CHEN, I. M., PEI, D., IACOBUCCI, I., VALENTINE, M., POUNDS, S. B., SHI, L., LI, Y., ZHANG, J., CHENG, C., RAMBALDI, A., TOSI, M., SPINELLI, O., RADICH, J. P., MINDEN, M. D., ROWE, J. M., LUGER, S., LITZOW, M. R., TALLMAN, M. S., WIERNIK, P. H., BHATIA, R., ALDOSS, I., KOHLSCHMIDT, J., MROZEK, K., MARCUCCI, G., BLOOMFIELD, C. D., STOCK, W., KORNBLAU, S., KANTARJIAN, H. M., KONOPLEVA, M., PAIETTA, E., WILLMAN, C. L. & MULLIGHAN, C. G. 2017. High Frequency and Poor Outcome of Philadelphia Chromosome-Like Acute Lymphoblastic Leukemia in Adults. *J Clin Oncol,* 35**,** 394-401.

ROBERTS, K. G., LI, Y., PAYNE-TURNER, D., HARVEY, R. C., YANG, Y. L., PEI, D., MCCASTLAIN, K., DING, L., LU, C., SONG, G., MA, J., BECKSFORT, J., RUSCH, M., CHEN, S. C., EASTON, J., CHENG, J., BOGGS, K., SANTIAGO-MORALES, N., IACOBUCCI, I., FULTON, R. S., WEN, J., VALENTINE, M., CHENG, C., PAUGH, S. W., DEVIDAS, M., CHEN, I. M., RESHMI, S., SMITH, A., HEDLUND, E., GUPTA, P., NAGAHAWATTE, P., WU, G., CHEN, X., YERGEAU, D., VADODARIA, B., MULDER, H., WINICK, N. J., LARSEN, E. C., CARROLL, W. L., HEEREMA, N. A., CARROLL, A. J., GRAYSON, G., TASIAN, S. K., MOORE, A. S., KELLER, F., FREI-JONES, M., WHITLOCK, J. A., RAETZ,

E. A., WHITE, D. L., HUGHES, T. P., GUIDRY AUVIL, J. M., SMITH, M. A., MARCUCCI, G., BLOOMFIELD, C. D., MROZEK, K., KOHLSCHMIDT, J., STOCK, W., KORNBLAU, S. M., KONOPLEVA, M., PAIETTA, E., PUI, C. H., JEHA, S., RELLING, M. V., EVANS, W. E., GERHARD, D. S., GASTIER-FOSTER, J. M., MARDIS, E., WILSON, R. K., LOH, M. L., DOWNING, J. R., HUNGER, S. P., WILLMAN, C. L., ZHANG, J. & MULLIGHAN, C. G. 2014. Targetable kinase-activating lesions in Ph-like acute lymphoblastic leukemia. *N Engl J Med,* 371**,** 1005-15.

ROBERTS, K. G., MORIN, R. D., ZHANG, J., HIRST, M., ZHAO, Y., SU, X., CHEN, S. C., PAYNE-TURNER, D., CHURCHMAN, M. L., HARVEY, R. C., CHEN, X., KASAP, C., YAN, C., BECKSFORT, J., FINNEY, R. P., TEACHEY, D. T., MAUDE, S. L., TSE, K., MOORE, R., JONES, S., MUNGALL, K., BIROL, I., EDMONSON, M. N., HU, Y., BUETOW, K. E., CHEN, I. M., CARROLL, W. L., WEI, L., MA, J., KLEPPE, M., LEVINE, R. L., GARCIA-MANERO, G., LARSEN, E., SHAH, N. P., DEVIDAS, M., REAMAN, G., SMITH, M., PAUGH, S. W., EVANS, W. E., GRUPP, S. A., JEHA, S., PUI, C. H., GERHARD, D. S., DOWNING, J. R., WILLMAN, C. L., LOH, M., HUNGER, S. P., MARRA, M. A. & MULLIGHAN, C. G. 2012. Genetic alterations activating kinase and cytokine receptor signaling in high-risk acute lymphoblastic leukemia. *Cancer Cell,* 22**,** 153-66.

ROGERS, J. H., GUPTA, R., REYES, J. M., BRUNETTI, L., GUNDRY, M. C., SONG, T., JOHNSON, C., CRISTOBAL, C. D. D., GOODELL, M. A. & RAU, R. E. 2018. Precise Modeling of IKZF1 Alterations in Human B-Cell Acute Lymphoblastic Leukemia Cell Lines Reveals Distinct Chemosensitivity, Homing, and Engraftment Properties. *Blood,* 132**,** 549-549.

ROUSSELOT, P., COUDÉ, M. M., GOKBUGET, N., GAMBACORTI PASSERINI, C., HAYETTE, S., CAYUELA, J. M., HUGUET, F., LEGUAY, T., CHEVALLIER, P., SALANOUBAT, C., BONMATI, C., ALEXIS, M., HUNAULT, M., GLAISNER, S., AGAPE, P., BERTHOU, C., JOURDAN, E., FERNANDES, J., SUTTON, L., BANOS, A., REMAN, O., LIOURE, B., THOMAS, X., IFRAH, N., LAFAGE-POCHITALOFF, M., BORNAND, A., MORISSET, L., ROBIN, V., PFEIFER, H., DELANNOY, A., RIBERA, J., BASSAN, R., DELORD, M., HOELZER, D., DOMBRET, H. & OTTMANN, O. G. 2016. Dasatinib and low-intensity chemotherapy in elderly patients with Philadelphia chromosome-positive ALL. *Blood,* 128**,** 774-82.

ROWE, J. M. 2010. Prognostic factors in adult acute lymphoblastic leukaemia. *British Journal of Haematology,* 150**,** 389-405.

ROWLEY, J. D. 1973. A New Consistent Chromosomal Abnormality in Chronic Myelogenous Leukaemia identified by Quinacrine Fluorescence and Giemsa Staining. *Nature,* 243**,** 290-293.

RUSSELL, L. J., CAPASSO, M., VATER, I., AKASAKA, T., BERNARD, O. A., CALASANZ, M. J., CHANDRASEKARAN, T., CHAPIRO, E., GESK, S., GRIFFITHS, M., GUTTERY, D. S., HAFERLACH, C., HARDER, L., HEIDENREICH, O., IRVING, J., KEARNEY, L., NGUYEN-KHAC, F., MACHADO, L., MINTO, L., MAJID, A., MOORMAN, A. V., MORRISON, H., RAND, V., STREFFORD, J. C., SCHWAB, C., TONNIES, H., DYER, M. J., SIEBERT, R. & HARRISON, C. J. 2009. Deregulated expression of

cytokine receptor gene, CRLF2, is involved in lymphoid transformation in B-cell precursor acute lymphoblastic leukemia. *Blood,* 114**,** 2688-98.

SAKANO, H., HÜPPI, K., HEINRICH, G. & TONEGAWA, S. 1979. Sequences at the somatic recombination sites of immunoglobulin light-chain genes. *Nature,* 280**,** 288-294.

SAMRA, B., JABBOUR, E., RAVANDI, F., KANTARJIAN, H. & SHORT, N. J. 2020. Evolving therapy of adult acute lymphoblastic leukemia: state-of-the-art treatment and future directions. *Journal of Hematology & Oncology,* 13**,** 70.

SCHEIJEN, B., BOER, J. M., MARKE, R., TIJCHON, E., VAN INGEN SCHENAU, D., WAANDERS, E., VAN EMST, L., VAN DER MEER, L. T., PIETERS, R., ESCHERICH, G., HORSTMANN, M. A., SONNEVELD, E., VENN, N., SUTTON, R., DALLA-POZZA, L., KUIPER, R. P., HOOGERBRUGGE, P. M., DEN BOER, M. L. & VAN LEEUWEN, F. N. 2017. Tumor suppressors BTG1 and IKZF1 cooperate during mouse leukemia development and increase relapse risk in B-cell precursor acute lymphoblastic leukemia patients. *Haematologica,* 102**,** 541-551.

SCHIECK, M., LENTES, J., THOMAY, K., HOFMANN, W., BEHRENS, Y. L., HAGEDORN, M., EBERSOLD, J., DAVENPORT, C. F., FAZIO, G., MÖRICKE, A., BUCHMANN, S., ALTEN, J., CARIO, G., SCHRAPPE, M., BERGMANN, A. K., STANULLA, M., STEINEMANN, D., SCHLEGELBERGER, B., CAZZANIGA, G. & GÖHRING, G. 2020. Implementation of RNA sequencing and array CGH in the diagnostic workflow of the AIEOP-BFM ALL 2017 trial on acute lymphoblastic leukemia. *Annals of Hematology,* 99**,** 809-818.

SCHJERVEN, H., MCLAUGHLIN, J., ARENZANA, T. L., FRIETZE, S., CHENG, D., WADSWORTH, S. E., LAWSON, G. W., BENSINGER, S. J., FARNHAM, P. J., WITTE, O. N. & SMALE, S. T. 2013. Selective regulation of lymphopoiesis and leukemogenesis by individual zinc fingers of Ikaros. *Nat Immunol,* 14**,** 1073-83.

SCHWICKERT, T. A., TAGOH, H., GULTEKIN, S., DAKIC, A., AXELSSON, E., MINNICH, M., EBERT, A., WERNER, B., ROTH, M., CIMMINO, L., DICKINS, R. A., ZUBER, J., JARITZ, M. & BUSSLINGER, M. 2014. Stage-specific control of early B cell development by the transcription factor Ikaros. *Nat Immunol,* 15**,** 283-93.

SCORE, J., CALASANZ, M. J., OTTMAN, O., PANE, F., YEH, R. F., SOBRINHO-SIMÕES, M. A., KREIL, S., WARD, D., HIDALGO-CURTIS, C., MELO, J. V., WIEMELS, J., NADEL, B., CROSS, N. C. P. & GRAND, F. H. 2010. Analysis of genomic breakpoints in p190 and p210 BCR–ABL indicate distinct mechanisms of formation. *Leukemia,* 24**,** 1742-1750.

SHEN, S., CHEN, X., CAI, J., YU, J., GAO, J., HU, S., ZHAI, X., LIANG, C., JU, X., JIANG, H., JIN, R., WU, X., WANG, N., TIAN, X., PAN, K., JIANG, H., SUN, L., FANG, Y., LI, C.-K., HU, Q., YANG, M., ZHU, Y., ZHANG, H., LI, C., PEI, D., JEHA, S., YANG, J. J., CHENG, C., TANG, J., ZHU, X. & PUI, C.-H. 2020. Effect of Dasatinib vs Imatinib in the Treatment of Pediatric Philadelphia Chromosome–Positive Acute Lymphoblastic Leukemia: A Randomized Clinical Trial. *JAMA Oncology,* 6**,** 358-366.

SHORT, N. J., KANTARJIAN, H. M., RAVANDI, F., DAVER, N. G., PEMMARAJU, N., THOMAS, D. A., YILMAZ, M., KADIA, T. M., SASAKI,

K., GARRIS, R., GARCIA-MANERO, G., DINARDO, C. D., KONOPLEVA, M., ESTROV, Z., JAIN, N., WIERDA, W. G., JEANIS, V., CORTES, J. E., O'BRIEN, S. M. & JABBOUR, E. 2017. Frontline hyper-CVAD plus ponatinib for patients with Philadelphia chromosome-positive acute lymphoblastic leukemia: Updated results of a phase II study. *Journal of Clinical Oncology,* 35**,** 7013-7013.

SIVE, J. I., BUCK, G., FIELDING, A., LAZARUS, H. M., LITZOW, M. R., LUGER, S., MARKS, D. I., MCMILLAN, A., MOORMAN, A. V., RICHARDS, S. M., ROWE, J. M., TALLMAN, M. S. & GOLDSTONE, A. H. 2012. Outcomes in older adults with acute lymphoblastic leukaemia (ALL): results from the international MRC UKALL XII/ECOG2993 trial. *Br J Haematol,* 157**,** 463-71.

SONG, C., GE, Z., DING, Y., TAN, B.-H., DESAI, D., GOWDA, K., AMIN, S., GOWDA, R., ROBERTSON, G. P., YUE, F., HUANG, S., SPIEGELMAN, V., PAYNE, J. L., REEVES, M. E., GUREL, Z., IYER, S., DHANYAMRAJU, P. K., XIANG, M., KAWASAWA, Y. I., CURY, N. M., YUNES, J. A., MCGRATH, M., SCHRAMM, J., SU, R., YANG, Y., ZHAO, Z., LYU, X., MUSCHEN, M., PAYNE, K. J., GOWDA, C. & DOVAT, S. 2020. IKAROS and CK2 regulate expression of BCL-XL and chemosensitivity in high-risk B-cell acute lymphoblastic leukemia. *Blood,* 136**,** 1520-1534.

SONG, C., PAN, X., GE, Z., GOWDA, C., DING, Y., LI, H., LI, Z., YOCHUM, G., MUSCHEN, M., LI, Q., PAYNE, K. J. & DOVAT, S. 2016. Epigenetic regulation of gene expression by Ikaros, HDAC1 and Casein Kinase II in leukemia. *Leukemia,* 30**,** 1436-40.

STANULLA, M., CAVÉ, H., MOORMAN, A. V. & FOR THE INTERNATIONAL, B. F. M. S. G. 2020. IKZF1 deletions in pediatric acute lymphoblastic leukemia: still a poor prognostic marker? *Blood,* 135**,** 252-260.

STANULLA, M., DAGDAN, E., ZALIOVA, M., MÖRICKE, A., PALMI, C., CAZZANIGA, G., ECKERT, C., TE KRONNIE, G., BOURQUIN, J.-P., BORNHAUSER, B., KOEHLER, R., BARTRAM, C. R., LUDWIG, W.-D., BLECKMANN, K., GROENEVELD-KRENTZ, S., SCHEWE, D., JUNK, S. V., HINZE, L., KLEIN, N., KRATZ, C. P., BIONDI, A., BORKHARDT, A., KULOZIK, A., MUCKENTHALER, M. U., BASSO, G., VALSECCHI, M. G., IZRAELI, S., PETERSEN, B.-S., FRANKE, A., DÖRGE, P., STEINEMANN, D., HAAS, O. A., PANZER-GRÜMAYER, R., CAVÉ, H., HOULSTON, R. S., CARIO, G., SCHRAPPE, M. & ZIMMERMANN, M. 2018. IKZF1plus Defines a New Minimal Residual Disease–Dependent Very-Poor Prognostic Profile in Pediatric B-Cell Precursor Acute Lymphoblastic Leukemia. *Journal of Clinical Oncology,* 36**,** 1240-1249.

STANULLA, M. & SCHRAPPE, M. 2009. Treatment of childhood acute lymphoblastic leukemia. *Semin Hematol,* 46**,** 52-63.

STEEGHS, E. M. P., BOER, J. M., HOOGKAMER, A. Q., BOEREE, A., DE HAAS, V., DE GROOT-KRUSEMAN, H. A., HORSTMANN, M. A., ESCHERICH, G., PIETERS, R. & DEN BOER, M. L. 2019. Copy number alterations in B-cell development genes, drug resistance, and clinical outcome in pediatric B-cell precursor acute lymphoblastic leukemia. *Scientific Reports,* 9**,** 4634.

SUGIYAMA, T., KOHARA, H., NODA, M. & NAGASAWA, T. 2006. Maintenance of the hematopoietic stem cell pool by CXCL12-CXCR4 chemokine signaling in bone marrow stromal cell niches. *Immunity,* 25**,** 977-88.

SUN, L., LIU, A. & GEORGOPOULOS, K. 1996. Zinc finger-mediated protein interactions modulate Ikaros activity, a molecular control of lymphocyte development. *The EMBO journal,* 15**,** 5358-5369.

SZCZEPANSKI, T., PONGERS-WILLEMSE, M. J., LANGERAK, A. W. & VAN DONGEN, J. J. 1999. Unusual immunoglobulin and T-cell receptor gene rearrangement patterns in acute lymphoblastic leukemias. *Curr Top Microbiol Immunol,* 246**,** 205-13; discussion 214-5.

TERWILLIGER, T. & ABDUL-HAY, M. 2017. Acute lymphoblastic leukemia: a comprehensive review and 2017 update. *Blood Cancer Journal,* 7**,** e577-e577.

THOMAS, R. M., CHEN, C., CHUNDER, N., MA, L., TAYLOR, J., PEARCE, E. J. & WELLS, A. D. 2010. Ikaros silences T-bet expression and interferon-gamma production during T helper 2 differentiation. *J Biol Chem,* 285**,** 2545-53.

TISSING, W. J., MEIJERINK, J. P., BRINKHOF, B., BROEKHUIS, M. J., MENEZES, R. X., DEN BOER, M. L. & PIETERS, R. 2006. Glucocorticoid-induced glucocorticoid-receptor expression and promoter usage is not linked to glucocorticoid resistance in childhood ALL. *Blood,* 108**,** 1045-9.

TRAGESER, D., IACOBUCCI, I., NAHAR, R., DUY, C., VON LEVETZOW, G., KLEMM, L., PARK, E., SCHUH, W., GRUBER, T., HERZOG, S., KIM, Y. M., HOFMANN, W. K., LI, A., STORLAZZI, C. T., JÄCK, H. M., GROFFEN, J., MARTINELLI, G., HEISTERKAMP, N., JUMAA, H. & MÜSCHEN, M. 2009. Pre-B cell receptor-mediated cell cycle arrest in Philadelphia chromosome-positive acute lymphoblastic leukemia requires IKAROS function. *J Exp Med,* 206**,** 1739-53.

TRAN, T. H. & HUNGER, S. P. 2020. The genomic landscape of pediatric acute lymphoblastic leukemia and precision medicine opportunities. *Semin Cancer Biol.*

TREVINO, L. R., YANG, W., FRENCH, D., HUNGER, S. P., CARROLL, W. L., DEVIDAS, M., WILLMAN, C., NEALE, G., DOWNING, J., RAIMONDI, S. C., PUI, C. H., EVANS, W. E. & RELLING, M. V. 2009. Germline genomic variants associated with childhood acute lymphoblastic leukemia. *Nat Genet,* 41**,** 1001-5.

TRINH, L. A., FERRINI, R., COBB, B. S., WEINMANN, A. S., HAHM, K., ERNST, P., GARRAWAY, I. P., MERKENSCHLAGER, M. & SMALE, S. T. 2001. Down-regulation of TDT transcription in CD4(+)CD8(+) thymocytes by Ikaros proteins in direct competition with an Ets activator. *Genes Dev,* 15**,** 1817-32.

VAN DER BURG, M., BARENDREGT, B. H., SZCZEPAÑSKI, T., VAN WERING, E. R., LANGERAK, A. W. & VAN DONGEN, J. J. M. 2002. Immunoglobulin light chain gene rearrangements display hierarchy in absence of selection for functionality in precursor-B-ALL. *Leukemia,* 16**,** 1448.

VAN DER VEER, A., ZALIOVA, M., MOTTADELLI, F., DE LORENZO, P., TE KRONNIE, G., HARRISON, C. J., CAVÉ, H., TRKA, J., SAHA, V., SCHRAPPE, M., PIETERS, R., BIONDI, A., VALSECCHI, M. G., STANULLA, M., DEN BOER, M. L. & CAZZANIGA, G. 2014a. IKZF1

status as a prognostic feature in BCR-ABL1-positive childhood ALL. *Blood,* 123**,** 1691-8.

VAN DER VEER, A., ZALIOVA, M., MOTTADELLI, F., DE LORENZO, P., TE KRONNIE, G., HARRISON, C. J., CAVÉ, H., TRKA, J., SAHA, V., SCHRAPPE, M., PIETERS, R., BIONDI, A., VALSECCHI, M. G., STANULLA, M., DEN BOER, M. L. & CAZZANIGA, G. 2014b. IKZF1 status as a prognostic feature in BCR-ABL1–positive childhood ALL. *Blood,* 123**,** 1691.

VAN DER VELDEN, V. H., CAZZANIGA, G., SCHRAUDER, A., HANCOCK, J., BADER, P., PANZER-GRUMAYER, E. R., FLOHR, T., SUTTON, R., CAVE, H., MADSEN, H. O., CAYUELA, J. M., TRKA, J., ECKERT, C., FORONI, L., ZUR STADT, U., BELDJORD, K., RAFF, T., VAN DER SCHOOT, C. E., VAN DONGEN, J. J. & EUROPEAN STUDY GROUP ON, M. R. D. D. I. A. L. L. 2007. Analysis of minimal residual disease by Ig/TCR gene rearrangements: guidelines for interpretation of real-time quantitative PCR data. *Leukemia,* 21**,** 604-11.

VAN GALEN, P., KRESO, A., WIENHOLDS, E., LAURENTI, E., EPPERT, K., LECHMAN, ERIC R., MBONG, N., HERMANS, K., DOBSON, S., APRIL, C., FAN, J.-B. & DICK, JOHN E. 2014. Reduced Lymphoid Lineage Priming Promotes Human Hematopoietic Stem Cell Expansion. *Cell Stem Cell,* 14**,** 94-106.

VENN, N. C., VAN DER VELDEN, V. H., DE BIE, M., WAANDERS, E., GILES, J. E., LAW, T., KUIPER, R. P., DE HAAS, V., MULLIGHAN, C. G., HABER, M., MARSHALL, G. M., MD, N., VAN DONGEN, J. J. & SUTTON, R. 2012. Highly sensitive MRD tests for ALL based on the IKZF1 Delta3-6 microdeletion. *Leukemia,* 26**,** 1414-6.

VIRELY, C., MOULIN, S., COBALEDA, C., LASGI, C., ALBERDI, A., SOULIER, J., SIGAUX, F., CHAN, S., KASTNER, P. & GHYSDAEL, J. 2010. Haploinsufficiency of the IKZF1 (IKAROS) tumor suppressor gene cooperates with BCR-ABL in a transgenic model of acute lymphoblastic leukemia. *Leukemia,* 24**,** 1200-4.

VORA, A., GOULDEN, N., WADE, R., MITCHELL, C., HANCOCK, J., HOUGH, R., ROWNTREE, C. & RICHARDS, S. 2013. Treatment reduction for children and young adults with low-risk acute lymphoblastic leukaemia defined by minimal residual disease (UKALL 2003): a randomised controlled trial. *Lancet Oncol,* 14**,** 199-209.

WAGNER, W., RODERBURG, C., WEIN, F., DIEHLMANN, A., FRANKHAUSER, M., SCHUBERT, R., ECKSTEIN, V. & HO, A. D. 2007. Molecular and Secretory Profiles of Human Mesenchymal Stromal Cells and Their Abilities to Maintain Primitive Hematopoietic Progenitors. *STEM CELLS,* 25**,** 2638-2647.

WANG, J. H., NICHOGIANNOPOULOU, A., WU, L., SUN, L., SHARPE, A. H., BIGBY, M. & GEORGOPOULOS, K. 1996. Selective defects in the development of the fetal and adult lymphoid system in mice with an Ikaros null mutation. *Immunity,* 5**,** 537-49.

WARBURG, O., POSENER, K. & NEGELEIN, E. 1924. Über den stoffwechsel der carcinomzelle. *Naturwissenschaften,* 12**,** 1131-1137.

WINANDY, S., WU, L., WANG, J. H. & GEORGOPOULOS, K. 1999. Pre-T cell receptor (TCR) and TCR-controlled checkpoints in T cell differentiation are set by Ikaros. *J Exp Med,* 190**,** 1039-48.

WINANDY, S., WU, P. & GEORGOPOULOS, K. 1995. A dominant mutation in the Ikaros gene leads to rapid development of leukemia and lymphoma. *Cell,* 83**,** 289-99.

WYLLIE, A. H. 1980. Glucocorticoid-induced thymocyte apoptosis is associated with endogenous endonuclease activation. *Nature,* 284**,** 555-556.

YADAV, V., GANESAN, P., VEERAMANI, R. & KUMAR V, D. 2021. Philadelphia-Like Acute Lymphoblastic Leukemia: A Systematic Review. *Clinical Lymphoma Myeloma and Leukemia,* 21**,** e57-e65.

YAMAZAKI, S., EMA, H., KARLSSON, G., YAMAGUCHI, T., MIYOSHI, H., SHIODA, S., TAKETO, M. M., KARLSSON, S., IWAMA, A. & NAKAUCHI, H. 2011. Nonmyelinating Schwann cells maintain hematopoietic stem cell hibernation in the bone marrow niche. *Cell,* 147**,** 1146-58.

YASUDA, T., TSUZUKI, S., KAWAZU, M., HAYAKAWA, F., KOJIMA, S., UENO, T., IMOTO, N., KOHSAKA, S., KUNITA, A., DOI, K., SAKURA, T., YUJIRI, T., KONDO, E., FUJIMAKI, K., UEDA, Y., AOYAMA, Y., OHTAKE, S., TAKITA, J., SAI, E., TANIWAKI, M., KUROKAWA, M., MORISHITA, S., FUKAYAMA, M., KIYOI, H., MIYAZAKI, Y., NAOE, T. & MANO, H. 2016. Recurrent DUX4 fusions in B cell acute lymphoblastic leukemia of adolescents and young adults. *Nature Genetics,* 48**,** 569-574.

YOSHIDA, T. & GEORGOPOULOS, K. 2014. Ikaros fingers on lymphocyte differentiation. *Int J Hematol,* 100**,** 220-9.

YOSHIDA, T., HU, Y., ZHANG, Z., EMMANUEL, A. O., GALANI, K., MUHIRE, B., SNIPPERT, H. J., WILLIAMS, C. J., TOLSTORUKOV, M. Y., GOUNARI, F. & GEORGOPOULOS, K. 2019. Chromatin restriction by the nucleosome remodeler Mi-2β and functional interplay with lineage-specific transcription regulators control B-cell differentiation. *Genes Dev,* 33**,** 763-781.

YOSHIDA, T., LANDHUIS, E., DOSE, M., HAZAN, I., ZHANG, J., NAITO, T., JACKSON, A. F., WU, J., PEROTTI, E. A., KAUFMANN, C., GOUNARI, F., MORGAN, B. A. & GEORGOPOULOS, K. 2013. Transcriptional regulation of the Ikzf1 locus. *Blood,* 122**,** 3149-3159.

ZAGELBAUM, J., SHIMAZAKI, N., ESGUERRA, Z. A., WATANABE, G., LIEBER, M. R. & ROTHENBERG, E. 2016. Real-time analysis of RAG complex activity in V(D)J recombination. *Proc Natl Acad Sci U S A,* 113**,** 11853-11858.

ZHANG, J., JACKSON, A. F., NAITO, T., DOSE, M., SEAVITT, J., LIU, F., HELLER, E. J., KASHIWAGI, M., YOSHIDA, T., GOUNARI, F., PETRIE, H. T. & GEORGOPOULOS, K. 2011. Harnessing of the nucleosome-remodeling-deacetylase complex controls lymphocyte development and prevents leukemogenesis. *Nature immunology,* 13**,** 86-94.

ZHANG, J., MCCASTLAIN, K., YOSHIHARA, H., XU, B., CHANG, Y., CHURCHMAN, M. L., WU, G., LI, Y., WEI, L., IACOBUCCI, I., LIU, Y., QU, C., WEN, J., EDMONSON, M., PAYNE-TURNER, D., KAUFMANN, K. B., TAKAYANAGI, S.-I., WIENHOLDS, E., WAANDERS, E., NTZIACHRISTOS, P., BAKOGIANNI, S., WANG, J., AIFANTIS, I., ROBERTS, K. G., MA, J., SONG, G., EASTON, J., MULDER, H. L.,

CHEN, X., NEWMAN, S., MA, X., RUSCH, M., GUPTA, P., BOGGS, K., VADODARIA, B., DALTON, J., LIU, Y., VALENTINE, M. L., DING, L., LU, C., FULTON, R. S., FULTON, L., TABIB, Y., OCHOA, K., DEVIDAS, M., PEI, D., CHENG, C., YANG, J., EVANS, W. E., RELLING, M. V., PUI, C.-H., JEHA, S., HARVEY, R. C., CHEN, I. M. L., WILLMAN, C. L., MARCUCCI, G., BLOOMFIELD, C. D., KOHLSCHMIDT, J., MRÓZEK, K., PAIETTA, E., TALLMAN, M. S., STOCK, W., FOSTER, M. C., RACEVSKIS, J., ROWE, J. M., LUGER, S., KORNBLAU, S. M., SHURTLEFF, S. A., RAIMONDI, S. C., MARDIS, E. R., WILSON, R. K., DICK, J. E., HUNGER, S. P., LOH, M. L., DOWNING, J. R., MULLIGHAN, C. G. & THE ST. JUDE CHILDREN'S RESEARCH HOSPITAL–WASHINGTON UNIVERSITY PEDIATRIC CANCER GENOME, P. 2016. Deregulation of DUX4 and ERG in acute lymphoblastic leukemia. *Nature Genetics,* 48**,** 1481-1489.

ZHAO, M., PERRY, J. M., MARSHALL, H., VENKATRAMAN, A., QIAN, P., HE, X. C., AHAMED, J. & LI, L. 2014. Megakaryocytes maintain homeostatic quiescence and promote post-injury regeneration of hematopoietic stem cells. *Nat Med,* 20**,** 1321-6.

ZHOU, T., COMMODORE, L., HUANG, W. S., WANG, Y., THOMAS, M., KEATS, J., XU, Q., RIVERA, V. M., SHAKESPEARE, W. C., CLACKSON, T., DALGARNO, D. C. & ZHU, X. 2011. Structural mechanism of the Pan-BCR-ABL inhibitor ponatinib (AP24534): lessons for overcoming kinase inhibitor resistance. *Chem Biol Drug Des,* 77**,** 1-11.